EVALUATION OF BANANA PEEL AND WATERMELON RIND COMPOSITE EXTRACTS AS A GREEN NANO-FERTILIZER

Nothando Clementine Madlala

201943751

orcid.org/ 0000-0002-5477-6651

Dissertation submitted in partial fulfilment of the requirements for the Master of Science degree in Agriculture.

Supervisor: Dr N. Khanyile

Co-Supervisor: Dr T.A. Masenya

School of Agricultural Sciences
Faculty of Agriculture and Natural Science
2026

DECLARATION

I, Nothando Madlala, affirm that this is my original research work and that this thesis has not been submitted before by anyone for examination for any degree at any other institution. I generated and analyzed the results presented in this paper. All the material and information from other sources have been indicated and acknowledged by reference.

Student's signature:	Date: 16/01/2026
Supervisor's signature:	Date: 22/04/2026
Co-supervisor's signature:	Date:

DEDICATION

I dedicate this dissertation to myself for the courage, resilience, and perseverance that sustained me through this journey. Through God's grace, I found the strength to finish what once seemed beyond my reach.

ACKNOWLEDGEMENTS

Above all, I am profoundly grateful to God for His unconditional love, and grace that sustained me during the hardships of this research. I extend my sincere gratitude to my supervisor Dr. Khanyile for her continuous mentorship and guidance throughout this research project. I am grateful for her patience and her time spent reviewing my work and providing constructive feedback. Her support has been instrumental in my journey. I am grateful to my co-supervisor Dr. Masenya for his support and guidance throughout my research journey. Special thanks to Dr. Mnyambo, for his constant support, mentorship and guidance, and for always extending his hand to help me. I would like to extend my heartfelt gratitude to my mother, grandmother, and siblings (Gugu and Zama), for their prayers, love, support, words of encouragement, and affirmation. I would like to appreciate my “farm squad”: Gugu, Siphesihle, Wisdom, Celuxolo, Musa, Manqoba and Katishi for assisting me with data collection and their consistency in checking up on me. I can’t forget to thank my lab mates, Sandra and Surprise, for assisting me with experiments and offering emotional support. My final gratitude goes to the financial support received from the National Research Foundation for my research study.

ABSTRACT

Rising demand for sustainable agriculture and expanding interest in alternatives to conventional fertilizers, which contribute to soil degradation, nutrient leaching, and environmental pollution, have stimulated research into eco-friendly nano-fertilizers. As a result, this study investigated the green synthesis method for producing nano-fertilizer using banana peel extract (BPE) and watermelon rind extract (WRE), with *Aloe vera* gel extract (ALvE) functioning as both a reducing and stabilizing agent. The objectives entailed synthesizing and characterizing composite nano-fertilizer derived from agricultural waste and assessing its agronomic performance on *Solanum lycopersicum* L. (tomato) and *Capsicum annuum* L. (bell pepper) crops under greenhouse conditions. A completely randomized factorial design ($2 \times 10 \times 4$) was used to evaluate crop type, composite formulation (BPE:WRE ratio of 50:50, 75:25 and 25:75 with *Aloe vera* gel extract concentrations of 5,10,15 mL, including appropriate control treatments), and application dose during the 2024 growing season. Physicochemical characterization was performed using Ultraviolet-visible (UV-Vis) spectroscopy, Transmission Electron Microscope (TEM), Scanning Electron Microscopy – Energy Dispersive Spectroscopy (SEM-EDS), and colorimetric phytochemical screening, followed by an evaluation of their impact on plant development and soil parameters. The results confirmed the successful formation of noncovalent composite nanoparticles rich in oxygen-containing phytochemicals (flavonoids, phenols, tannins, saponins) and essential nutrients (potassium (K), magnesium (Mg), calcium (Ca)). Lower ALvE content (5 mL) produced well-dispersed nanoparticles, whereas higher ALvE levels (10 mL) caused polymer bridging and particle agglomeration (>500 nm). Consequently, crop type, composite formulation, dose, and their interactions significantly influenced plant growth and soil parameters, with tomato crops generally outperforming bell peppers across most evaluated growth parameters. In particular, 5 mL of ALvE composites at reduced application doses improved seed emergence percentage and plant height, whereas higher doses had the opposite effects. Leaf traits, stem diameter, flowering and biomass traits varied depending on crop type and composite formulation. Soil pH and electrical conductivity declined after application of the nano-fertilizer, indicating nutrient uptake and rhizosphere modification. This study demonstrates that effective nano-fertilizers capable of improving agronomic performance can be produced from agricultural waste without inorganic salt precursors, highlighting a promising avenue for sustainable agricultural practices

Keywords: Green synthesis, nano-fertilizer, banana peel extract, watermelon rind extract, aloe vera gel extract, seed emergence, plant growth, soil pH and EC.

TABLE OF CONTENTS

DECLARATION .... **II**

DEDICATION .... **III**

ACKNOWLEDGEMENTS .... **IV**

ABSTRACT .... **V**

TABLE OF CONTENTS .... **VII**

LIST OF APPENDICES .... **XI**

LIST OF TABLES .... **XIII**

LIST OF FIGURES .... **XVI**

LIST OF ABBREVIATIONS .... **XXI**

ACADEMIC CONTRIBUTIONS AND ACHIEVEMENTS .... **XXIV**

CHAPTER 1 .... **1**

BACKGROUND **1**

1.1 INTRODUCTION 1

1.2 PROBLEM STATEMENT 4

1.3 JUSTIFICATION OF THE STUDY 5

1.4 NOVELTY OF THE STUDY 6

1.5 PURPOSE OF THE STUDY 7

1.5.1 Aim *7*

1.5.2 Objectives *7*

1.5.3 Hypotheses *7*

1.6 RELIABILITY, VALIDITY, AND OBJECTIVITY 7

1.7 BIAS 8

1.8 SUMMARY OF CHAPTER 1 8

1.9 OUTLINE OF THE DISSERTATION 8

CHAPTER 2 .... **10**

LITERATURE REVIEW **10**

2.1 INTRODUCTION 10

2.2 ATTRIBUTES THAT QUALIFY A MATERIAL TO BE CLASSIFIED AS A FERTILIZER 12

2.3 ORGANIC AND INORGANIC FERTILIZERS 13

2.4 UTILIZATION OF ORGANIC MATERIALS AS SOURCES OF NUTRIENTS IN THE SYNTHESIS OF NANO-FERTILIZERS 15

2.4.1 The banana plant *15*

2.4.2 The watermelon plant *21*

2.5 THE COALITION OF STUDIES FOR BANANA PEELS AND WATERMELON RINDS AND THE UNFILLED RESEARCH GAP…………….. 25

2.6 NANO-FERTILIZERS 26

2.7 GREEN SYNTHESIS OF NANO-FERTILIZERS 33

2.7.1 Plant extracts in the synthesis of nano-fertilizers *34*

2.7.2 The effect of concentration of the plant extracts used in synthesizing nanoparticles *35*

2.8 PROPERTIES OF NANO-FERTILIZERS 42

2.9 EFFECT OF CONCENTRATION ON NANO-FERTILIZER PERFORMANCE 43

2.10 THE TOMATO (*SOLANUM LYCOPERSICUM* L.) PLANT 45

2.11 *CAPSICUM ANNUUM* L (BELL PEPPERS) 46

2.12 POTENTIAL OF NANO-FERTILIZERS AND THEIR CURRENT LIMITATIONS IN PLANT 47

2.13 CONCLUSION 49

CHAPTER 3 .... **51**

SYNTHESIS AND CHARACTERIZATION OF GREEN NANO-FERTILIZER USING BANANA PEELS, WATERMELON RINDS AND *ALOE VERA* GEL EXTRACT **51**

3.1 INTRODUCTION 51

3.2 MATERIALS 54

3.2.1 Source of plant extracts *54*

3.2.2 Source of chemicals and consumables *54*

3.3 METHODS 55

3.3.1 Preparation of Aloe vera gel extract (ALvE) *55*

3.3.2 The synthesis of green nano-fertilizer *56*

3.4 CHARACTERIZATION OF EXTRACTED MATERIAL 58

3.4.1 Ultraviolet- Visible (UV-Vis) spectroscopy analysis *58*

3.4.2 Phytochemical screening *59*

3.4.3 The pH and Electrical Conductivity (EC) *61*

3.4.4 Transmission Electron Microscopy (TEM) analysis *61*

3.4.5 Scanning Electron Microscopy (SEM)- Energy-Dispersive X-ray Spectroscopy EDS) analysis *61*

3.5 RESULTS AND DISCUSSION 62

3.5.1 UV-Vis spectroscopic analysis *63*

3.5.2 Phytochemical screening *66*

3.5.3 The pH and Electrical Conductivity (EC) *71*

3.5.4 Morphology and elemental composition of individual plant extracts *73*

3.5.5 The greenness of the byproduct or synthesis approach *107*

3.6 CONCLUSION 109

CHAPTER 4 110

THE IMPACT OF GREEN NANO-FERTILIZER ON SEED EMERGENCE PERCENTAGE AND PLANT GROWTH OF TOMATOES AND BELL PEPPERS UNDER GREENHOUSE CONDITIONS 110

4.1 INTRODUCTION 110

4.2 MATERIALS AND METHODS 113

4.2.1 The study location *113*

4.2.2 Experimental design and cultural practices *113*

4.2.3 Data collection *115*

4.2.4 Statistical analysis *117*

4.3 RESULTS 118

4.3.1 Seed emergence percentage *118*

4.3.2 Plant growth parameters *129*

4.3.3 Soil variables *153*

4.4 DISCUSSION 155

4.4.1 Seed emergence percentage *155*

4.4.2 Plant growth variables *157*

4.4.3 Soil variables ... 164

4.5 CONCLUSION ... 166

CHAPTER 5 ... 168

SYNTHESIS OF FINDINGS, SIGNIFICANCE, AND PROSPECTS ... 168

5.1 SUMMARY ... 168

5.2 IMPLICATIONS OF THE FINDINGS OF THIS STUDY ... 168

5.3 RECOMMENDATIONS AND DIRECTIONS FOR FUTURE RESEARCH ... 169

5.4 CONCLUSIONS ... 170

REFERENCES ... 172

APPENDICES ... 232

LIST OF APPENDICES

Appendix 1: Ethical approval 232

Appendix 2 :Topic change approval 233

Appendix 3:Published manuscript 234

Appendix 4:Published manuscript 235

Appendix 5: Book chapter invitation 236

Appendix 6: DSTI-Dr Ivy Matsepe-Casaburri Master's Fellowships 237

Appendix 7: Similarity index 238

Appendix 8: Analysis of variance for seed emergence percentage in Experiment 1 239

Appendix 9: Analysis of variance for seed emergence percentage in Experiment 2 239

Appendix 10: Analysis of variance for plant height in Experiment 1 240

Appendix 11: Analysis of variance for plant height in Experiment 2 241

Appendix 12: Analysis of variance for stem diameter in Experiment 1 241

Appendix 13: Analysis of variance for stem diameter in Experiment 2 242

Appendix 14 :Analysis of variance for chlorophyll content in Experiment 1 243

Appendix 15: Analysis of variance for chlorophyll content in Experiment 2 243

Appendix 16 :Analysis of variance for leaf length in Experiment 1 244

Appendix 17: Analysis of variance for leaf length in Experiment 2 245

Appendix 18: Analysis of variance for leaf width in Experiment 1 245

Appendix 19: Analysis of variance for leaf width in Experiment 2 246

Appendix 20: Analysis of variance for leaf area in Experiment 1 247

Appendix 21: Analysis of variance for leaf area in Experiment 2 248

Appendix 22: Analysis of variance for number of flowers in Experiment 1 249

Appendix 23: Analysis of variance for number of flowers in Experiment 2 249

Appendix 24: Analysis of variance for number of fruits in Experiment 1 250

Appendix 25: Analysis of variance for number of fruits in Experiment 2 250

Appendix 26: Analysis of variance for fruit mass in Experiment 1 251

Appendix 27: Analysis of variance for fruit mass in Experiment 2 252

Appendix 28: Analysis of variance for dry shoot mass in Experiment 1 253

Appendix 29: Analysis of variance for dry shoot mass in Experiment 2 254

Appendix 30: Analysis of variance for fresh root mass in Experiment 1 255

Appendix 31: Analysis of variance for fresh root mass in Experiment 2 255

Appendix 32: Analysis of variance for dry root mass in Experiment 1 256

Appendix 33: Analysis of variance for dry root mass in Experiment 2 256

Appendix 34: Analysis of variance for pH in Experiment 1 257

Appendix 35: Analysis of variance for pH in Experiment 2 257

Appendix 36: Analysis of variance for EC in Experiment 1 258

Appendix 37: Analysis of variance for EC in Experiment 2 258

LIST OF TABLES

Table 2.1: The different applications of fruit peels across various industries………………… 17

Table 2.2: The watermelon rind powder mineral profile……………………………………… 23

Table 2.3: Summaries of studies on the impact of different types of nano-fertilizers on crop performance……………………………………………………………………………….. 29

Table 2.4: The effect of concentration of plant extracts in the synthesis of nanoparticles…….. 37

Table 3.1: Ratios of banana to watermelon peels for the synthesis of the green nano-fertilizers 57

Table 3.2: Composite of banana peel extracts (BPE), watermelon peel extracts (WPE) and Aloe vera extracts (ALvE). 58

Table 3.3:The phytochemical screening of plant extracts 67

Table 3.4: The pH and EC of extracted material from banana peel extract (BPE), watermelon rind extract (WRE), Aloe vera gel extract (ALvE) 72

Table 4.1: The 2 × 10 × 4 factorial design employed in the present study 113

Table 4.2: Partitioning mean sum squares for the effect of green nano-fertilizer on seed emergence percentage in experiments 1 (February to June) and experiment 2 (June to October) at 14 days after applying the treatments. 118

Table 4.3: The impact of interaction between crop type, composite of plant extract, and dose on seed emergence in Experiment 1 123

Table 4.4: The effect of interaction between crop type and CPE in Experiment 2 127

Table 4.5: The effect of the interaction between the composite of plant extract and dose in Experiment 2 128

Table 4.6: Partitioning mean sum squares for the effect of green nano-fertilizer on plant height, and stem diameter in experiments 1 (February to June) and experiment 2 (June to October) under greenhouse conditions at 120 days after applying the treatments (n=240) 131

Table 4.7:Partitioning mean sum squares for the effect of green nano-fertilizer on leaf length and leaf width in Experiments(February to June) and experiment 2 (June to October) under greenhouse conditions at 120 days after applying the treatments (n=240) 132

Table 4.8: Partitioning mean sum squares for the effect of green nano-fertilizer on leaf area in Experiment 1(February to June) and leaf area as well as chlorophyll content in Experiment 2 (June to October) under greenhouse conditions at 120 days after applying the treatments (n=240) ... 133

Table 4.9: Partitioning mean sum squares for the effect of green nano-fertilizer on the number of flowers, the number of fruits, and fruit mass, in Experiment 1 and the number of flowers in Experiment 2, under greenhouse conditions at 120 days after applying the treatments............ 135

Table 4.10:Partitioning mean sum squares for the effect of green nano-fertilizer on fresh root mass in Experiment 1 (February to June), and dry shoot mass, fresh root mass and dry root mass in Experiment 2 (June to October) under greenhouse conditions at 120 days after applying the treatments (n=240) 136

Table 4.11: The effect of CPE on stem diameter, leaf length, leaf width, leaf area, number of flowers, and fresh root mass in Experiment 1 (February to June) 145

Table 4.12: The effect of CPE on plant height, stem diameter, leaf length, leaf width, leaf area, dry shoot mass, fresh root mass, and dry root mass in Experiment 2 (June to October)........... 146

Table 4.13: The effect of interaction between crop type, CPE, and dose on stem diameter and number of flowers in Experiment 1 (February to June)... 149

Table 4.14: The effect of interaction between crop type and composite of plant extracts on stem diameter in Experiment 2 (June to October).. 152

Table 4.15: Source of variation affecting pH and EC in experiments 1 (February to June) and experiment 2 (June to October)..153

Table 4.16: The effect of CPE on EC in experiments 1 (February to June) and experiment 2 (June to October) 155

LIST OF FIGURES

Figure 2.1:Mechanism of fertilizer application in enhancing plant growth. (A) plant receiving nutrients via compost shows healthy development of flowers and fruits. (B) Plant without nutrients shows stunted growth and discolored leaves. Source: Author's own illustration........................13

Figure 2.2: Citrulline chemical structure 24

Figure 2.3: The key principles of green synthesis approach of synthesizing nano-fertilizers.....33

Figure 2.4: The bio-reduction of gold nanoparticles using *Aloe vera* gel extract as a reducing and stabilizing agent. Authors own' 35

Figure 3.1: The synthesis of *Aloe vera* gel extract...56

Figure 3.2: Schematical diagram of the green synthesis of composite of banana and watermelon peel extracts 57

Figure 3.3: The composite of 75%BPE+25%WPE (D), 75%BPE+25%WPE+15 mL ALvE (C), 75%BPE+25%WPE+10 mL ALvE (B), 75%BPE+25%WPE+5 mL ALvE (A) 62

Figure 3.4: The UV-Vis absorption spectra of the clean extracts and composite material; (A) the absorption spectrum of watermelon rind extract (WRE); (B) banana peel extract (BPE); (C) composite material of 50% BPE + 50% WRE + 10 mL ALvE; (D) *Aloe vera* gel extract (ALvE). 63

Figure 3.5: The phytochemical screening showing the presents of various phytochemicals for the plant extracts. 69

Figure 3.6: (a) TEM image of BPE, exhibiting quasi-spherical nanoparticles (scale bar =20 nm). (b) Histogram illustrating the particle size distribution (n=23), with an average diameter of 9.9 nm. 74

Figure 3.7: SEM-EDS analysis of BPE. (a) SEM image illustrating the surface morphology (500 nm) (b) EDS spectrum confirming O, Mg, Na, Si, S, Cl, and K. (c) Overlay elemental map. (d) Individual elemental maps. 75

Figure 3.8: Self-assembly into nanostructures induced by higher pH and heat, "oxidative polymerization process". (a) effectively capped nanoparticles. (b) poorly capped nanoparticles. Adapted from Pal et al. (2024)..77

Figure 3.9: (a) TEM image of WRE (scale bar = 20 nm). (b) Histogram illustrating the particle size distribution (n = 10), with an average diameter of 11.2 nm. 78

Figure 3.10: SEM-EDS analysis of WRE. (a) SEM image showing the surface morphology (500 nm) (b) EDS spectrum confirming O, Na, Mg, Si, P, S, Cl, K and Ca. (c) Overlay elemental map. (d) Individual elemental maps. 79

Figure 3.11: (a) TEM image of ALvE (scale bar = 1000 nm). (b) Histogram illustrating the particle size distribution (n = 17), with an average diameter of 58.1 nm. 80

Figure 3.12: SEM-EDS analysis of ALvE. (a) SEM image showing the surface morphology (500 nm) (b) EDS spectrum confirming O, Na, Mg, Si, P, Cl, K, Ca, and Mn. (c) Overlay elemental map. (d) Individual elemental maps...81

Figure 3.13:The formation of ALvE nanoparticles through the process called "evaporation-induced self-assembly". Adapted from Cusola et al. (2018). 82

Figure 3.14: (a) TEM image of 50 % BPE+50%WRE (scale bar= 200 nm). (b) Histogram illustrating the particle size distribution (n=52), with an average diameter of 37.3 nm. (c) SAED image of 505BPE+50%WRE. (d) EDS spectrum of 50%BPE+50%WRE 84

Figure 3.15: (a) TEM image of 75 % BPE+25%WRE (scale bar = 20 nm). (b) Histogram illustrating the particle size distribution (n = 90), with an average diameter of 4.4 nm. 85

Figure 3.16: SEM-EDS analysis of 75%BPE + 25%WRE. (a) SEM image showing the surface morphology (500 nm) (b) EDS spectrum confirming O, Si, P, S, Cl, and K. (c) Overlay elemental map. (d) Individual elemental maps...86

Figure 3.17: TEM image of 75%WRE+25%BPE (scale bar = 100 nm). (b) Histogram illustrates the particle size distribution (n= 5), with an average diameter of 81.6 nm (c) EDS spectrum of 75%WRE+25%BPE. 88

Figure 3.18: (a) TEM image of 50 % BPE+50%WRE +5 mL ALvE (scale bar = 20 nm), (b) the histogram illustrates the particle size distribution (n = 12), with an average diameter of 7.7 nm. 89

Figure 3.19: SEM-EDS analysis of 50%BPE + 50%WRE+ 5 ml ALvE. (a) SEM image showing the surface morphology (500 nm) (b) EDS spectrum confirming K, Cl, Mg, O, Si, and Na. (c) Overlay elemental map. (d) Individual elemental maps. 90

Figure 3.20: The formation of nanoparticles through heat-assisted post-synthetic polymer encapsulation. Inspired by (Aguilar et al., 2021), with modifications 92

Figure 3.21:(a) TEM image of 50 % BPE+50%WRE +10 mL ALvE (scale bar = 2000 nm). (b) Histogram illustrating the particle size distribution (n = 13), with an average diameter of 528.8 nm. (c) SAED structure of 50%BPE+50%WRE+10mL. 93

Figure 3.22: The polymer bridging of nanoparticles process. Adapted from Liang et al. (2023). 94

Figure 3.23: 50%BPE+50%WRE+15 mL (a) TEM image (scale bar = 500 nm). (b) Histogram illustrates the particle size distribution (n = 4), with an average diameter of 540.8 nm. (c) SAED pattern. (d) EDS spectrum 95

Figure 3.24: The 75%BPE+25%WRE_5mL ALvE (a) TEM image (scale bar = 500 nm). (b) Histogram illustrating the particle size distribution (n = 3), with an average diameter of 365.3 nm. (c) SAED pattern. (d) EDS spectrum 97

Figure 3.25: 75%BPE+25%WRE+10 mL AlvE (a) TEM image (scale bar = 500 nm). (b) Histogram illustrating the particle size distribution (n= 5), with an average diameter of 433.5 nm. (c) SAED pattern. (d) EDS spectrum 99

Figure 3.26: 75%BPE+25%WRE+15 mL AlvE (a)TEM image of 75 % BPE+25 %WRE +15 mL ALvE (scale bar =200 nm). (b) Histogram illustrating the particle size distribution (n = 4), with an average diameter of 113.9 nm. (c) SAED pattern. (d) EDS spectrum. 100

Figure 3.27:75%WRE+25%BPE+5 mL ALvE (a) TEM image (scale bar =100 nm). (b) Histogram illustrating the particle size distribution (n = 23), with an average diameter of 4.6 nm. (c) SAED image. (d) EDS spectrum. 102

Figure 3.28: The 75%WRE+25%BPE+10 mL ALvE (a) TEM image (scale bar = 500 nm). (b) Histogram illustrating the particle size distribution (n= 7), with an average diameter of 289.2 nm. (c) SAED image. (d) EDS spectrum. 104

Figure 3.29: (a) TEM image of 75 % WRE +25 %BPE +15 mL ALvE (scale bar = 20 nm). (b) Histogram illustrating the particle size distribution (n= 10), with an average diameter of 23.5 nm. 105

Figure 3.30: The EDS spectrum of 75%WRE+25%BPE +10 mL ALvE. (a) SEM image showing the surface morphology (500 nm) (b) EDS spectrum confirming O, Na, Mg, Si, S, Cl, and K. (c) Overlay elemental map. (d) Individual elemental maps. 106

Figure 4.1: The experimental layout 115

Figure 4.2:Air dried samples of sandy loam soils 117

Figure 4.3: The effect of the composite of plant extracts on seed emergence percentage in Experiment 1. 119

Figure 4.4: The effect of the composite of plant extracts on seed emergence percentage in Experiment 2. 120

Figure 4.5: The effect of dose on seed emergence percentage in Experiment 1 121

Figure 4.6: The effect of dose on seed emergence percentage in Experiment 2 121

Figure 4.7: The effect of crop type on plant height in Experiments 1 and 2. 137

Figure 4.8: The effect of crop type on stem diameter in Experiments 1 and 2. 138

Figure 4.9: The effect of crop type on leaf length in Experiment 1 and 2. 138

Figure 4.10: The effect of crop type on leaf width in Experiments 1 and 2 139

Figure 4.11: The effect of crop type on leaf area in Experiments 1 and 2 139

Figure 4.12: The effect of crop type on chlorophyll content in Experiment 2. 140

Figure 4.13: The effect of crop type on the number of flowers in Experiments 1 and 2. 141

Figure 4.14: The effect of crop type on the number of fruits in Experiment 1. 141

Figure 4.15: The effect of crop type on fruit mass in Experiment 1. 142

Figure 4.16: The effect of crop type on dry shoot mass in Experiment 2. 142

Figure 4.17: The effect of crop type on fresh root mass in Experiment 2. 143

Figure 4.18: The effect of crop type on dry root mass in Experiment 2. 143

Figure 4.19: The effect of dose on plant height in Experiment 2. 147

Figure 4.20: The effect of the interaction between crop type and dose in Experiment 2. 152

Figure 4.21: The effect of crop type on soil pH in Experiment 1. 154

Figure 4.22: The effect of crop type on EC in Experiment 1 154

LIST OF ABBREVIATIONS

AgNPs:	Silver Nanoparticles
ALvE:	*Aloe Vera* Gel Extract
AuNPs:	Gold Nanoparticles
BPB:	Banana Peel Biochar
BPE:	Banana Peel Extract
BPs:	Banana Peels
CPE:	Composite of Plant Extracts
Cu:	Copper
CuO NPs:	Copper Oxide Nanoparticles
DM:	Dry Matter
DNA:	Deoxyribonucleic Acid
EC:	Electrical Conductivity
Fe_2O_3:	Iron (III) Oxide
Fe_2Cl_2:	Iron (II) Chloride
$FeSO_4$:	Ferrous Sulfate
FTIR:	Fourier Transform Infrared Spectroscopy

K:	Potassium
KCl:	Potassium Chloride
LAI:	Leaf Area Index
LOF:	Liquid Organic Fertilizer
MnO NPs:	Manganese (II) Oxide Nanoparticles
NFs:	Nano-Fertilizers
NPs:	Nanoparticles
NUE:	Nutrient-Use Efficiency
P:	Phosphorous
RND:	Recommended Nitrogen Doses
ROS:	Reactive Oxygen Species
RuNPs:	Ruthenium Nanoparticles
SEA:	South-East Asia
SEM-EDS:	Scanning Electron Microscopy – Energy Dispersive Spectroscopy
TEM:	Transmission Electron Microscopy
TiO_2:	Titanium Oxide
UV-Vis:	Ultraviolet-Visible Spectroscopy
WRE:	Watermelon Rind Extract

WRs:	Watermelon Rinds
WUE:	Water-Use Efficiency
XRD:	X-Ray Diffraction
Zn:	Zinc
ZnO NPs:	Zinc Oxide Nanoparticles

ACADEMIC CONTRIBUTIONS AND ACHIEVEMENTS

Published review articles

- Madlala, N.C., Khanyile, N. and Masenya, A., 2024. Examining the correlation between the inorganic nano-fertilizer physical properties and their impact on crop performance and nutrient uptake efficiency. *Nanomaterials*, 14(15), p.1263.
- Khanyile, N., Dlamini, N., Masenya, A., Madlala, N.C. and Shezi, S., 2024. Preparation of Biofertilizers from Banana Peels: Their Impact on Soil and Crop Enhancement. *Agriculture*, 14(11), p.1894.

Manuscript under review

- Madlala, N.C., Khanyile, N. and Masenya, A., 2025. Advances on the Use of Plant Extracts for Green Synthesized Nano-Fertilizers: Recent Developments and Proposed Research Themes (under review).
- Madlala, N.C., Khanyile, N. and Masenya. Nano-Enabled Edible Coatings as Postharvest Treatments for Preserving Quality of and Extending Shelf-Life of Deciduous Fruits – A Review. International journal of Fruit Science (under review).

Invited Book chapter (under review)

Madlala, N.C., Khanyile, N. and Masenya, A., Shezi, S. 2025. Impact of Nanomaterial Properties on Nano-fertilizer Efficiency. Springer (under review).

Awards and achievements

DSTI 2025 SAWISA Master's Fellowship Recipient: Awarded by the Department of Science, Technology and Innovation as part of the South African Women in Science Award fellowship, in recognition of outstanding achievement and research potential among female postgraduates.

CHAPTER 1

BACKGROUND

1.1 Introduction

In pursuit of addressing global challenges such as access to adequate and nutritious food, soil degradation and climate fluctuations, sustainable agriculture has become essential in addressing these challenges (Saleem et al., 2024). Contemporary agricultural practices prove to be insufficient against inefficient delivery of nutrients, declining soil health and environmental pollution as a result of excessive application of conventional fertilizers (Saurabh et al., 2024). The modern agricultural ideology seeks to allow for the generation of high profits with minimal investment, ensuring that no biotic or abiotic factors of life are interrupted (Saravana kumari et al., 2024). In efforts to ensure this objective is achieved, governments have set targets to promote sustainable agricultural initiatives due to growing consumer demand and the belief that organically produced food has a positive impact on public health. In light of this, the advent of novel sustainable organic farming practices has gained traction (Anand and Rai, 2024).

As previously mentioned, current agricultural food systems have been criticized for their lack of environmental sustainability and for perpetuating economic and social inequalities. Within it, there is a heavy reliance on monoculture and high levels of synthetic chemical applications, which require an intense amount of energy and resources. Nonetheless, amid all the aforementioned, the justification for continued practice lies in short-term productivity and profitability over long-term ecological health (Zhang, 2024). Conventional fertilizers tend to release nutrients in bulk, exceeding the rate of plant uptake (Saleem et al., 2022). The residual nutrients from conventional fertilizers interact with soil and microbial systems, which leads to transformations such as the volatilization of gaseous products, precipitation of insoluble salts, and leaching of soluble ions. In addition, redox-driven processes such as nitrification and denitrification reduce nutrient bioavailability (Giordano et al., 2021; Tian et al., 2023).

In response to these challenges, nanotechnology-based fertilizers, commonly known as nano-fertilizers (NFs), have emerged as innovative tools in modern agriculture. Nano-fertilizers can improve nutrient use efficiency and crop productivity, thereby supporting more sustainable agricultural practices. These fertilizers stand out from their counterparts as they are capable of being acclimatized to specific crop needs in line with nutrient requirements grounded on soil conditions, environmental factors and crop growth stages (Kak et al., 2024).

Nano-fertilizers operate at the nanoscale by using particles of at least 1 billionth of a meter i.e., between 1 to 100 nanometers (Pudhuvai et al., 2024). This gives rise to their unique properties such as their high surface area to volume ratio and improved reactivity, allowing for a dedicated modifiable release of nutrients to crops. This, in turn, reduces the environmental effect that comes with over-fertilization practices. Therefore, the improved nutrient accessibility in the rhizosphere and facilitation of nutrient uptake improve crop quality and yields (Amanullah, 2024).

The green synthesis of nano-fertilizers using plant extracts as reducing and stabilizing agents has gained attention as a sustainable approach (Bairwa et al., 2023). This approach is characterized by being facile, eco-friendly, benign, cost-effective and biocompatible (Perumalsamy et al., 2024). Plant extracts are rich in phytochemicals such as polyphenols (e.g. flavonoids, tannins), alkaloids, and organic acids, capable of donating electrons to reduce metal ions and form protective barriers to prevent nanoparticle agglomeration (El Shafey, 2020). These phytochemicals also act as natural chelating agents by binding metal ions to form stable complexes (Nobahar et al., 2021). Chelating agents improve the bioavailability of nutrients in plants by preventing nutrient loss and keeping them soluble and stable in forms that are readily available to plants (Hussein et al., 2019). Hence, the identification of precise phytochemicals in plant extracts is imperative in the synthesis of green nano-fertilizer, as it brings about the modification of nanoparticles with the desired characteristics.

Plant extracts are not only rich in phytochemicals, but have also long been recognized as organic fertilizers, primarily due to their beneficial and diverse nutrient composition (El-Serafy et al., 2023). Prior studies have revealed that combining agricultural wastes, such as fruit peels, is an innovative approach to enhance the efficiency and nutrient profile of fertilizers (Khanyile et al., 2024; Ma'mor et al., 2023). Different plant materials often possess unique properties that, when combined, can complement each other and result in improved outcomes compared to using a single material (Khanyile et al., 2024; Ma'mor et al., 2023). Fruit peel residues, particularly banana peels (BPs), have received increasing attention as plant-derived materials because their extracts contain several essential nutrients, including magnesium (Mg), potassium (K), nitrogen (N), calcium (Ca), manganese (Mn), zinc (Zn), sodium (Na), and copper (Cu), which contribute to their potential use as bio-fertilizers (Oyeyinka and Afolayan, 2019). As reported by Gladvin et al. (2017), watermelon rind extracts contain similar minerals present in BPs and play a role in enriching soil organic matter and improving soil fertility (Kitundu et al., 2024).

Therefore, the present study aims to synthesize a green nano-fertilizer from a composite of banana peel extract (BPE) and watermelon rind (WRE) extract using *Aloe vera* gel extract (ALvE). The efficacy of the prepared material was evaluated on *Solanum lycopersicum* L. (tomato) and *Capsicum annuum* L. (bell pepper) crops. The prepared material aims to promote the adoption of green materials at the nanoscale, addressing the growing demand for organic food and encouraging the sustainability of the environment.

1.2 Problem statement

The exponential, sudden human population growth calls for a direct proportional increase in food production to meet the escalating demand (Hong et al., 2024). Despite anything to the contrary, sustainable agricultural practices should be employed as a solution to ensure productivity, and prioritized in a manner that does not endanger the environment (Gomiero, 2016). Enacting from these so-called practices, the application of organic nano-fertilizer advocates great possibilities that can serve as an antidote to the spreading food insecurity issue, as they function by enhancing the ability of the soil to supply essential crop nutrients (Liu et al., 2024). Hence, the development of novel agricultural approaches is pivotal in ensuring the global need for enough and healthy, nutritious food is met (Varzakas and Smaoui, 2024).

It is worth pointing out, though, that extensive application of conventional fertilizer is a culprit contributing to environmental degradation (Gaytancıoğlu and Yılmaz, 2024). Topsoil loss through leaching, eutrophication of water bodies because of nutrient accumulation, culminating in the growth of algae, aquatic biodiversity loss, and elimination of oxygen, are some of the unfavorable environmental effects (Luna Juncal et al., 2023). Furthermore, these synthetic conventional fertilizers claim a hefty price, thereby rendering them hardly accessible to small-scale farmers, leading to reduced crop yields and therefore aggravating food security issues further (Zhuang et al., 2024). It has therefore become an urgent pressing issue to innovate solutions in addressing the negative environmental impact concerns linked with the popular application of chemical fertilizers for the protection of ecosystems, promotion of sustainable agriculture, and tackling food insecurity issues for vulnerable populations (Pandian et al., 2024).

Long-term reliance on chemical fertilizers can result in residue accumulation in food, which may pose potential risks to environmental sustainability and human health. Research illustrates that continuous agrochemical residue exposure has the potential to cause adverse health issues, which can include neurological disorders and cancer (Khan et al., 2022; Said, 2023). Applying organic materials for fertilization decreases the presence of harmful chemical remains on food. This is because food produced from organic fertilizers has lower accumulation of nitrates, pesticides, metals, and antibiotics in relation to food produced from conventional fertilizers. Hence, organic food becomes safer and healthier because of the reduced harmful contaminants (Giampieri et al., 2022). Apart from that, essential nutrients, vitamins and antioxidants are obtained from organic foods and these offer more nutritional value. This, therefore, restrains the long-term influence of consumption on chemically grown food (Rahman et al., 2024).

Irrespective of the well-known setbacks of applying chemical fertilizers, as already discussed above, they are still undoubtedly popular and common in the production of food (Chen et al., 2018). Consequently, production in agriculture is likely to fall into a popular concept of the law of diminishing returns, producing low yields and lowering soil health (Xiong and Zhao, 2024). Taking such concerns into account, this research aims to investigate the possibility of using a green nano-fertilizer derived from the composite of banana and watermelon peel extracts as an environmentally friendly alternative.

1.3 Justification of the study

The study holds the potential to address a concerning matter in agriculture: the need for sustainable and environmentally friendly fertilizers. Amid ongoing climate change, which demands climate-smart agriculture, the use of inorganic fertilizers has been a response to the threat of food insecurity. However, the current study introduces an underexplored approach to synthesizing a liquid green nano-fertilizer using banana and watermelon peel extracts. Its ultimate goal is to reduce dependence on chemical fertilizers while simultaneously enhancing productivity. Through this approach, the study will contribute to promoting environmental conservation as it will assist in reducing the application of hazardous chemicals, which can contaminate soil, air, and water.

The proposed fruit peels, as previously mentioned, are organic materials that would otherwise be discarded. Poor management can contribute to environmental pollution. The intervention of the current study is to bridge the gap between the mismanagement of fruit peels (BPE and WRE) and the valorization of these organic materials for the benefit of agricultural food production whilst reducing waste. The banana and watermelon peels have been chosen, owing to their abundant availability and easier access since synthesizing green nano-fertilizer from such materials is simpler, energy efficient, which may lead to reduced operational costs. In addition, efforts by farmers to grow food organically will also be boosted via the study. The effectiveness of green nano-fertilizers in promoting plant growth is largely associated with their nanoscale characteristics. Their extremely small particle size and large surface-area-to-volume ratio enhance nutrient interaction and mobility, allowing nutrients to be retained and released more efficiently. As a result, plants can access nutrients more readily, which supports improved growth and development.

1.4 Novelty of the study

This study presents a significant advancement in sustainable agriculture by using composite peel extracts synthesized from BPE and WRE as the primary materials for the synthesis of the nano-fertilizer, demonstrating a synergistic effect with the potential to enhance crop attributes more effectively than when applied individually.

In addition, this study explores a new approach of using ALvE as a reducing and stabilizing agent for the synthesis of nano-fertilizer from BPE and WRE. Previous studies have used ALvE to synthesize various nanoparticles, including metallic and non-metallic nanoparticles. This study presents an approach that uses only organic materials and incorporates ALvE with BPE and WRE to produce a nano-fertilizer containing all the benefits of the three materials, resulting in an eco-friendly material with enhanced properties.

1.5 Purpose of the study

1.5.1 Aim

The study aimed to investigate the efficacy of banana and watermelon composite peel extracts as a green nano-fertilizer in promoting plant growth, specifically in tomato and bell pepper crops.

1.5.2 Objectives

i. To synthesize and characterize a liquid green nano-fertilizer derived from composite banana and watermelon peel extracts using *Aloe vera* gel extract as a stabilizing agent.

ii. To evaluate the impact of the prepared material on the growth parameters of tomato and bell pepper crops.

1.5.3 Hypotheses

i. A green nano-fertilizer synthesized from a composite of banana and watermelon peel extracts using *Aloe vera* gel extract will exhibit physicochemical and structural properties characteristic of nano-fertilizer systems, including appropriate particle size, morphology, nutrient availability, and phytochemical composition.

ii. The banana and watermelon composite peel extract will have a positive impact on the seed emergence and growth parameters of the tomato and bell pepper crops.

1.6 Reliability, validity, and objectivity

Data reliability was assessed through statistical analysis using a significance level of 5%. The validity of the findings was ensured by repeating the experimental treatments. Objectivity in the study was maintained by relying on empirical evidence during data interpretation, thereby minimizing subjective influence in the analysis.

1.7 Bias

To mitigate bias, it was ensured that each experiment was conducted with sufficient replications to account for potential errors (Leedy et al., 2019).

1.8 Summary of Chapter 1

This chapter introduces the thesis and addresses the importance of implementing eco-friendly agricultural practices. Problems associated with the extensive application of chemical fertilizers regarding the environment and the food chain system are discussed. Considering this, the study proposes the application of organic waste materials, banana and watermelon peels in particular, for the synthesis of green nano-fertilizer. The chapter establishes the justification, aim, objectives, hypotheses, and the novelty of the study. In addition, this chapter also presents how the study will ensure that results are not biased. The assurance is backed by the deployment of comprehensive measures, including statistical analysis, replication of experiments, and reliance on empirical evidence.

1.9 Outline of the dissertation

This dissertation comprises five chapters. **Chapter 1** establishes the overall research framework of this study and outlines the overall research approach adopted, encompassing key methodological elements. **Chapter 2** provides a critical review of relevant literature, highlighting previous studies on the green synthesis of nano-fertilizer using plant extracts, developments in the use of nano-fertilizers, and identifies the research gap this research aims to address. **Chapter 3** details the materials and methods used in the synthesis of the green nano-fertilizer, and the characterization of the green nano-fertilizer. **Chapter 4** presents agronomic practices related to the application of prepared green nano-fertilizer. **Chapter 5** presents a summary, discussion of the findings and conclusions drawn from the study and offers future recommendations.

CHAPTER 2

LITERATURE REVIEW

2.1 Introduction

There is a compelling dilemma in agriculture, one that entails uncovering the optimal solution to meet sustainable global food demands without exacerbating soil degradation and depleting water and other natural resources (Kumari et al., 2024). Conventional fertilizers, though highly efficient in enhancing crop yields, are prone to initiating environmental repercussions. These issues include, but are not limited to soil degradation, nutrient runoff, and water contamination (Luna Juncal et al., 2023; Madjar et al., 2024). By virtue of this phenomenon, a new paradigm shift has been enacted, prompting the world to gravitate towards more sustainable production techniques (Moodley et al., 2024). Hence, the growing interest in organic alternatives is becoming prominent, with a major focus on enhancing crop yields while minimizing environmental impact (Wang et al., 2024). As a countermeasure against the environmental threats posed by traditional chemical fertilizers, green nano-fertilizers have come to the rescue as a promising alternative, offering potential solutions for enhanced agricultural production with reduced ecological effects (Arora et al., 2024; Elsabagh et al., 2024). Nano-fertilizers represent a novel class of fertilizers developed through nanotechnology to improve the efficiency of nutrient delivery to plants (Kekeli et al., 2025). These fertilizers are composed of nanoparticles with a typical size between 1 and 100 nm (Kumar et al., 2025), which can completely enclose essential nutrients, including N, P, K, and micronutrients efficiently (Mim et al., 2025). Their minute size allows for an increased surface area and enhanced interaction with plant cells through the facilitation of better nutrient utilization and absorption (Demeke et al., 2025). This specific delivery system has the potential to reduce nutrient losses, environmental impact, and improve crop yields, contrary to their counterparts i.e., conventional fertilizers (Goyal et al., 2025). These nano-fertilizers share a similar formulation as they can be synthesized from both inorganic and organic materials (Ayenew et al., 2025).

Numerous studies have reported that metallic and metal oxide nanoparticles (NPs) can promote plant growth by improving crop yield, nutrient uptake, and fruit quality (Aqeel et al., 2022; Özgören Can et al., 2024). Commonly studied nanoparticles include titanium oxide (TiO_2), iron oxide (Fe_2O_3), silver (Ag), zinc oxide (ZnO), and gold (Au). Their unique physicochemical characteristics enable effective interaction with plant systems, which can enhance several physiological processes (Keita et al., 2025). However, despite their good properties, they have an undesirable loophole in their mechanism of action. Studies have reported issues such as toxicity, negative effects on non-target organisms, and possible accumulation within the food chain (Islam, 2025a; Zhang et al., 2025). Utilization of plant extracts, which are now gaining traction in the synthesis of nano-fertilizer (Wanapat et al., 2024).

It has become common practice to discard plant extracts, especially fruit peels, which add to the build-up of waste, creating health and environmental issues (Hasan et al., 2024). Nonetheless, recycling these fruit peels into valuable material is feasible, such as using them as bio-fertilizers and as an additive to livestock feed (Bishnoi et al., 2023). Banana peels present a promising antidote for becoming a potential bio-fertilizer and this discovery finds its anchors in several studies. Sampling out from these studies, According to Sogani et al. (2023), the application of BPs as a bio-stimulatory fertilizer significantly enhanced the germination performance of black gram crops. To support this, the study showed an increase in the germination rate of gram crops to 100% with $12mL^{-1}$ application of the biofertilizer compared to the low 12% in the control group. In a separate study, Hussain et al. (2023) discovered that the growth of flax plants is significantly improved by the application of liquid fertilizer synthesized from banana and apple peels. Various vegetative characteristics, including plant height, shoot fresh weight, root fresh weight, and levels of photosynthetic pigments, were used to compare treated plants with the control group.

Similarly, BPs and WRs are often disposed of as agricultural waste, which holds nutritional value (Ben Romdhane et al., 2024). To truly harness the maximum production of bio-fertilizer from WRs in the most efficient way possible is through the use of Response Surface Methodology, provided that the conditions identified give a 20 day retention with a water ratio of 400 mL for significant nutrient content of primary nutrients (N,P,K) and this is brought forth by the findings of Eurogo et al. (2022). Plant-derived extracts, including those from banana and orange peels, have been widely used due to their dual function as bio-fertilizers, acting as reducing and stabilizing agents in synthesizing nanoparticles (Goh et al., 2023) . However, there is still an untapped area in this topic; as far as the existing body of knowledge is concerned, no study appears to have utilized plant extracts as both the source of nutrients, reducing and stabilizing agent in the synthesis of bio-fertilizers let alone using the same plant extracts solemnly for both as a nutrient source and as a reducing agent in synthesizing nanoparticles with the intention to use them as bio-fertilizers. Thus, the aim of this literature review is to delve deeper into current research on the utilization of plant extracts as bio-fertilizers, focusing on BPE and WRE. Additionally, investigate a green approach to synthesizing nano-fertilizers. Then, explore the effects of these organic nano-fertilizers on how they affect the development of plants in general.

2.2 Attributes that qualify a material to be classified as a fertilizer

Fertilizers are the pillars of agricultural production as they replenish essential nutrients, thereby improving crop growth, yields and soil fertility (Asadu et al., 2024). The process is initiated by the absorption of nutrients from fertilizers. These nutrients are assimilated by plant roots, which, as a result, boost the main physiological functions such as photosynthesis. In response, plants improve in growth, tolerating stress and eventually their yield is improved (Anbarasan and Ramesh, 2021; Guo et al., 2021) (Figure 2.1). Should a material contain at least one macronutrient, for example, N, P, K, and hold the capability of releasing these nutrients in a bioavailable form i.e., accessed and absorbed by plants' roots with ease, then such a material can be regarded as fertilizer (Chakraborty et al., 2022). For efficiency, fertilizers are often formulated to be absorbed in soluble form and release nutrients in this manner, which allows for efficient uptake by plants. They can be categorized into organic and inorganic types, primarily based on their origin and composition (Asadu et al., 2024).

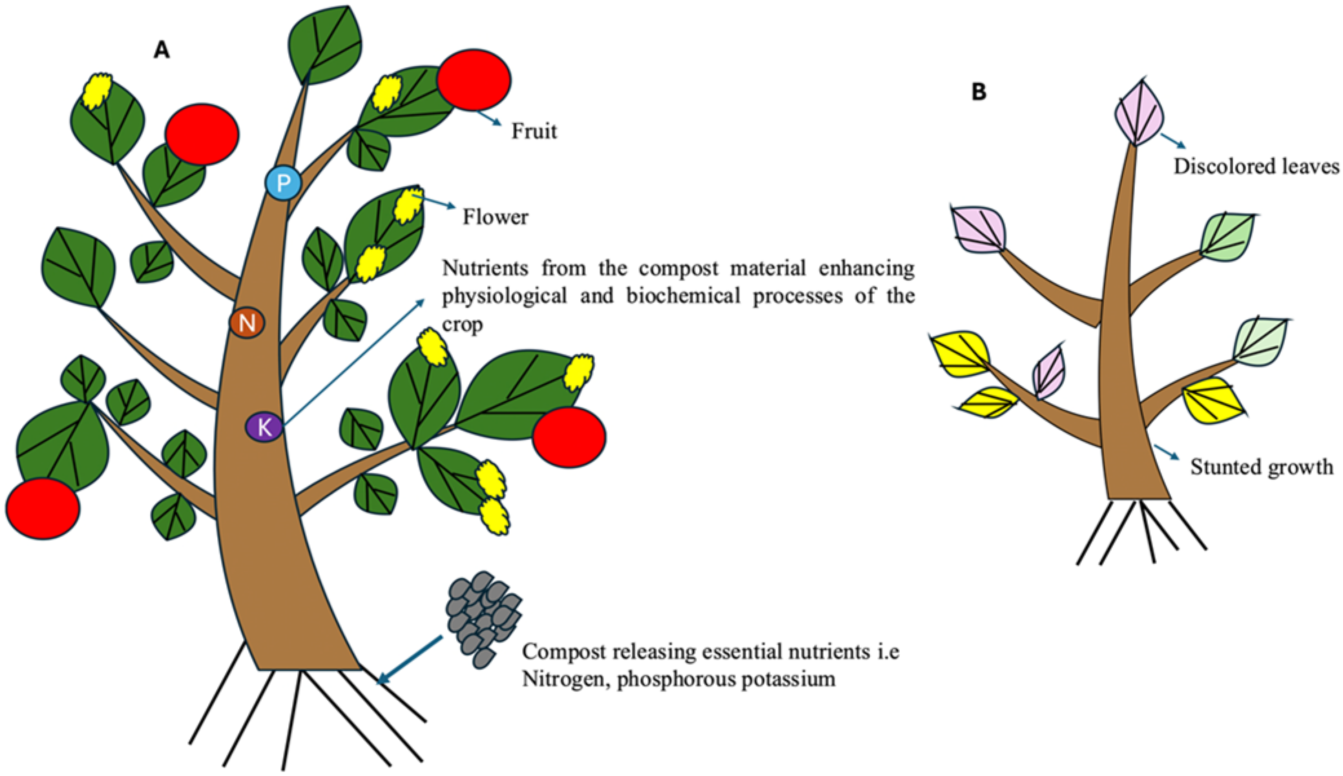

Figure 0.1:Mechanism of fertilizer application in enhancing plant growth. (A) plant receiving nutrients via compost shows healthy development of flowers and fruits. (B) Plant without nutrients shows stunted growth and discolored leaves. Source: Author's own illustration.

2.3 Organic and inorganic fertilizers

Organic fertilizers are natural substances derived from plants or animals that supply essential nutrients to plants and serve a vital function in sustainable agricultural practices through the promotion of environmental health and improving soil fertility (Khan et al., 2024). The following are examples of fertilizers: manure, bone meal, and fish emulsion (Ullah, 2023). Contrary to organic fertilizers, inorganic fertilizers are artificial and based on minerals that supply nutrients in readily available forms. This gesture buys the attention of farmers looking to improve their crop yield within a short space of time (Quddus et al., 2025). The most common inorganic fertilizer examples include, but are not limited to, potassium chloride, superphosphate, ammonium nitrate etc. (Cabrera and Solis-Perez, 2017).

Both the aforementioned fertilizer types present their own challenges, though the focus here is on the limitations imposed by organic fertilizers. For example, the hefty price to manage the nutrient budget of organic fertilizers is due to their low nutrient profile and variability in mineralization dynamics. This challenge emanates from their organic physique, which makes it difficult to predict the availability of nutrients effectively to meet the demand required by crops (Goldan et al., 2023; Lazicki et al., 2020). Manure and bone fish meal are just some examples with considerably varying nutrient content (Ahuja et al., 2020; Rayne and Aula, 2020). Careful management to ensure balanced soil fertility is thus a requirement for managing these varying nutrients (Singh et al., 2024). As mentioned earlier, their outstanding feature is their low nutrient concentration, which necessitates bulk supplementation. However, this creates challenges in terms of transportation and handling (Velthof et al., 2024).

Hence, the continued widespread use of chemical fertilizers is due to the confidence farmers have in them to achieve acceptable yields through their application (Aryal et al., 2021). Therefore, to address these limitations, nano-fertilizers are now being introduced into agricultural production, promising increased yields without compromising the environment. However, the increased use comes with empirical development of supporting data through research.

2.4 Utilization of organic materials as sources of nutrients in the synthesis of nano-fertilizers

2.4.1 The banana plant

The origin of banana crops has its descent rooting from the wet tropics of South-East Asia (SEA), before being distributed in over 130 countries (Uwimana et al., 2020) through cultivation and trade (Salas-Pascual and Cáceres-Lorenzo, 2022). Banana plant, also scientifically known as *Musa spp.* belong to the Musaceae family. These crops thrive better in wet climatic regions i.e., tropical and subtropical climates (Maseko et al., 2024).

Their large leaves, a key physical attribute, make them heavy feeders, thereby increasing the demand for a continuous supply of both primary and secondary nutrients to promote optimal production and development (Santosh et al., 2022). According to Hussain et al. (2016), the nutrients required for optimum development of banana plants are N, P and K (primary nutrients) and Mg, Ca, Mn, Fe, Zn and B (secondary nutrients).

Due to their high requirement for K (Chen et al., 2022), a substantial amount (1000-1500 kg/ha) of potassium oxide equivalent K_2O is needed for optimum growth and fruiting (Shira et al., 2013; Villaseñor-Ortiz et al., 2022).

2.4.1.1 Banana fruit and peel composition

The banana fruit represents the primary economic component of the crop and is ranked among the most valuable agricultural commodities globally, following wheat (*Triticum aestivum* L. (wheat), *Zea mays* L. (maize), and *Oryza sativa* L. (rice) (Osorio-Guarin et al., 2024). On average, a banana fruit weighs approximately 125g and consists of about 25% dry matter (DM) and 75% water content (Hikal et al., 2022).

Structurally, the fruit is composed of two main parts: pulp, which is the edible portion, and the peel, which serves as an outer protective layer (Vishala and Singh, 2021; Yasin et al., 2025). Although the pulp is primarily consumed, the peel constitutes a significant proportion of the fruit biomass and is rich in macro-and micromicronutrients, bioactive compounds, and structural carbohydrates (Ranjha et al., 2022).

These peels are continuously generated year-round due to the continuous availability of the banana fruit (de Angelis-Pereira et al., 2016). These peels tend to become a major waste problem for households and fruit markets, leading to increased daily waste. The abundance of waste then produces gases via the process of anaerobic respiration, creating an unpleasant odour and disturbing the natural air balance (Kumari et al., 2023). As a result, various industries, including agriculture, beverages, paper manufacturing, cosmetics, food processing, bio-absorbents, energy resources, biofuel production, medicine, and textiles (Table 2.1), have ventured into the use of fruit peels for different applications (Castillo et al., 2023).

Table 0.1: The different applications of fruit peels across various industries

Industry	**Fruit Peels**	**Uses**	**Reference**
Agriculture	Banana, sweet lime and papaya peels	Used as bio-fertilizer	(Devi et al., 2023)
Cosmetics	Banana and pomegranate peels	Used in skin care for their antioxidant and antibacterial properties for skin care.	(Khang et al., 2021)
Food processing	Banana, apples, pineapple and pomegranate peels	Used for extending food shelf-life due to their antioxidant properties.	(Rather et al., 2023)
Bio-absorbents	Banana, orange and pomegranate peels	Used as bio-absorbents for absorbing pollutants from wastewater.	(Ngole-Jeme and Ntumba, 2024)
Bio-fuel production	Orange and banana peels.	They can be converted into bioethanol and biodiesel through fermentation and transesterification.	(Hamzah et al., 2019)

Medicines	Citrus peels and banana peels	Are used for their bioactive compounds to treat cough, digestive problems, infection, muscle pain and skin inflammation.	(Hussain et al., 2022)
Textiles	Banana and orange peels	Are used for creating sustainable and biodegradable fabric	(Redko, 2017)

2.4.1.2 Banana peel nutritional value

The banana peel is rich in essential nutrients (Khanyile et al., 2024) necessary for the development of NFs. Tsado et al. (2021) discovered that sodium (Na) is the most abundant element in banana peels, with a concentration of 58.16±2.73 mg/100g, followed by magnesium; 49.32 ±0.74 mg/100g; potassium; 38.22 ±0.16 mg/100g; phosphorous; 22.64 ±0.38 mg/100g; calcium; 17.85 ±0.25 mg/100g; zinc; 11.60 ±0.03 mg/100g; manganese; 10.38 ±0.04 mg/100g; iron and copper were found to be the least element, containing 5.06 ±0.07 mg/100g and 1.35 ±0.05 mg/100g, respectively.

Siahaan et al. (2023) also observed that BPs can be used as liquid organic fertilizer (LOF), and this is due to their high N content (4.070%), which meets the LOF's N content standard (3-6%). Based on this approach, the LOF synthesized from banana peels has the potential to serve as an alternative to potassium chloride (KCl) fertilizer as a K source (Hariyono et al., 2021), and this is also confirmed by Islam et al. (2019) through banana peel biochar (BPB). The application of banana peels has demonstrated positive results as a sustainable amendment of the soil, but studies have indicated that combining them with other organic materials offers synergistic benefits (Nurseha et al., 2023).

An eco-friendly compost was developed by Fernando and Weerasinghe (2023) by combining papaya peels, eggshells, banana peels, and onion peels in equal proportions. To ascertain the efficiency of the compost, it was tested on the growth performance of *Capsicum annuum* L. (bell pepper) seedlings. The findings indicated that the high K content from banana peels and the high Ca content from eggshells increased the seedling performance of *C. annuum* L. This confirmed that banana peels, combined with eggshells and other organic materials, make them a better soil amendment and contribute significantly to crop productivity, as found by Ma'mor et al. (2023). Their study combined banana, orange, and papaya peels with eggshells, resulting in improved maize growth performance. The key point from the aforementioned is that banana peels and eggshells, combined with other organic materials, can be a feasible, sustainable approach to enhance the productivity of agriculture.

The biochemical constituents contained bring forth an abundance of phytochemical compounds. These include flavonoids (tannins), carotenoids, alkaloids, biogenic amines, quinones, polyphenols, saponins, phytosterols, phenols, and monoterpenes (John Isa, 2024; Sheidu et al., 2021). Plant phenolic compounds offer several benefits for plant development as they are used as functional polymers, ultraviolet protectors (flavonoids), antioxidants, attractants (carotenoids and flavonoids), phytoalexins, protection chemicals, and flash signals (salicylic acid) (Chowdary et al., 2022; Lin et al., 2016). Apart from that, these compounds also serve as regulators of plant growth, allelopathic compounds, and plant defense mechanisms (Ali et al., 2024; Cheng et al., 2024). Various investigations have unraveled those bioactive compounds, including saponins, terpenoids, flavonoids, anthocyanins, lycopene, phenolics, tannins, and alkaloids, which have antimicrobial activities (Al-Hajj, 2021). Owing to their phenolic content, banana peel extracts scavenge and neutralize free radicals in plants (Nasir et al., 2020). These free radicals, like the reactive oxygen species (ROS), induce dire consequences on plants as they disrupt their cellular homeostasis and initiate oxidative stress (Rai and Kaushik, 2023), resulting in damaged Deoxyribonucleic Acid (DNA), proteins, and cell membranes (Sachdev et al., 2023). Therefore, the vitality of using banana peels in producing fertilizers should not be undermined since they exhibit properties that improve the growth performance of plants.

2.4.2 The watermelon plant

Watermelon *(Citrullus lanatus)* belongs to the Cucurbitaceae family (Devi et al., 2020) and it is native to Africa, where it has been cultivated for centuries (Paris, 2015). The watermelon is characterized as a large, sprawling annual plant with coarse, hairy, pinnately lobed leaves and yellow flowers. However, the watermelon fruit is featured with a smooth, thick, deep green exterior rind with vertical stripes that can be either light green or grey (Tomar, 2018). The plants are grown for their edible fruit, which is eaten fresh or utilized in different culinary dishes (Nadeem et al., 2022; Olalekan et al., 2025). Dry and warm climatic environments are the most preferred to grow watermelons effectively as they are not frost-tolerant (Burdulis et al., 2025; Ali et al., 2017). The suitable temperature range to grow productive watermelon plants is from 18-35 °C (Jang et al., 2022). Warm temperatures during the ripening stage encourage superior-quality fruit. Chemical fertilizers, especially N, play a significant role in enhancing their yield and maintaining quality (da Silva et al., 2020).

The physical appearance of a ripe watermelon features a green outer rind and red flesh where the rind is situated. The rind itself is light green in color and has a plethora of bioactive compounds, minerals, and phytochemicals (Kataria and Kaur, 2023). The fruit is composed of a low-energy fruit matrix packed with a high nutrient capacity, including vitamins A, C, B_1, B_6; potassium; magnesium; dietary fiber, antioxidants such as lycopene and has a high-water volume (Manivannan et al., 2020; Nissar et al., 2025). Taken as a whole, all these constituents play a huge role in various functions such as hydration, cardiometabolic regulation, gastrointestinal function, exercise recovery, and cutaneous antioxidant protection (Bailey et al., 2016; Gu et al., 2023; Volino-Souza et al., 2022). Nonetheless, despite all these benefits, the use of WRE remains limited due to a lack of awareness and an underrated perspective.

Generally, one-third of the fruit is the watermelon rind (WR), yet it is discarded because of its unappealing flavor. This is why a broad view of WRE is largely confined to a single frame of reference, yet so many benefits can be realized by valorizing watermelon rinds (WRs) across different industries. In a bid to leverage the often-overlooked benefits of fruit rinds, varying industries are already applying them in different ways. These industries include food, cosmetics, and pharmaceutical industries, as well as industrial applications in biofuel production and eco-friendly packaging. The versatile nature of the watermelon rind presents itself as an exciting research area that may encourage researchers to uncover new applications and improve the existing ones (Dubey et al., 2021; Manikishore et al., 2025; Zia et al., 2024).

2.4.2.1 Chemical composition of watermelon rinds

Previous studies have shown that the watermelon rinds contain essential nutrients required for optimum plant development (Zia et al., 2021). Table 2.2 lists nine minerals identified in the watermelon rind powder by Gladvin et al. (2017) and Egbuonu (2015), excluding the quantity of minerals present in the rinds.

Table 0.2: The watermelon rind powder mineral profile

No.	Mineral	Content (mg/100g)	
		(Gladvin et al., 2017)	(Egbuonu, 2015).
1	Phosphorus	129.70	135.24
2	Magnesium	30.40	1.48
3	Calcium	28.00	29.15
4	Potassium	21.70	1.37
5	Sodium	11.40	12.65
6	Iron	4.63	1.29
7	Manganese	1.30	1.48
8	Zinc	1.25	1.29
9	Copper	0.40	0.45

Both studies converge on a high phosphorus (P) content and the least amounts of zinc (Zn) and copper (Cu). This may be attributed to their similar methods of extraction and material analysis. Nonetheless, the nutrient content of the WR presented in Table 2.2 varied between the two authors and this might be ascribed to cultivar and variety. This observation is supported by Gladvin et al. (2017) and Ashoka et al. (2022), who reported that different watermelon cultivars have varying mineral compositions. Moreover, independent authors have also unraveled many other factors contributing to this such as soil, pH and nutrient availability. For example, watermelon fruits cultivated on soil rich in nutrients will have different minerals (Romelle et al., 2016). The same author highlighted that agricultural practices such as fertilizer, pesticide use, and irrigation methods can also alter the mineral composition of fruit peels. Other factors are environmental, such as climate conditions like humidity, temperature and rainfall during earlier stages of development, which can also influence crop nutrient uptake of minerals. This, in turn, leads to variations in nutrient composition of agri-waste (Czech et al., 2020).

According to Mo et al. (2016), the watermelon N content in the rinds makes them suitable sources of N, allowing them to serve as N precursors in the production of N-doped activated carbon. Studies conducted previously have reported that WRs contain an amino acid known as citrulline (Joshi et al., 2019; Volino-Souza et al., 2023), which contains three nitrogen atoms in its chemical structure as shown in Figure 2.2. As a result, the presence of citrulline in watermelon rinds indicates the presence of N.

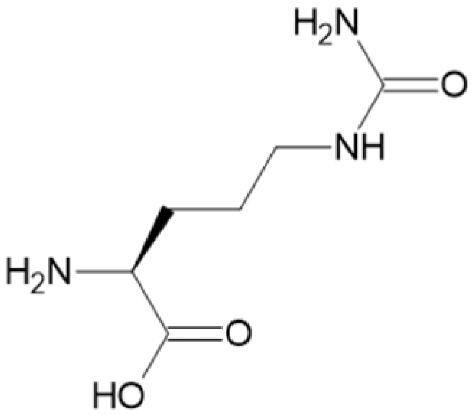

Figure 0.2: Citrulline chemical structure.

Phytochemical compounds present in WRs contribute to plant defense mechanisms and reproductive development by promoting pigment synthesis in flowers and fruits (Manivannan et al., 2020). Erugo et al. (2022) produced a bio-fertilizer using WRs through fermentation. The study focused on determining the ideal conditions for biofertilizer production. It was found that fermenting WRs for 20 days with 400 mL of water gave optimal results, with high levels of N (26.2824%), P (94.5099%), and K (0.0005%) observed. Another study also utilized WRs with other agricultural waste materials to produce a bio-fertilizer in combination with cow dung through anaerobic digestion (Hassan and Abdulsalam, 2017). Prior to digestion, the N content in the substrates was calibrated at 14 mg/L, while the P content expressed as phosphorous pentoxide equivalent (P_2O_5) and K content expressed as potassium oxide equivalent (K_2O) were at 2.75 mg/L and 2.6 mg/L, respectively. Post digestion, a significant increase in nutrient composition was observed, confirmed by a rise in N content to 25 mg/L, representing a 78.57% increase. Likewise, P content increased to 5.2 mg/L, demonstrating a significant increase of 89.09%. In addition, K content increased to 4.8 mg/L, marking an increase of 84.62%.

Mahmud et al. (2019) converted solid waste, including the following materials: paper, banana peel, watermelon rind, pineapple peel, and orange peel, and mixed them all into bio-fertilizer through vermicomposting. Amongst these compositions, the mixture exhibited the highest level of nutrients, resulting in N, P and K concentrations of 17.2%, 10.24%, and 48.32%, respectively.

The studies of Mahmud et al. (2019) and Hassan and Abdulsalam (2017) further underscores the incorporation of WRs with other solid waste materials, as it improves the composition of nutrients in the fertilizer. Therefore, their studies form a suitable coalition with the above findings from other esteemed sources in the production of organically backed fertilizer from plant extracts.

2.5 The coalition of studies for banana peels and watermelon rinds and the unfilled research gap

The studies on both BPs and WRs give us a huge insight into the production of organic fertilizers using BPE and WRE with different organic materials because of the high nutrient elements that emerge alongside the discovery of phytochemicals, fibers, minerals and vitamins. Various methods of producing these peel-backed organic fertilizers also vary considerably, including converting them into liquid fertilizer (Siahaan et al., 2023), turning them into powder, and fermenting them (Mahmud et al., 2019; Egbuonu, 2015). While previous studies provide substantial evidence supporting the use of BPs and watermelon rinds (WRs) in organic fertilizer development, limited research has explored their combined application at the nanoscale. Previous studies seem mainly focused on using these peels for their nutrient content and biochemical constituents in a traditional sense, rather than on improving their novelty. As a result, the literature on converting agricultural waste into nanoscale particles using only organic materials, without adding chemical fertilizers, is scant and insufficient. Hence, the proposed nanoscale approach.

2.6 Nano-fertilizers

As discussed earlier in the introduction to this chapter, particularly pertaining to the third paragraph, the distinct characteristics of nano-fertilizer set them apart from their conventional counterparts. Their minute nanoscale dimension permits distinct physicochemical properties, notably enhancing their functionality (Avila-Quezada et al., 2022). Evidence from multiple studies indicates that nano-fertilizers can significantly enhance crop performance, suggesting their promising application in sustainable agricultural systems (Abdel et al., 2018; Latef et al., 2018; Midde et al., 2024; Nazir et al., 2024). As such, various nano-fertilizer types have been investigated in three-fold: for their capability to improve nutrient uptake by plants, increase yields, and enhance overall crop quality.

The study by Latef et al. (2018) investigated the potential of titanium oxide nanoparticles (TiO_2 NPs) to counteract the adverse effects of soil salinity on the growth of *Vicia faba* L. (broad bean) during the vegetative stage. Three concentrations (0.01%, 0.02%, and 0.03%) were evaluated based on plant growth and stress responses. The findings indicated that 0.01% TiO_2 NPs improved leaf area, shoot length, root dry weight, soluble sugars, chlorophyll, proline, and antioxidant enzyme activities under both normal and saline conditions. The study further revealed that the positive effects were concentration-dependent, with 0.01% being most effective, while higher concentrations were either ineffective or reduced effectiveness, possibly due to agglomeration or genotoxic effects. These results highlight the potential of TiO_2 NPs as a stress-ameliorative agent in improving crop resilience under saline conditions.

Midde et al. (2022) evaluated the impact of nano urea on growth and yield parameters of *Oryza sativa* L. (rice), focusing on enhancing nitrogen use-efficiency (NUE) and reducing fertilizer consumption. Treatments included recommended nitrogen doses (RDN), conventional urea, and nano urea, as well as combinations such as 50% RDN + 50% nano urea. Growth parameters measured included plant height, number of trillers, leaf area index (LAI), and dry matter production. The combination of 50% RND +50% nano urea displayed the highest dry matter production and improved LAI, with significant effects on grain yield and related yield components. The study concluded that partial substitution of conventional urea with nano urea improves growth and yield while reducing fertilizer input costs.

Nazir et al. (2024) investigated the effects of phyto-generated zinc oxide (ZnO) NPs on the growth and yield of *Triticum aestivum* L. (wheat) and Zn biofortification. Different Zn concentrations (0, 25, 50, 100, 200 mg/L) were compared to Zn acetate at 100 mg/L. The findings showed that zinc nanoparticles improved wheat growth, particularly plant height, leaf number and area, with the most observed increase recorded at 25 mg/L (23% improvement compared with the control). Significant increases in biochemical parameters such as carotenoids, carbohydrates, chlorophyll, protein content, and antioxidant enzyme activity were also reported. These findings underpin the potential of nanoparticles in enhancing crop growth and stress tolerance.

In summary, Abdel et al. (2018), demonstrated that the positive effects of managing crop stress TiO_2 NPs are dependent on the precise lower (0.01%) concentration of these particles. Any increase above this level is likely to have no effect or be reduced due to agglomeration or genotoxic effects. Midde et al. (2022) also employed the same “nano particle precise approach”, emphasizing that the growth and yield of rice crops in terms of producing the highest grain and straw is dependent upon 50% RDN combined with 50% nano Urea, thereby eliminating the need for conventional urea. In addition, Nazir et al. (2024) also emphasized a precise concentration of ZnO NPs at 25 mg/L to observe better Triticum aestivum L.(wheat) crop performance in terms of height, biochemical constituents, and antioxidant enzymes.

Table 0.3: Summaries of studies on the impact of different types of nano-fertilizers on crop performance

Type of nano-fertilizers	Crop	Observed benefits	Reference
TiO_2 NPs	*Vicia faba* L. (broad bean)	• Enhanced plant growth • Increased soluble sugars and mino cids • Osmo protection under saline conditions • Enhanced antioxidant activities	(Abdel Latef et al., 2018)
ZnO nano-fertilizer	*Triticum aestivum* L. (wheat)	• Enhnaced growth and yield • Morpho-anatomical changes • Biochemical enhancements	(Nazir et al., 2024)

MARDI nano-Fertilizer	*Cucumis melo* L. (rockmelon)	• Improved growth metrics • Optimal development and quality of rock melon • Increased photosynthetic pigments	(Fadzil et al., 2024)
Copper nano-fertilizer	*Mentha* × *piperita* L. (peppermint)	• Increased the number of branches and leaves, total leaf area of peppermint plants • Increased production of menthone and Menthol	(Alkhlefawi, 2022)
Nano- urea	*Oryza sativa* L. (rice)	• Enhanced growth attributes • Increased yield • Early flowering	(Midde et al., 2022)
Nano-Potassium Fertilizer	*Glycine max* (L.) Merr. (soybeans)	• Potassium nano-fertilizer significantly affected soybean protein and oil percentages	(Rostami Ajirloo and Amiri, 2022)

		• Improved plant height, the number of leaves, and the number of lateral branches • The highest yield of 3.17 tons per hectare was achieved • Potassium nano-fertilizer decreased the adverse effects of drought stress by about 25% • Increased water use efficiency (WUE)	
Nano-phosphorous	*Triticum aestivum* L. (wheat)	• Improved Nutrient Use Efficiency (NUE) • The application of nano-P fertilizers has been shown to improve growth, yield, and yield-attributing properties of wheat	(Poudel et al., 2023)

In reference to the studies summarized in Table 2.3, the role of nano-fertilizers in improving the performance of plants has been illustrated. The research points out the advantages of different kinds of nano-fertilizers for various crops. As previously discussed, the unique properties of nano-fertilizers are a major contributor to their exceptional performance. In the most vital sense, these properties are closely linked to the synthesis method employed. The synthesis of nano-fertilizers can be done using several approaches and these can be chemical, physical, and green synthesis methods (Banjara et al., 2024). Each method provides unique properties, which influence the emerging nano-fertilizer. This difference underpins the necessity for researchers to take extra precautions in their synthesis methods as the choices made directly impact the characteristics of nano-fertilizer and, consequently, their efficiency in agricultural applications (Afroz et al., 2021). For the purpose of this study, only the green synthesis method will be discussed.

There has been a growing interest in green synthesis as a viable approach to fabricating nano-fertilizers. This method not only promotes environmental sustainability, but also offers unique benefits in terms of the properties of the resulting nanoparticles (Channab et al., 2024; Zafar et al., 2024). Understanding how green synthesis influences these properties is crucial, as it allows researchers to tailor nano-fertilizers to meet specific agricultural needs (Faizan et al., 2024). As such, delving deeper into the impacts of green synthesis on the characteristics and subsequent performance of nano-fertilizers is a pivotal area of exploration that aligns with current research trends in sustainable agriculture. This focus on green synthesis will enable advancements in the development of effective and eco-friendly nano-fertilizers that can significantly contribute to enhancing crop productivity (Wahab et al., 2024).

2.7 Green synthesis of nano-fertilizers

Green synthesis correlates to sustainable methods with the aim of satisfying contemporary necessities while protecting the capacity of generations to come, so they can meet their own (Hariram et al., 2023). The approach puts emphasis on the use of renewable and sustainable sources, including plant extracts, microbes, and agricultural waste, for synthesis, as these resources are readily available and do not deplete limited reserves (Aswathi et al., 2023). Plant extracts used in synthesizing nano-fertilizers through the application of green synthesis constitute the following: stems, fruit peels, roots, leaves, bark, seeds and flowers (Saifuddin et al., 2024). These plant extracts function as natural stabilizing and reducing agents and assist in outmaneuvering chemical reducing and stabilizing agents (Singh et al., 2023). Apart from that, microbes like algae, fungi, bacteria and yeasts can also be incorporated into green synthesis (Bahrulolum et al., 2021). The principles of green nano-fertilizers are summarized in Figure 2.3.

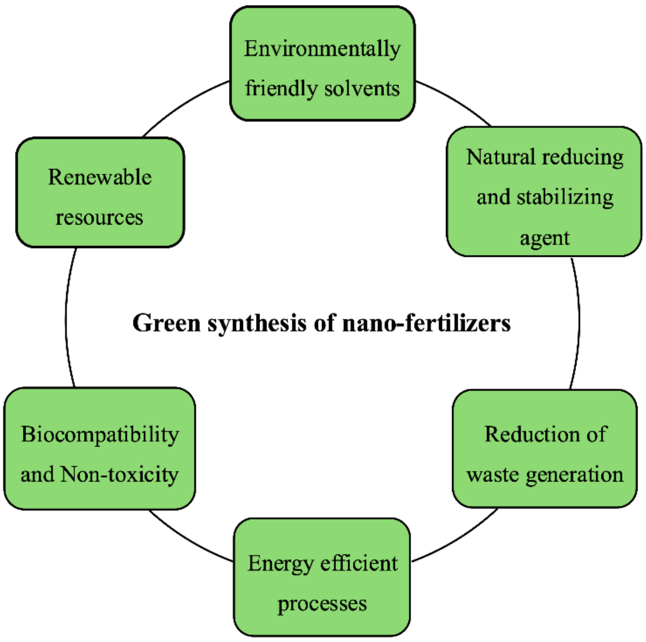

Figure 0.3: The key principles of green synthesis approach of synthesizing nano-fertilizers

2.7.1 Plant extracts in the synthesis of nano-fertilizers

Plant extracts contain bioactive compounds in abundance, and these are the secondary metabolites that are tailored for various applications such as functional and therapeutic properties (Twaij and Hasan, 2022). The reported plant extracts by various researchers include, but are not limited to the following: flavonoids, alkaloids, phenolic acids, polysaccharides (sugars), quinines, tannins, ascorbic acid, terpenoids and saponins (Riaz et al., 2023; Sun and Shahrajabian, 2023). Owing to their bioactive compounds, plant extracts are involved in oxidation reactions to reduce metal ions from a higher oxidation state to a lower neutral state (El Shafey, 2020). In general, nanoparticles are highly reactive and need to be functionalized to maintain stability and halt or prevent undesirable changes such as oxidation or agglomeration. This is due to their large surface area to volume ratio, making them susceptible to being volatile to surrounding molecules, including other nanoparticles (Xu et al., 2018). However, plant extracts also function as capping and stabilizing agents to prevent agglomeration of nanoparticles. Figure 2.4 mimics a simplified bio-reduction process of metallic elements using *Aloe vera gel* extract as the reducing and capping agent (Ahmad et al., 2024).

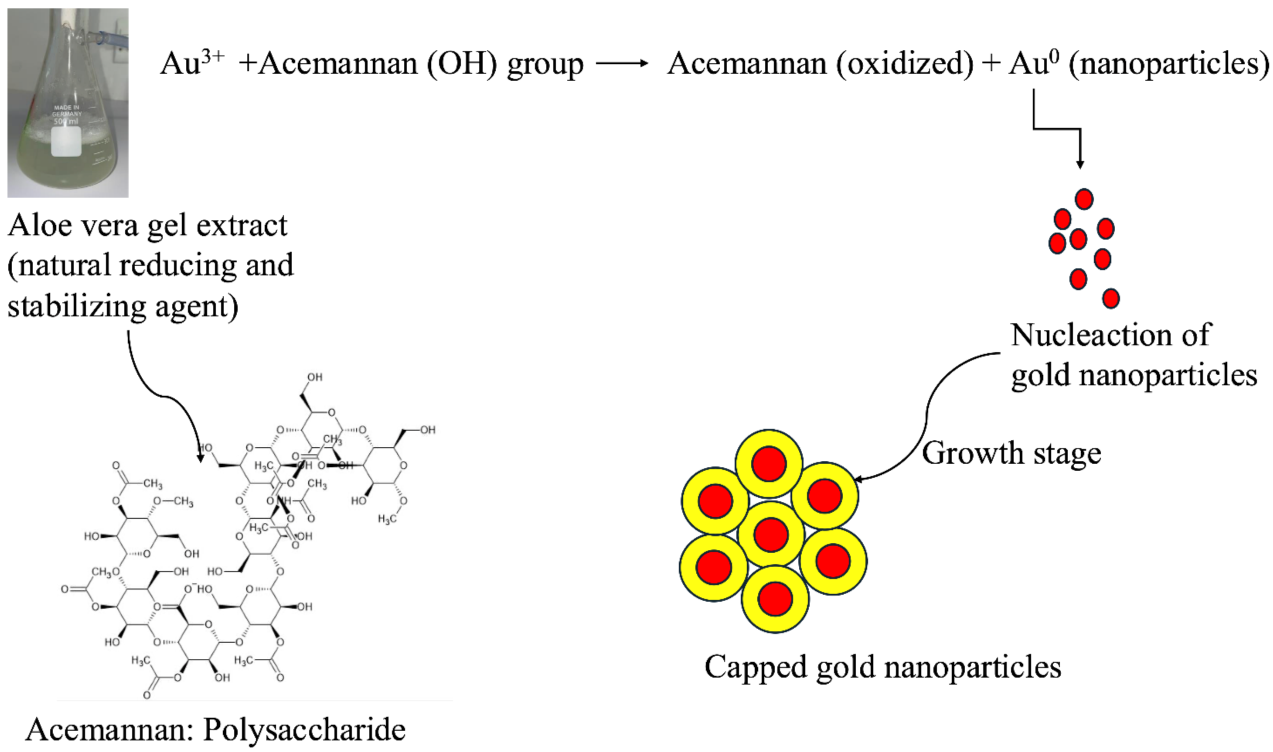

Figure 0.4: The bio-reduction of gold nanoparticles using *Aloe vera* gel extract as a reducing and stabilizing agent. Authors own'

2.7.2 The effect of concentration of the plant extracts used in synthesizing nanoparticles

The concentration of plant extracts has a vital role in nanoparticle synthesis as it influences their shape, size and overall properties. Various studies have employed different concentrations of plant extracts as reducing and stabilizing agents for the synthesis of inorganic nanoparticles. The example by Ahemed et al. (2023) synthesized TiO_2 NPs using *Aloe vera* gel extract as a reducing and capping agent. Three concentrations (10, 20, and 30 mL) were employed. The results showed inhibition zone sizes of 20.8 mm, 19 mm, and 17.2 mm, respectively. Structural properties were confirmed using X-ray diffraction (XRD), Fourier transform infrared spectroscopy (FTIR), and Raman spectroscopy. The study demonstrated that increasing the concentration of *Aloe vera* gel extract reduced TiO_2 crystal size, indicating an indirect proportional relationship between extract concentration and nanoparticle size.

These findings correlate with those of Villagrán et al. (2024) as they also discovered that the concentration of the reducing agent, particularly referring to orange peel extracts, alters the properties of ZnO NPs to a great degree. Their study further revealed that adding 50 mL of orange peel extract to 100 mL of zinc nitrate dihydrate solution resulted in the quick synthesis of nanoparticles composed of uniform sizes, a narrower optical band gap, and increased surface energy. Contrary to the aforementioned, lower concentrations (25 mL and 35mL) resulted in slower formation. Meanwhile, 1:1 v/v (orange peel extract: zinc nitrate dihydrate solution) yielded non-uniform nanoparticles. This, therefore, emphasizes the importance of optimizing the concentration of plant extracts in tailoring nanoparticle characteristics.

Table 0.4: The effect of concentration of plant extracts in the synthesis of nanoparticles

Type of nanoparticles	Plant extract	Plant extract amount: metal salt solution (ml)	Nanoparticle size (nm)	Nanoparticle shape	Reference
Ag NPs	*Aloe vera* gel extract	5 mL: 45mL (1:9)	25.26 nm	Spherical	(Ibrahim et al., 2020)
Ag NPs	*Aloe vera* gel extract	10 mL: 40 mL (1:4)	66.6 nm	Spherical	(Sohal et al., 2019)
Ag NPs	*Hibiscus sabdariffa* L. (roselle) leaves extract	26 mL:100 mL (13:50)	25 nm	Spherical-shaped	(Khan et al., 2024)
Ag NPs	*Lysiloma acapulcense (* Tepehuaje*)* stem and roots extracts	2.5ml: 2.5 ml (1:1)	5 nm	Spherical and quasi-spherical nanoparticles	(Garibo et al., 2020)
Ag NPs	*Aloe vera* gel extract	20 mL: 5 mL (4:1)	12-40 nm	Spherical shaped	

Au NPs			15 nm		(Kamala Nalini and Vijayaraghavan ,2020)
Ag NPs	*Lawsonia inermis* L. (henna) leaves extract	10 mL:50 mL (1:5)	3.48- 19.34 nm	Spherical shaped	(Said et al., 2024)
ZnO NPs	Scallion's onion peel extract	50 mL	Spherical=40-100 nm Rod shaped= above 200 nm	Spherical and rod-shaped particles	(Soltani et al., 2023)
ZnO NPs	*Punica granatum* L. (pomegranate) peel extract	95 mL:5 mL (19:1)	118.6 nm	hexagonal crystalline shape	(Abdelmigid et al., 2022a)
ZnO NPs	Neem leaf extracts	20 mL:100 mL (1:5)	25.26 nm	Hexagonal	

CuO NPs		20 mL:80 mL (1:4)	18.42 nm	Monoclinic	(Yadeta Gemachu and Lealem Birhanu, 2024)
NiO NPs		20 mL:100 mL (1:5)	10.50 nm	Cubic	
TiO_2 NPs	*Aloe vera* gel extract	10 mL:100 mL (1:10)	20.8 nm	Irregular shape	(Ahmed et al., 2023
		20 mL:100 mL (1:5)	19 nm		
		30 mL:100 mL (3:10)	17.2 nm		
CuO NPs	Watermelon seed shell extract	25 mL:5 mL (1:2)	50–100 nm	Irregular spherical shaped	(Ekinci et al., 2023)
MnO NPs			20–50 nm	Spherical agglomerates	
CuO NPs	*Aloe vera* gel extract	100 mL:100 mL (1:1)	272 nm	Spherical shaped	(Khanna et al., 2024)

$FeCl_2$ NPs	Spinach leaf extract	20 mL:40 mL (1:2)	10-70 nm	-	(Tyagi et al., 2021)
	Banana peel extract		20-50 nm		
Ruthenium (Ru NPs)	*Aloe vera* gel extract	100 mL: 100 mL (1:1)	1.57 nm	Hexagonal	(Begum et al., 2025)

As shown in Table 2.4, *Aloe vera* gel, as a plant extract, influences nanoparticle production at varying ratios of plant extract to metal solution. Smaller sizes of AgNPs (from 12-40 nm) were achieved at a ratio of 4:1, whilst larger sizes (66 nm) were achieved at a ratio of 1:4. This suggests that increasing the plant extract concentration, in relation to the metal salt, typically reduces the nanoparticle size. This phenomenon is still observed from other plant extracts such as *Lawsonia inermis* L. (henna) and *Punica granatum* L. (pomegranate) peel, which shows small NPs at 3.48–19.34 nm at 1:5 ratio. *Hibiscus sabdariffa* L. (roselle) plant extract also produced small-sized NPs at 25 nm at a ratio of 13:50. Moreover, the spherical shapes seem to dominate most of the plant extracts used, especially those Ag-NPs synthesized using various plant extracts. Despite this, specific nanoparticle shapes such as hexagonal (from ZnO NPs, Neem leaves extract) or monoclinic (from CuO NPs) result from specific plant extracts or types of nanoparticles. Thus, suggesting that the morphology of nanoparticles is influenced by both the extract and the nanoparticle type.

Since the nanoparticles were synthesized using different plant extracts, they yielded different results. From the data in Table 2.4, AgNPs typically range from 3.48 nm to 66.6 nm, depending on the plant extract used and the conditions of the synthesis. A larger range is exhibited by ZnO NPs (from 40 nm to above 200 nm), which reflects the potential for different morphologies and crystal shapes, for example, hexagonal, crystalline or rod-shaped particles. Copper oxide (CuO) and TiO_2 tend to remain under 100 nm when synthesized with *Aloe vera* gel, watermelon seed shell extract, indicating their efficiency in terms of nanoparticle size reduction.

A direct proportional trend is observed in the ratio of plant extract to metal salt solution, for example, 1:1 or 1:5 ratios. From these ratios, it can be concluded that lower ratios of plant extract to metal salt solution often yield smaller NPs and the same is true for higher ratios (e.g., at 19:1). This trend demonstrates a critical role of concentration in the control of nanoparticle size during synthesis.

Aloe vera gel extract seems to be capable of producing smaller nanoparticles compared to all the other plant extracts and this includes Ag NPs, CuO NPs, TiO_2 NPs and Ru NPs. Both *Aloe vera* gel and *Lawsonia inermis* L.(henna) consistently produce smaller nanoparticles across various studies, indicating their strong reducing and capping abilities. Larger-sized nanoparticles are obtained from onion peel and *Punica granatum* L. (pomegranate) extracts, indicating differences in bioactive compounds required for nanoparticle synthesis.

Zinc oxide nanoparticles produced from onion peel extract exhibited dual shapes (spherical and rod-shaped) depending on particle size. On the other hand, RuNPs combined with *Aloe vera* gel extract resulted in the smallest nanoparticle size of 1.57 nm. Higher extract concentration in relation to the metal salt solution generally yields smaller nanoparticles. Most plant extracts tend to produce spherical shapes, even though exceptions of other shapes exist, such as hexagonal and rod shapes, based on the plant type or metal. Among the plant extracts used, *Aloe vera* seems to be highly versatile and efficient in the synthesis of nanoparticles across various metals with controlled size and shape.

2.8 Properties of nano-fertilizers

Nanoparticle penetration into plant tissues must be ensured, as it allows them to be available to plants for their metabolic processes (Sembada and Lenggoro, 2024). The process is governed by several pathways and mechanisms that influence the routes of entry for nanoparticles, not the system of plants, which determines the required size (Khan et al., 2022). One of these routes of entry is foliar entry, where nanoparticles enter the plant via the stomata or cuticular pores

(Avellan et al., 2021). In the quest for entrance, smaller-sized nanoparticles prove to be the most successful as they can pass through the cell wall and enter the membrane (Zhao and Stenzel, 2018). On the other hand, larger nanoparticles have been found to accumulate outside the cell wall (Banerjee et al., 2019). Nanoparticle routes of entry are not the only dictating factor to nanoparticle assimilation to plant tissues, but the plant species also play a role as they have varying cell wall pores, owing to their morphology. Factoring this nanoparticle property will ensure that nano-fertilizers with particle sizes smaller than the cell walls and membrane of targeted plants are developed efficiently for their absorption (Madlala et al., 2024).

2.9 Effect of concentration on nano-fertilizer performance

Even though the properties and size of nano-fertilizers are critical factors, the concentration at which these fertilizers are applied is vital for them to function effectively. Maximized nutrient uptake, promotion of healthy growth and improved crop yield can be realized at the right concentration of nano-fertilizers to avoid stress and toxicity, ensuring that the plants utilize resources effectively. Studies have reported that varying concentrations of nanoparticles affect the performance of plants. For example, a study conducted by Mustafa et al. (2021) examined the toxicological and beneficial effects of plant-based TiO_2 NPs when plants are exposed to saline stress. TiO_2 NPs were synthesized using *Buddleja asiatica* L. (asian butterfly bush)leaf extract and characterized them via the application of various technologies. The technologies included UV-visible spectroscopy, SEM, FTIR, and EDX.

On another note, two wheat varieties, Faisalabad-08 (salinity-tolerant) and NARC-11 (salinity-susceptible), were treated with varying concentrations of sodium chloride (NaCl) at 100 nm and 150 nm, respectively, with TiO_2 NPs of different concentrations at 20, 40, 60, and 80 mg/L.

The study found that TiO_2 NPs at 40 mg/L significantly improved plant height, fresh and dry weight, shoot and root length, and chlorophyll content under saline stress. Yet, higher concentrations displayed a decrease in these positive effects, highlighting potential toxicity. Therefore, the results suggest that plant-based TiO_2 NPs can improve the growth and physiological characteristics of wheat under saline stress, presenting a promising antidote for enhancing crop defense via the application of nanotechnology.

Özgören Can et al. (2024) independently investigated the synthesis of iron oxide nanoparticles (Fe_3O_4 NPs), ZnO NPs, and TiO_2 NPs using bay leaf extracts. The nanoparticles synthesized were examined as biofertilizers on sunflower plants at 5 ppm and 20 ppm. Whereby the lower concentration greatly improved the root length, fresh weight, leaf surface area and chlorophyll. Meanwhile, those at 20 ppm resulted in reduced growth parameters. The findings extend as far as pointing to the influence of nano-fertilizer on crop performance.

A study by Singh et al. (2024) evaluated biologically synthesized iron oxide (Fe_3O_4) NPs using *Emblica officinalis* L. (indian gooseberry) fruit extract on the growth and metabolic activity of *Solanum lycopersicum* L. (tomato)seedlings. Concentrations of 10, 50, and 100 mg/L were compared with ferrous sulfate ($FeSO_4$) under greenhouse conditions. The results showed that 10 mg/L Fe_3O_4 NPs significantly improved germination rate, root and shoot length, chlorophyll content, and nitrate reductase activity compared to the control and $FeSO_4$ treatments. However, higher concentrations (100 mg/L) inhibited growth parameters and increased oxidative stress. The study indicates that Fe_3O_4 NPs act as effective nano-fertilizers at optimal concentrations.

All three studies are in coalition with one another as they synthesized various NPs using different plant extracts on various crops, but all emphasize that for significantly enhanced plant growth, nanoparticles in the nano-fertilizer must be maintained at lower concentrations. However, the study by Gosavi et al. (2020) evaluated the effects of various concentrations of Ag NPs of 5 mL, 10 mL, and 15 mL on crop growth. The findings of their study showed that lower concentrations (5 mL) reduced plant vigor and fresh weight in relation to higher concentrations (10 mL and 15 mL). Of the three studies discussed above, which are in agreement with one another, the findings of Gosavi et al. (2020) offer a different viewpoint as lower concentrations of silver nanoparticles reduced crop growth attributes. Emphasizing that different plants and their growth stages have varying nutrient requirements. This has a major influence on the ideal concentration of nano-fertilizers (Arora et al., 2024), soil properties (Reddy et al., 2024), the properties of nanoparticles (Fathy et al., 2024) and the application method (Iqbal et al., 2019).

2.10 The tomato (*Solanum lycopersicum* L.) plant

The tomato crop, scientifically known as *Solanum lycopersicum* L. is a widely cultivated fruit crop due to its versatile use in the culinary, nutritional industry, and economic value (Knapp and Peralta, 2016). Originally from the South American continent, its cultivation has spread to other regions of the world, particularly in subtropical and tropical regions. As a major nutrient and vitamin source, especially potassium, vitamin A and C, this crop holds a significant role in various diets globally (Denham, 2020). Apart from that, the cultivation of the crop supports millions of commercial and smallholder farmers, giving the local and international markets a substantial economic upper hand (Naika, 2005).

To ensure proper cultivation and optimal growth of tomato crops, well-drained fertile soils of optimal pH levels between the range of 6.0 and 7.0 (Astija, 2020), supported by warm temperatures, enough sunlight and a moderate supply of water (Somefun et al., 2024; Zheng et al., 2023). Their morphological structure demonstrates compound leaves, small yellow flowers, and varying fruit sizes and shapes (Nakayama et al., 2023).

Despite the aforementioned ideal characteristics and crop requirements regarding tomatoes, the crop remains ravished by several challenges owing to its susceptibility to biotic and abiotic stresses (Shi et al., 2025). These can include fungal diseases such as late blight (resulting from Phytophthora infectants) and infections from bacteria like bacterial wilt (Dufková et al., 2023). In addition, they are prone to a lack of nutrients such as potassium, nitrogen, and calcium, which can lead to additional infections such as blossom end rot (Ghimirey et al., 2024). Extreme temperatures, drought and waterlogging have the capability of causing adverse effects. At post-harvest, the fruit has a relatively shorter life span as it is prone to quick ripening and spoilage, thus propagating spoilage and senescence (Ngcobo and Bertling, 2021).

2.11 *Capsicum annuum* L (Bell peppers)

Capsicum annuum L. (bell pepper), commonly known as pepper, is an extensively cultivated high-value crop due to its nutritional and economic significance (Öztürk et al., 2021). Originating in the heart of Central South America, the crop has now stretched its roots across various regions of the world, especially in warm, temperate climatic regions (Swamy, 2023). The crop has become a source of income for smallholder farmers, making it a key player in both local and international markets, and contributing to the economic sector. Its versatile nature in culinary uses and rich nutrient profile render it a valuable source of vitamins A and C, dietary fiber, and antioxidants such as carotenoids. (Mutayoba and Ngaruko, 2018). Adding to that, substantial opportunities for employment come as a result of bell pepper cultivation, contributing to agricultural revenues in major production regions (Anaya-Esparza et al., 2021).

Their adaptability to protected cultivation such as greenhouse farming, allows them to be produced all year round. Further boosting their economic value (Montejo et al., 2024). Demand for fresh and processed bell peppers in local and international markets underpins their importance in the trade of agricultural produce worldwide (Thakur et al., 2024). For proper cultivation and growth, they require well-drained, fertile soil with a pH range between 6.0 and 7.0, supported by warm temperatures from 20-25°C (Kanabar et al., 2024). Bushy growth, dark green leaves, and large, hollow fruits with a color range from green to red, yellow, orange or even purple (dependent upon variety and ripening stage) define their morphological characteristics (Zhigila et al., 2014).

Irrespective of the proper cultivation technique used to obtain the ideal characteristics described above, these crops remain susceptible to various biological crop stresses (Xu et al., 2022). One being their weak defense against fungal infections such as anthracnose and bacterial infections like leaf spots (Ali et al., 2016) . In addition, nutrient deficiencies, especially calcium deficiency, lead to physiological disorders resulting in diseases such as blossom end rot (Massimi and Radocz, 2021). Furthermore, their sensitive nature to temperature fluctuations and excessive soil moisture further exacerbates yield and quality reduction (Preet et al., 2020).

2.12 Potential of nano-fertilizers and their current limitations in plant

The reviewed literature in the current study vividly demonstrates that nano-fertilizers can successfully enhance nutrient use efficiency (NUE) and also improve plant development. The effect aligns with their physicochemical properties, making them particularly suitable for crops such as tomato and bell pepper, because such crops are characterized by high nutrient demands based on each of the stages of their growth cycles.

The production of these crops depends on a steady supply of available nutrients, and any compromise that directly imposes limits on several factors affecting their growth. These can be their vegetative growth, flowering, and fruit set (Fidler et al., 2025; Lisboa et al., 2024; Ortas, 2013). Irrespective of the success of nano-fertilizers as a potential sustainable mitigating strategy to this dilemma, acknowledging the limits of their technology that which is still in its infancy, is important (Luo et al., 2025).

Gathered from the nano-fertilizer literature, much emphasis is placed on their experimental application in seed germination assays, early seedling tests, and short controlled experiments rather than full crop growth cycle evaluations. To achieve these, often researchers use petri dishes, hydroponics systems or small pot assays as supported by Szőllősi et al. (2020). Consistent with these findings, Garg et al. (2023) further added that researchers would even use high nano-fertilizer concentrations exceeding agricultural applications. These findings point towards a common coalition area of necessity; the need for long-term studies beyond the petri dishes, since their behavior in them and the soil environment is not yet fully understood (Maaz et al., 2025). The lack of comprehensive crop cycle evaluations pertaining to nano-fertilizers risks giving them a superficial status that does not reflect their true agronomic potential. As highlighted previously, plant nutrient demands vary with each growth stage. This, therefore, means that observed effects during germination or early vegetative growth cannot be used to inherently estimate flowering, fruit set, or yield formation. All the presented views by Maaz et al. (2025), Szőllősi et al. (2020), and Garg et al. (2023) emphasize the vitality of evaluating nano-fertilizers across the entire crop growth stage. This is to determine whether early growth effects that come as a result of nano-fertilizers translate to sustainable uptake of nutrients, physiological improvement and final yield benefits under real production conditions. However, neglecting these nuances risks falsely making conclusions based only on short-term data and hence an overestimate of the nano-fertilizer technology's true field-level value.

2.13 Conclusion

Evidence gathered from various studies indicates that nano-fertilizers offer solutions to the contemporary problems faced in agriculture. The use of plant extracts in the green synthesis of nano-fertilizers provides a sustainable alternative that is environmentally friendly, energy-efficient, and economically viable, while aligning with the principles of green chemistry. The use of plant extracts as reducing and stabilizing agents due to their properties significantly influences the properties of nano-fertilizers. Overlooking their concentration is a huge mistake, as these extracts produce nano-fertilizer with varying properties and the efficacy of the plant extracts depends on the antioxidant capacity. The effectiveness of nano-fertilizers depends on the plant being able to assimilate these materials and its capability to use them for physiological and biochemical processes. Apart from their effectiveness, plant cell size also plays a significant role, as larger nanoparticles fail to penetrate the plant cell wall. Hence, it is imperative to factor in the physiology of the targeted crop to enhance the efficiency of the nano-fertilizer. The concentration of nano-fertilizer applied significantly affects its performance, as some plants perform better with a lower concentration, and vice versa. Therefore, it becomes pivotal to consider the plant requirement, stage of the plant, soil properties and environmental conditions to maximize its performance and ensure the optimum application rate of nano-fertilizers. Plant extracts for the synthesis of nano-fertilizers appear to offer a better alternative as they can be used as reducing and stabilizing agents. Yet again, they are widely used as a source of nutrients to synthesize fertilizers (bio-fertilizers) through various methodologies such as composting, vermicompost, and ash. In light of the substantial research on plant-based peels used as organic nano-fertilizers, not much has been reported on their use as reducing agents to convert other plant extracts, serving as sources of nutrients for other plants. Numerous studies have explored the use of plant extracts in synthesizing inorganic nano-fertilizers, which still raises many questions about their long-term effects because the precursors are still chemicals. Therefore, exploring the method of converting organic material into nanoscale can offer a more sustainable solution.

CHAPTER 3

SYNTHESIS AND CHARACTERIZATION OF GREEN NANO-FERTILIZER USING BANANA PEELS, WATERMELON RINDS AND *ALOE VERA* GEL EXTRACT

3.1 Introduction

Achieving high crop productivity and maintaining global food security has been strongly associated with the extensive use of chemical fertilizers in contemporary agricultural practice (Penuelas et al., 2023). Researchers indicate that, without them, current food output would be reduced by approximately half (Alkhader, 2023; Rodríguez et al., 2024). Notwithstanding their advantages, numerous studies highlight growing concerns regarding the environmental consequences of chemical fertilizers and their potential risks to human health (Pal et al., 2025). Due to rapid hydrolysis, chemical fertilizers often release nutrients at a rate that exceeds the plant root absorption capacity (Liu et al., 2014). The lack of synchrony between nutrient supply and plant demand reduces fertilizer use efficiency (FUE) and facilitates nutrient losses through pathways including leaching, runoff, denitrification, and volatilization (Cantarella et al., 2018; Motasim et al., 2024). Another concern associated with phosphate-based fertilizers is their role in introducing heavy metals such as cadmium, lead, and mercury into agricultural soils. Continuous accumulation of these elements in soils poses significant long-term risks because they can be mobilized and transferred through the food chain (Govinda et al., 2023).

The increasing recognition of the environmental and agronomic limitations of chemical fertilizers has stimulated interest in nano-fertilizers as a viable alternative (Kekeli et al., 2025). Nano-fertilizers are nutrient delivery systems developed through nanotechnology, where the active components are engineered within the nanoscale range of approximately 1–100 nm. Within nano-fertilizer formulations, nutrients may originate from the nanomaterials themselves or from encapsulated conventional fertilizers that are engineered to release nutrients gradually over time (Basavegowda and Baek, 2021; Nongbet et al., 2022; Shalaby et al., 2022). Compared with conventional fertilizers, the use of nano-fertilizers has been associated with improved crop productivity and increased economic returns for farmers, as reported in recent studies (Abhiram, 2023; Goyal et al., 2025). Key physicochemical characteristics, including nanoscale particle dimensions, high surface-area-to-volume ratios, and increased surface reactivity, are largely responsible for the improved performance observed in nano-fertilizers (Yadav et al., 2023).

While nano-fertilizers have demonstrated the potential to improve agronomic performance and NUE, it is pertinent to highlight certain limitations. Most existing nano-fertilizers still rely on energy-intensive methods (Abhiram, 2023; Pohshna et al., 2020; Pohshna and Mailapalli, 2023), as well as expensive, hazardous chemical reagents, and complex synthesis conditions and equipment (Diao et al., 2023; Bhattacharjee et al., 2025). For instance, conventional methods such as the Sol-gel process and chemical vapor deposition are known for producing toxic by-products and their high energy consumption (Yadav and Yadav, 2025). In contrast, green synthesis methods present a compelling avenue for sustainable agricultural production (Yadav et al., 2025). Green synthesis promotes the production of nanomaterials using renewable resources, such as agricultural waste, to minimize waste production and the use of hazardous chemicals (Abady et al., 2025).

In parallel, there is a growing shift toward health-oriented diets in society, which significantly increases the production and processing of fruits (Meena et al., 2023). Consequently, this trend generates a considerable volume of fruit peel waste, accounting for approximately 25-30%

(Sharma et al., 2025). Fruit peels are intrinsically valuable, rich in minerals, phytochemicals, and natural polymers that can serve as green precursors for nano-fertilizer synthesis (Usman et al., 2025).

Plant-derived aqueous extracts, including those from banana peels, watermelon rinds, and *Aloe vera* gel, have been extensively used in green synthesis as reducing and stabilizing agents to produce metal-based nanoparticles with smaller dimensions (Kumar et al., 2025; Ndikau et al., 2017; Pawar and Kakde, 2022). Even though their effectiveness as natural reducing and stabilizing agents has been widely reported, their practical application in green synthesis has not yet been fully explored. This limited integration is mainly caused by the reliance on inorganic salt precursors as nutrient sources (Villagrán et al., 2024). However, it is well established that fruit peels have historically been used as a nutrient source in traditional agricultural practices, owing to their mineral and biochemical composition (Khanyile et al., 2024). Plant extracts contain macronutrients, micronutrient minerals, and a diverse array of bioactive compounds (Añibarro-Ortega et al., 2025). A limited number of studies have explored the direct use of fruit peel extracts as nutrient sources in nano-fertilizer synthesis; one example is the study by Hussein et al. (2019). In that study, a green nano-fertilizer was synthesized from banana peel extract using citric acid as a chelating agent and urea as a nutrient carrier. The formulation yielded nanoparticles ranging from 19-55 nm and significantly enhanced germination rates in tomato and fenugreek seeds.

Previous research indicates that plant extracts can act as natural reducing and stabilizing agents during the green synthesis of nano-fertilizers. Findings from other studies reveal that plant extracts naturally contain essential nutrients and phytohormones that promote plant development (Añibarro-Ortega et al., 2025; Khanyile et al., 2024). In many green synthesis strategies, inorganic salts continue to serve as the primary nutrient precursors, whereas plant extracts are typically used only to facilitate reduction and stabilization during nanoparticle formation. As a result, the development of nano-fertilizers that rely on plant extracts as both nutrient sources and synthesis agents remains insufficiently explored.

The present study sought to synthesize a green nano-fertilizer using a composite of banana peel extract (BPE) and watermelon rind extract (WRE), with *Aloe vera* gel extract (ALvE) serving as a reducing and stabilizing agent. The central hypothesis of this study is that green nano-fertilizers can be successfully synthesized using exclusively plant-derived extracts, without relying on inorganic precursor materials. In addition, combining extracts from banana peels and watermelon rinds was expected to produce a formulation with a broader and more balanced nutrient profile.

3.2 Materials

3.2.1 Source of plant extracts

3.2.1.1 Banana and watermelon fruits were bought at a local supermarket in Mbombela. Mpumalanga Province (25°27′57″S 30°59′07″E), South Africa. *Aloe vera* leaves were collected from naturally established plants within the University of Mpumalanga, Mbombela campus. Mpumalanga Province (25.4371° S, 30.9818° E) of South Africa.

3.2.2 Source of chemicals and consumables

Potassium hydroxide pellets (85%, Analytical Reagent grade, AR) were supplied by VWR chemicals BDH ® (United States). Hydrochloric acid (32% Analytical Reagent grade), sodium carbonate anhydrous (≥ 99%), and copper (II) sulfate pentahydrate (99.0-1005. %, iodometric) were sourced from Merck (Germany). Tri-sodium citrate dihydrate (assay 99-101%, dried basis), acetic acid glacial (≥ 99.8%, Analytical Reagent grade), sulfuric acid 98%, and sodium hydroxide pellets (≥ 97%) were supplied by MINEMA chemicals from South Africa. Ferric chloride (≥ 99 %,) was supplied by GlassWorld from South Africa. All chemicals were of analytical grade and used as received. All dilutions were done using distilled water. Distilled water was prepared using an Elix system with A10 TOC monitor, incorporating Milli-Q Integral 10 technology from Merck (Milford, MA, USA).

3.3 Methods

3.3.1 Preparation of *Aloe vera* gel extract (ALvE)

The preparation of *Aloe vera* gel extract was done following a method by Kamala Nalini and Vijayaraghavan (2020), minor modifications. Smooth, thick, and large *Aloe vera* leaves were cut close to the trunk using a sterile, sharp knife. The *Aloe vera* leaves were taken to the chemistry laboratory, thoroughly washed with tap water, and subsequently rinsed with distilled water. The leaves were incised, and gel was separated using a sterile knife. The gel was subjected to a mechanical blender for blending with distilled water in a 1:2 (w/v) ratio (gel extract: distilled water). The resulting extract was filtered with a Whatman No. 1 filter paper. The aqueous extract was stored in a refrigerator at 4°C for later use as a reducing and stabilizing agent in the green nano-fertilizer synthesis. Figure 3.1 demonstrates the method used to synthesize the *Aloe vera* gel extract.

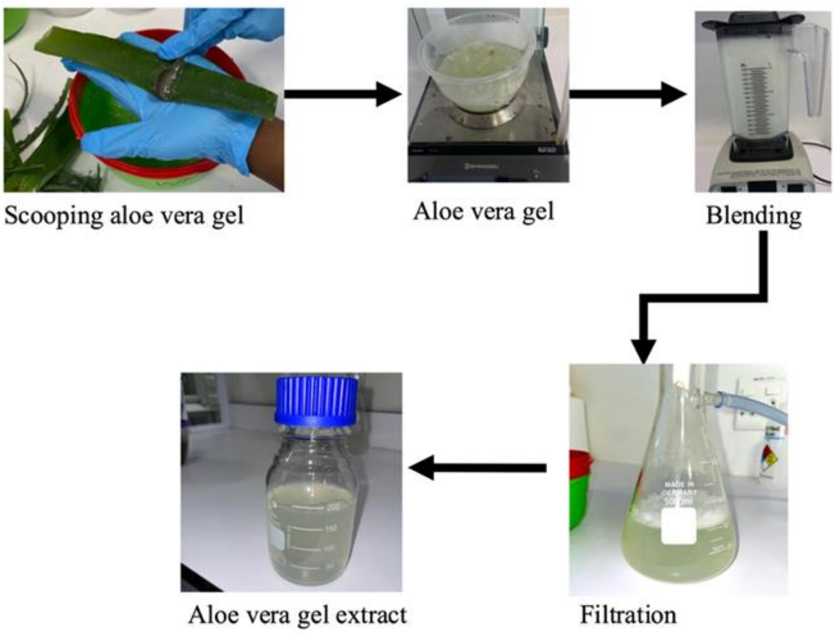

Figure 0.5: The synthesis of *Aloe vera* gel extract.

3.3.2 The synthesis of green nano-fertilizer

The synthesis process for the green nano-fertilizer was conducted using a modified protocol derived from the method reported by Hussein et al. (2019). Prior to processing, banana peels and watermelon rinds were washed thoroughly with distilled water to remove impurities and then cut into smaller pieces. These smaller pieces were blended, and the extraction ratio was maintained at 1:2 (fruit peels: distilled water). The peels were combined in three different ratios, as illustrated in Table 3.1. After blending, the slurry was mixed with 10 g of potassium hydroxide, serving as the extracting agent, and subjected to boiling and continuous stirring for 30 minutes. Subsequently, the slurry was allowed to cool and then filtered with a vacuum filter. The clear solution obtained was heated with continuous stirring until it reached a temperature of 70 °C. The solution was left at room temperature for cooling purposes before it was stored in a refrigerator at 4 °C. This procedure was repeated for each different peel ratio. Figure 3.2

presents a schematic representation of the green synthesis process used to produce composites from banana peel and watermelon rind extracts.

Table 0.1: Ratios of banana to watermelon peels for the synthesis of the green nano-fertilizers

Ratio	**Weight (g)**
50% of banana peels + 50% watermelon peels	250 g of banana peels + 250 g watermelon peels
75% of banana peels + 25% of watermelon peels	375 g of banana peels + 125 g of watermelon peels
25% of banana peels + 75% of watermelon peels	125 g of banana peels + 375 g of watermelon peels

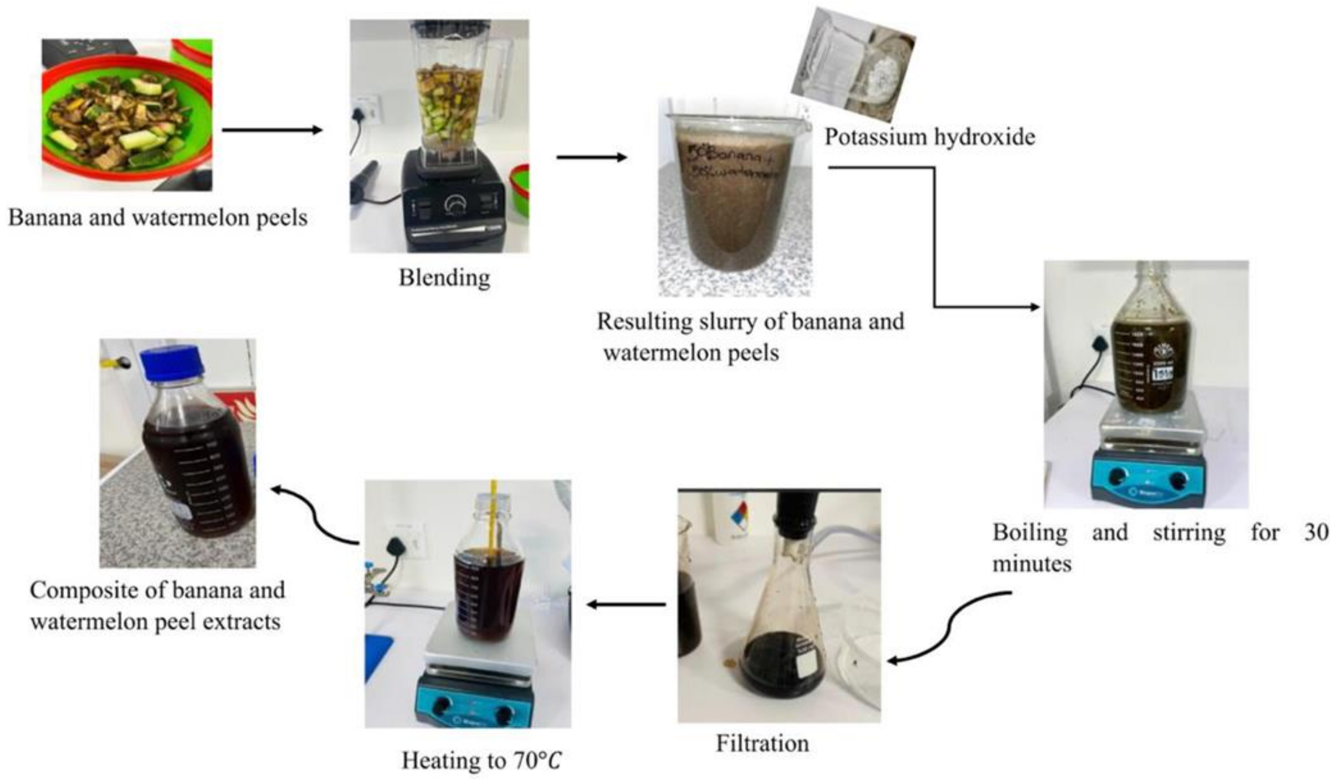

Figure 0.6: Schematical diagram of the green synthesis of composite of banana and watermelon peel extracts.

The different amounts (5 mL, 10 mL, and 15 mL) of *Aloe vera* gel extract were taken from the solution prepared in Section 3.2 and added dropwise to the extracted materials under constant stirring. The details of the resulting composite of plant extracts are specified in Table 3.2

Table 0.2: Composite of banana peel extracts (BPE), watermelon peel extracts (WPE) and *Aloe vera* extracts (ALvE).

Composite of plant extracts
50% BPE + 50% WPE +5 mL of ALvE
50% BPE+ 50% WPE +10 mL ALvE
50% BPE+ 50% WPE +15 mL of ALvE
75% BPE+ 25% WPE +5 mL ALvE
75% BPE+25% WPE +10 mL ALvE
75% BPE+ 25% WPE +15 mL ALvE
75% WRE + 25% BPE +5 mL ALvE
75% WRE + 25% BPE +10 mL ALvE
75% WRE+ 25%BPE +15 mL ALvE

3.4 Characterization of extracted material

3.4.1 Ultraviolet- Visible (UV-Vis) spectroscopy analysis

A UV-Vis spectroscopy analysis was carried out to determine the composition of the extracted material. The analysis was performed within the wavelength range of 200 to 700 nm. The Perkin Elmer Lambda 265 spectrophotometer was used with 1 cm pathlength glass quartz cuvettes placed in the cuvette holder. Distilled water was used as a blank. The results were analyzed using WinLab software. The Savitzky-Golay method was employed to smooth the UV-Vis spectra with an 11-point window size and a polynomial order of 2 in Origin version 24b. This was performed to reduce noise and enhance the visibility of the spectral features.

3.4.2 Phytochemical screening

All phytochemical screening procedures were carried out using a method described by Shaikh and Pati (2020).

3.4.2.1 Flavonoid detection

The presence of flavonoids was evaluated using an alkaline test in which 2 mL of the extract was placed in a test tube followed by the addition of 2 mL of 2% sodium hydroxide solution. The presence of flavonoids was verified by the development of a yellow coloration that diminished following the addition of several drops of hydrochloric acid.

3.4.2.2 Phenolic detection

Phenolic compounds were assessed using the ferric chloride test, in which 2 mL of the extract was placed in a test tube followed by the addition of a few drops of 2% ferric chloride solution. Confirmation of phenolic compounds was based on the development of a blackish color observed in the test tube.

3.4.2.3 Tannin detection

Detection of tannins was carried out using Braemer's assay by mixing 1 mL of plant extract with 2 mL of distilled water, after which the mixture was boiled and filtered. The filtrate obtained after boiling and filtration was reacted with several drops of 5% ferric chloride solution. Tannin presence was confirmed by the development of a dark-green coloration.

3.4.2.4 Saponin detection

Detection of saponins was carried out by adding 2 mL of the plant extract to 5 mL of distilled water. Confirmation of saponins was based on the formation of foam after the solution had been shaken vigorously.

3.4.2.5 Anthraquinones detection

The presence of anthraquinones was detected by the Bontrager's test. The procedure involved mixing 2 mL of the extract with 10 mL of a 10% ammonium solution in a test tube, followed by vigorous agitation for approximately 30 seconds. The development of a pink coloration indicated the presence of anthraquinones.

3.4.2.6 Glycosides detection

The presence of glycosides was assessed using the Keller–Killani test, where 2 mL of plant extract was reacted with 2 mL of concentrated H_2SO_4 in a test tube. The mixture was further reacted with 2 mL of glacial acetic acid, after which several drops of a 2% $FeCl_3$ solution were added. Confirmation of cardiac steroidal glycosides was based on the observation of a brown ring formed between the layers of the solution.

3.4.2.7 Carbohydrate detection

The presence of carbohydrates was determined using the Benedict test. To prepare the Benedict reagent, solutions A and B were prepared. Solution A was prepared by dissolving 173 g trisodium citrate together with 100 g sodium carbonate in 800 mL of distilled water using a volumetric flask. For solution B, 17.3 g of copper sulphate was dissolved in 100 mL of distilled water. The previously prepared solutions were mixed . Carbohydrate presence was evaluated by combining 2 mL of the extract with 2 mL of Benedict's reagent in a test tube, followed by boiling the mixture for 5 minutes. A greenish coloration in the solution confirmed the presence of carbohydrates.

3.4.3 The pH and Electrical Conductivity (EC)

The pH and EC of the extracted materials were measured using a calibrated Thermo Orion Star A211 pH/ EC meter.

3.4.4 Transmission Electron Microscopy (TEM) analysis

Nanoparticle morphology was determined using a TEM (JEM-2100, Jeol, Japan) operated at 200 kV. For the sample preparation, 10 microliters (µL) of the sample were drop-cast onto a holey carbon-coated 200 mesh copper TEM grid (SPA, USA) and left to dry overnight in a desiccator. After drying, the sample was analyzed for distribution, size, and shape. The particle size distribution was investigated using ImageJ software (NIH, USA) (Schneider et al., 2012). Origin Lab 2024b software was used to plot the histogram graphs.

3.4.5 Scanning Electron Microscopy (SEM)- Energy-Dispersive X-ray Spectroscopy EDS) analysis

Morphological characteristics of the extracted material were determined using SEM (FEGSEM Zeiss Ultraplus). The samples were placed on a carbon tape adhered to a clean aluminum stub. Samples were subsequently coated with gold and analyzed by SEM with concurrent EDS at 20 kV to determine elemental composition. The analysis was performed using AZTEC software from Oxford Instruments Nano Analysis.

3.5 Results and discussion

Visual observation of the reaction mixtures provided preliminary evidence of composite formation. After the addition of *Aloe vera* gel extract in the composite of banana and watermelon peel extracts, a color change was observed, transitioning from dark black to light brown in the composite of 75%BPE+25%WPE (Figure 3.3). In the composite containing 75% WPE + 25% BPE, upon addition of ALvE, the color changed from brown to light brown. Whereas in the composite of 50%BPE + 50%WPE, there was a change from dark brown to light brown.

Figure 0.7: The composite of 75%BPE+25%WPE (D), 75%BPE+25%WPE+15 mL ALvE (C), 75%BPE+25%WPE+10 mL ALvE (B), 75%BPE+25%WPE+5 mL ALvE (A).

3.5.1 UV-Vis spectroscopic analysis

The study recorded the UV-Vis spectra of BPE, WRE, ALvE and composite material between 200 and 700 nm to investigate the spectral fingerprints of phytochemicals and confirm the formation of the composite material (Fig. 3.4).

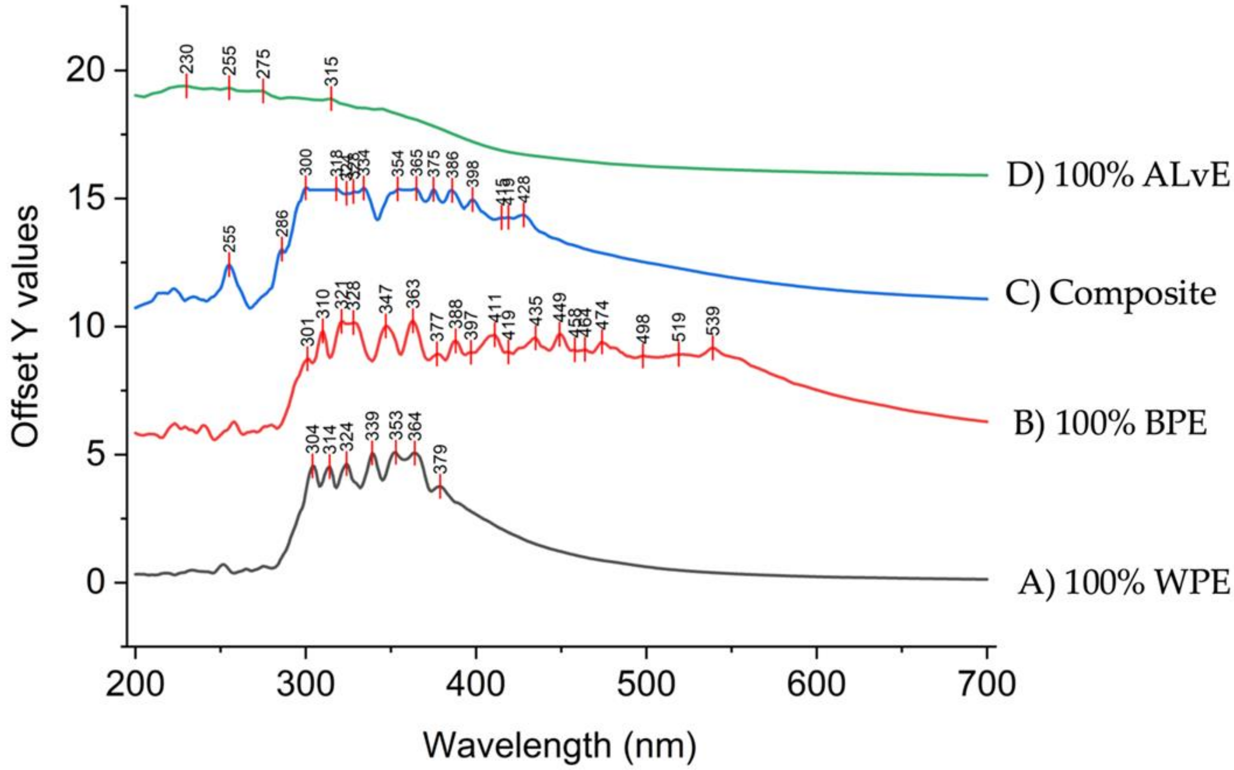

Figure 0.8: The UV-Vis absorption spectra of the clean extracts and composite material; (A) the absorption spectrum of watermelon rind extract (WRE); (B) banana peel extract (BPE); (C) composite material of 50% BPE + 50% WRE + 10 mL ALvE; (D) *Aloe vera* gel extract (ALvE).

The BPE and WRE, primarily utilized as nutrient sources in the present study, are also rich in phytochemicals. The spectral profile of WRE is dominated by phenolic acids (304-324 nm) (Adnan et al., 2020; Kaeswurm et al., 2021) and flavonoids (339-379 nm) (Nistor and Butnariu,

2023) (Fig 3.4 A).On the other hand, BPE exhibited the diverse and richest spectral profile compared to the other extracts with the UV-Vis spectrum of BPE showing the following absorption bands assignable to phenolic acids (301-328 nm) (Sádecká et al., 2025), flavonoids (347-388 nm) (Nistor and Butnariu, 2023; Lu et al., 2019; Grevsen et al., 2009), chlorophyll (411-419 nm) (He et al., 2023), carotenoids (435-489 nm) (Yahya et al., 2021), and anthocyanins (519-535 nm) (Ng and Choo, 2016; Xue et al., 2024). The spectral profile of ALvE (Fig. 3.4 D) revealed the absorption peaks corresponding to anthraquinone (230-275 nm) (Borges-Argáez et al., 2019; Gansukh et al., 2018) and an absorption peak at 315 nm attributed to phenolic acid (Kaeswurm et al., 2021).

The three clean extracts served as a benchmark to evaluate the synthesis of the composite material, providing reference spectra for identifying the emergence of new peaks, spectral shifts and retained peaks. The spectrum of the composite material (Fig. 3.4 C) exhibits a split absorption band in the 300-334 nm region. The λmax at 324 nm (characteristics of WRE) and λmax at 328 nm (characteristics of BPE) were retained in the composite material. Additionally, the composite material retains the BPE peak at 419 nm and the ALvE peak at 255 nm, indicating that all three parent extracts are present and contribute to the optical properties of the composite material.

In the 300-334 nm region, the composite spectrum exhibits a split absorption band with closely spaced peaks at 324 nm and 328 nm. Likewise, two nearby absorption maxima are noted at 415 nm and 419 nm in the visible region. These features indicate that the absorption peaks of BPE and WRE occur in the same spectral region, resulting in unresolved overlapping peaks (Spano and Silva, 2014). Relative to the absorption band at 275 nm (characteristics of ALvE), the composite material exhibited a bathochromic shift to 286 nm (Δλ = +11 nm). Alongside this, the absorption peaks at 315 nm (characteristic of ALvE) and 314 nm (characteristic of WRE) both shifted to 318 nm in the composite material (bathochromic shift). Furthermore, an additional bathochromic shift was noted in the composite, with BPE peak shifting from 411 nm to 415 nm. Previous studies reported that bathochromic shifts in the UV-Vis spectra are likely due to increased electron delocalization resulting from π - π stacking and J-type aggregation of aromatic systems (Deng et al., 2012; Hema et al., 2020). In addition, stabilization of excited states in a heterogeneous dielectric or polar environment is likely to cause a bathochromic shift (Sıdır and Sıdır, 2025) .

A 5 nm hypsochromic shift was observed for the WRE phenolic absorption band, from 339 nm to 334 nm, in the composite. Similarly, the BPE chlorophyll band shifted 7 nm towards shorter wavelengths, from 435 to 428 nm, in the composite material. These hypsochromic shifts are consistent with Hp- π interaction (Hema et al., 2020) and H-type aggregation (Ma et al., 2021). Altogether, the combination of retained absorption bands from clean extracts and the small spectral red and blue shifts aligns with the formation of a noncovalent composite. For instance, Marcia et al. (2018) found that a composite film synthesized from graphene and ZnO nanoparticles retains the parent fingerprint features and exhibits slightly bathochromic displacements with broadened bands in the UV-Vis and Raman analysis. Such spectral perturbations were attributed to interfacial noncovalent forces, particularly electrostatic interactions, π - π stacking and van der Waals attractions. Consistent with Marcia et al. (2018), Georgakilas et al. (2016) reported that hybrids are stabilized by H-bonding, ionic interactions, π–π stacking and van der Waals interaction without loss of parent spectral signatures. Such interactions produce only minor spectral changes, consistent with noncovalent functionalization of graphene and graphene oxide. On this basis, the material synthesized from BPE, WRE and ALvE in this study can be best described as a noncovalent composite.

3.5.2 Phytochemical screening

The results of the qualitative phytochemical screening to test the presence of the flavonoids, phenols, saponins, cardiac glycosides, steroids, carbohydrates and anthraquinones are shown in Table 3.3. The preliminary phytochemical screening study revealed that the plant extracts listed in Table 3.3 contain flavonoids, phenols, tannins, saponins, steroids, glycosides and carbohydrates. However, it is worth noting that the anthraquinones were detected only in the clean extract of *Aloe vera* gel.

Table 0.3:The phytochemical screening of plant extracts

Plant extract	Flavonoids	Phenols	Tannins	Saponins	Anthraquinones	Steroids	Glycosides	Carbohydrates
ALvE	+	+	+	+	+	+	+	+
BPE	+	+	+	+	−	+	+	+
WRE	+	+	+	+	−	+	+	+
50%BPE+50%WRE	+	+	+	+	−	+	+	+
50%BPE+50%WRE+5 mL ALvE	+	+	+	+	−	+	+	+
50%BPE+50%WRE+10 ml ALvE	+	+	+	+	−	+	+	+
50%BPE+50%WRE+15 mL ALvE	+	+	+	+	−	+	+	+
75%BPE+25%WRE	+	+	+	+	−	+	+	+
75%BPE+25%WRE+5 mL ALvE	+	+	+	+	_	+	+	+
75%BPE+25%WRE+10 mL ALvE	+	+	+	+	−	+	+	+

75%BPE+25%WRE+15 mL ALvE	+	+	+	+	_	+	+	+
75WRE+25%BPE	+	+	+	+	_	+	+	+
75%WRE+25% BPE+5 mL ALvE	+	+	+	+	_	+	+	+
75%WRE+25%BPE+10 mL ALvE	+	+	+	+	_	+	+	+
75%WRE+25%BPE+15 mL ALvE	+	+	+	+	_	+	+	+

Legend: +: indicate present; _ : indicate absent

Figure 3.5 A-P below presents the observed findings of the phytochemical screening of the plant extracts, whereby the flavonoids were observed in 100%ALvE (A), 100%BPE (B) and in 50%BPE+50%WPE+15 mL ALvE (C). Phenols were present in 100% ALvE (D), 100%BPE (E), and in 100%WPE (F). Glycosides were indicated in 100% WPE (G), 100% BPE (H), 100% 75%WPE+25%BPE+5 mL ALvE (I) and in 100% ALvE (J). Saponins were indicated in 100% ALvE (K), 100% ALvE (Q) and 100% WPE (L). Anthraquinones were indicated in 100% ALvE (M) and in 100% WPE (N). Tannins were only indicated in 100% BPE (O), whereas carbohydrates were indicated only in 75%BPE+25%WPE+ 10 mL (P) (Fig 3.4).

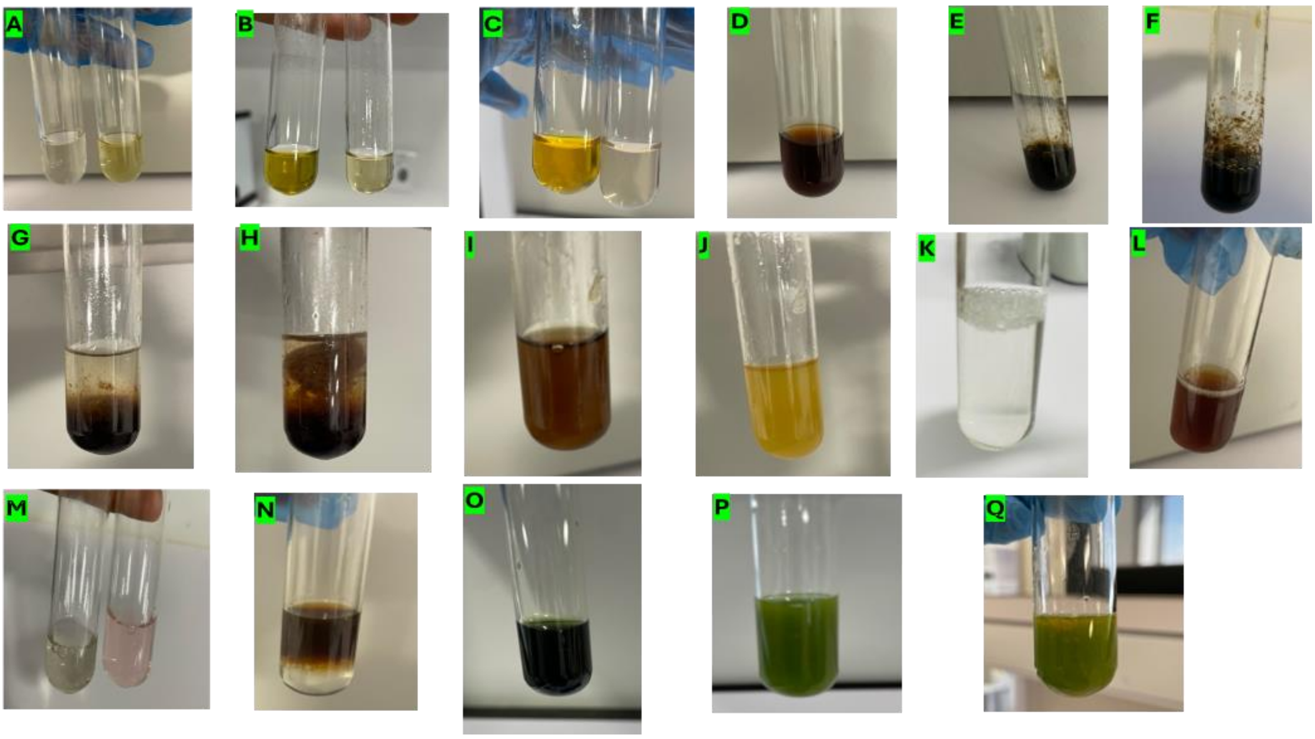

Figure 0.9: The phytochemical screening showing the presents of various phytochemicals for the plant extracts.

The phytochemical profile of the composite extracts indicates that the formulation contains an abundance of multifunctional biomolecules that can mediate nano-fertilizer synthesis. All the extracts and their combinations consistently contained phenols, flavonoids, and tannins. Researchers have revealed that these polyphenolic molecules can serve as chelating agents by binding to nutrient cations such as Zn^{2+}, Cu^{2+}, and $Fe^{2+/3+}$, etc via coordination through carbonyl and hydroxyl groups (Borowska et al., 2020; Marković et al., 2011; Lakey-Beitia et al., 2021). In addition, they also function as reducing agents by donating electrons (Villagrán et al., 2024).

In green synthesis studies, reducing agents are usually discussed in the context of reducing exogenously added metal salts into their zero-valent nanoscale counterparts. In contrast, in this study, no metal salt precursor was used. However, the system contains endogenous mineral ions such as K^{+}, Ca^{2+}, Mg^{2+}, Na^{2+}, Cu^{2+}, Mn^{2+}, etc., from the extracts (Jaroszewska et al., 2023; Kamble et al., 2022; Khanyile et al., 2024). These cations do not undergo reduction to metallic nanoparticles; instead, they are stabilized through chelation and partial redox interactions within the phytochemical matrix (Liu et al., 2024). Saponins and glycosides were detected in all composite extracts. Saponins are naturally occurring amphiphilic glycosides (Rai et al., 2021). Their surface-active behavior enables them to adsorb at interfaces (Dziza et al., 2025), and can act as stabilizing agents to prevent aggregation and maintain colloidal stability (Adnan et al., 2023). In addition, carbohydrates and saponins, which were detected in all the extracts, are known as capping agents to prevent the aggregation of nanoparticles (Pattnaik et al., 2025).

Whereas, Anthraquinones were found exclusively in the ALvE, aligning with the known phytochemistry of aloe as a source of anthracene-based polyketides, such as aloin and emodin (Sadiq et al., 2022). Studies have demonstrated that anthraquinones can chelate transition metal ions via their hydroxyl and carbonyl groups. For example, Zhao and Zheng (2023) describe the mechanism by which anthraquinone derivatives coordinate with metal ions (Mn^{2+}, Fe^{2+}, Cu^{2+},

Zn^{2+}) via phenolic hydroxyl oxygen atoms and 9-carbonyl, resulting in the formation of stable coordination complexes. Furthermore, the research conducted by Selyutina et al. (2024) demonstrated that anthraquinone derivatives (such as Q3) can bind Cu^{2+} and Fe^{3+} via chelation, as confirmed by NMR and UV-Vis analysis.

Collectively, the phytochemical profile confirmed the presence of phenols, flavonoids, tannins, saponins, glycosides, steroids, and carbohydrates across the composite extracts. These compounds function synergistically to facilitate the formation of nano-fertilizers by donating electrons, chelating vital cations, and stabilizing the resulting nanoscale complexes.

3.5.3 The pH and Electrical Conductivity (EC)

Table 3.4 summarizes the pH and electrical conductivity (EC) measurements for both the clean extracts and their composite materials. The three plant extracts exhibited a wide range of pH (5.23-13.24) and EC (0.53-12.26 mS cm^{-1}), influenced by composition and extraction method. The pH values of BPE (12.69) and WRE (13.24) demonstrated significant alkalinity, along with high conductivity of 7.92 and 12.26 mS cm^{-1}, respectively. Conversely, AlvE exhibited an acidic pH of 5.23 and a weak EC of 0.53 mS cm^{-1}. A strong acidifying effect is observed with increasing concentrations of *Aloe vera* gel, as evidenced by both pH and EC.

Table 0.4: The pH and EC of extracted material from banana peel extract (BPE), watermelon rind extract (WRE), *Aloe vera* gel extract (ALvE)

Plant extract	Ph	EC
BPE	12.69	7.92
WRE	13.24	12.26
ALvE	5.23	0.53
50%BPE+50%WRE	12.37	9.31
50%BPE+50%WRE+5 mL ALvE	10.77	7.48
50%BPE+50%WRE+10 mL ALvE	10.59	9.21
50%BPE+50%WRE+15 mL ALvE	9.78	8.23
75%BPE+25%WRE	12.67	8.94
75%BPE+25%WRE+5 mL ALvE	11.92	8.79
75%BPE+25%WRE+10 mL ALvE	11.69	7.57
75%BPE+25%WRE+15 mL ALvE	11.34	7.12
75%WRE+25%BPE	12.83	11.82
75%WRE+25%BPE +5 mL ALvE	12.66	7.67
75%WRE+25%BPE +10 mL ALvE	12.56	9.97
75%WRE+25%BPE +15 mL ALvE	12.44	8.63

Previous studies have revealed that banana peels have a slightly acidic pH. For example, Mohd Dom et al. (2021) showed that powdered banana peel mixed with water resulted in supernatant with mild acidity levels of 6.16 and 6.46, depending on particle size. In line with Kalibbala et al. (2023), banana peel supernatant had a pH of 6.92 and anEC of 1.093 mS cm^{-1}. Pérez-Juárez et al. (2025) demonstrated that watermelon rind flour mixed with water had an acidic pH between 4.60 and 5.25. Odogwu et al. (2022) reported that exhibited a pH of 5.2-3.8 and an EC of 3.38-3.41 µS cm^{-1}. According to Munoz et al. (2015), *Aloe vera* gel extract exhibited a pH of 5.24 and an EC of 4.09 mS cm^{-1} (Soltani et al., 2023).

The measured pH and EC values for ALvE, recorded at 5.23 and 0.53 mS cm^{-1}, respectively, are in excellent alignment with existing literature on natural gels, which generally exhibit mildly acidic characteristics and weak conductivity (Leal, 2015). On the other hand, BPE and WRE demonstrated significantly alkaline pH levels (12.69-13.24) with corresponding higher EC (7.92-12.26 mS cm^{-1}). The observed discrepancies in relation to the reported near-neutral values by (Kalibbala et al., 2023; Mohd Dom et al., 2021; Odogwu et al., 2022; Pérez-Juárez et al., 2025) may be ascribed to the utilization of KOH as the extracting agent. When potassium hydroxide (KOH) interacts with water, it undergoes dissociation into potassium ions (K^+) and hydroxide ions (OH^-), resulting in the formation of a highly alkaline, ion-rich medium (Hausmann et al., 2021). Hussein et al. (2019) revealed that as the KOH concentration increases, the extracted potassium from BP increases from 46g/L at 4g of KOH to 87.8 g/L at 20 g of KOH. Furthermore, citric acid and urea were employed to reduce the alkalinity of the BPE to a pH of 5. In this study, *Aloe vera* gel was used and it can be observed that as the concentration of ALvE increases, the pH and EC slightly decrease, indicating a partial neutralization effect rather than a complete acidification.

3.5.4 Morphology and elemental composition of individual plant extracts

3.5.4.1 Banana peel extract (BPE)

The TEM image of BPE presents discrete, quasi-spherical particles organized into small, loose chains with no neck formation or visible sintering (Fig.3.6A). The corresponding histogram

(Fig. 3.6B) shows a narrow, quasi-monodisperse distribution of particles, ranging from 4 to 14 nm, with an average particle size of 9.9 nm.

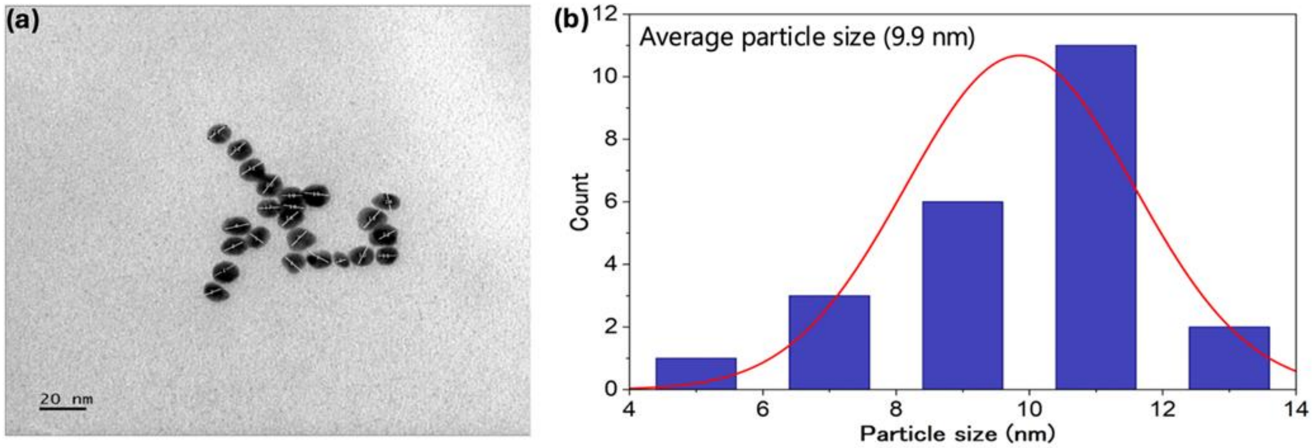

Figure 0.10: (a) TEM image of BPE, exhibiting quasi-spherical nanoparticles (scale bar =20 nm). (b) Histogram illustrating the particle size distribution (n=23), with an average diameter of 9.9 nm.

SEM imaging (Fig.3.7a) displays a uniform, wrinkled surface morphology with bright nanoscale spots. Alongside the bright dots, a curved, ridged-like nanostructure is visible, indicating that nanoparticles tend to gather into a denser and stretched-out form rather than spreading evenly across the surface. In Fig.3.7 b, the EDS spectrum indicates that K (48.45%) and O (46.42%) are the dominant elements in the BPE, whereas S, Na, Cl, Mg, and Si are present in smaller amounts. Elemental mapping at the 500 nm scale (Fig.3.7 c-d) indicates that the nutrient ions are evenly distributed, without forming separate phases or concentrated zones.

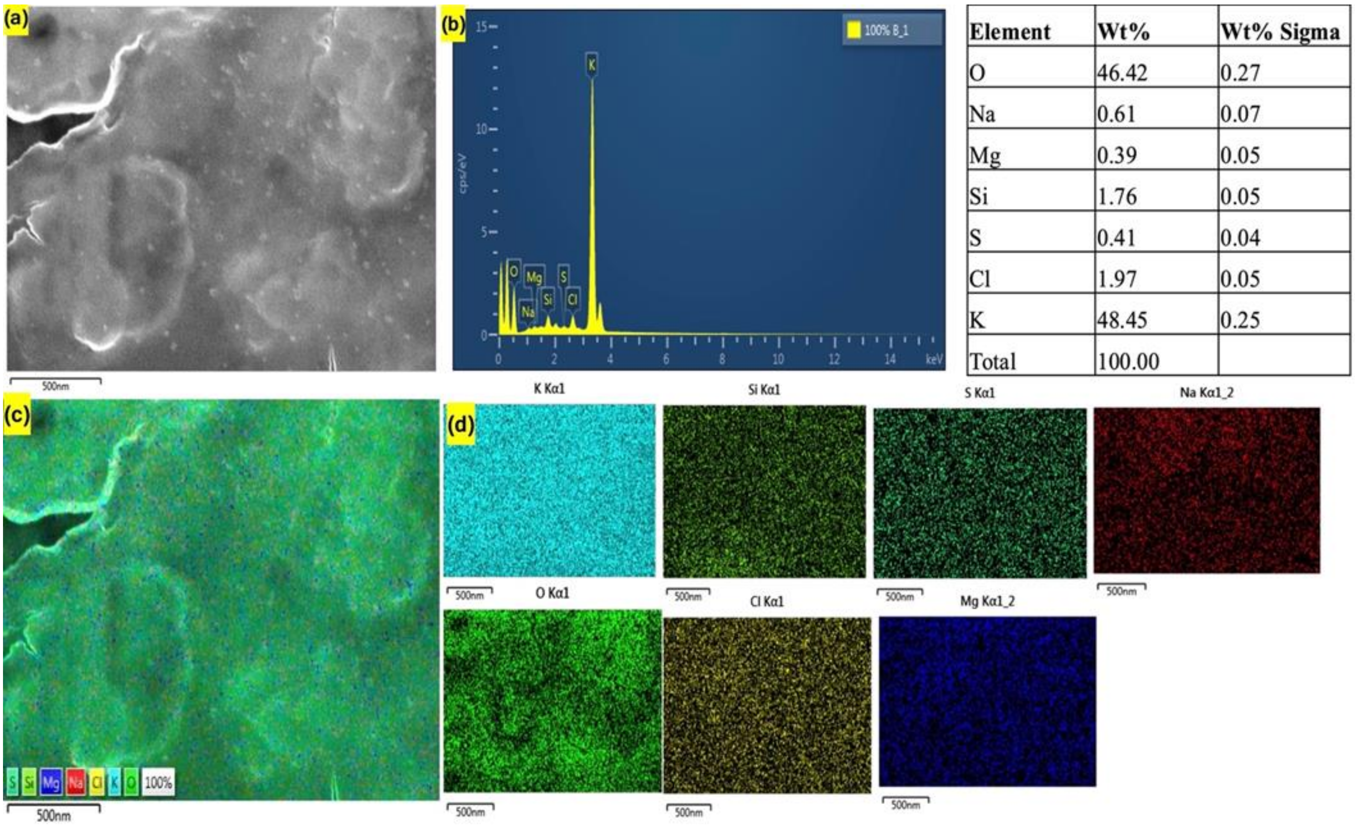

Element	Wt%	Wt% Sigma
O	46.42	0.27
Na	0.61	0.07
Mg	0.39	0.05
Si	1.76	0.05
S	0.41	0.04
Cl	1.97	0.05
K	48.45	0.25
Total	100.00	

Figure 0.11: SEM-EDS analysis of BPE. (a) SEM image illustrating the surface morphology (500 nm) (b) EDS spectrum confirming O, Mg, Na, Si, S, Cl, and K. (c) Overlay elemental map. (d) Individual elemental maps.

The qualitative phytochemical screening (Table 3.3) and the UV-Vis spectrum of BPE revealed the presence of phytochemical compounds. The phytochemicals were phenols, flavonoids, saponins, tannins, carbohydrates, steroids, and glycosides.

The banana peels and watermelon rinds were extracted under highly alkaline and heat conditions. High alkaline conditions are vital for modulating nanoparticle morphology and their stability in green synthesis systems (Velgosova et al., 2025). As a result of these conditions, the inherent phytochemicals of the banana peels were likely deprotonated (Yang et al., 2022; Yuuki and Takeshi, 2023). The deprotonated phytochemicals most probably underwent oxidative polymerization and subsequently self-assembly into nanostructures.

The observed chain-like structure in TEM is likely due to oxidative polymerization, as depicted in Figure 3.8. In addition, the wrinkled, interconnected surface observed in SEM indicates that the discrete, chain-like particles seen in TEM coalesce into a larger, organized structure. The consistency observed between TEM and SEM images supports the idea that the BPE nanoparticles did not form randomly; they developed through a stepwise, self-directed assembly process. The smaller particle size observed in TEM suggests that rapid-burst nucleation occurred. This is evident under higher pH and abundant phytochemicals (Azad et al., 2023; kazemi et al., 2023). The high oxygen content observed in the EDS spectrum of BPE (Fig. 3.7b) is typical in plant-derived materials, as these materials contain oxygen-rich phytochemicals (Pradeep et al., 2022), as observed in Table 3.3.

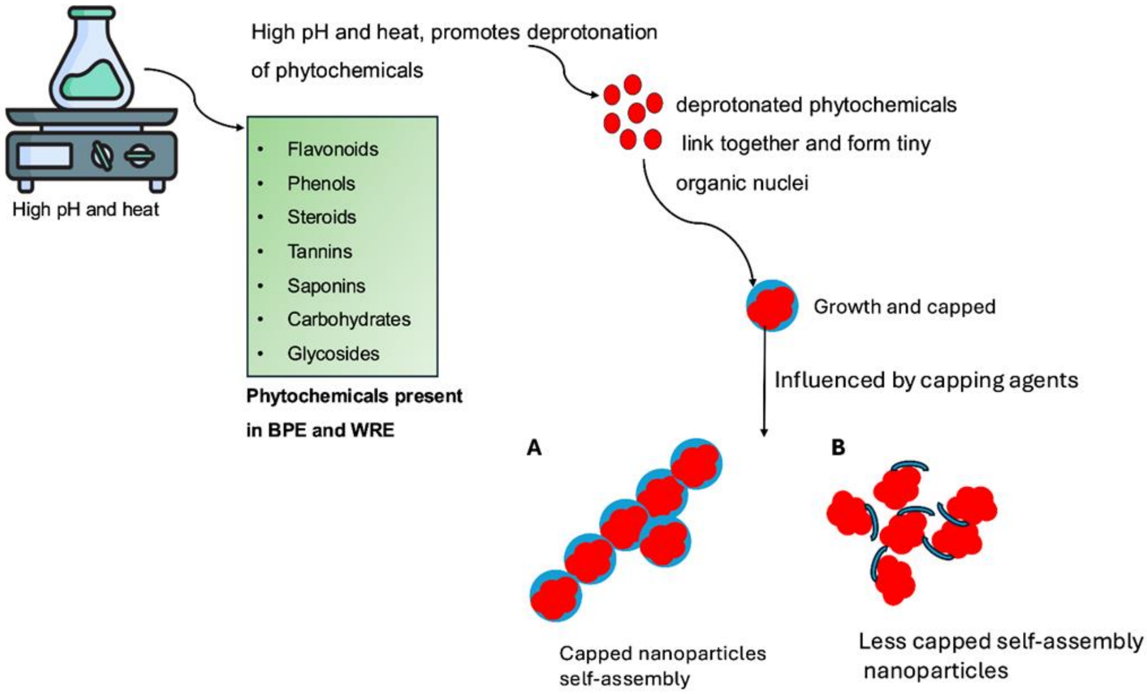

Figure 0.12: Self-assembly into nanostructures induced by higher pH and heat, "oxidative polymerization process". (a) effectively capped nanoparticles. (b) poorly capped nanoparticles. Adapted from Pal et al. (2024).

3.5.4.2 Watermelon rind extract (WRE)

The TEM micrograph (Fig.3.9a) exhibits quasi-spherical to slightly irregular-shaped nanoparticles. Nanoparticles are partially agglomerated and arranged in a grape-like cluster. The nanoparticles exhibit a unimodal distribution, which is highly polydisperse, with an average particle size of 11.2 nm (Fig. 3.9 b).

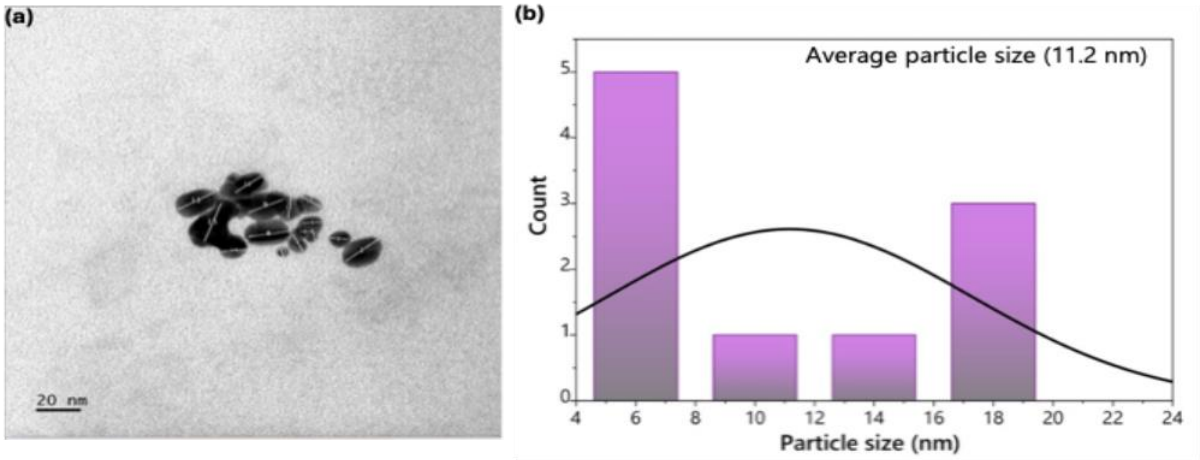

Figure 0.13: (a) TEM image of WRE (scale bar = 20 nm). (b) Histogram illustrating the particle size distribution (n = 10), with an average diameter of 11.2 nm.

The SEM image of WRE (Fig. 3.10a) reveals a smooth, sheet-like, and continuous surface with few pores and no sharp edges. The EDS spectra and qualitative analysis (Fig. 3.10b) reveal that WRE contains a high abundance of O and K, with minor amounts of Na, Mg, Si, P, S, Cl, and Ca. The overlay map and elemental maps (Fig. 3.10c-d) display a uniform distribution of elements, suggesting a good homogeneity with no segregation of elements.

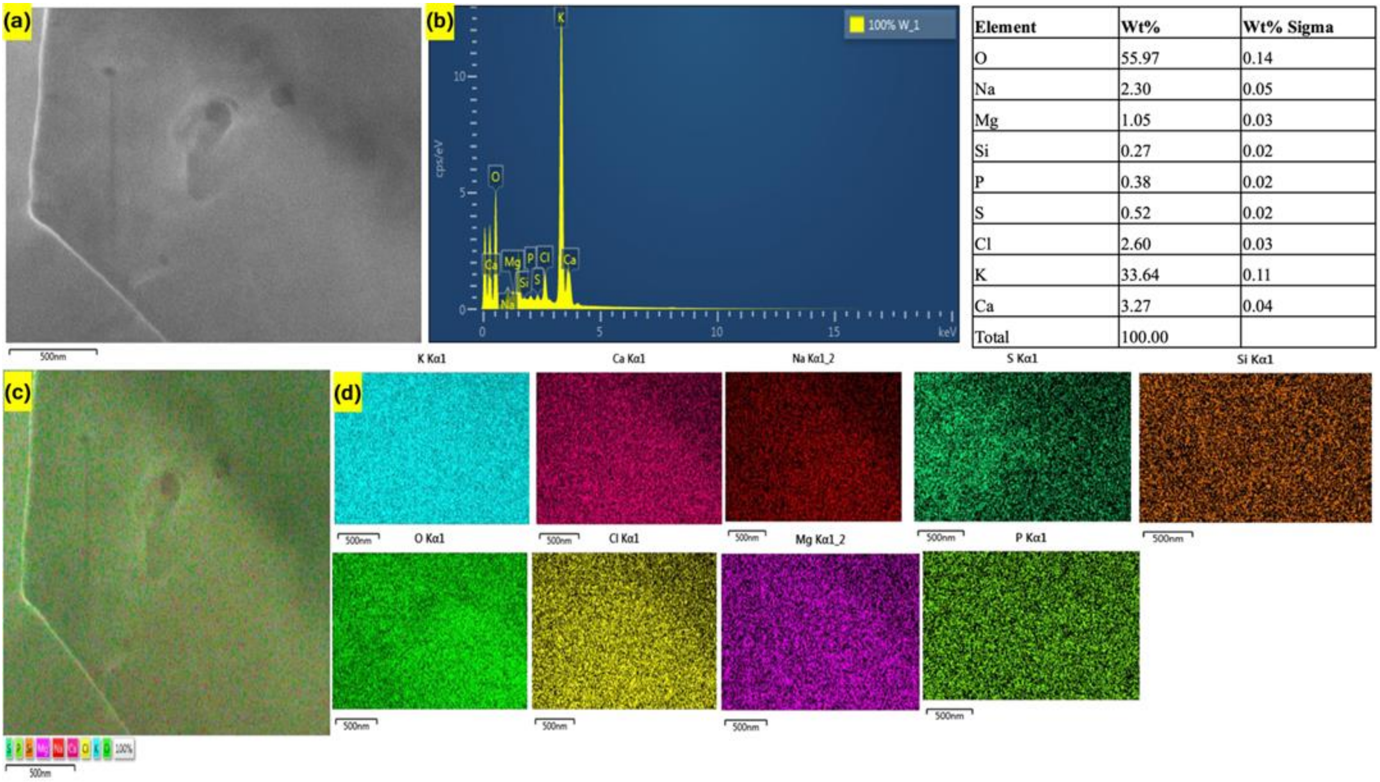

Element	Wt%	Wt% Sigma
O	55.97	0.14
Na	2.30	0.05
Mg	1.05	0.03
Si	0.27	0.02
P	0.38	0.02
S	0.52	0.02
Cl	2.60	0.03
K	33.64	0.11
Ca	3.27	0.04
Total	100.00	

Figure 0.14: SEM-EDS analysis of WRE. (a) SEM image showing the surface morphology (500 nm) (b) EDS spectrum confirming O, Na, Mg, Si, P, S, Cl, K and Ca. (c) Overlay elemental map. (d) Individual elemental maps.

The particle size (11.2 nm) seen in WRE (Fig. 3.9) is comparable to that of BPE. This behaviour is consistent with the mechanism already described for BPE (Fig. 3.8), which indicates a similar pattern of particle formation. However, the particles for WRE were slightly aggregated, suggesting poorer capping than for BPE. Tarkas et al. (2024) found that in the absence of capping agents, particles underwent rapid nucleation followed by aggregation driven by van der Waals forces, leading to larger, irregular particles. As the sample dries for SEM, solvent loss can cause nanoparticles to coalesce (Du et al., 2018; Wu and Briscoe, 2018), which might explain the surface morphology observed in WRE. The higher oxygen content and mineral elements detected by EDS (3.10) indicate that these compounds are incorporated into the sheet-like film observed in SEM. In addition, the mineral elements observed in the EDS spectrum of WRE, are consistent with the results reported by Kouniba et al. (2024) in which the EDX of watermelon rind powder indicates the presence of C, O, K, Cl, Ca, Al, P, Fe, Mg, Cu and Zn.

3.5.4.3 Aloe vera gel extract (ALvE)

The TEM images reveal nanoparticles that are discrete and dispersed, with a large, fuzzy dark patch in the middle (Fig.3.11a). The corresponding histogram graph (Fig.3.11b) shows that the nanoparticles range between 20 nm and 100 nm, with an average of 58.1 nm,

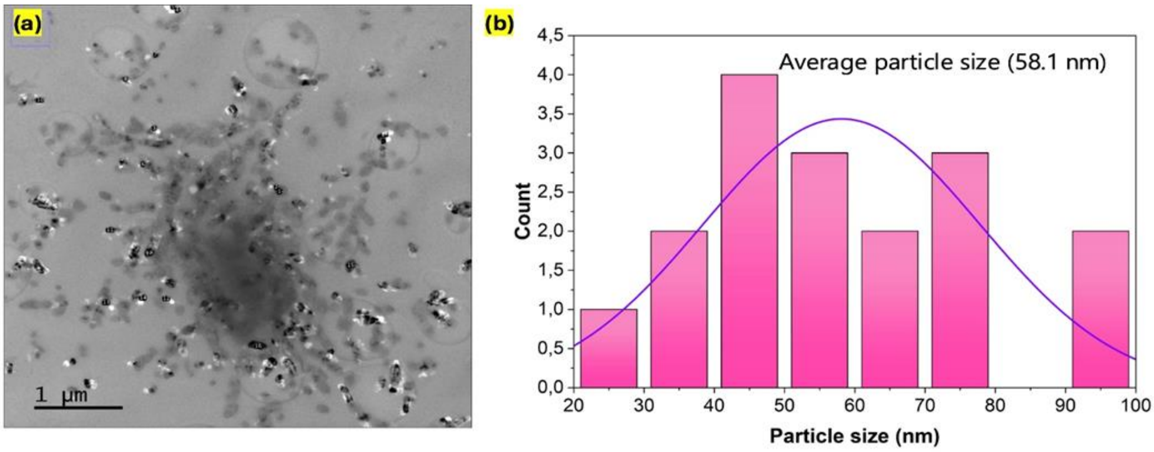

Figure 0.15: (a) TEM image of ALvE (scale bar = 1000 nm). (b) Histogram illustrating the particle size distribution (n = 17), with an average diameter of 58.1 nm.

The SEM micrographs for ALvE revealed well-faceted nanocubes (Fig. 3.12a). The EDS analysis indicated that ALvE contained a higher concentration of potassium (47.83 wt%) and chloride (40.22 wt%) and lower concentrations of oxygen and sodium, as illustrated in Fig. 3.12 b.

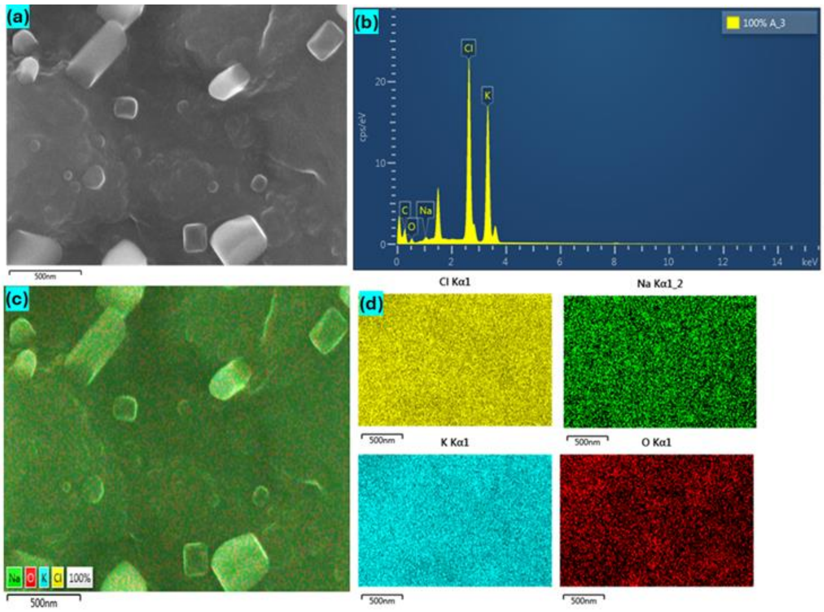

Element	Wt%	Wt% Sigma
O	10.71	0.20
Na	1.24	0.04
Cl	40.22	0.11
K	47.83	0.13
Total	100.00	

Figure 0.16: SEM-EDS analysis of ALvE. (a) SEM image showing the surface morphology (500 nm) (b) EDS spectrum confirming O, Na, Mg, Si, P, Cl, K, Ca, and Mn. (c) Overlay elemental map. (d) Individual elemental maps.

Aloe vera gel extract exhibits distinct behavior compared to BPE and WRE. Both BPE and WRE were boiled and highly alkaline, which activated oxidative polymerization and the subsequent self-assembly of nanostructures. *Aloe vera* gel differed because it was not heated and had a low pH (5.23); Thus, the molecules were less reactive. *Aloe vera* gel behaves in a way similar to what Brinker et al. (1999) described as "evaporation-induced self-assembly", in which drying alone brings molecules together and causes the polymers to organize themselves at the nanoscale. This can explain why the ALvE appears as 20-100 nm nanoparticles, with an average particle size of 58.1 nm, as seen in the TEM image of the ALvE (Figure 3.11a). Figure 3.13 illustrates the formation of nanoparticles of ALvE.

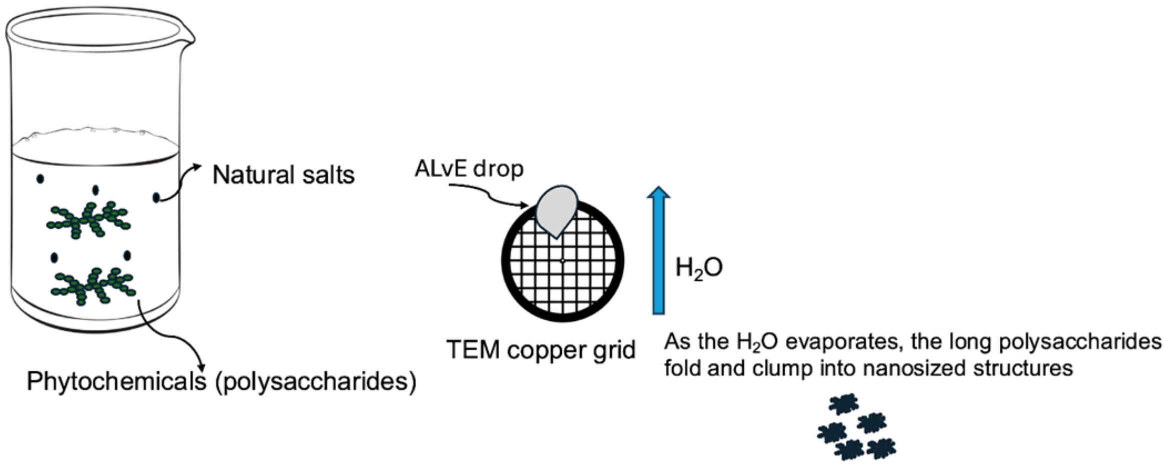

Figure 0.17:The formation of ALvE nanoparticles through the process called "evaporation-induced self-assembly". Adapted from Cusola et al. (2018).

The formation of nano cubes in the ALvE can be explained by the crystallization of naturally occurring potassium and ions in the plant extracts, which can form potassium chloride (KCl). Potassium chloride is known for forming well-faceted cubic crystals because of its symmetrical crystal lattice nature (Castillo-Quevedo et al., 2020). This is consistent with the findings of Sun et al. (2024), who confirmed that K^+ and Cl^- in solution yield well-defined, cubic crystals. Even though this study did not use micellar templates or exogenous KCl, the results suggest that biogenic K^+ and Cl^- can crystallize during solvent evaporation, potentially leading to the formation of faceted KCl nanocubes. The overlay mapping (Fig. 3.12 c-d) demonstrates that the elements were evenly distributed across the surface, with no evidence of phase separation.

The EDS analysis of WRE, BPE, and ALvE revealed that all three biogenic extracts contained a high content of potassium. The high content of potassium in BPE, WRE, and ALvE is likely due to the inherent richness of potassium ions in plant tissues (Asafa et al., 2024; Kamble et al., 2022; Oyeyinka and Afolayan, 2019) .In addition, the three extracts indicated the presence of oxygen, although this element was higher in BPE and WRE. The high oxygen content can be ascribed to oxygen-rich organic molecules such as organic acids, polysaccharides, and pectins (Chandel et al., 2022; Freitas et al., 2021; Mohammed et al., 2021). Regarding BPE and WRE samples, the addition of KOH as an extracting agent during synthesis may have contributed to the higher potassium and oxygen content observed. Notably, even though KOH was not used during ALvE synthesis, potassium levels were still elevated. This indicates that potassium may be derived from the intrinsic composition of the plant material (ALvE) rather than from the reagent alone. High oxygen signals observed in FTIR, EDX, and XPS spectra are commonly attributed to oxygen-containing biomolecules derived from plant extracts used in green synthesis. The oxygen-rich biomolecules help drive nanoparticle formation by serving as both reducing and stabilizing agents (Bashir et al., 2020; Batool et al., 2021; Ikhuoria et al., 2023). The high oxygen content observed in BPE and WRE indicates that the extracts contain more oxygen-rich biomolecules, making them potent reducing and stabilizing agents. On the other hand, ALvE exhibited lower oxygen content, which could make it a weaker reducing and stabilizing agent.

3.5.4.4 Composite of 50% BPE+50% WRE

The TEM analysis of the composite 50% BPE+50% WRE revealed that the nanoparticles were discrete, exhibited low contrast and a quasi-spherical shape with minimal agglomeration (Fig. 3.14a). The nanoparticles are widely distributed, ranging from 20 to 100 nm with an average particle size of 37.3 nm (Fig. 3.14b). Selected Area Electron Diffraction (SAED) was employed to evaluate the crystallinity of the nanocomposite derived from BPE, WRE, and ALvE at the nanoscale. The SAED pattern for the composite of 50% BPE +50% WRE (Fig. 3.14c) exhibits a broad diffuse background with faint spots, indicating a low degree of crystallinity, which leans toward an amorphous structure. The EDS spectrum of this composite indicates the presence of higher K (76.66 wt%), and the presence of Cu (17.05 wt%) and S (6.29 wt%) (Fig. 3.14c).

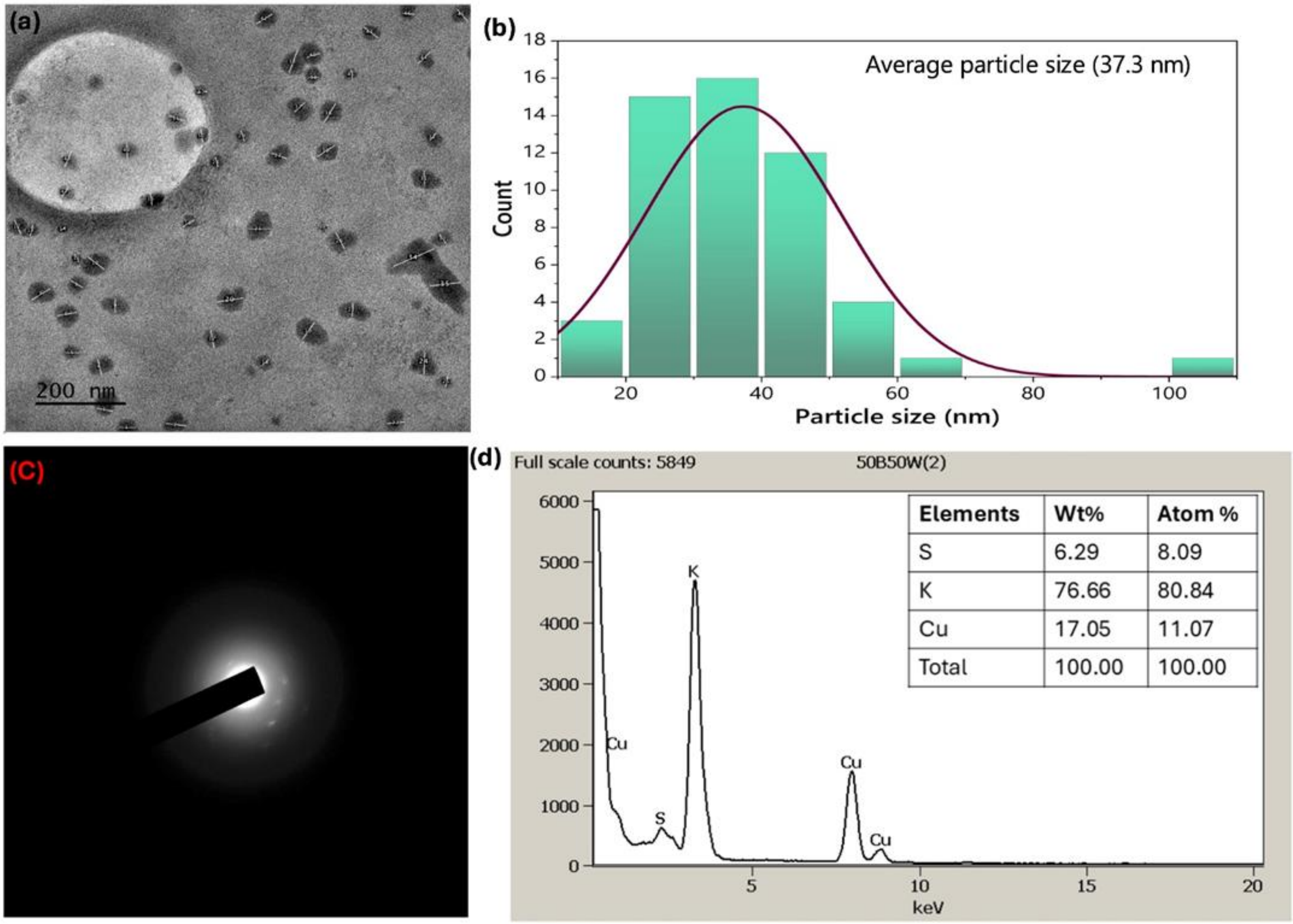

Figure 0.18: (a) TEM image of 50 % BPE+50%WRE (scale bar= 200 nm). (b) Histogram illustrating the particle size distribution (n=52), with an average diameter of 37.3 nm. (c) SAED image of 505BPE+50%WRE. (d) EDS spectrum of 50%BPE+50%WRE.

When equal amounts of BPE and WRE were combined, nanoparticles with moderate particle size were formed. The process behind their formation was likely similar to what is shown in Figure 3.8, as the composite was subjected to the same conditions. Crystallinity significantly influences nano-fertilizer performance by determining nutrient dissolution and release behavior (Madlala et al., 2024). The amorphous pattern observed in SAED is consistent with a polymeric matrix commonly found in organic materials (Thomas et al., 2024), and aligns with the low-contrast nanoparticles observed in TEM (Muchenski et al., 2021). Moreover, amorphous phases are usually associated with an enhanced ion-exchange capacity (Simancas et al., 2023) and a faster dissolution than their crystalline counterparts. Thus, amorphous phases release nutrients rapidly and have improved bioavailability (Carmona et al., 2020). This suggests that the composite of 50%BPE+50%WRE can be optimized for immediate nutrient release rather than gradual and sustained release. The BPE and WRE are both rich in potassium (Ben Romdhane et al., 2024; Hikal et al., 2022). Combining the plant extracts and adding the extracting agent likely increased the potassium content.

3.5.4.5 Composite of 75% BPE+25% WRE

The TEM image of 75% BPE+25% WRE showed discrete, dispersed quasi-spherical nanoparticles that are very small and exhibit no obvious necking or sintering (Fig. 3.1Aa). The nanoparticle had a minimal mean diameter of 4.4 nm, with the nanoparticle size ranging between 1-9 nm (Fig. 3.15b).

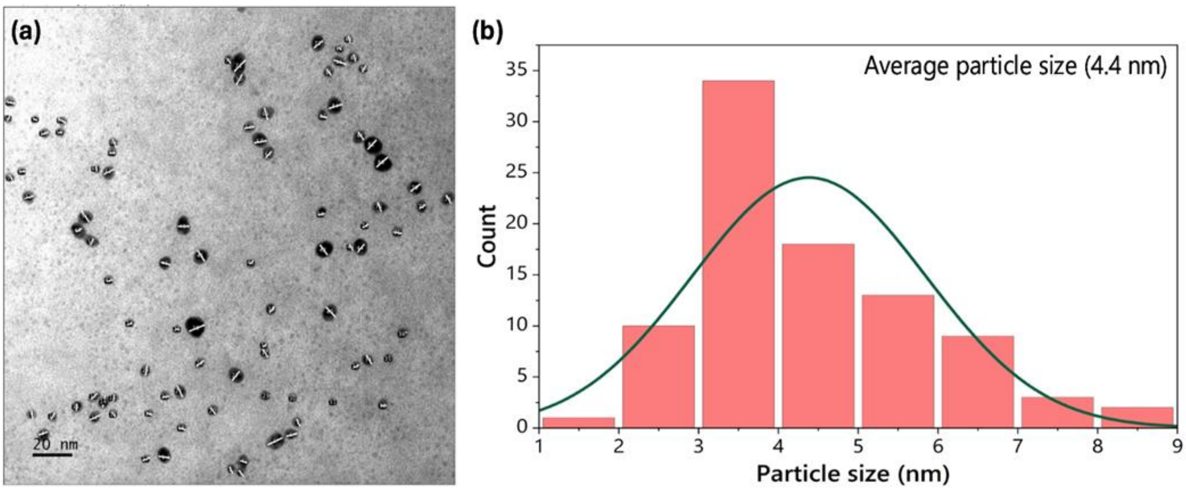

Figure 0.19: (a) TEM image of 75 % BPE+25%WRE (scale bar = 20 nm). (b) Histogram illustrating the particle size distribution (n = 90), with an average diameter of 4.4 nm.

The SEM image for 75%BPE+ 25%WRE (Fig. 3.16a) reveals compact, cloud-shaped clusters composed of rounded and partially fused particles, creating a smooth and continuous surface morphology. The corresponding EDS spectrum (Fig. 3.1b) indicates that oxygen and potassium are the main elements present, accompanied by smaller concentrations of chlorine, phosphorous, silicon and sulfur. The elemental overlay (Fig. 3.16c-d) indicates that the detected elements are evenly distributed throughout the analyzed area.

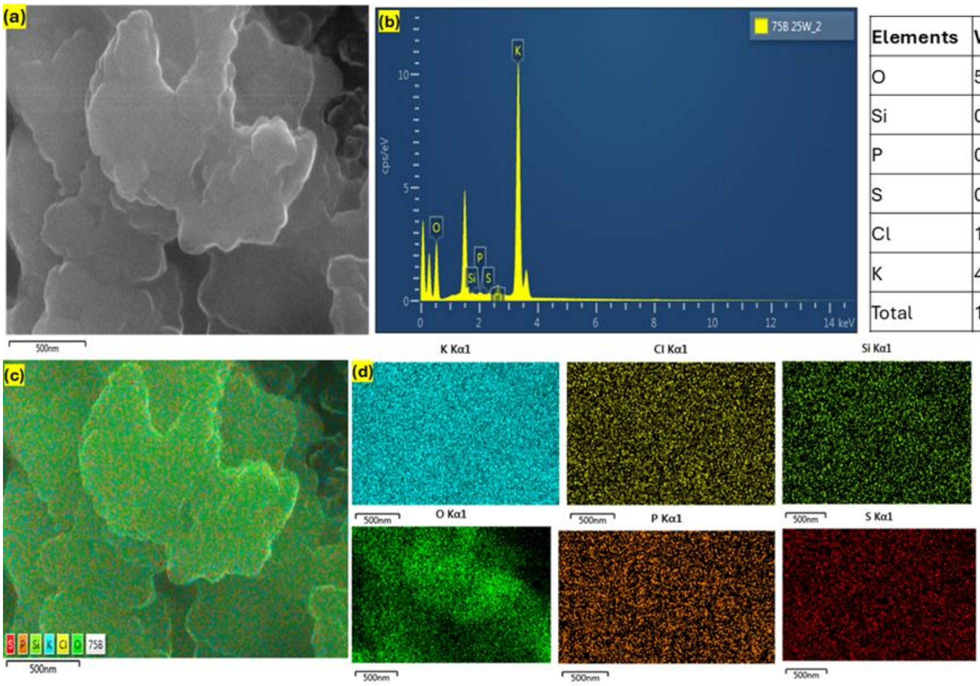

Elements	Wt%	Wt% Sigma
O	52.88	0.25
Si	0.36	0.04
P	0.27	0.04
S	0.20	0.04
Cl	1.29	0.05
K	44.99	0.24
Total	100.00	

Figure 0.20: SEM-EDS analysis of 75%BPE + 25%WRE. (a) SEM image showing the surface morphology (500 nm) (b) EDS spectrum confirming O, Si, P, S, Cl, and K. (c) Overlay elemental map. (d) Individual elemental maps.

The formation of smaller nanoparticles in the 75%BPE+25%WRE composite likely followed the same procedure depicted in Figure 3.8. The nanoparticles were smaller and more dispersed, indicating that nucleation likely occurred faster (Farshad and Rasaiah, 2023), and were effectively capped (Gharibshahian and Tafreshi, 2021; Mahlambi and Moloto, 2022). The observed fused nanoparticles in the SEM image most probably formed as a result of drying artifacts and this is well reported in previous studies. In support of this claim, Michen et al. (2015) reported that drying has a tendency to introduce artifacts and these artifacts can prevent the dispersion state of nanoparticles following drying. In expanding on this report, Brydson (2015) also stated that drying can induce nanoparticle agglomeration or break up formed agglomerates. Following the previous claims, Teulon et al. (2019) further stated that Microscopy-based techniques suffer from a common issue: severe artifact induction resulting from drying, largely due to the retraction of the liquid meniscus, which can either disrupt or promote agglomerates. Together, the observations made by Teulon et al. (2019), Brydson (2015) and Michen et al. (2015) share a common revelation that indeed drying can alter nanoparticle formation during SEM and TEM sample preparation. This can occur either by encouraging the formation of artificial agglomerates or by disrupting those that already exist. In light of this, microscopy techniques alone are not reliable for resolving the real state of dispersion or morphology concerning nanoparticles in their natural colloidal environment. Other advanced techniques, including but not limited to complementary solution-phase techniques e.g., Dynamic Light Scattering (DLS) and zeta potential analysis, are required to fill the gap of characterizing particle size and stability under their actual suspension conditions (Pochapski et al., 2021; Rodriguez-Loya et al., 2023). The minerals identified by EDS were present in all individual plant extracts.

3.5.4.6 Composite of 75% WRE+25% BPE

The formulation of 75% WRE + 25% BPE presents particles with irregular, flake-like aggregates with ragged outlines, and the primary particles are not resolved (Fig. 3.17a). The histogram of the same sample shows a wide particle distribution with an average particle size of 81.6 nm (Fig. 3.17b). The EDS spectrum results for 75%WRE+25%BPE (Fig. 3.17c) present magnesium as the dominant element (51.92 wt%), with notable amounts of potassium, calcium, and sulfur. Trace levels of titanium, copper, and barium were also detected. The strong magnesium and potassium signals suggest that the surface is enriched with alkaline earth and alkali metals.

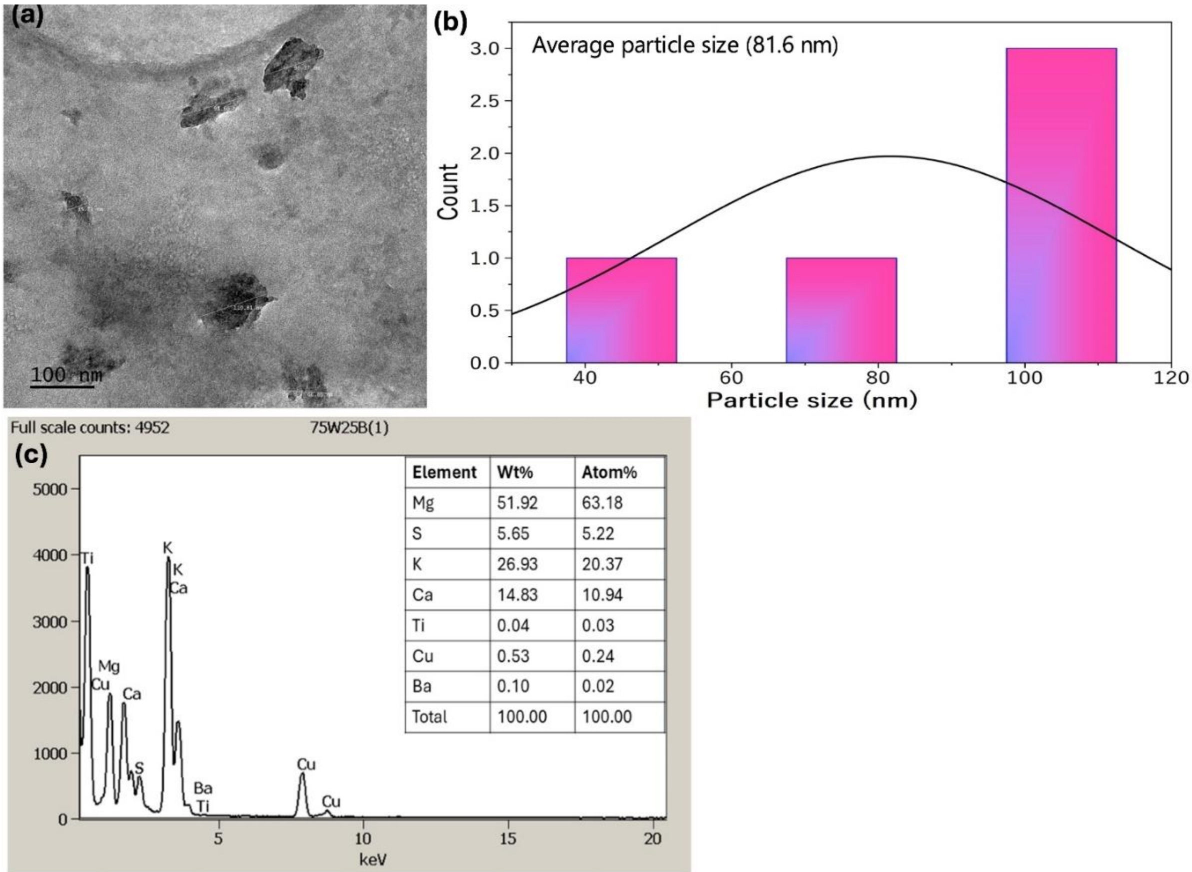

Figure 0.21: TEM image of 75%WRE+25%BPE (scale bar = 100 nm). (b) Histogram illustrates the particle size distribution (n= 5), with an average diameter of 81.6 nm (c) EDS spectrum of 75%WRE+25%BPE.

The formation of nanoparticles for 75%WRE+25%BPE, followed the same procedure described in Figure 3.8. However, combining higher amounts of WRE with BPE produced slightly larger nanoparticles, likely due to poor capping (Sharma et al., 2020). The higher magnesium content observed in EDS for this formulation aligns with the findings by Acun et al. (2025) and Ashoka et al. (2022), who revealed that watermelon rinds are rich in magnesium, potassium and other trace elements.

3.5.4.7 Composite of 50%BPE+50%WRE+5 mL ALvE

The TEM image of the 50%BPE+50%WRE+5mL ALvE depicts discrete, quasi-spherical nanoparticles. The nanoparticles appear compact but loosely aggregated, with each particle having its unique structure despite the close packing (Fig. 3.18a). The histogram illustrates narrowly distributed, nearly monodispersed particles with an average size of 7.7 nm (Fig. 3.18b).

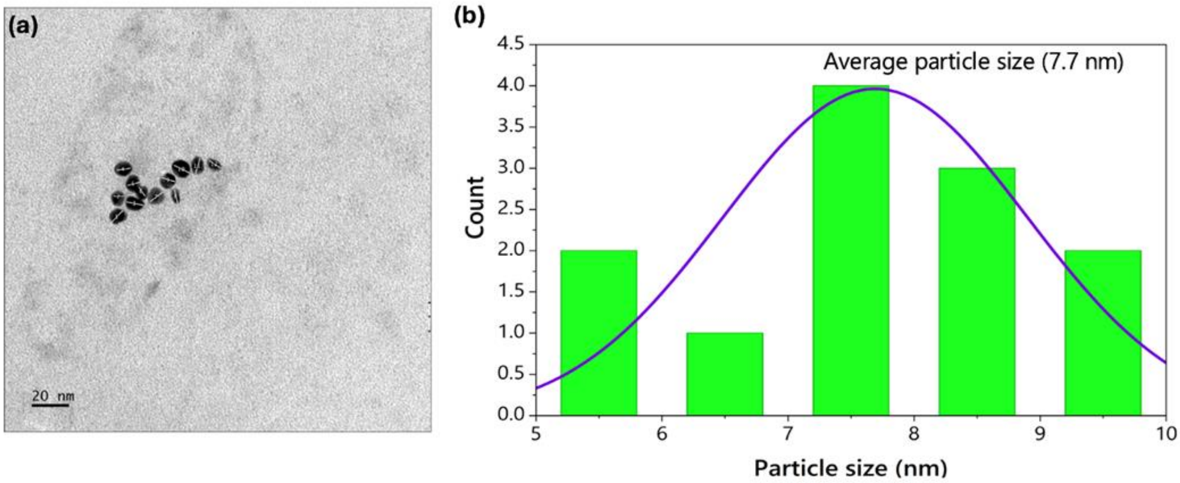

Figure 0.22: (a) TEM image of 50 % BPE+50%WRE +5 mL ALvE (scale bar = 20 nm), (b) the histogram illustrates the particle size distribution (n = 12), with an average diameter of 7.7 nm.

The SEM micrograph for 50%BPE+50%WRE +5mL ALvE (Fig.3.19a) displays loosely packed, cloud-like agglomerates formed by the merging of rounded particles, resulting in a smooth and compact morphology. The EDS (Fig. 3.19b) results reveal strong signals for potassium and oxygen, along with weaker peaks for sodium, silicon, magnesium, and chlorine.

The elemental overlay maps (Fig. 3.19c-d) illustrate that the elements are evenly distributed throughout the surface. However, the oxygen signal appears slightly less intense in the upper or dark regions.

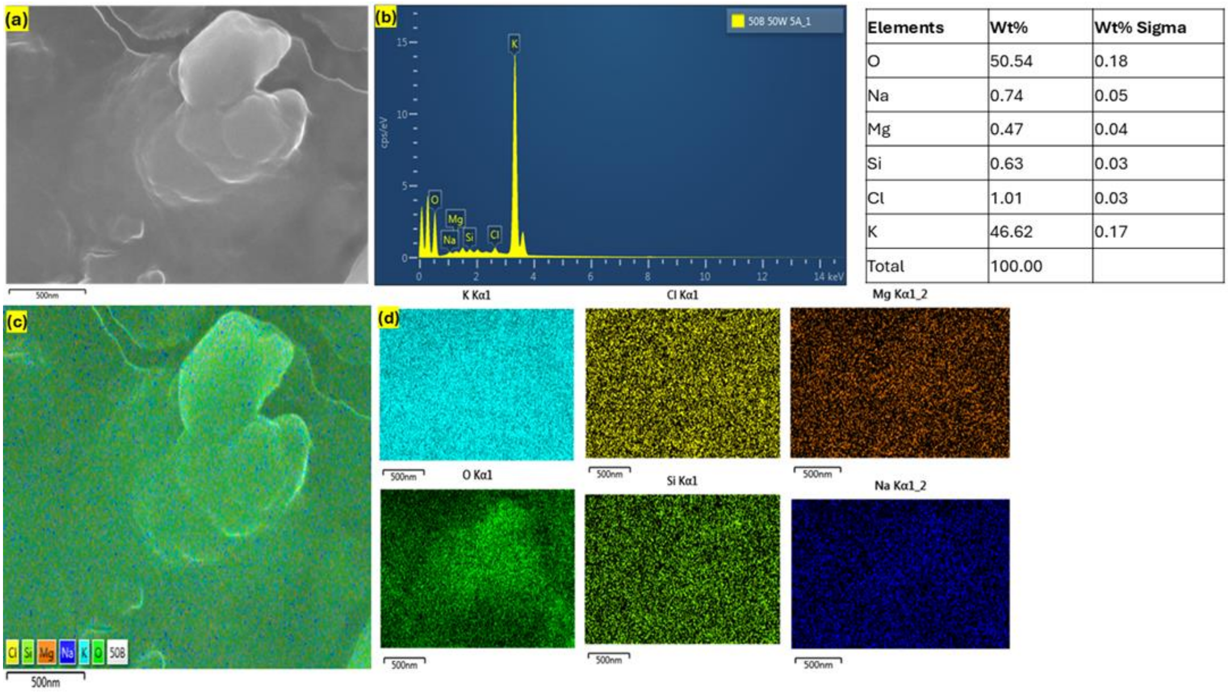

Elements	Wt%	Wt% Sigma
O	50.54	0.18
Na	0.74	0.05
Mg	0.47	0.04
Si	0.63	0.03
Cl	1.01	0.03
K	46.62	0.17
Total	100.00	

Figure 0.23: SEM-EDS analysis of 50%BPE + 50%WRE+ 5 ml ALvE. (a) SEM image showing the surface morphology (500 nm) (b) EDS spectrum confirming K, Cl, Mg, O, Si, and Na. (c) Overlay elemental map. (d) Individual elemental maps.

The cloud-like shape observed in the SEM image (Figure 3.19a) likely formed because of the closely packed, loosely aggregated nanoparticles observed in the TEM image (Figure 3.18a). Lesaine et al. (2020), noted that this phenomenon is common, and the final morphology of the nanoparticles during drying is mainly influenced by the rate at which evaporation and aggregation occur. It has been noted that the composite of 50%BPE+50%WRE yielded 37.3 nm nanoparticles through an oxidative polymerization route. Before introducing ALvE to the composites of BPE and WRE, the composites were heated to 70 ºC. Previous studies have reported that temperature can significantly influence the surface layer of nanoparticles. Widmer-Cooper and Geissler (2016) temperature changes drive ligand coatings on nanoparticles to transition from ordered to disordered forms. Moreover, Huang et al. (2024) demonstrated that increased temperature can boost molecular motion, thereby increasing ligand mobility and promoting disordered conformations. These findings suggest that heat can disturb or loosen the surface coating on a nanoparticle. Heating the composite to a temperature of 70 ºC appears to have loosened molecular interactions. As a result, the ALvE polysaccharides insert themselves more efficiently during post-synthetic capping, yielding smaller particles. This implies that ALvE served as an effective capping agent (Javed et al., 2020).

The mechanism by which the nanoparticles formed is shown in Figure 3.20. The EDS results indicate that this composite retained elements from the individual extracts, which were subsequently incorporated into the organic matrix of the materials.

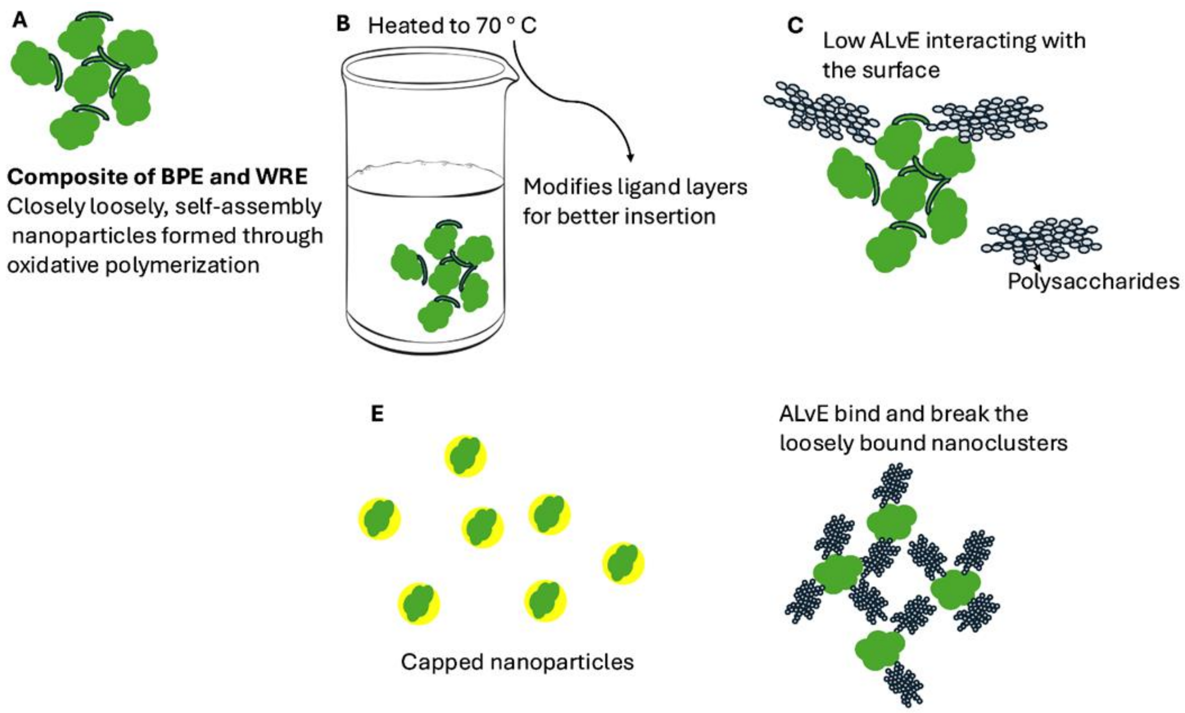

Figure 0.24: The formation of nanoparticles through heat-assisted post-synthetic polymer encapsulation. Inspired by (Aguilar et al., 2021), with modifications

3.5.4.8 Composite of 50%BPE+50%WRE+10 mL ALvE

Increasing the amount of ALvE to 10 mL in the 50%BPE and 50% WRE composite yielded nanoparticles with elongated rod-like and capsule shapes. The particles are relatively large and form secondary agglomerates arranged in a short chain (Fig. 3.21a). The histogram revealed that the particles were widely distributed and polydisperse, exhibiting an average particle size of 528.nm (Fig. 3.21b). The SAED pattern displayed concentric rings with clear, discrete spots, consistent with a polycrystalline structure (Figure 3.21c).

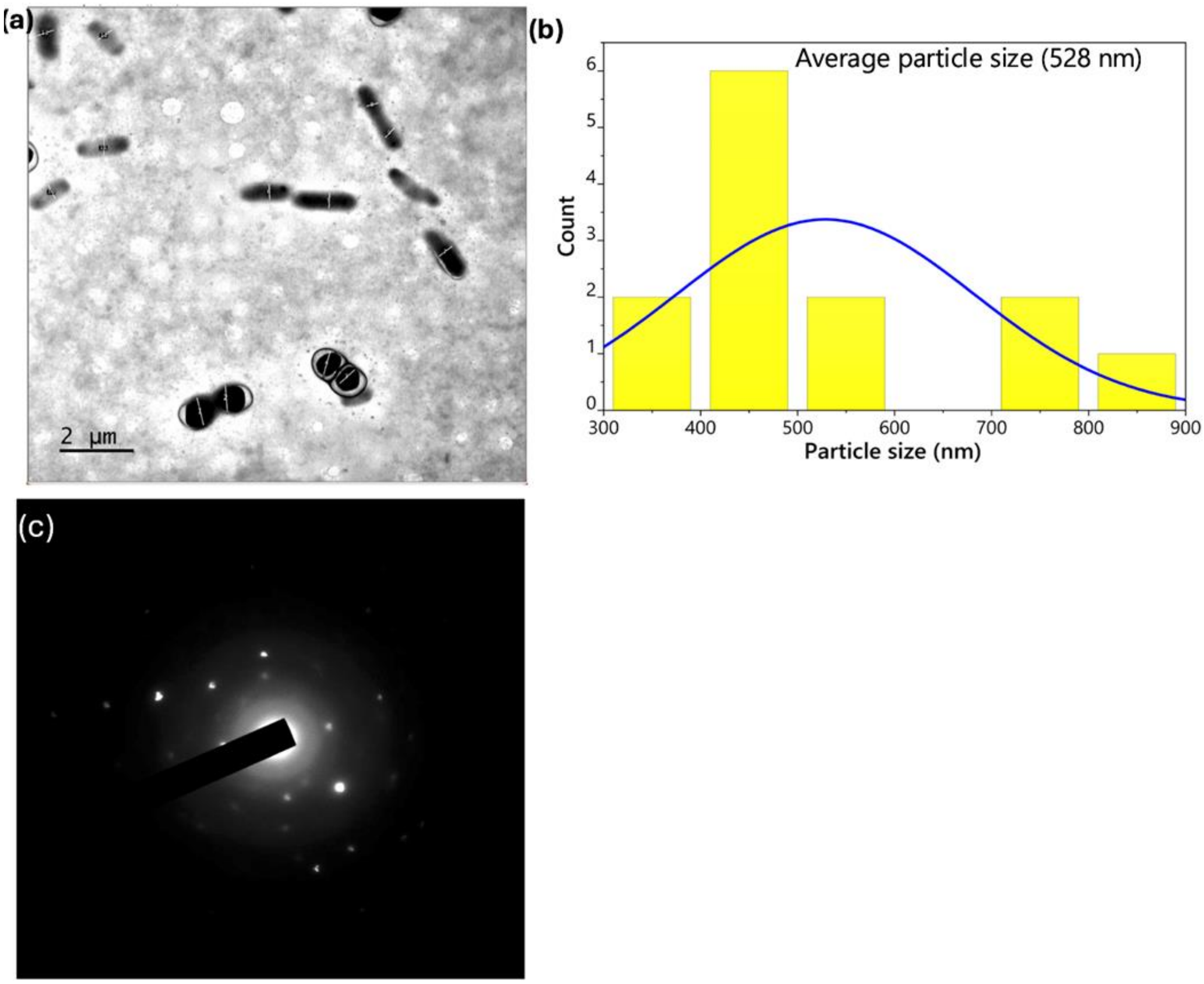

Figure 0.25:(a) TEM image of 50 % BPE+50%WRE +10 mL ALvE (scale bar = 2000 nm). (b) Histogram illustrating the particle size distribution (n = 13), with an average diameter of 528.8 nm. (c) SAED structure of 50%BPE+50%WRE+10mL.

The observation of larger aggregates after the addition of 10 mL of ALvE to the composite of 50%BPE+50%WRE aligns with a bridging effect between particles mediated by polymer chains. Hogg (2013) documented that this mechanism occurs when larger polymer molecules bind to multiple particles simultaneously. Maćczak et al. (2020) noted that when a polymer chain attaches to a particle surface, it can form loops and tails in the solution, which have the ability to bind adjacent particles, thereby driving the formation of larger aggregates (Fig. 3.22).

This could explain why the nanoparticles seen in the TEM image connected to form nanorod-like structures with larger particles. The 50%BPE+50%WRE+10mL ALvE displayed a polycrystalline pattern, suggesting the elements were incorporated within polycrystalline grains.

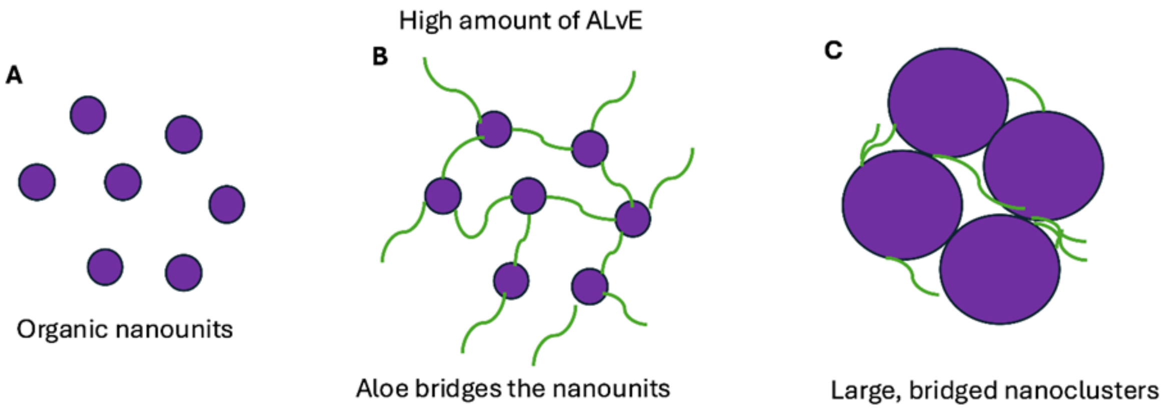

Figure 0.26: The polymer bridging of nanoparticles process. Adapted from Liang et al. (2023).

3.5.4.9 Composite of 50%BPE+50%WRE+15 mL ALvE

Larger irregularly shaped particles that were angular and faceted were displayed by the TEM micrograph of the 50%BPE+50%WRE +15 mL ALvE. The particles undergo partial sintering; however, they remain distinct and do not fuse into a single crystallite (Fig.3.23a). The histogram presents a wide distribution of particle sizes and polydisperse particles, with an average particle size of 540.8 nm (Fig. 3.23b). The SAED pattern of 50%BPE+50%WRE+15 mL ALvE displayed concentric rings with sharp spots, confirming the polycrystalline nature of the nanoparticles. The composite of 50%BPE +50%WRE +15 mL ALvE EDS spectrum (Fig.3.23c) represented a higher oxygen content (87.75 wt%). It also contained two macronutrients: potassium (11.06 wt%) and phosphorus (1.19 wt%), along with two trace elements, copper (1.09 wt%) and zinc (0.19 wt%).

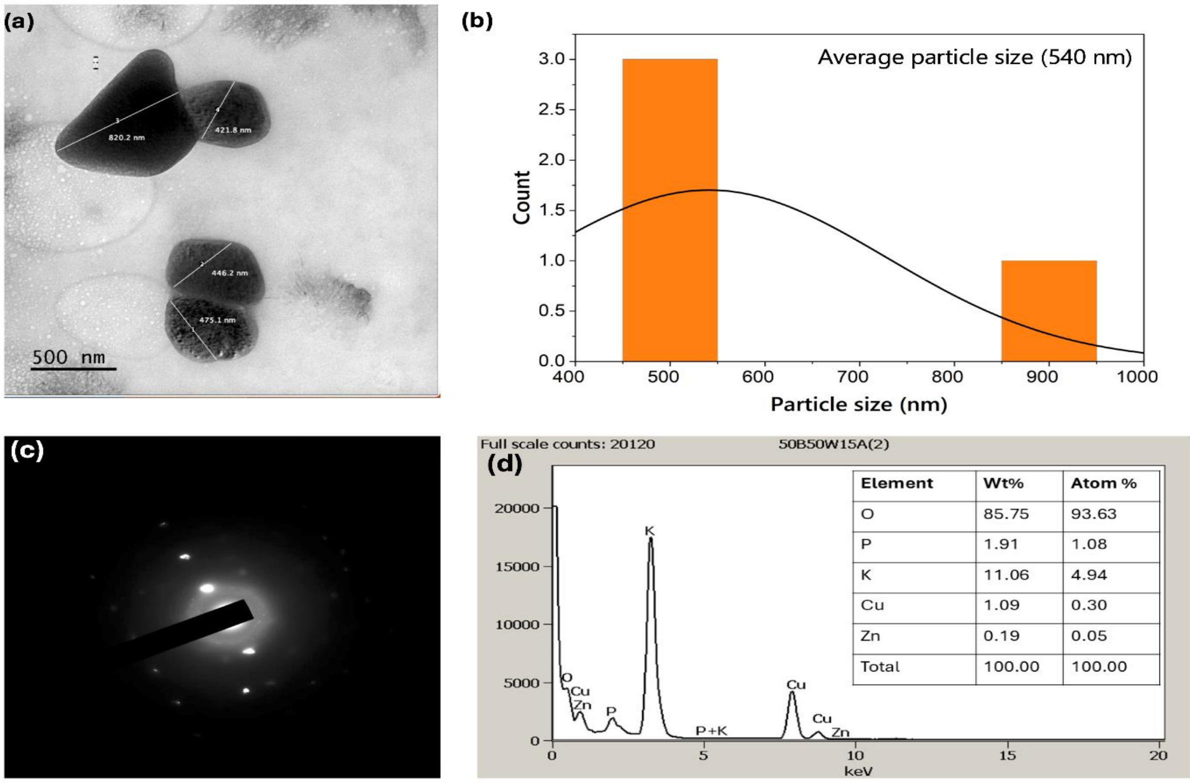

Figure 0.27: 50%BPE+50%WRE+15 mL (a) TEM image (scale bar = 500 nm). (b) Histogram illustrates the particle size distribution (n = 4), with an average diameter of 540.8 nm. (c) SAED pattern. (d) EDS spectrum.

The larger, irregular-shaped particles seen in the TEM image of 50%BPE+50%WRE+15 mL are consistent with the bridging flocculation mechanism presented in Figure 3.22. The SAED pattern indicates that the elements were incorporated within the polycrystalline grain as observed with the formulation of 50%BPE+50%WRE+15 mL ALvE. The higher oxygen content observed in the EDS could be due to the presence of high levels of plant-derived polysaccharides and phenolics, which contain numerous oxygen-rich groups. Moreover, the

EDS reveals that this formation contains elements that are present in the individual plant extracts.

3.5.4.10 Composite of 75%BPE+25%WRE+5 mL ALvE

The TEM micrograph for 75%BPE+25%WRE+5 mL ALvE revealed much larger, elongated or ellipsoidal particles that are well separated (Fig. 3.24a). The particles exhibited a narrow size distribution, ranging from 300 to 450 nm, with an average particle size of 365.3 nm (Fig. 3.24b). The composite of 75%BPE+25%WRE with 5mL AlvE exhibited a broad diffuse halo with almost no distinct rings, indicating an amorphous structure (Fig. 3.24c). The formulation of 75%BPE+25%WRE +5 mL ALvE EDS spectrum (Fig. 3.24d) revealed peaks for all three primary plant nutrients (NPK) and two trace elements (Cl and Cu). Nitrogen was detected at a higher content, accounting for 86.08 wt%.

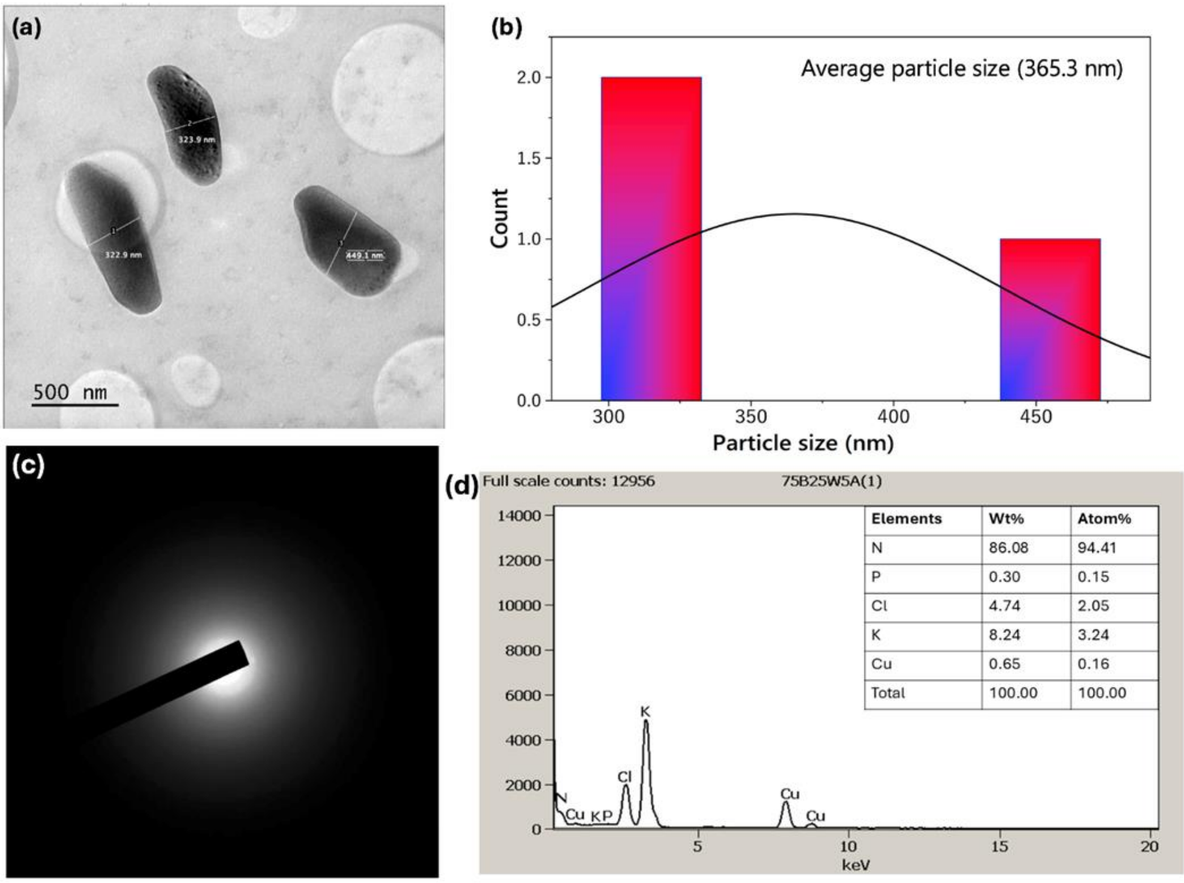

Figure 0.28: The 75%BPE+25%WRE_5mL ALvE (a) TEM image (scale bar = 500 nm). (b) Histogram illustrating the particle size distribution (n = 3), with an average diameter of 365.3 nm. (c) SAED pattern. (d) EDS spectrum.

The composite of BPE and WRE yielded discrete, dispersed, and smaller particles with an average particle size of 4.4 nm. When 5 mL of ALvE was added to the composite, the TEM illustrated bigger, elongated particles with an average particle size of 365.3 nm. *Aloe vera* gel extract is rich in natural polymers, and a study by Gamagedara et al. (2018) reported that the addition of a synthetic polymer (polyethylene oxide) to small, spherical nanoparticles induced self-assembly and elongation into rod shapes. This is because the polymer binds to each surface of the nanoparticle, directing its growth into a rod-shaped structure. This aligns with the morphology observed in the TEM image (Fig. 3.24), suggesting that ALvE can also serve as a soft template. The amorphous structure indicates that the elements were incorporated within an amorphous structure. The EDS indicates that this formulation contains all three plant nutrients required for proper development; however, nitrogen was not detected in the individual plant extracts. As noted earlier in the previous sections, plant extracts contain high amounts of capping agents and when combined in different amounts, they impose surface alterations and also mask or expose some elements when the surface is thick. This therefore suggests that the composites are likely to facilitate easier detection of nitrogen (Reda et al., 2019).

Expanding from this view, it must also be considered that the elemental analysis by EDS does impose some limitations whereby some elements may not be detected due to several limitations of the instruments, especially concerning plant tissues. For instance, low-energy x-rays ($Z \leq 10$) are strongly absorbed by the specimens, rendering elements like C, O and N undetectable, as well as Na, depending on whether the surface is thick or heterogeneous. This effect increases with surface thickness and the density of the specimen (MyScope, 2025). Not only that, but detection limits are also influenced by the surface matrix coupled with conditions. This means that various factors, such as the beam energy, material and geometry, are major contributors. Typical detection limits range from 0.1% or above. This implies that thin layers may not be detected if they fall below this threshold (Jeol, 2025). Lastly, in practice, simulations and applications demonstrate that the limits of detection (LODs) and detectability shift with increasing voltage, absorption paths and detector geometry. Based on this fact, thicker surfaces worsen detectability for certain elements (Burgess, 2022).

3.5.4.11 Composite of 75%BPE+25%WRE+10 mL ALvE

Large, dense, rounded particles, forming agglomerates, are displayed in the TEM image for 75%BPE+25%WPE+10mL ALvE (Fig.3.25a). The nanoparticles exhibited narrow distribution, with an average particle size of 433.5 nm (Fig. 3.25B). The SAED pattern reveals few weak discrete spots superimposed on a diffuse background, indicating a poor crystalline state (Fig. 3.25c).

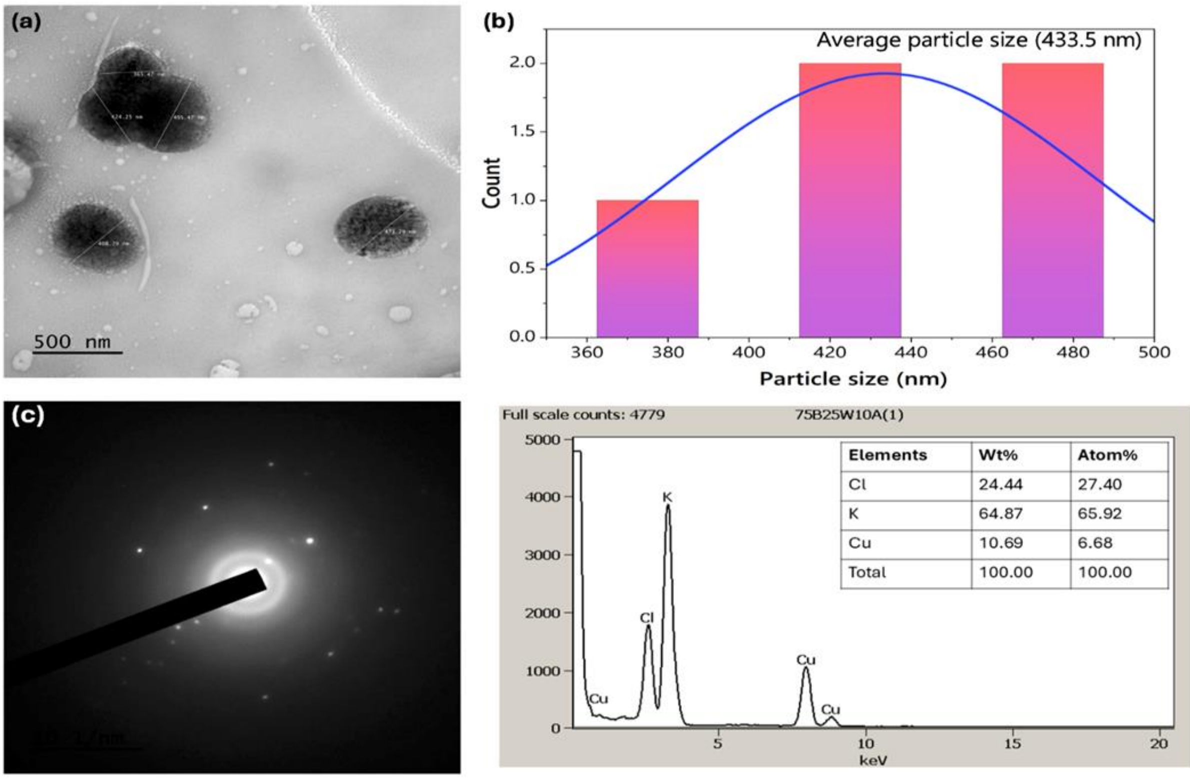

Figure 0.29: 75%BPE+25%WRE+10 mL AlvE (a) TEM image (scale bar = 500 nm). (b) Histogram illustrating the particle size distribution (n= 5), with an average diameter of 433.5 nm. (c) SAED pattern. (d) EDS spectrum.

Similarly, the larger particle size observed in TEM likely formed through the bridging of polymer approach illustrated in Figure 3.20. The elements were embedded within the poorly crystalline structure of 75%BPE+ 25%WRE+10 mL ALvE.

3.5.4.12 Composite of 75%BPE+25%WRE+15 mL ALvE

The TEM image for 75%BPE+25%WRE+15 mL ALvE (Fig. 3.26 a) brought about discrete, mostly rounded particles with minimal agglomeration. The histogram (Fig. 3.26b) showed that the particles were polydisperse, with most diameters ranging from 100 to 400 nm and an average diameter of 113.9 nm. The SAED image shows a broad, diffuse halo with no sharp rings and very faint diffraction spots, indicating an amorphous structure (Fig. 3 .26C). The EDS spectrum indicated a higher potassium content, along with smaller amounts of chlorine and copper.

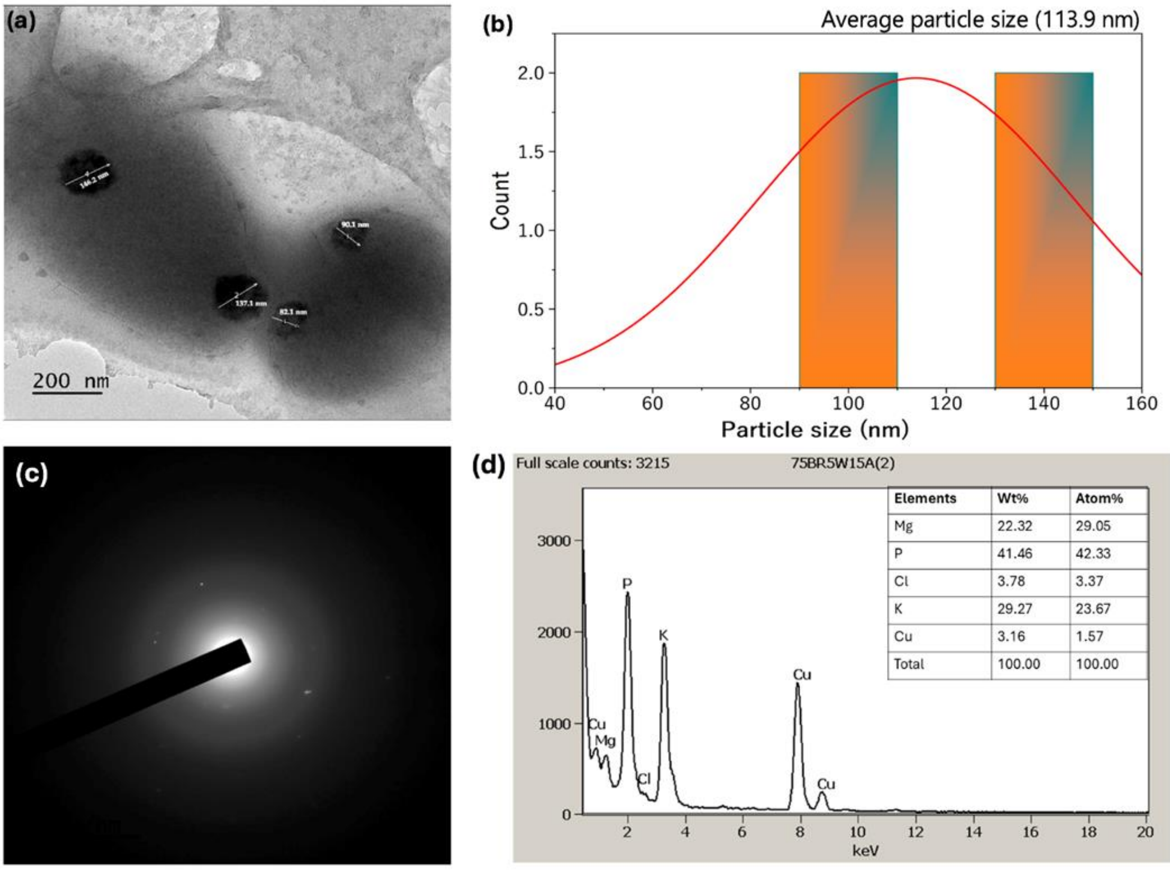

Figure 0.30: 75%BPE+25%WRE+15 mL AlvE (a)TEM image of 75 % BPE+25 %WRE +15 mL ALvE (scale bar =200 nm). (b) Histogram illustrating the particle size distribution (n = 4), with an average diameter of 113.9 nm. (c) SAED pattern. (d) EDS spectrum.

It can be observed that the nanoparticles were slightly larger, but they were dispersed. This may indicate that nucleation was slow (Farshad and Rasaiah, 2023) and steric stabilization took place, preventing nanoparticles from clustering (Javed et al., 2020). The EDS results showed that the material contained a higher content of magnesium and phosphorus, which were relatively low in the individual plant extracts.

3.5.4.13 Composite of 75%WRE +25%BPE+ 5mL ALvE

The composite of 75%WRE+25%BPE+5 mL ALvE (Fig. 3.27a) revealed numerous, very small, near-spherical particles, with sharp interfaces and minimal agglomeration. The corresponding histogram (Fig. 3.27b) shows that the particles were broadly polydisperse, skewed toward smaller sizes, with an average particle size of 4.6 nm. The SAED pattern reveals a broad halo with no distinct rings or sharp spots, indicating an amorphous structure (Fig. 3.27c). The EDS spectrum (Fig. 3.27d) identifies oxygen (76.99 wt%) as the most abundant element, followed by potassium and magnesium. Trace amounts of silicon, copper and sulfur were also detected.

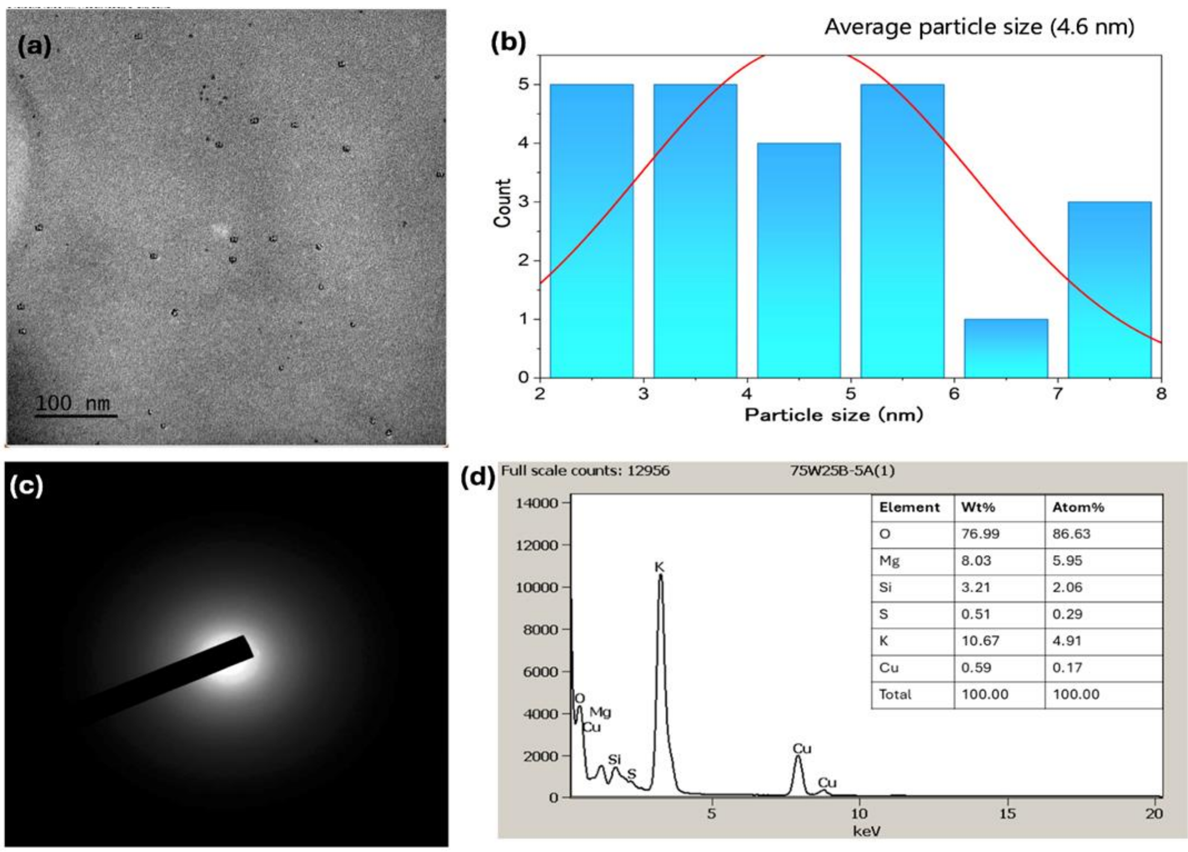

Figure 0.31:75%WRE+25%BPE+5 mL ALvE (a) TEM image (scale bar =100 nm). (b) Histogram illustrating the particle size distribution (n = 23), with an average diameter of 4.6 nm. (c) SAED image. (d) EDS spectrum.

The discrete, evenly dispersed nanoparticles seen in the TEM image (Fig. 3.27a) likely suggest that these nanostructures are products of post-synthetic or pre-formed nanoparticles. As shown in Fig. 3.20, the constituents of *Aloe vera* gel extract likely adsorb non-covalently onto the surface of nanoparticles, disrupting weak agglomeration and resulting in the encapsulation of individual particles. The elements detected by EDS were present in the individual plant extracts and they were incorporated within the amorphous matrix.

3.5.4.14 Composite of 75%WRE+25%BPE+10mL ALvE

A few large, rounded aggregates with smooth margins displaying spheroidal or ovoid particles are seen from the TEM image (Figure 4.28a). The corresponding histogram (Fig. 3.28b) indicates that particle size was widely distributed between 100 and 430 nm, exhibiting an average of 289.2 nm. The SAED image further illustrates sharp, well defined discrete spots arranged in a symmetric pattern, which is characteristic of a single-crystalline structure (Figure 3.28c). The EDS results (Fig. 3.28d) reveal that oxygen (74.23 wt%) dominates the sample surface. Moderate potassium (19.12 wt%) and small amounts of copper (2.35 wt%), chlorine (2.02 wt%), sulfur (1.34 wt%), and silicon (0.95 wt%) were detected.

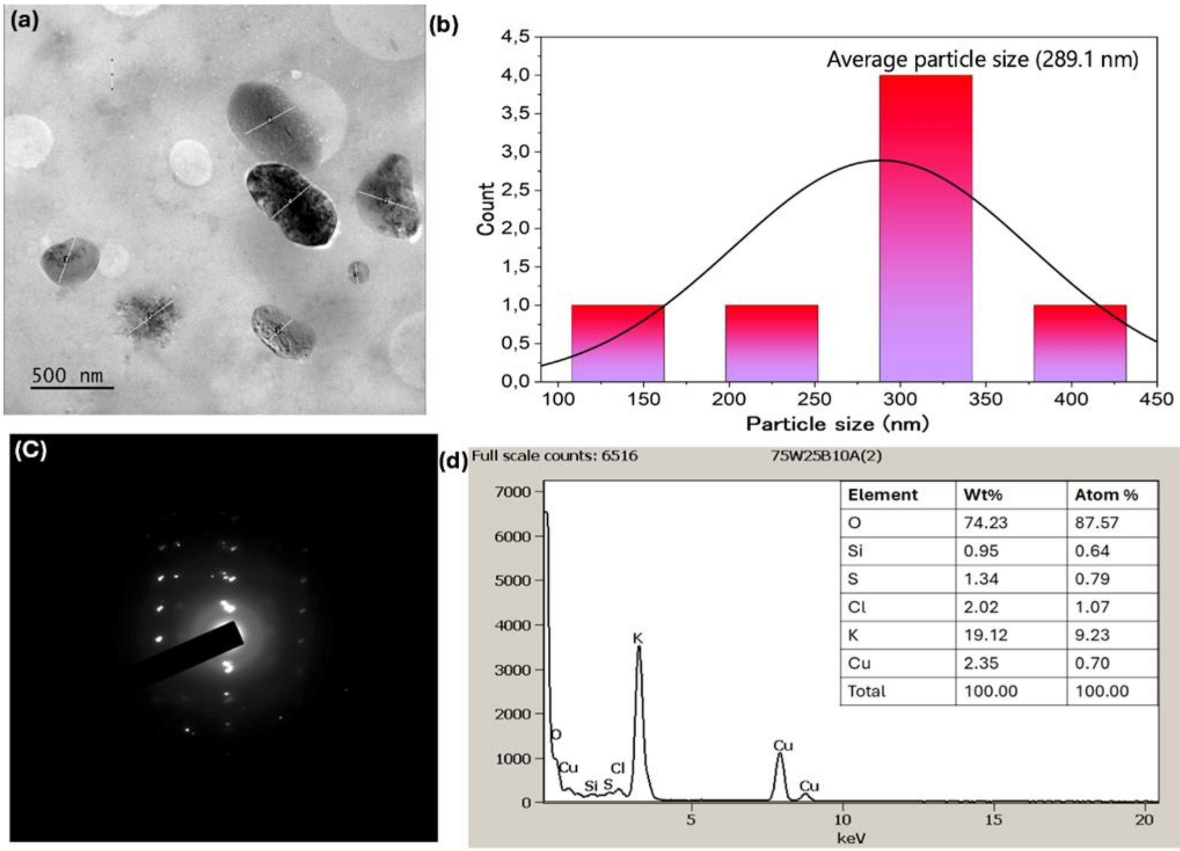

Figure 0.32: The 75%WRE+25%BPE+10 mL ALvE (a) TEM image (scale bar = 500 nm). (b) Histogram illustrating the particle size distribution (n= 7), with an average diameter of 289.2 nm. (c) SAED image. (d) EDS spectrum.

The nanoparticles observed in the TEM image are consistent with the previously noted polymer template. The EDS results showed the presence of elements detected in the individual plant extracts and they were incorporated within a single crystalline domain. The single-crystal structure exhibits slower nutrient release behavior than the polycrystalline structure because it has highly ordered, stable crystal faces and fewer reactive sites for dissolution (Kurganskaya and Luttge, 2023; Morales-Cámara et al., 2025).

3.5.4.15 Composite of 75%WRE+25%BPE+15 mL ALvE

The TEM micrograph of the same sample showed small, quasi-spherical or irregular nanoparticles forming loose clusters with partial necks. However, the primary particles remain distinguishable (Fig. 3.29a). The histogram reveals a broadly polydisperse population with an average of 23.5 nm (Fig. 3.29b).

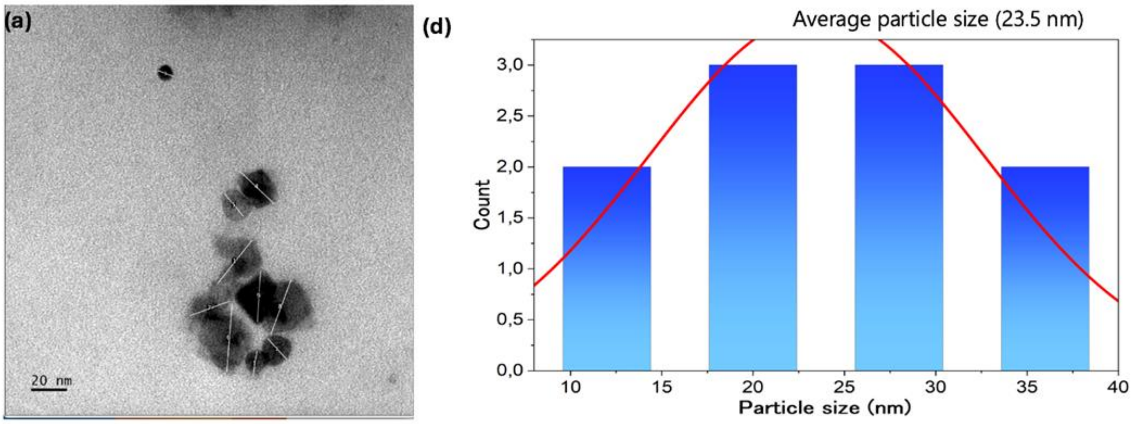

Figure 0.33: (a) TEM image of 75 % WRE +25 %BPE +15 mL ALvE (scale bar = 20 nm). (b) Histogram illustrating the particle size distribution (n= 10), with an average diameter of 23.5 nm.

The SEM micrograph for 75%WRE+25%BPE+15 mL ALvE (Fig. 3.30a) shows a group of rounded particles forming tight, cloud-like agglomerates characterized by smooth and well-defined boundaries. The EDS spectrum (Fig. 3.30b) reveals dominant peaks of oxygen, potassium and chlorine, with smaller contributions from sulfur, magnesium, silicon, and sodium. The elemental overlay map indicates an overall even distribution of the elements throughout the analyzed area (Fig. 3.30 c-d).

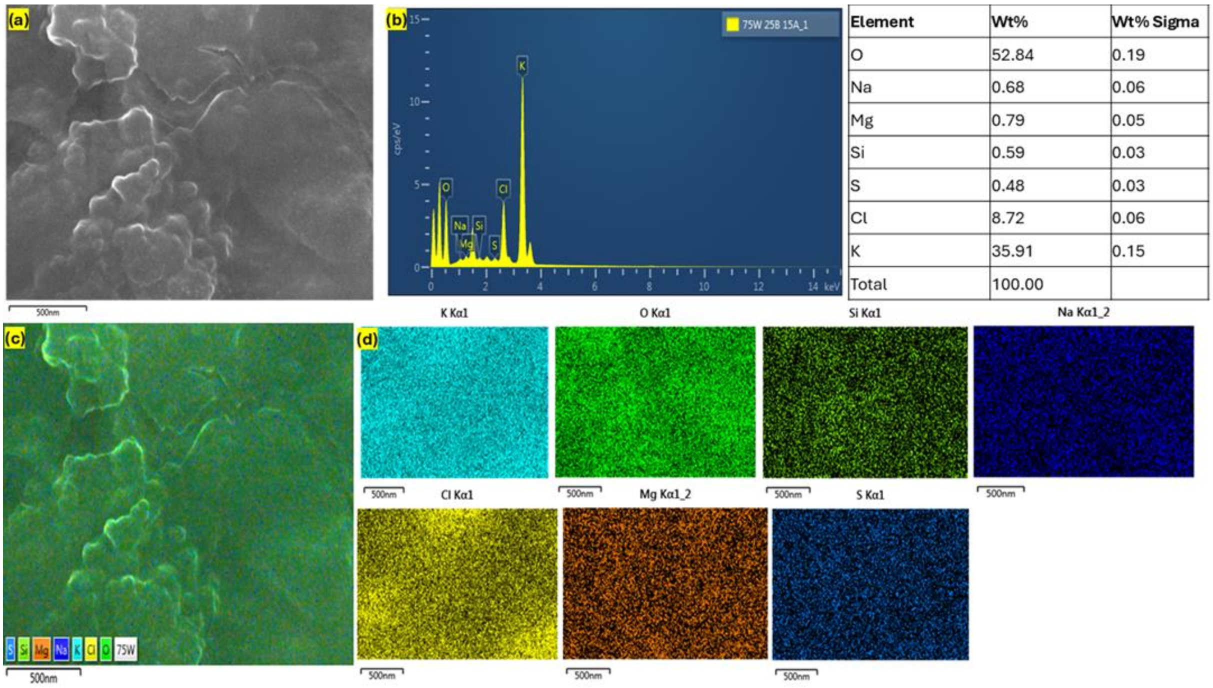

Element	Wt%	Wt% Sigma
O	52.84	0.19
Na	0.68	0.06
Mg	0.79	0.05
Si	0.59	0.03
S	0.48	0.03
Cl	8.72	0.06
K	35.91	0.15
Total	100.00	

Figure 0.34: The EDS spectrum of 75%WRE+25%BPE +10 mL ALvE. (a) SEM image showing the surface morphology (500 nm) (b) EDS spectrum confirming O, Na, Mg, Si, S, Cl, and K. (c) Overlay elemental map. (d) Individual elemental maps.

The TEM image showed that the nanoparticles were closely packed together, and the SEM image showed that the nanoparticles were likely clustered, indicating that the capping agent was not effective in keeping the nanoparticles dispersed (Javed et al., 2020). The EDS reveals elements detected in the individual plant extracts.

3.5.4.16 The effect of the ALvE on the morphology of the composite of BPE and WRE

Despite ALvE's role as a stabilizing and reducing agent, the findings gathered from this study indicate that it was not the only source of influence regarding nanoparticle formation. It has been observed that BPE and WRE also modulate nanoparticle morphology in various ways, as they contain high levels of phytochemicals. However, the addition of ALvE leads to dramatic size tuning since prior to its addition, the composites maintained a nanoscale size. An opposing effect to this dramatic size change was observed with lower amounts of AlvE; hence, the ALvE effects in the different composites were non-monotonic. The large particle size could be attributed to ALvE introducing sufficient capping agents to break the nanostructures within the composite, owing to the so-called bridging effect, as detailed in previous discussions. These observations collectively demonstrate the sensitivity of green nanoparticle formation to extract composition, yielding synergistic effects. This is especially important in the design of effective nano-fertilizers, which involve characterizing extracts based on polymer content, pH, ionic strength and careful control of dosages.

3.5.5 The greenness of the byproduct or synthesis approach

Green products are referred to as those that have been manufactured by employing procedures that lead to the production of less harmful substances and waste, as backed by green chemistry principles (Kharissova et al., 2019).The discussion of all subsequent points here owes its origin to green chemistry principles as outlined by Ogodo and Abosede (2025). The process of synthesizing nano-fertilizer is heavily centred on the transformation of agricultural waste, i.e., banana peels and watermelon rinds, into primary raw product inputs. By virtue of this conversion, the principles of green chemistry are adhered to as they prioritize waste prevention and the use of renewable resources. Valorizing banana peels and watermelon through nano-fertilizer synthesis leads to the reduction in landfill waste and pollution linked with the decay and burning of waste. Often, the waste generated from these raw materials is discarded. However, this process helps extend their use beyond mere consumption. Therefore, in place of applying harsh chemical reagents to fabricate nano-fertilizer, the study has employed the reducing and stabilizing effects of *Aloe vera* gel.

In addition, water has been used as a solvent, allowing safer application than organic solvents. Beyond this, the synthesis conditions have been further set to adhere to green chemistry principles, as the samples required only 30 minutes of boiling under constant stirring, free from extreme temperatures or pressures. Based on these principles, the resulting nano-fertilizer produced blend is in perfect harmony with the environment, as the material inputs are derived from natural organic molecules that can also biodegrade. Supporting this idea is the EDS analysis, which showed that the synthesized material contained no heavy metals. This, in practice, means that if the same material is not absorbed by plants, it can either degrade or become part of soil organic matter without harming the ecosystem. This aligns with the green chemistry principle of degradation design and benign byproducts (Priya et al., 2023).

By this approach, the SDG goal 12 is thus supported, as the valorization of biowaste into useful input materials prevents waste generation and promotes the circulation of resources. This is achieved through the conversion of residues into biodegradable products, allowing them to integrate into the soil system without becoming a pollutant (Priya et al., 2023). Furthermore, the application of KOH as an extracting agent also qualifies it for compliance with green chemistry principles. Even though such a bold claim can spark controversy. The alignment of sodium hydroxide with green chemistry principles lies in its incorporation, with almost all its atoms used (alignment with atom economy). Another aspect that qualifies it for the green chemistry contest is the presence of potassium ions, which are important for serving as design chemicals since they form essential plant nutrients and are environmentally benign. Hence, overall, considering these alignment factors, the synthesis method and byproduct are deemed green.

The application of bio-based, eco-friendly nano-fertilizers is in line with the first two SDG goals (no poverty, zero hunger") as they can improve the use of nutrients efficiently and crop productivity. Crop productivity has a direct impact on food security and also improves the livelihood of farmers (Khundi et al., 2025; Zafar et al., 2024).

3.6 Conclusion

Rising research trends in sustainable materials science largely focus on the use of agricultural waste for the production of nanomaterials. In line with this, the current study successfully demonstrated that BPE, WRE, and ALvE can be utilized as renewable precursors for synthesizing green nano-fertilizers. The production of a non-covalent nanocomposite through the incorporation of these materials exemplifies the application of green chemistry in manufacturing agricultural inputs from low-value biomass.

Systemic control of environmental parameters, including alkaline pH, thermal conditions, and extract ratios, was accounted for during fabrication. Optimization of these factors enabled successful nanoparticle nucleation and stabilization through plant-derived agents. It was observed that higher concentrations of *Aloe vera* resulted in larger nanoparticles, highlighting the importance of compositional balance in tailoring physicochemical characteristics for agricultural applications.

Based on these findings, the study confirms the feasibility of synthesizing plant extract-mediated nano-fertilizers under controlled conditions. The results therefore support the hypothesis that these renewable biological resources can serve as effective precursors for the green synthesis of nano-fertilizers.

CHAPTER 4

THE IMPACT OF GREEN NANO-FERTILIZER ON SEED EMERGENCE PERCENTAGE AND PLANT GROWTH OF TOMATOES AND BELL PEPPERS UNDER GREENHOUSE CONDITIONS

4.1 Introduction

Ensuring adequate food production under the pressures of climate change and population growth requires the development and adoption of efficient and sustainable fertilizer sources (Pagano et al., 2025). One promising strategy that has recently gained attention involves the use of green nano-fertilizers synthesized from plant-derived extracts (Maaz et al., 2025). The concept of nano-fertilizers involves embedding or coating nutrients within nanomaterials, which facilitates a controlled nutrient release mechanism and enhances nutrient distribution and availability in soils (Demeke et al., 2025). The performance of nano-fertilizers may also be enhanced through nanoscale carriers that support interactions with beneficial soil microbes, resulting in reduced pathogen pressure and improved soil health and plant growth (Oyediran et al., 2025).

Green-synthesized nano-fertilizers sourced from plant extracts have successfully improved crop physiology, biochemical status and nutrient uptake of plants while improving the soil's nutrient capacity. For instance, efficient mobilization of exchangeable soil potassium in support of nutrient cycling at the root interface has been recognized via the application of potassium nanoparticles derived from *Artocarpus hirsutus* (wild jackfruit) (Peddi, 2025). Improved biomass and iron accumulation in plants has also been achieved with biogenic nanoparticles synthesized from *Calendula officinalis* (pot marigold) (Malekzadeh et al., 2024). On another note, zinc oxide nanoparticles that were fabricated using *Aloe vera* gel and *Coriandrum sativum* (coriander) extracts have driven the stimulation of root development, seed vigour, biomass responses and chlorophyll content in plants. This effect has also been shown to have a close association between rhizosphere activity and soil nutrient uptake (Singh et al., 2019; Ukidave and Ingale, 2022).

Further evidence echoes the preceding findings, as nanoparticles derived from banana peels have shown support for the early establishment of seeds (Hussein et al., 2019). Meanwhile, extended reinforcement emanates from *M. oleifera* (moringa)-based sulphur nanoparticles, which have proven to enhance osmolyte levels, photosynthesis and antioxidant activities in plants. Feeding into high nutrient returns and the rhizosphere health of crops (Khalifa et al., 2024). Nonetheless, despite the overwhelming positive feedback of plant-derived nanoparticles, some of them, like *Punica granatum* L. (pomegranate) peel-derived nano-hydroxyapatite, are subject to optimization by dosage as a result of pigment reduction effects (Abdelmigid et al., 2022b). Given these reports, the consensus amongst researchers is that plant-derived nano-fertilizers are a promising tool for spearheading improvements in plant growth by enhancing nutrient availability and soil biochemical activity. This effect has thus placed them at the cornerstone of agricultural innovation for sustainable soil fertility management.

In Chapter 4 of the present study, the impact of nano-fertilizer derived from a composite of banana peel extract (BPE) and watermelon rind extract (WRE), used as a nutrient source, and *Aloe vera* gel extracts (ALvE), used as a reducing and stabilizing agent, was evaluated. In this chapter, the performance of the resulting formulation was evaluated using seed emergence percentage and growth parameters of tomatoes and bell peppers. The approach aims to promote sustainable nutrient management by reducing reliance on inorganic salt precursors through the use of plant-derived materials, advocating for a circular economy.

Seedling establishment is a crucial stage in crop development, as successful emergence determines plant population and significantly influences overall crop productivity (Reed et al., 2022 ; Girgel, 2025). Adetimirin (2008), noted that emergence percentage offers notable selection index for assessing stand establishment and early field vigour. Similarly, it is often preferred because it serves as a more generalisable and intuitive metric for assessing stand establishment across different sites and years (Loarca et al., 2024). According to Božena Šerá (2023), seed-emergence percentage is among the most frequently reported parameters used to evaluate establishment potential in agricultural crops, cultivated trees, and wild plant species.

For the initial assessment, *Solanum lycopersicum* L. (tomato) and *Capsicum annuum* L. (bell pepper) were selected as the test species. Previous studies indicate that high-vigour seed lots of both species germinate rapidly and within a relatively narrow and uniform period when incubated near their thermal optimum (Demir et al., 2008; Jafari et al., 2024). Residual dormancy may delay and stagger seed emergence, thereby complicating the accurate assessment of treatment effects. Therefore, many reviews and experimental protocols recommend the use of fully after-ripened, high-vigour seed lots that exhibit rapid and uniform germination. This approach ensures that any observed differences in emergence can be attributed to the treatments rather than to inherent variation in seed physiology (Finch-Savage and Leubner-Metzger, 2006; Finch-Savage, and Bassel, 2016: Soppe and Bentsink, 2020; Marcinkowska et al., 2025).

Because the nano-fertilizer formulated in this study represents a novel plant-based system, with both the nutrient sources and synthesis agents derived from plant materials, its performance required initial evaluation under reliable germination conditions. This step was necessary to verify its biological effectiveness during early plant development. Determining baseline effectiveness under controlled emergence conditions creates a strong basis for future research that can extend the evaluation to crops with more complex germination patterns.

4.2 Materials and Methods

4.2.1 The study location

The study was carried out in a greenhouse facility at the University of Mpumalanga located in Mbombela, Mpumalanga Province, South Africa (25.4365° S, 30.9818° E). The Mbombela region receives an average annual rainfall of less than 867 mm. During the experiment, greenhouse temperatures were maintained between 25 °C and 30 °C using thermostatically controlled fans and wet wall cooling systems positioned at opposite ends of the structure.

4.2.2 Experimental design and cultural practices

Two separate experiments were conducted during two different growing seasons: February to June (Experiment 1) and June to October (Experiment 2) in 2024. The experiments were arranged in a 2 × 10 × 4 factorial design laid out in a completely randomized design (CRD), replicated three times. The factors included in the factorial design were crop type, composite of plant extracts (CPE) and the dosages as presented in Table 4.1.

Table 0.5: The 2 × 10 × 4 factorial design employed in the present study

Crop type	Composite of plant extracts (CPE)	Dose (mL)
Tomato	50%BPE+50%WRE+5mL ALvE (C1)	4 mL
Bell pepper	50%BPE+50%WRE+10mL ALvE (C2)	8 mL
	50%BPE+50%WRE+15mL ALvE (C3)	12 mL

75%BPE+25%WRE+5mL ALvE (C4)	16 mL
75%BPE+25%WRE+10mL ALvE (C5)	
75%BPE+25%WRE+15mL ALvE (C6)	
75%WRE+25%BPE+5mL ALvE (C7)	
75%WRE+25%BPE+10mL ALvE (C8)	
75%WRE+25%BPE+15mL ALvE (C9)	
Control (C10)	

Twenty-centimeter plastic pots, each containing approximately 2700 mL steam-pasteurized loam and sandy soil at a ratio of 3:1 (v/v) were placed in a 0.1 m intra and 0.3 inter- row spacings on the greenhouse floor. Seeds of tomato (*Solanum lycopersicum* L., cultivar Heinz 1370) and bell pepper (*Capsicum annuum* L., cultivar California Wonder) were purchased from a local supermarket in Mbombela, Mpumalanga Province, South Africa. The seeds were sown separately, with five seeds per pot. The treatments were applied at planting and every second week throughout the study period. As true leaves began showing, the seedlings were thinned with the aim of leaving one healthy plant per pot. Each pot was irrigated every second week with 250 mL of tap water. Weeds that emerged in the pots were manually removed by hand. During the entire period of the study (120 days) plant protection activities were carried out, such as scouting for pests and insects. Leaf miner and whiteflies presence were noticed and were treated with Karate Zeon pesticide at recommended dosage rates.

Figure 0.35: The experimental layout

4.2.3 Data collection

4.2.3.1 Seedling emergence percentage

The seed emergence percentage was determined by regularly monitoring the number of seeds that emerged from the soil surface over a period of 14 days. This process involved counting the emerged seedlings and calculating the percentage of seeds that successfully germinated using the formula demonstrated in Eq. 1 (Chen et al., 2023).

$$\text{Seedling emergency \%} = \frac{\text{Number of emerged seedlings}}{\text{Total number of seeds sown}} \times 100 \qquad (1)$$

4.2.3.2 Plant variables

Plant growth variables were recorded at 120 days after planting, and plant height was determined by measuring the distance from the crown to the tip of the flag leaf of each plant using a measuring tape. The number of flowers was manually counted when visible. Using a digital Vernier caliper (Model 464-9952, RS PRO, Midrand, South Africa), stem diameter was recorded at a position 5 cm above the cut end. The chlorophyll measurements were taken around the edge of the top leaf of each crop using a chlorophyll meter (Minolta spad-502, Hangzhou, China). The leaf length of the tomato and bell peppers was measured following a method described by Ding et al. (2020)

The leaf area was measured as reported by Cheng et al. (2023) using the relation shown in Eq. 2.

$$Leaf\ Area = L \times \mathrm{W} \quad (2)$$

Where, L is longest leaf length and W is maximum leaf width.

Roots were carefully collected from each pot and rinsed in water to remove adhering soil particles. Excess moisture was removed by gently blotting the roots with a laboratory towel before weighing. The samples were then oven-dried at 52 °C for 72 h to determine their dry matter content. Fruit mass was measured using an electronic top-loading digital laboratory balance (Model ELB 1200, Japan).

4.2.3.3 Soil variables

Soil from each pot was first thoroughly homogenized, after which 250 g samples were collected for the determination of electrical conductivity (EC) and pH. The collected samples were air-dried and passed through a 2 mm sieve prior to analysis. A 10 g subsample of the dried soil was transferred into a glass beaker containing 25 mL of distilled water, and the suspension was stirred vigorously for approximately 5 seconds using a glass rod. The mixture was then incubated for 50 minutes following the procedure described by Rayment and Higginson (1992). After incubation, the suspension was stirred again and left to settle for 10 minutes. The pH of the supernatant was measured using a calibrated pH meter, while electrical conductivity (EC) was determined using a calibrated EC meter (Thermo Orion Star A211 pH/EC meter).

Figure 0.36:Air dried samples of sandy loam soils

4.2.4 Statistical analysis

The normality of the data was evaluated using the Shapiro-Wilk test (Ghasemi and Zahediasl, 2012; Shapiro and Wilk, 1965). Statistical analyses were performed using Statistix version 10.0. The degrees of freedom and corresponding mean sum of squares (MSS) were partitioned to quantify the contribution of different sources of variation to the total treatment variation (TTV) of the measured variables. Mean separation was performed using Tukey's HSD test at a significance level of 5% (Mashela et al., 2015). Only parameters that were statistically significant at $p \leq 0.05$ were considered in the discussion, unless otherwise indicated (Mashela et al., 2015).

4.3 Results

4.3.1 Seed emergence percentage

The results have shown that for the computed seed emergence percentage, there was a significant difference for the composite of plant extracts (CPE), dose, and the interaction between crop type × composite of plant extracts × dose ($p \leq 0.05$), with TTV of 42.36%, 29.25%, and 4.97% in Experiment 1, respectively (Table 4.1). In Experiment 2, the results have shown that for the seed emergence percentage, there was a significant difference for CPE, dose, and the interaction between crop type × CPE as well as CPE × dose ($p \leq 0.05$), with TTV of 51.73%, 25.56%, 5.32%, and 4.55%, respectively (Table 4.4).

Table 0.6: Partitioning mean sum squares for the effect of green nano-fertilizer on seed emergence percentage in experiments 1 (February to June) and experiment 2 (June to October) at 14 days after applying the treatments.

		Experiment 1		Experiment 2	
Source	DF	MS	TTV (%)	MS	TTV (%)
Replication	2	26.7	0.33 ns	155	2.78 ns
Crop	1	735.0	9.21 ns	281.67	5.06 ns
CPE	9	3 381.7	42.36 ***	2 881.67	51.73 ***
Dose	3	2 335.0	29.25 ***	1 423.89	25.56 ***
Crop × CPE	9	235.0	2.94 ns	296.48	5.32 **
Crop × Dose	3	432.8	5.42 ns	41.67	0.75 ns
CPE × Dose	27	225.1	2.82 ns	253.52	4.55 **
Crop × CPE × Dose	27	397.0	4.97 ***	110.8	1.99 ns
Error	158	215,7	2,70	126.31	2.27
Total	239	7 983.9	100.00	5571.01	100.00

***Highly significant at p ≤0.001, **significant at p ≤0.05, ns not significant, TTV (%) Total treatment Variation

4.3.1.1 Effect of composite of plant extract (CPE)

The application of C7 recorded the highest seed emergence percentages (80%), followed by C1 (76.7%) and the lowest seed emergence percentage occurred on C9 (41.7%) in Experiment 1 (Figure 4.3). A pattern comparable to that observed in Experiment 1 was also observed in Experiment 2 for the composite of plant extracts. The formulation C7 produced the highest seed emergence (81.7%), followed by C1 (77.5%), and the lowest seed emergence occurred in C6 and C9 (50.8%) (Figure 4.4).

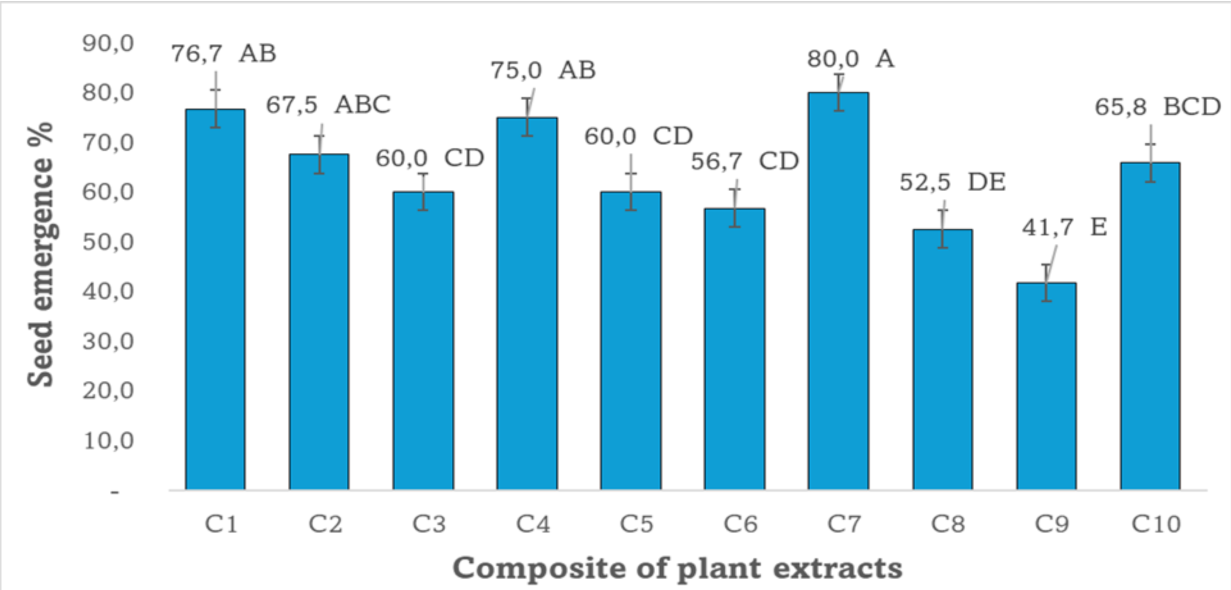

Figure 0.37: The effect of the composite of plant extracts on seed emergence percentage in Experiment 1.

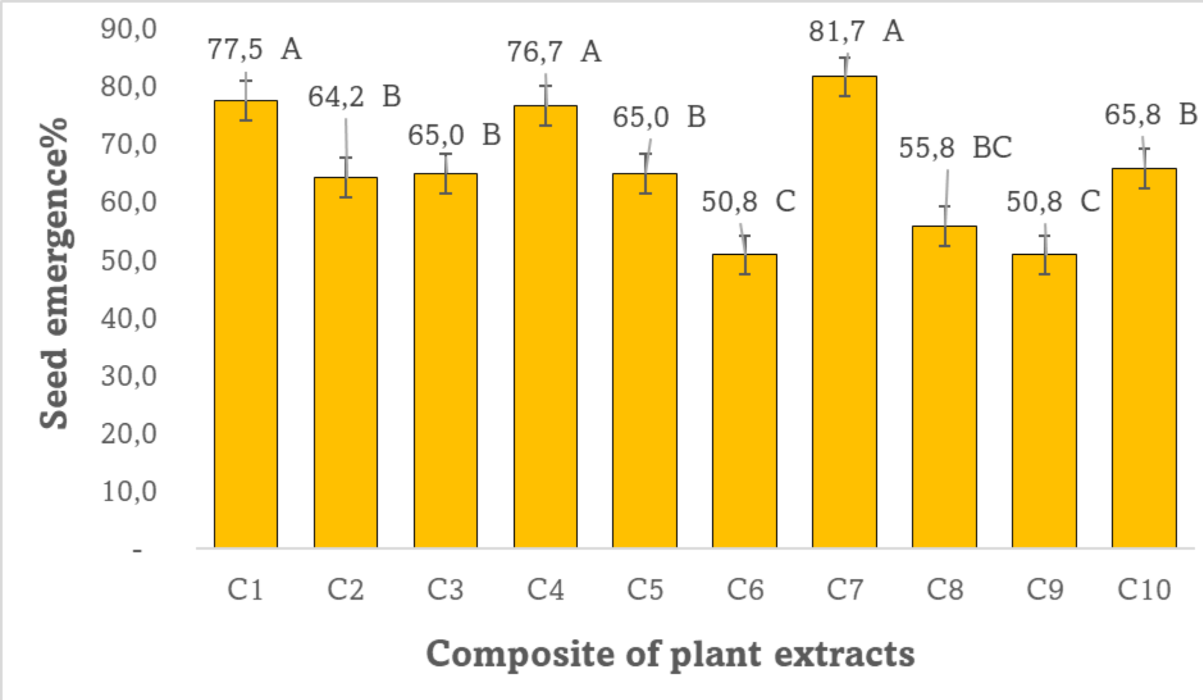

Figure 0.38: The effect of the composite of plant extracts on seed emergence percentage in Experiment 2.

4.3.1.2 Effect of dose

The lower application dose of 4 mL resulted in the highest seed emergence percentages (72.7%) and differed significantly from the other application doses, whereas the applications (8 mL, 12 mL, and 16 mL) were similar to each other and the application of 16 mL recorded the lowest seed emergence of 58.7% in Experiment 1 (Figure 4.5). The applications of 4 mL and 8mL did not differ from each other significantly, and exhibited a greater seed emergence of 69.3%. The application of 4 mL improved seed emergence in both experiments. In contrast, the application of 12 mL and 16 mL were significantly similar to each other, with 16 mL recording the lowest seed emergence (59.7%) (Figure 4.6).

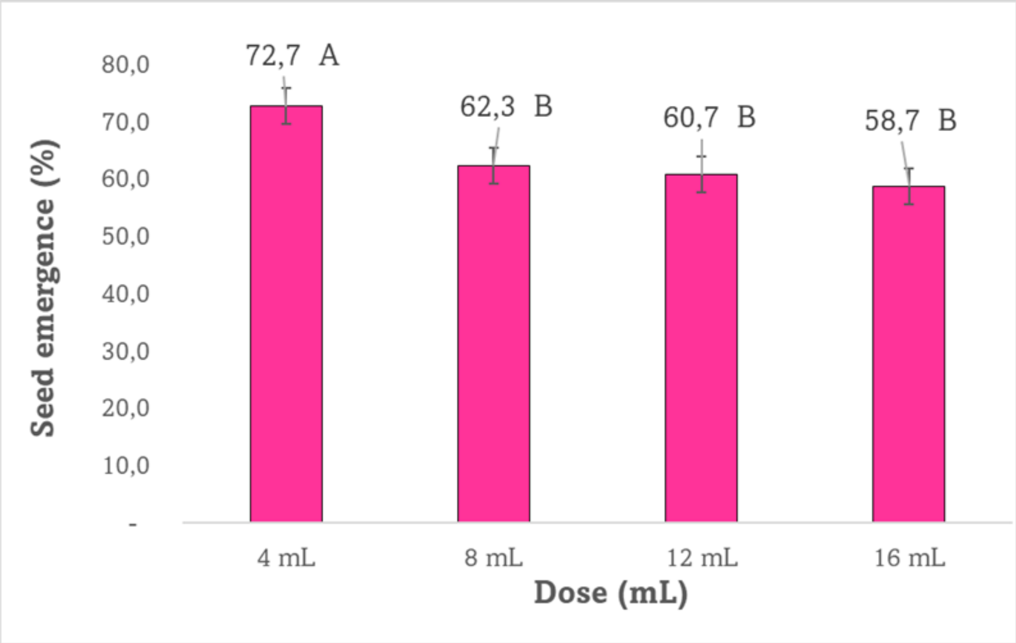

Figure 0.39: The effect of dose on seed emergence percentage in Experiment 1.

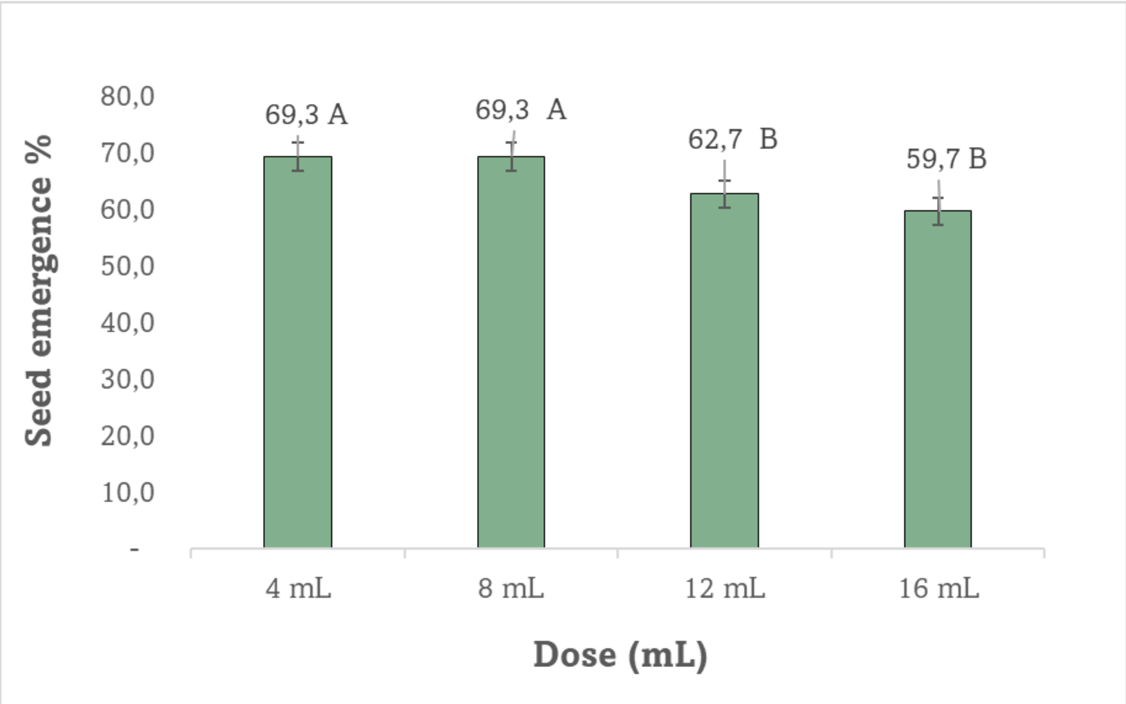

Figure 0.40: The effect of dose on seed emergence percentage in Experiment 2.

4.3.1.3 Effect of interaction

The results show that treatments had a positive influence in Experiment 1. Seed emergence increased in tomato crops with the application of C1 at 4 mL and C7 at 8 mL, reaching 93.3%, while the application of C9 at 12 mL led to lower seed emergence of 33,3%. In bell peppers, application of C1 and C7 at 4ml resulted in higher seed emergence of 86.7%, whereas the C9 at 12 mL yielded lower seed emergence of 20.0% (Table 4.3).

Table 0.7: The impact of interaction between crop type, composite of plant extract, and dose on seed emergence in Experiment 1

CPE	Dose	Tomato	Bell pepper
C1	4 mL	93.3^{a}	86.7^{ab}
	8 mL	80.0^{abc}	66.7^{abcd}
	12 mL	73.3^{abc}	73.3^{abc}
	16 mL	73.3^{abc}	66.7^{abcd}
C2	4 mL	73.3^{abc}	80.0^{abc}
	8mL	73.3^{abc}	66.7^{abcd}
	12 mL	60.0^{abcd}	60.0^{abcd}
	16 mL	66.7^{abcd}	60.0^{abcd}

C3	4mL	73.3^{abc}	53.3^{abcd}
	8mL	40.0^{bcd}	53.3^{abcd}
	12mL	60.0^{abcd}	73.3^{abc}
	16mL	80.0^{abc}	46.7^{abcd}
C4	4 mL	80.0^{abc}	80.0^{abc}
	8 mL	80.0^{abc}	73.3^{abc}
	12mL	60.0^{abcd}	73.3^{abc}
	16mL	73.3^{abc}	80.0^{abc}
C5	4mL	86.7^{ab}	53.3^{abcd}
	8mL	53.3^{abcd}	73.3^{abc}
	12mL	66.7^{abcd}	46.7^{abcd}

	16mL	46.7^{abcd}	53.3^{abcd}
C6	4mL	86.7^{ab}	66.7^{abcd}
	8mL	46.7^{abcd}	53.3^{abcd}
	12mL	40.0^{bcd}	73.3^{abc}
	16mL	40.0^{bcd}	46.7^{abcd}
C7	4 mL	86.7^{ab}	86.7^{ab}
	8 mL	93.3^{a}	73.3^{abc}
	12 mL	80.0^{abc}	73.3^{abc}
	16 mL	80.0^{abc}	66.7^{abcd}
C8	4 mL	66.7^{abcd}	66.7^{abcd}
	8 mL	53.3^{abcd}	53.3^{abcd}

	12 mL	46.7^{abcd}	40.0^{bcd}
	16 mL	46.7^{abcd}	46.7^{abcd}
C9	4 mL	66.7^{abcd}	33.3^{cd}
	8 mL	40.0^{bcd}	46.7^{abcd}
	12 mL	33.3^{cd}	40.0^{bcd}
	16 mL	53.3^{abcd}	20.0^{d}
C10		66.7^{abcd}	66.7^{abcd}

In Experiment 2, the application of C7 in tomato resulted in the highest seed emergence (78.3%), while C6 had the lowest (41.7%). Similarly, in bell pepper, the application of C7 resulted in higher seed emergence of 85.0%, and the application of C9 produced the lowest seed emergence of 48.3% (Table 4.4).

Table 0.8: The effect of interaction between crop type and CPE in Experiment 2

CPE	Crop type	
	Tomato	Bell pepper
C1	73.3^{ab}	76.7^{abc}
C2	63.3^{bcdefg}	65.0^{bcdef}
C3	63.3^{bcdefg}	66.7^{bcdef}
C4	78.3^{ab}	75.0^{abcd}
C5	61.7^{cdefg}	68.3^{bcde}
C6	41.7^{h}	60.0^{defg}
C7	78.3^{ab}	85.0^{a}
C8	58.3^{efg}	53.3^{efgh}
C9	51.7^{fgh}	48.3^{gh}
C10	66.7^{bcdef}	65.0^{bcdef}

The results showed that for most of the CPE, a lower dose resulted in higher seed emergence and as the dose level increased, seed emergence declined. However, an exception to this trend was observed with C4: increasing the dosage was associated with increased seed emergence. The highest seed emergence was achieved when 4 mL of C1 (90.0%) was applied and the lowest seed emergence occurred when C9 was applied at 16 mL (43.3%) (Table 4.5).

Table 0.9: The effect of the interaction between the composite of plant extract and dose in Experiment 2

CPE	Dose	Seed emergence
C1	4 mL	90.0[a]
	8 mL	76.7[abcd]
	12 mL	70.0[abcde]
	16 mL	73.3[abcde]
C2	4 mL	70.0[abcde]
	8 mL	70.0[abcde]
	12 mL	63.3[bcdef]
	16 mL	53.3[defg]
C3	4 mL	70.0[abcde]
	8 mL	73.3[abcde]
	12 mL	53.3[defg]
	16 mL	63.3[bcdef]
C4	4 mL	66.7[abcdef]
	8 mL	76.7[abcd]
	12 mL	80.0[abc]
	16 mL	83.3[ab]
C5	4 mL	70.0[abcde]
	8 mL	70.0[abcde]
	12 mL	56.7[cdef]
	16 mL	63.3[bcef]
C6	4 mL	60.0[bcdef]
	8 mL	63.3[bcdef]

	12 mL	30.0^{g}
	16 mL	50.0^{efg}
C7	4 mL	83.3^{ab}
	8 mL	80.0^{abc}
	12 mL	80.0^{abc}
	16 mL	83.3^{ab}
C8	4 mL	56.7^{cdef}
	8 mL	60.0^{bcdef}
	12 mL	53.3^{defg}
	16 mL	53.3^{defg}
C9	4 mL	53.3^{defg}
	8 mL	53.3^{defg}
	12 mL	50.0^{efg}
	16 mL	43.3^{fg}
C10	0	66.7^{abcdef}

4.3.2 Plant growth parameters

At day 120, after the initiation of treatments, it was observed that in Experiment 1, the different crop types had a significant effect on plant height and stem diameter ($p \leq 0.05$), with TTV of 51.77% and 59.44%, respectively. In addition to crop type, stem diameter was also influenced by the interactions of CPE and crop type and of CPE and dose ($p \leq 0.05$), with TTVs of 10.14% and 6.02%, respectively. However, in Experiment 2, plant height was significantly influenced by the crop type, CPE, and dose ($p \leq 0.05$), with TTV of 53.61%, 19.77%, and 9.32%, respectively. For stem diameter, crop type, CPE, interaction between crop type and CPE, and interaction between crop type and dose, with TTV ($p \leq 0.05$), with TTV of 63.06%, 11.80%, 5.65%, and 5.43%, respectively (Table 4.6).

It can be noted from Table 4.7 that the leaf length and leaf width were significantly influenced by both crop type and CPE ($p \leq 0.05$) in Experiments 1 and 2. The interaction of crop type and

CPE accounted for 98.36% and 0.48% of the TTV in Experiment 1 for leaf length, while for leaf width, the crop type and CPE contributed to 98.37% and 0.55%, respectively. In Experiment 2, crop type and CPE accounted for 91.40% and 5.26% of the TTV in leaf length, respectively. For leaf width, crop type and CPE accounted for TTVs of 92.15% and 3.69%, respectively (Table 4.7).

The results of Experiment 1 indicate that leaf area was significantly influenced by crop type and CPE, resulting in TTVs of 98.69% and 0.45%, respectively. However, the findings indicated that there was no significant difference ($p > 0.05$) across the factors for chlorophyll content in Exp 1. In Exp 2, it was noted that leaf area was significantly affected by crop type, with CPE of 92.60% and 3.23%, respectively. The chlorophyll content was significantly affected by crop type, only with TTV of 78.36% (Table 4.8).

Table 0.10: Partitioning mean sum squares for the effect of green nano-fertilizer on plant height, and stem diameter in experiments 1 (February to June) and experiment 2 (June to October) under greenhouse conditions at 120 days after applying the treatments (n=240)

		Experiment 1				Experiment 2			
		Plant height		Stem diameter		Plant height		Stem diameter	
Source	DF	MS	TTV (%)	MS	TTV (%)	MS	TTV	MS	TTV
Replications	2	8.95	1.58 ns	1.58	8.19	21.14	0.96 ns	7.01	6.14
Crops	1	294.15	51.77 ***	11.44	59.44 ***	1178.38	53.61***	71.94	63.06***
CPE	9	65.60	11.55 ns	1.95	10.14 ***	434.57	19.77 ***	13.46	11.80**
Dose	3	2.18	0.38 ns	0.76	3.94ns	204.79	9.32 **	2.83	2.48
Crops × CPE	9	65.79	11.58 ns	0.87	4.54ns	101.11	4.60 ns	6.45	5.65 ***
Crop type × Dose	3	8.61	1.52 ns	0.14	0.75ns	43.68	1.99 ns	6.19	5.43 **
CPE × Dose	27	31.39	5.52 ns	0.71	3.71ns	63.78	2.90 ns	2.31	2.02
Crop × CPE × Dose	27	54.98	9.68 ns	1.16	6.02 **	75.50	3.43 ns	1.71	1.50
Error	158	36.53	6.43	0.63	3.27	75.10	3.42	2.18	1.91
Total	239	568.18	100.00	19.25	100.00	2198.05	100.00	114.09	100.00

***Highly significant at $p \leq 0.001$. **significant at $p \leq 0.05$. ns not significant. TTV (%) Total treatment Variation

Table 0.11:Partitioning mean sum squares for the effect of green nano-fertilizer on leaf length and leaf width in Experiments(February to June) and experiment 2 (June to October) under greenhouse conditions at 120 days after applying the treatments (n=240)

		Experiment 1				Experiment 2			
		Leaf length		Leaf width		Leaf length		Leaf width	
Source	DF	MS	TTV (%)	MS	TTV (%)	MS	TTV	MS	TTV
Replications	2	1.73	0.12^{ns}	0.22	0.05^{ns}	2.65	0.22^{ns}	3.10	0.77
Crop	1	1450.42	98.36^{***}	402.23	98.37^{***}	1115.43	91.40^{**}	372.75	92.15^{***}
CPE	9	7.15	0.48^{**}	2.23	0.55^{**}	64.23	5.26^{**}	14.94	3.69^{***}
Dose	3	2.34	0.16^{ns}	0.05	0.01^{ns}	1.22	0.10^{ns}	1.01	0.25^{ns}
Crop × CPE	9	1.67	0.11^{ns}	0.88	0.21^{ns}	5.35	0.44^{ns}	2.65	0.66^{ns}
Crop × Dose	3	2.54	0.17^{ns}	0.43	0.10^{ns}	1.01	0.08^{ns}	0.70	0.17^{ns}
CPE × Dose	27	2.15	0.15^{ns}	0.72	0.18^{ns}	10.56	0.87^{ns}	3.53	0.87^{ns}
Crop × CPE × Dose	27	3.65	0.25^{ns}	1.15	0.28	11.48	0.94^{ns}	2.98	0.74^{ns}
Error	158	3.02	0.20	0.98	0.24	8.48	0.69^{ns}	2.82	0.70
Total	239	1474.67	100.00	408.88	100.00	1220.41	100.00	404.49	100.00

***Highly significant at $p \leq 0.001$. **significant at $p \leq 0.05$. ^{ns} not significant. TTV (%) Total treatment Variation

Table 0.12: Partitioning mean sum squares for the effect of green nano-fertilizer on leaf area in Experiment 1(February to June) and leaf area as well as chlorophyll content in Experiment 2 (June to October) under greenhouse conditions at 120 days after applying the treatments (n=240)

	Experiment 1			Experiment 2			
	Leaf area			Leaf area		Chlorophyll content	
Source	DF	MS	TTV (%)	MS	TTV	MS	TTV
Reps	2	12.0	0.02^{ns}	254.8	0.29 ^{ns}	432.27	9.77
Crop	1	71463.3	98.69***	81756.5	92.60 ***	3465.60	78.36***
CPE	9	324.1	0.45**	2850.1	3.23 ***	126.61	2.86
Dose	3	79.0	0.11^{ns}	190.7	0.22 ^{ns}	50.65	1.15
Crop × CPE	9	53.2	0.07^{ns}	793.9	0.90 ^{ns}	108.92	2.46
Crop × Dose	3	97.8	0.14^{ns}	201.3	0.23 ^{ns}	18.42	0.42
CPE × Dose	27	93.3	0.13^{ns}	871.2	0.99 ^{ns}	73.33	1.66
Crop × CPE × Dose	27	159.3	0.22^{ns}	812.9	0.92 ^{ns}	73.12	1.65
Error	158	127.2	0.18	558.2	0.63	73.66	1.67
Total	239	72409.20	100.00	88 289.60	100.00	4422.58	100.00

***Highly significant at p ≤0.001. **significant at p ≤0.05. ^{ns} not significant. TTV (%) Total treatment Variation

In Experiment 1, the source of variation aligned with crop type, CPE and the interaction of crop type, CPE and dose significantly influenced the number of flowers. The crop type contributed a major TTV of 71.71%, whereas CPE accounted for 6.61%. The interaction of crop type, composite of plant extracts and dose contributed to a TTV of 5.93%. Moreover, crop type significantly influenced fruit number and fruit mass, with TTVs of 68.49% and 64.93%, respectively. On the other hand, crop type significantly influenced the number of flowers, contributing to a TTV of 81.92% (Table 4.9). Among the biomass variables collected, fresh root was significant for CPE, accounting for 23.11% of the TTV in Experiment 1.

For Experiment 2, dry shoot mass, fresh root mass, and dry root mass were significantly influenced by source of variation aligned to crop type and CPE ($p \leq 0.05$). For dry shoot mass, crop type accounted for a TTV of 78.00%, while CPE contributed to a TTV of 6.79%. For fresh root mass, crop type contributed to a TTV of 62.10% and CPE accounted for a TTV of 12.12%. Crop type accounted for a TTV of 65.88% and 9.74% for CPE in dry root mass (Table 4.10).

Table 0.13: Partitioning mean sum squares for the effect of green nano-fertilizer on the number of flowers, the number of fruits, and fruit mass, in Experiment 1 and the number of flowers in Experiment 2, under greenhouse conditions at 120 days after applying the treatments

		Experiment 1						Experiment 2	
		Number of flowers		Number of fruits		Fruit mass		Number of flowers	
Source	DF	MS	TTV	MS	TTV	MS	TTV	MS	TTV
Replications	2	0.32	0.69^{ns}	0.99	16.89^{ns}	59.01	17.00^{ns}	15.43	6.38
Crop	1	23.44	71.71^{***}	4.00	68.49^{***}	225.39	64.93^{***}	198.02	81.92^{***}
CPE	9	2.16	6.61^{**}	0.09	1.59^{ns}	5.48	1.58^{ns}	6.05	2.50^{ns}
Dose	3	0.68	2.09^{ns}	0.08	1.40^{ns}	10.61	3.06^{ns}	2.96	1.22^{ns}
Crop × CPE	9	0.97	2.95^{ns}	0.08	1.34^{ns}	4.47	1.29^{ns}	5.48	2.27^{ns}
Crop × Dose	3	0.58	1.78^{ns}	0.04	0.64^{ns}	7.26	2.09^{ns}	0.49	0.20^{ns}
CPE × Dose	27	1.49	4.57^{ns}	0.21	3.51^{ns}	12.80	3.69^{ns}	4.69	1.94^{ns}
Crop × CPE × Dose	27	1.94	5.93^{**}	0.21	3.60^{ns}	12.22	3.52^{ns}	5.03	2.08^{ns}
Error	158	1.11	3.40	0.15	2.53	9.88	2.85	3.57	1.48
Total	239	32.69	100.00	5.85	100.00	347.13	100.00	241.73	100.00

***Highly significant at $p \leq 0.001$. **significant at $p \leq 0.05$. ^{ns} not significant. TTV (%) Total treatment Variation

Table 0.14:Partitioning mean sum squares for the effect of green nano-fertilizer on fresh root mass in Experiment 1 (February to June), and dry shoot mass, fresh root mass and dry root mass in Experiment 2 (June to October) under greenhouse conditions at 120 days after applying the treatments (n=240)

		Experiment 1		Experiment 2					
		Fresh root mass		Dry shoot mass		Fresh root mass		Dry root mass	
Source	DF	MS	TTV	MS	TTV	MS	TTV	MS	TTV
Replications	2	21.79	20.92	4.95	2.05^{ns}	18.63	2.46^{ns}	0.51	2.12^{ns}
Crop	1	4.50	4.32^{ns}	188.63	78.00***	470.37	62.10***	15.73	65.88***
CPE	9	24.06	23.11**	16.41	6.79***	91.80	12.12**	2.33	9.74**
Dose	3	3.89	3.74^{ns}	5.68	2.35^{ns}	15.96	2.11^{ns}	1.33	5.59^{ns}
Crop × CPE	9	16.99	16.32^{ns}	8.47	3.50^{ns}	50.80	6.71^{ns}	1.10	4.60^{ns}
Crop × Dose	3	7.020	6.74^{ns}	0.92	0.38^{ns}	22.02	2.91^{ns}	0.07	0.29^{ns}
CPE × Dose	27	7.60	7.30^{ns}	6.22	2.57^{ns}	26.03	3.44^{ns}	1.05	4.40^{ns}
Crop × CPE × Dose	27	7.91	7.60^{ns}	5.74	2.37^{ns}	26.84	3.54^{ns}	0.84	3.52^{ns}
Error	158	10.37	9.96	4.81	1.99	34.98	4.62	0.92	3.85
Total	239	104.13	100.00	241.83	100.00	757.42	100.00	23.87	100.00

***Highly significant at p ≤0.001. **significant at p ≤0.05. ^{ns} not significant. TTV (%) Total treatment Variation

4.3.2.1 Effect of crop type

The analysis revealed that crop types differed in their growth measures. In both Experiment 1 and 2, tomato plants recorded the highest plant height among bell pepper plants (Figure 4.7). A similar pattern was observed for stem diameter; tomato plants produced greater stem diameter than bell pepper plants in both Experiment 1 and 2 (Figure 4.8).

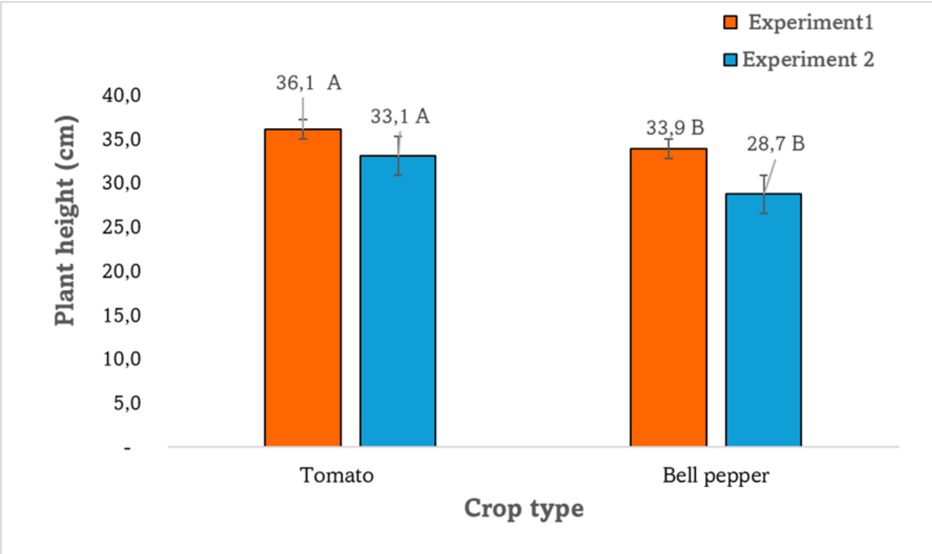

Figure 0.41: The effect of crop type on plant height in Experiments 1 and 2.

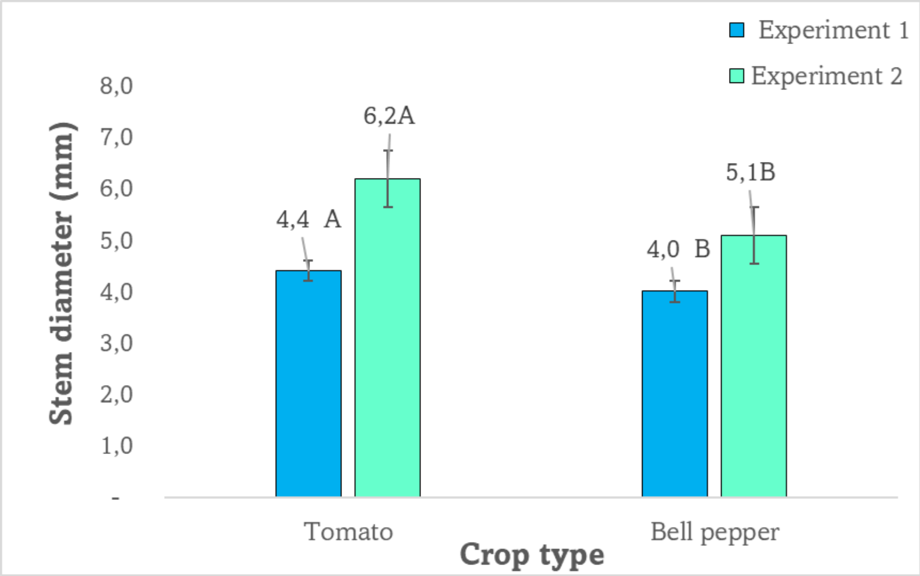

Figure 0.42: The effect of crop type on stem diameter in Experiments 1 and 2.

On the other hand, bell peppers showed superior leaf traits compared to tomato plants. In both Experiment 1 and 2, bell peppers recorded the highest leaf length (Figure 4.9), leaf width (Figure 4.10) and leaf area (Figure 4.11) than tomato plants. In addition, bell pepper plants recorded the highest chlorophyll content than bell pepper plants in Experiment 2 (Figure 4.12).

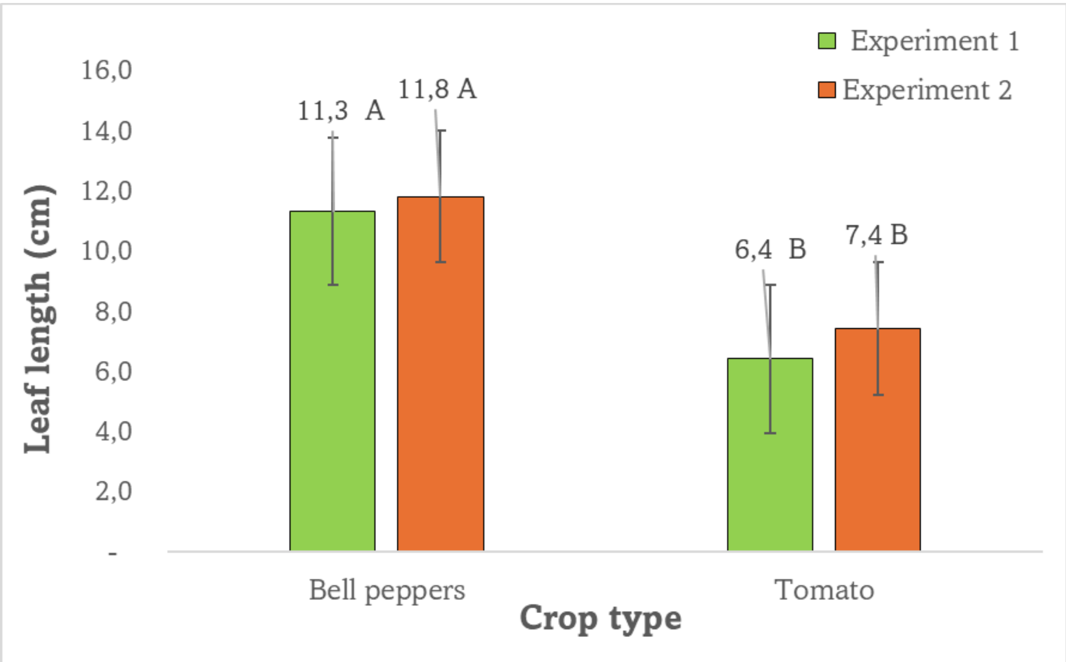

Figure 0.43: The effect of crop type on leaf length in Experiment 1 and 2.

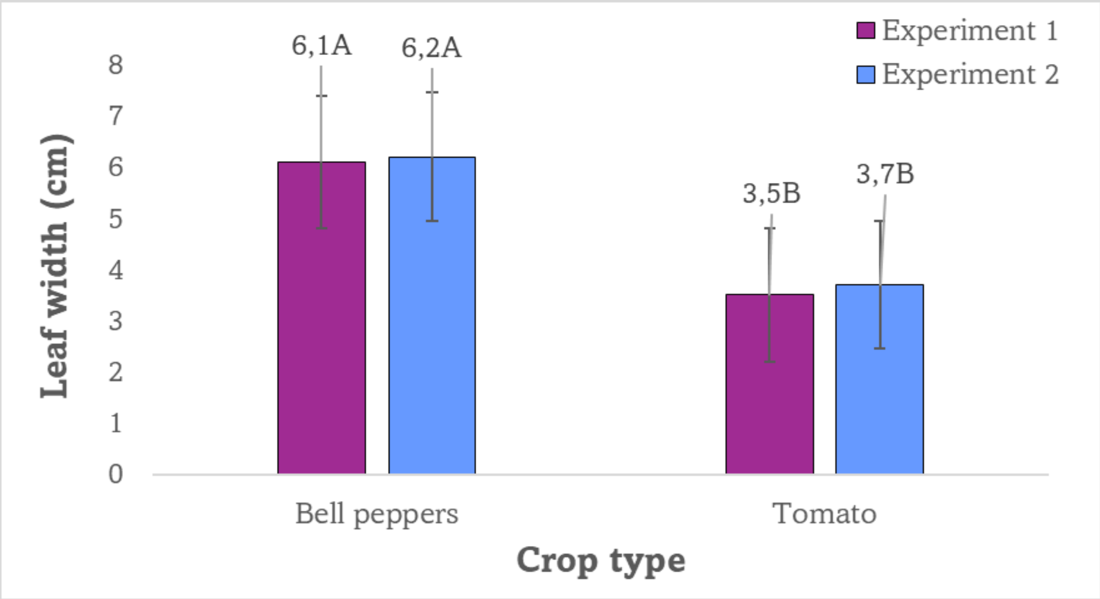

Figure 0.44: The effect of crop type on leaf width in Experiments 1 and 2

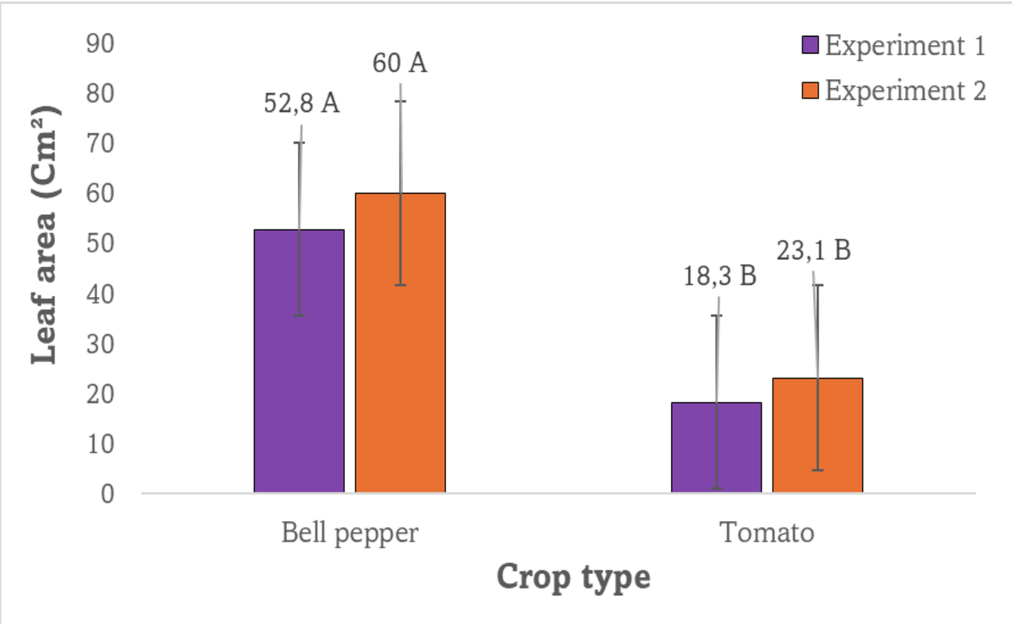

Figure 0.45: The effect of crop type on leaf area in Experiments 1 and 2

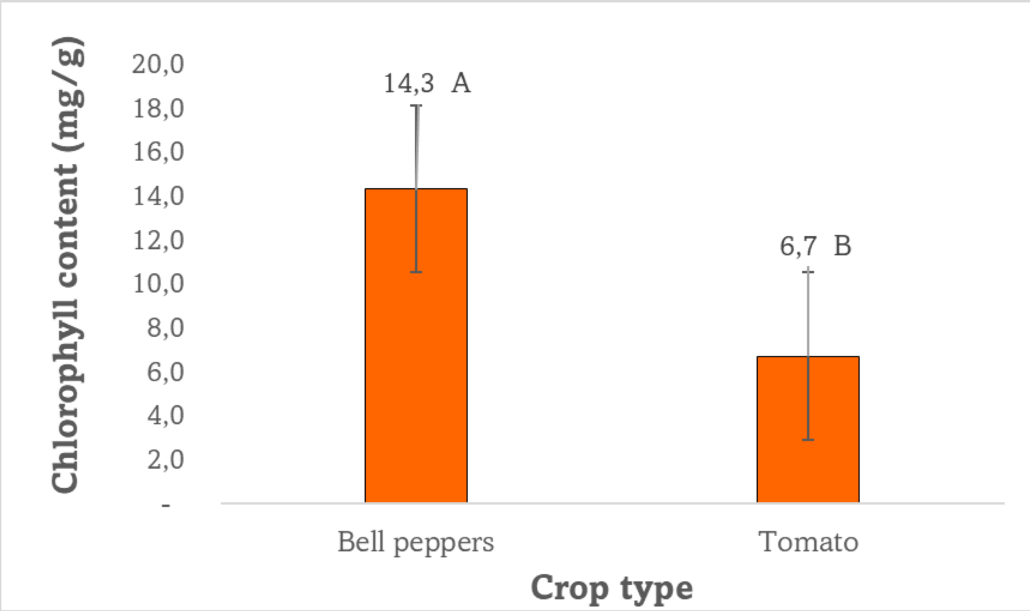

Figure 0.46: The effect of crop type on chlorophyll content in Experiment 2.

Tomato plants exhibited the highest flower count in Experiment 1 compared to bell pepper plants; however, in Experiment 2, the highest flower count was recorded in bell pepper plants and the lowest was achieved in tomato plants (Figure 4.13). Bell pepper crops recorded the highest number of fruits (Figure 4.14) and fruit mass (Figure 4.15) than tomato plants in Experiment 1.

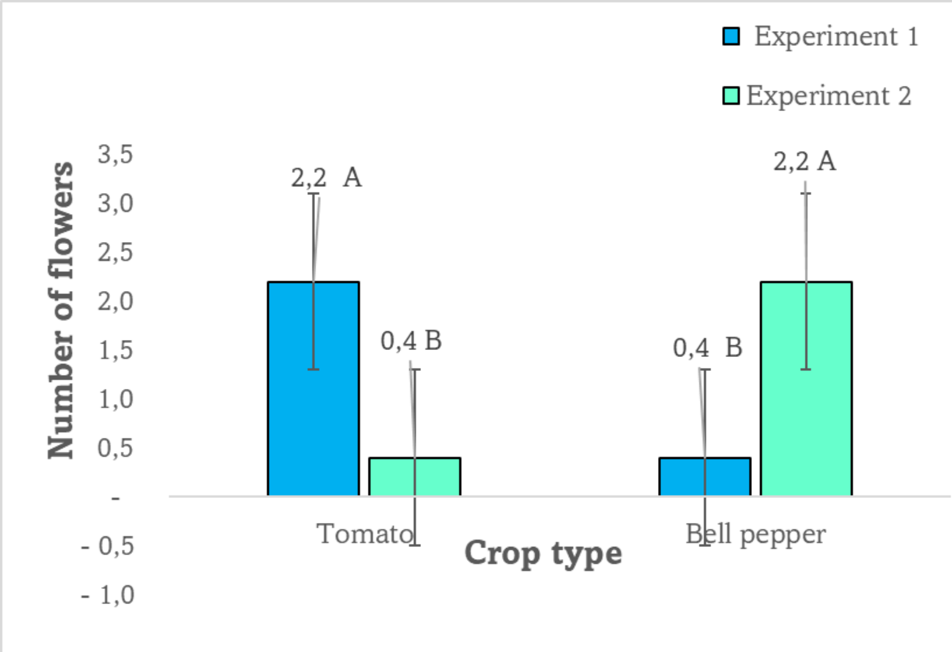

Figure 0.47: The effect of crop type on the number of flowers in Experiments 1 and 2.

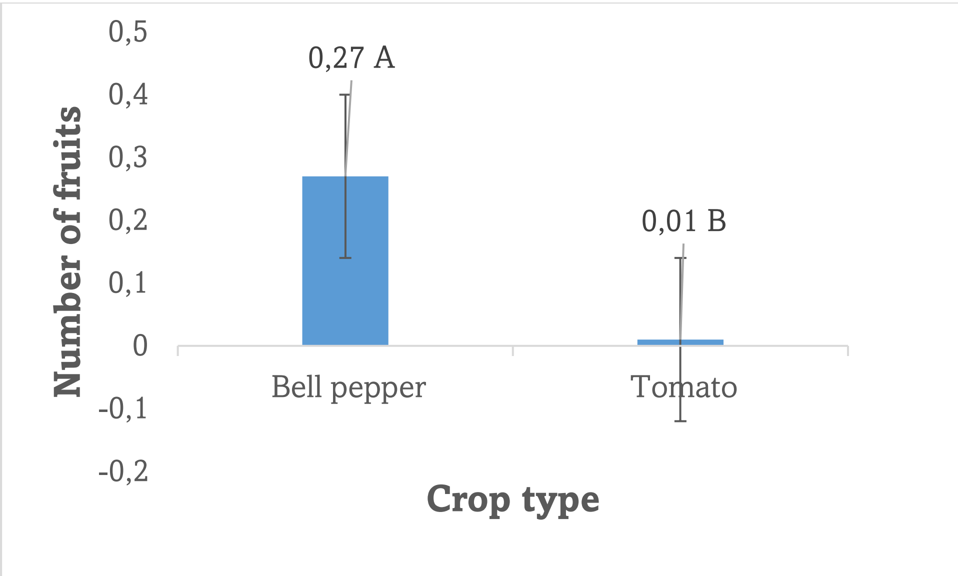

Figure 0.48: The effect of crop type on the number of fruits in Experiment 1.

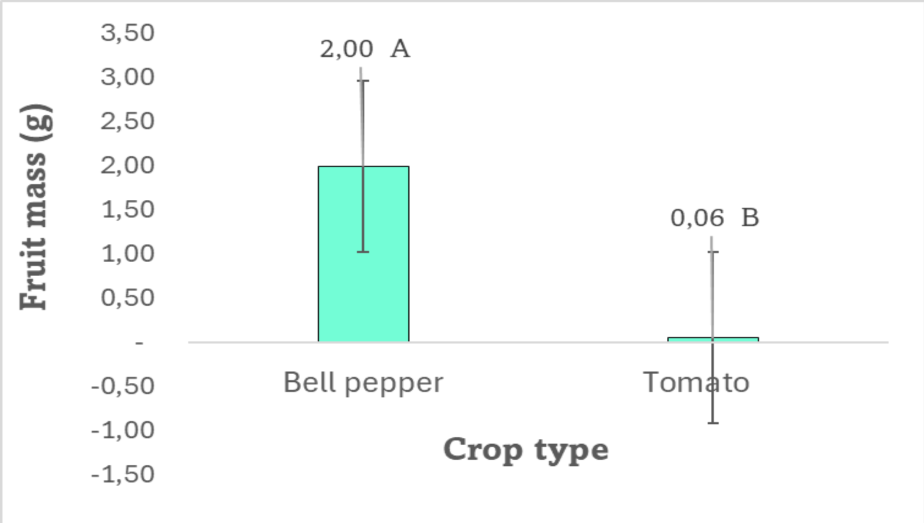

Figure 0.49: The effect of crop type on fruit mass in Experiment 1.

The effect of crop type on the biomass traits was more pronounced in Experiment 2. Tomato exhibited higher dry shoot mass (Figure 4.16), fresh root mass (Figure 4.17) and dry root mass (Figure 4.18) than bell peppers in Experiment 2.

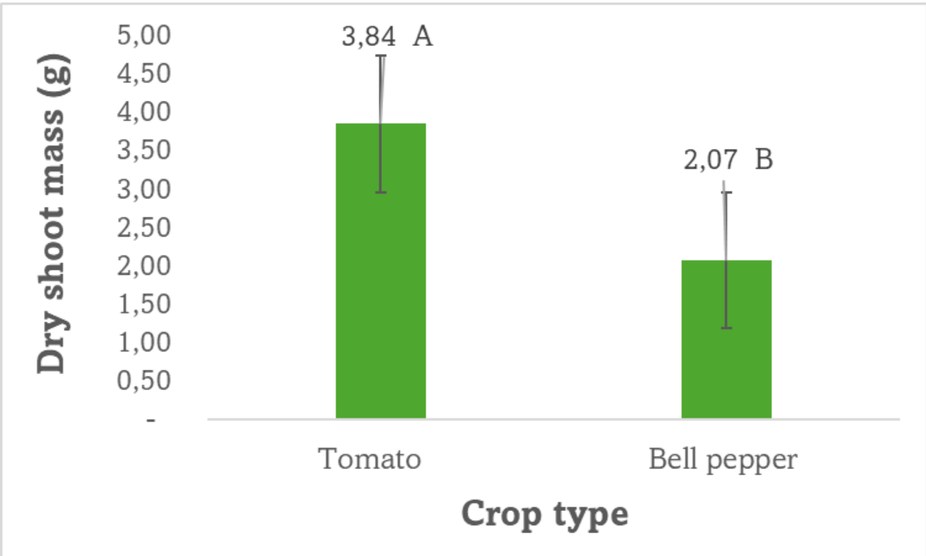

Figure 0.50: The effect of crop type on dry shoot mass in Experiment 2.

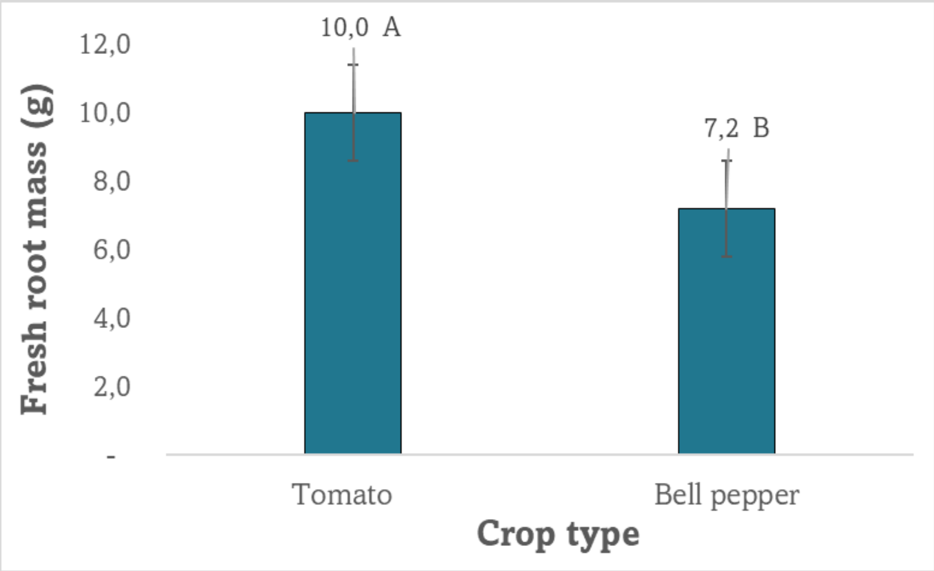

Figure 0.51: The effect of crop type on fresh root mass in Experiment 2.

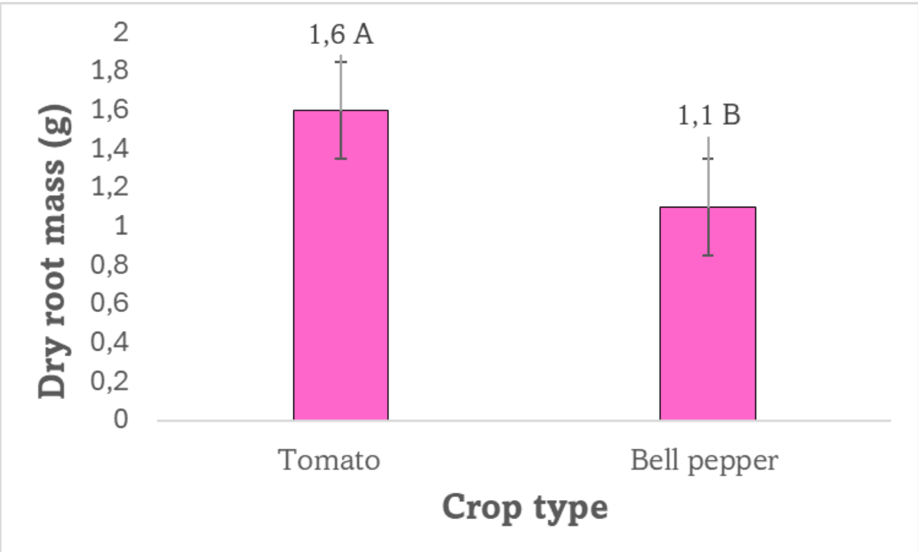

Figure 0.52: The effect of crop type on dry root mass in Experiment 2.

4.3.2.2 Effect of composite of plant extract (CPE)

The analysis showed that across the different CPE applied in Experiment 1, C1 produced the highest stem diameter and the control exhibited the lowest stem diameter. For leaf length, leaf width, and leaf area, despite the ANOVA indicating a significant difference among the CPE, the mean separation showed no distinction in mean letter designations. With regards to the number of flowers, the application of C1 produced the highest flower count, whereas the control produced zero flowers. The application of C7 resulted in higher fresh root mass and the control produced the lowest fresh root mass (Table 4.12).

In Experiment 2, the different CPEs performed similarly for plant height, except the C10, which produced the lowest plant height. A similar pattern was observed for stem diameter: there was no difference among the CPE, but they differed from C10, which produced a smaller stem diameter. With regards to leaf length and leaf area, the application of C8 exhibited greater values and was significantly different from C10, which recorded lower values. For the biomass traits (dry shoot mass, fresh root mass, and dry root mass), the application of C3 exhibited the greatest values and was significantly different from C10, which exhibited the lowest values (Table 4.13).

Table 0.15: The effect of CPE on stem diameter, leaf length, leaf width, leaf area, number of flowers, and fresh root mass in Experiment 1 (February to June)

CPE	Stem diameter (mm)	Leaf length (cm)	Leaf width (cm)	Leaf area (cm^2)	Number of flowers	Fresh root mass (g)
C1	4.80^{a}	8.6^{a}	4.8^{a}	34.7^{a}	1.1^{a}	5.5^{ab}
C2	4.48^{ab}	8.6^{a}	4.6^{a}	32.7^{a}	0.4^{ab}	3.9^{ab}
C3	4.16^{abc}	9.2^{a}	5.0^{a}	37.7^{a}	0.3^{ab}	3.6^{ab}
C4	4.11^{abc}	9.6^{a}	5.2^{a}	40.4^{a}	0.4^{ab}	4.7^{ab}
C5	4.07^{bc}	8.5^{a}	4.5^{a}	32.4^{a}	0.6^{ab}	4.7^{ab}
C6	4.27^{abc}	9.5^{a}	5.2^{a}	39.9^{a}	0.3^{ab}	5.2^{ab}
C7	4.05^{bc}	8.4^{a}	4.5^{a}	31.0^{a}	0.5^{ab}	6.3^{a}
C8	4.10^{abc}	9.5^{a}	5.2^{a}	40.1^{a}	0.6^{ab}	4.8^{ab}
C9	4.29^{abc}	8.5^{a}	4.0^{a}	34.2^{a}	0.8^{ab}	5.5^{ab}
C10	3.73^{c}	8.2^{a}	4.6^{a}	32.1^{a}	0^{b}	3.0^{ab}

Table 0.16: The effect of CPE on plant height, stem diameter, leaf length, leaf width, leaf area, dry shoot mass, fresh root mass, and dry root mass in Experiment 2 (June to October)

CPE	Plant height (cm)	Stem diameter (mm)	Leaf length (cm)	Leaf width (cm)	Leaf area (cm^2)	Dry shoot mass (g)	Fresh root mass (g)	Dry root mass (g)
C1	30.3^{a}	5.68^{a}	10.2^{ab}	5.0^{a}	44.1^{ab}	3.1^{a}	9.1^{ab}	1.3^{ab}
C2	34^{a}	6.33^{a}	10.4^{ab}	5.3^{a}	45.5^{ab}	3.4^{a}	9.7^{a}	1.4^{ab}
C3	34.3^{a}	6.34^{a}	11.2^{ab}	5.5^{a}	50.6^{ab}	4.0^{a}	11.3^{a}	1.9^{a}
C4	31.6^{a}	5.26^{a}	8.6^{b}	4.4^{ab}	33.7^{bc}	3.0^{a}	8.4^{ab}	1.2^{ab}
C5	30.7^{a}	5.88^{a}	9.5^{ab}	4.9^{a}	42.5^{ab}	3.6^{a}	9.7^{a}	1.7^{a}
C6	32.4^{a}	5.39^{a}	9.8^{ab}	5.1^{a}	39.7^{ab}	2.8^{ab}	8.9^{ab}	1.4^{ab}
C7	29.4^{a}	5.80^{a}	9.6^{ab}	5.4^{a}	43.9^{ab}	2.6^{ab}	7.7^{ab}	1.3^{ab}
C8	34.7^{a}	6.35^{a}	11.5^{a}	5.7^{a}	55.7^{a}	2.9^{ab}	9.4^{a}	1.3^{ab}
C9	31.8^{a}	5.80^{a}	9.8^{ab}	5.2^{a}	44.4^{ab}	3.1^{a}	7.8^{ab}	1.5^{ab}
C10	19.9^{b}	3.83^{b}	5.6^{c}	3.0^{b}	15.4^{c}	0.9^{b}	3.9^{b}	0.7^{b}

4.3.2.3 Effects of dose

The findings of this study revealed that dose only influenced plant height in Experiment 2, with the lower dose (4 mL) promoting greater plant height than the higher dose (16 mL) (Figure 4.19).

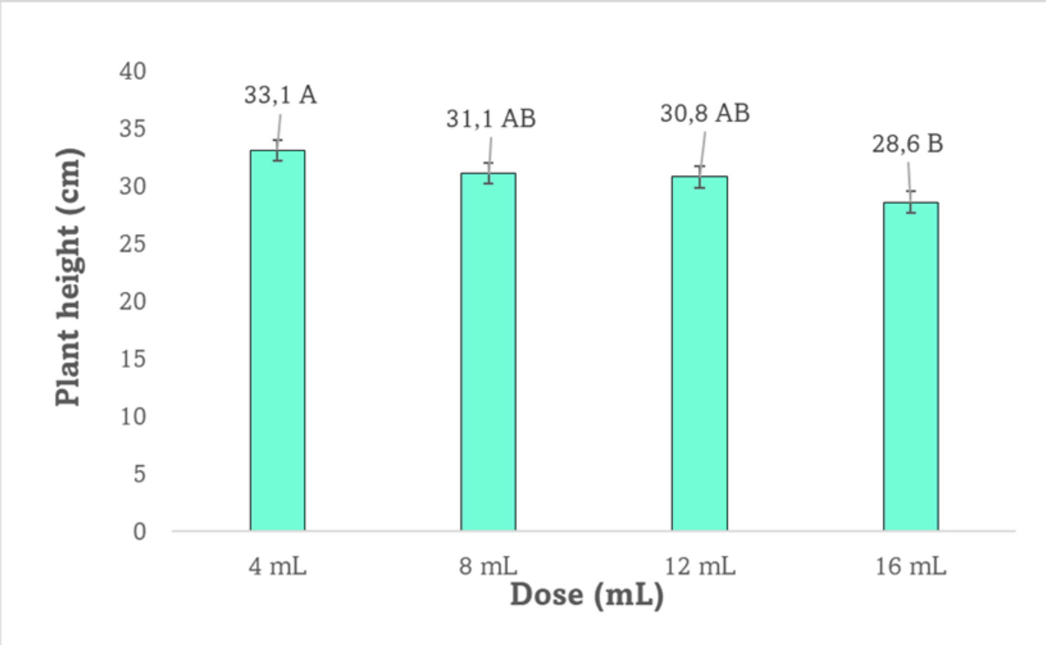

Figure 0.53: The effect of dose on plant height in Experiment 2.

4.3.2.4 Effect of interaction

In Experiment 1, tomato and bell peppers showed different responses with regard to stem diameter. For tomato plants, the application of C6 at 8 mL produced thicker stem diameters than C8 at 4 mL, whereas bell pepper plants responded similarly regardless of CPE or dose (Table 4.14). On the other hand, in Experiment 2, the interaction between crop type and CPE showed that crop types responded differently to the applied CPE with respect to stem diameter. In tomatoes, the application of C3 produced the highest stem diameter and was significantly different from C10, which recorded the lowest stem diameter. While in bell pepper, the highest stem diameter occurred when C8 was applied and C10 remained the lowest for bell peppers as well (Table 4.15). Following the interaction between crop type and dose, both tomato and bell pepper crops showed that differences in dose did not influence stem diameter, indicating that stem growth did not vary across all application levels (Figure 4.14). Even though ANOVA identified a significant difference (crop type × CPE × dose) interaction for the number of flowers in Experiment 1, the mean separation test indicated that treatment combinations performed similarly (Table 4.14).

Table 0.17: The effect of interaction between crop type, CPE, and dose on stem diameter and number of flowers in Experiment 1 (February to June)

CPE	Dose (mL)	Stem diameter (mm)		Number of flowers	
		Tomato	Bell pepper	Tomato	Bell pepper
C1	4 mL	5.67^{ab}	3.60^{abc}	0.0^{a}	2.3^{a}
	8 mL	4.87^{abc}	5.07^{abc}	3.3^{a}	0.0^{a}
	12 mL	5.60^{ab}	4.77^{abc}	0.0^{a}	1.3^{a}
	16 mL	5.53^{abc}	3.33^{abc}	1.0^{a}	0.7^{a}
C2	4 mL	3.93^{abc}	3.83^{abc}	0.0^{a}	0.0^{a}
	8mL	4.63^{abc}	5.23^{abc}	0.0^{a}	2.0^{a}
	12 mL	4.67^{abc}	4.23^{abc}	0.0^{a}	0.0^{a}
	16 mL	5.30^{abc}	3.97^{abc}	0.0^{a}	1.3^{a}
C3	4 mL	4.12^{abc}	3.57^{abc}	0.0^{a}	0.3^{a}
	8 mL	3.97^{abc}	4.33^{abc}	0.0^{a}	0.0^{a}
	12 mL	5.17^{abc}	3.40^{abc}	0.0^{a}	0.7^{a}
	16 mL	4.80^{abc}	3.90^{abc}	0.7^{a}	1.0^{a}
C4	4 mL	4.70^{abc}	3.67^{abc}	0.0^{a}	2.0^{a}
	8 mL	4.60^{abc}	3.80^{abc}	0.0^{a}	0.0^{a}

	12 mL	4.67^{abc}	3.63^{abc}	0.0^{a}	1.0^{a}
	16 mL	3.57^{abc}	4.23^{abc}	0.0^{a}	0.0^{a}
C5	4 mL	3.67^{abc}	4.00^{abc}	0.0^{a}	0.3^{a}
	8 mL	4.43^{abc}	2.97^{bc}	0.0^{a}	2.3^{a}
	12 mL	3.53^{abc}	4.07^{abc}	0.0^{a}	1.7^{a}
	16 mL	4.57^{abc}	4.33^{abc}	0.0^{a}	0.3^{a}
C6	4 mL	4.12^{abc}	4.33^{abc}	0.0^{a}	1.0^{a}
	8 mL	5.70^{a}	3.67^{abc}	0.0^{a}	0.0^{a}
	12 mL	4.07^{abc}	3.73^{abc}	0.0^{a}	0.0^{a}
	16 mL	4.23^{abc}	4.27^{abc}	0.0^{a}	2.0^{a}
C7	4mL	4.33^{abc}	4.10^{abc}	0.0^{a}	0.0^{a}
	8mL	4.67^{abc}	3.60^{abc}	0.0^{a}	1.7^{a}
	12mL	3.03^{abc}	4.50^{abc}	0.0^{a}	1.3^{a}
	16mL	3.80^{abc}	4.37^{abc}	0.3^{a}	0.7^{a}
C8	4mL	2.87^{c}	3.67^{abc}	0.0^{a}	1.0^{a}
	8mL	4.53^{abc}	3.73^{abc}	0.0^{a}	2.0^{a}
	12mL	4.8^{abc}	4.07^{abc}	0.0^{a}	1.0^{a}
	16mL	4.87^{abc}	4.30^{abc}	0.7^{a}	0.3^{a}
C9	4mL	4.33^{abc}	4.20^{abc}	0.0^{a}	0.0^{a}
	8mL	4.63^{abc}	3.97^{abc}	0.0^{a}	0.0^{a}
	12mL	4.20^{abc}	3.47^{abc}	1.3^{a}	3.0^{a}

	16mL	4.77^{abc}	4.73^{abc}	0.0^{a}	2.0^{a}
C10		3.47^{abc}	3.72^{abc}	0.0^{a}	0.0^{a}

Table 0.18: The effect of interaction between crop type and composite of plant extracts on stem diameter in Experiment 2 (June to October)

	Crop type	
CPE	Tomato	Bell pepper
C1	5.89[abcd]	5.46[bcde]
C2	7.46[ab]	5.20[cde]
C3	7.85[a]	4.83[cde]
C4	6.25[abcd]	4.28[de]
C5	6.36[abcd]	5.40[bcde]
C6	5.99[abcd]	4.78[cde]
C7	5.73[abcd]	5.88[abcd]
C8	6.61[abc]	6.10[abcd]
C9	5.65[bcd]	5.74[abcd]
C10	4.25[de]	3.41[e]

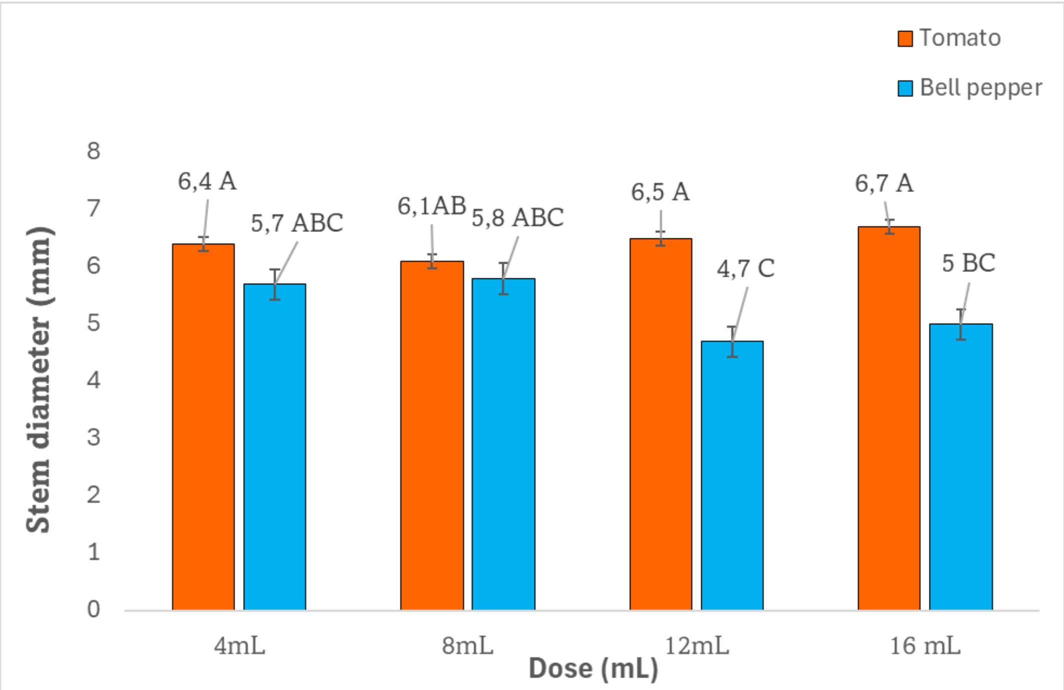

Figure 0.54: The effect of the interaction between crop type and dose in Experiment 2.

4.3.3 Soil variables

The soil samples collected before application of the treatments had a pH of 7.01 and an electrical conductivity (EC) of 0.77 dS/m. Crop type had a significant effect ($p \leq 0.05$) on soil pH only in Experiment 1. In the Experiment, all the factors had no significant effect on soil pH. The crop type accounted for a TTV of 58.01%. For EC, in Experiment 1, both the crop type and CPE had a significant effect ($p \leq 0.05$), contributing to a TTV of 52.91%, and 39.06%, respectively, whereas in Experiment 2, only the CPE had a significant effect on the EC, accounting for a TTV of 78.58% (Table 4.15).

Table 0.19: Source of variation affecting pH and EC in experiments 1 (February to June) and experiment 2 (June to October)

		Experiment 1				Experiment 2	
		pH		EC		EC	
Source	**DF**	**MS**	**TTV (%)**	**MS**	**TTV (%)**	**MS**	**TTV (%)**
Crop	1	0.74	58.01^{**}	0.11	52.91^{**}	0.004	2.12^{ns}
CPE	9	0.19	14.54^{ns}	0.08	39.06^{***}	0.130	78.58^{***}
Dose	3	0.21	16.16^{ns}	0.00	0.25^{ns}	0.008	4.90^{ns}
Error	60	0.14	11.28	0.02	7.79	0.024	14.40
Total	73	1.28	100.00	0.20	100.00	0.166	100.00

4.3.3.1 The effect of crop type

Bell pepper crop reduced the soil pH from 7.01 to 6.89 and tomato crop reduced the soil pH to 6.69 (Figure 4.21). On the other hand, the initial electrical conductivity (EC) measured was 0.77 dS/m; after crop growth, EC decreased in both soils, to 0.18 dS/m under bell peppers and 0.11 dS/m under tomato plants (Figure 4.22).

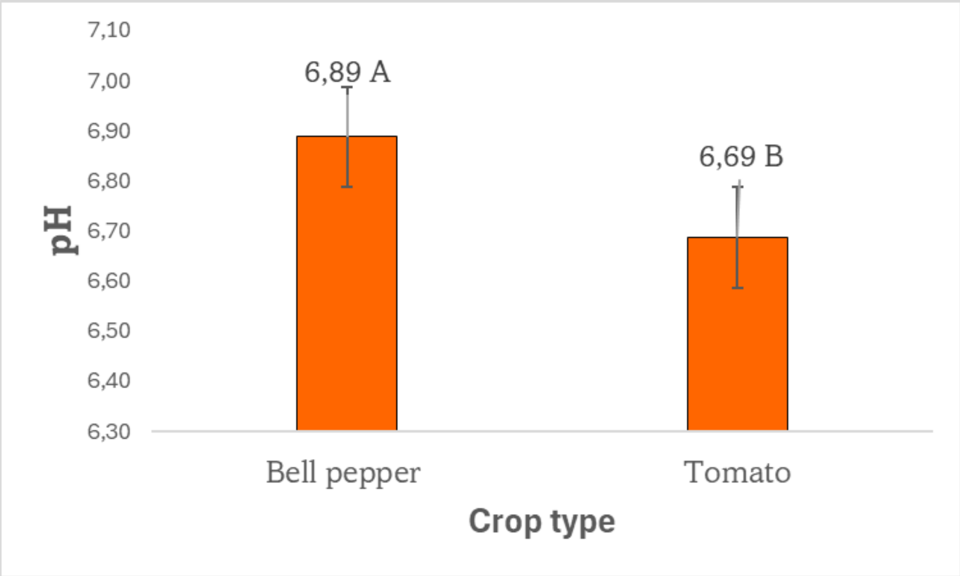

Figure 0.55: The effect of crop type on soil pH in Experiment 1.

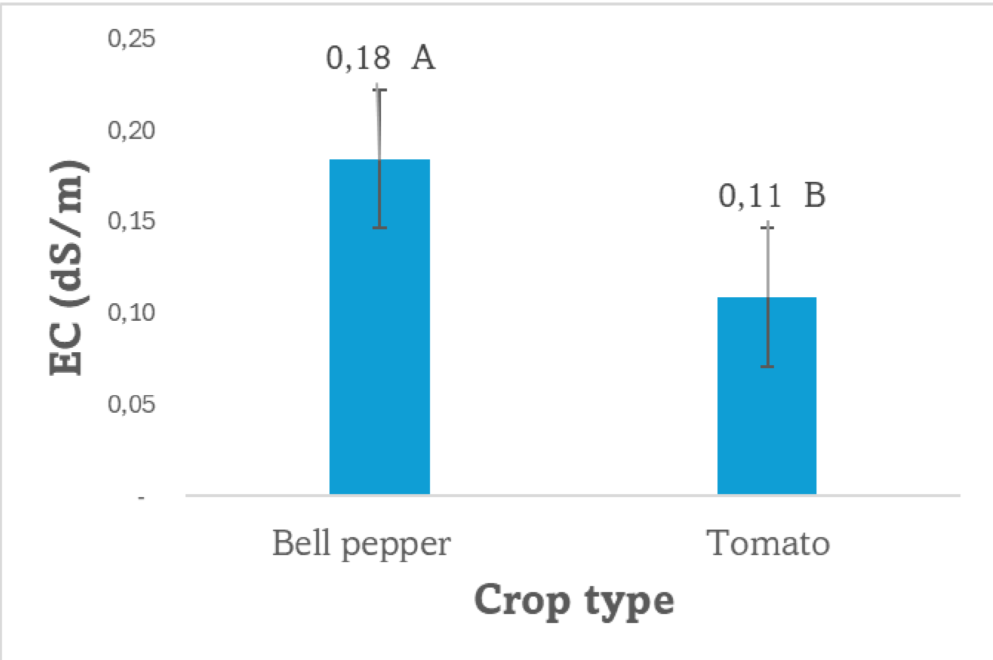

Figure 0.56: The effect of crop type on EC in Experiment 1

4.3.3.2 Effect of CPE

Soil EC was 0.77 dS/m before the application of the treatments. In Experiment 1, post-application of the CPE, the soil EC dropped across all the treatments; however, the extent of decline varied. The C10 application decreased EC to 0.40 dS/m, while the soil with CPE (C1-

C9) declined sharply to 0.07-0.36 dS/m. A similar trend was observed in Experiment 2, where C10 EC changed very little from 0.77 dS/m to 0.72 dS/m, while the soils treated with CPE had lower EC from 0.08-0.43 dS/m.

Table 0.20: The effect of CPE on EC in experiments 1 (February to June) and experiment 2 (June to October)

CPE	Experiment 1	Experiment 2
C1	0.36 ^{a}	0.43^{ab}
C2	0.08^{ab}	0.24^{bc}
C3	0.07^{ab}	0.21^{bc}
C4	0.08^{ab}	0.16^{c}
C5	0.11^{ab}	0.20^{bc}
C6	0.07^{b}	0.08^{c}
C7	0.13^{ab}	0.12^{c}
C8	0.09^{ab}	0.12^{c}
C9	0.08^{ab}	0.18^{bc}
C10	0.40^{a}	0.72^{a}

4.4 Discussion

4.4.1 Seed emergence percentage

Seed emergence percentage depends on numerous factors, including nutrient availability in the growth environment (Yadav et al., 2024). In this study, the factors influencing seed emergence percentage only differed slightly between the two experiments. The results showed that for the computed seed emergence percentage, there was a significant difference for the CPE, dose, and the interaction between crop type × CPE × dose in Experiments 1 and 2. From this observation, we hypothesize that, even under greenhouse conditions, microclimatic heterogeneity can occur, with variations in temperature, carbon dioxide concentration, and humidity influencing plant physiological responses (Jerszurki et al., 2021).

In both Experiment 1 and 2, a similar trend was observed: formulations containing a lower amount of *Aloe vera* gel extract (below 5 mL) resulted in higher seed emergence percentage, whereas formulations containing a higher amount of *Aloe vera* gel extract showed a decline in seed emergence percentage (Figures 4.3 and 4.4). Hakeem et al. (2025), demonstrated that ALvE contains plant growth regulators such as Benzylaminopurine (BAP), indole-3-acetic acid (IAA), and gibberellic acid (GA_3). At lower concentrations, the extract of *Aloe vera* gel may function as a biostimulant, providing a small amount of natural phytohormones, enhancing enzyme activity and stimulating cell elongation and division, improving seed germination and seedling development (Lalitha et al., 2016; Moharana et al., 2018; Sajjad et al., 2020).

Although ALvE has the potential to enhance seed germination, its stimulatory effect is strongly influenced by the applied concentration. This is substantiated by Al-Maathedi and Mohammad (2020), who reported that increasing the concentration levels of ALvE from 5%-20% significantly reduced the seed germination rate of *Senna siamea* (Kassod) and *Cassia surattensis* (Scrambled egg) seedlings. The authors attributed this decline to the presence of allelochemicals in ALvE extract, which may exert inhibitory effects on germination and negatively influence physiological processes and cell division. In addition, when plant extract concentrations are too high, they increase the osmotic pressure around the seeds, thus preventing the seeds from taking up enough water, which in turn lowers germination (Salam et al., 2018).

Moreover, the observed decline in Experiment 1 and 2, for seed emergence percentage with increasing dose in formulations containing a higher amount of *Aloe vera* gel extract, supports the characteristic biphasic response associated with hormesis. This response is well documented in prior studies, which describe how low concentrations of biostimulants enhance germination, while higher doses inhibit it (Pannacci et al., 2022; Agathokleous et al., 2023). Ali et al. (2020) revealed that a lower dose of *Cuscuta reflexa* (Giant dodder) extract stimulated germination-related enzymes such as protease and α-amylase improved water uptake by lowering osmotic potential. At higher doses, however, the opposite effect occurred. It is therefore important to optimize the plant extract formulation to determine which formulation promotes the best performance.

4.4.2 Plant growth variables

The crop type displayed a vivid and consistent effect on plant growth in Experiments 1 and 2 (Figure 4.7-4.18). The findings revealed that tomato plants showed stronger structural growth, whilst bell pepper crops showed greater leaf development. In light of this observation, the contrasting trend highlights distinct growth strategies among the two crop types. Higher biomass accumulation was observed in tomato crops, whereas bell pepper crops showed greater leaf expansion and photosynthetic potential, as indicated by high chlorophyll content. This growth trend is backed by several reports, which have pointed out that crop genotypes tend to yield different structural growth traits as a result of genetic vigor and different growth responses to growth-regulating factors among varying plant species (Miao et al., 2024; Yoshiyama et al., 2024).

Despite similar growth conditions to which the crops were exposed in both Experiments, the CPE applied produced varying growth responses across all trials (Li and Mattson, 2019). This is because greenhouse conditions rarely follow a perfect uniform consistency of environmental conditions due to varying crop geometry and greenhouse management (Santosh et al., 2017). Santosh et al. (2017)'s observation was confirmed in a tomato crop study by Šalagovič et al. (2024) under greenhouse conditions for three consecutive years. Their study found that the temperature and humidity varied from each zone, yielding differences in stem growth, fruit growth rate and final yield due to varying microclimates within the greenhouse itself. In another study by Triana et al. (2024), it was found that peppers grown in one corner of the greenhouse received a cooler, more humid microclimate and had lower vapor-pressure deficit than other parts. Placing emphasis on micro-environment variability due to the location status of each plant within the greenhouse. Further inferring the view that even if the plants are given the same fertilizer treatment, differences in their individual local climates may still affect their growth responses, causing them to vary. This view is further reinforced by Choi and Yang (2025), who found that, despite the typical gradual, near-linear transitions of greenhouse microclimates, the occurrence of abrupt external weather conditions and actuator operations imposes nonlinear dynamics that increase the complexity of accurately predicting and interpreting greenhouse microclimate conditions.

In Experiment 1, some treatment combinations, such as C1, improved stem diameter and flower production, whereas C7 treatments excelled at improving root mass, with the remaining CPE yielding minimal improvements, slightly above the control group. In Experiment 2, more pronounced effects of CPE treatments were observed, with the control group showing consistently lower values; meanwhile, composites such as C3 and C8 showed increased biomass and leaf development. This trend reveals that different CPE treatments have varying effects on plant growth, as widely reported in biostimulant research (Cristofano et al., 2021; El-Nakhel et al., 2023). Their studies revealed that the plant’s response is closely linked to the concentration and composition of three major factors, viz. phytohormones, antioxidants, and other bioactive compounds in each formulation (El-Nakhel et al., 2023). This means that observed physiological effects on plant growth parameters are heavily influenced by the formulation's chemical composition. In a review by Ali et al. (2021), it is revealed that biostimulants can selectively improve the architecture of the roots, chlorophyll within leaves, flowers, as well as the setting of the fruits, hence the varying effects of some of the CPEs being “root/shoot focused” whilst others were “flower focused.”

Several research publications over accumulated decades (Oliveira et al., 2023; Schwab et al., 2016) also reveal that the diameter of each particle can still alter the shape of the entire plant-nanomaterial interaction process, from root entry to physiological effects. Nutrient uptake studies have shown that particles below 20 nm are readily susceptible to migration into the 5-20 nm pores of the primary cell wall and can even move through the plasmodesmata. This can then lead to rapid whole-plant translocation and, at times, provide a dramatic germination boost, as well as support or improve photosynthesis and micronutrient status. However, the 20 nm threshold is not absolute, as some studies also reflect that nanoparticles as large as 50 nm can still very much penetrate the plant cell wall (Djanaguiraman et al., 2024; Djanaguiraman et al., 2018;González-Melendi et al., 2008; Ha et al., 2021). This suggests that other factors, such as cell-wall plasticity, pore enlargement, aggregation state, and nanoparticle chemistry, also play a huge role in nutrient uptake (Djanaguiraman et al., 2024).

Recent reports indicate that large particles lying above 50-300 nm enter plant tissues and the findings were confirmed via TEM that silicon dioxide nanoparticles sized at 54 nm could enter the leaves of *Arabidopsis thaliana* (El-Shetehy et al., 2021). Lian et al. (2021) also observed via TEM that polystyrene nanoplastic particles at an average size of 93.3 nm were detected on lettuce leaves through stomatal uptake. Jia-Yi et al. (2022) also tested chitosan-based silicon particles with an average size of 166 nm and found that they were successfully absorbed by rice leaves and spread across their cells. Another study by Lin et al. (2021) on *Camellia Oleifera* (oil tea plant) seedlings found that hydroxyapatite nanoparticles as a phosphorus source improved plant height, stem diameter, and lettuce biomass. Noting that nanoparticles of smaller size (20 nm) were more mobile and hence led to a higher loss of phosphorus compared to 200 nm sized ones, not due to better penetration, but the larger particles stayed in the rhizosphere and released the phosphorus accurately and slowly. Meanwhile, these larger particles were successfully absorbed by crops. Zhao et al. (2018) confirmed that fluorescein isothiocyanate (FITC)-labeled mesoporous nanoparticles (MSNs), even at larger sizes of 200-300 nm, could still be absorbed by cucumber leaves. In view of these findings, it is scientifically proven that the common ≤20 nm plant cell wall absorption does not disqualify the benefits of larger particles, since other factors such as cell wall plasticity, pore enlargement, aggregation state, and NP chemistry also come into play.

The emphasis here is that larger particles do not necessarily penetrate the plant cell wall directly but do so via a slow-release mechanism, in which they enter plant tissues via apoplastic/stomatal and cuticular epidermal pathways before being absorbed by cells (Wang et al., 2023). In fact, according to a review by Schwab et al. (2016b), it was reported that a vast number of studies have reflected that the "uptake, clogging, or translocation in the apoplast of plants" has mostly been observed from nanoparticles much larger than the 5-20 nm size exclusion limit of plant cell walls. Besides these pathways, some particle absorptions impose a rather "forceful entrance" into plant cell walls, as observed in the epidermal cells of root cell walls, with minute pores causing large particles to be impermeable, yet they remain semi-permeable (Pérez-de-Luque, 2017). Therefore, when the roots lack the exodermal layer, nanoparticles may still penetrate via the xylem central column. However, this just hints at the core mechanism of anomality. Previous studies have found that some nanoparticles can disrupt the plasma membrane and thus induce new pore formation in the epidermal layer of the cell wall, thereby increasing permeability to larger particles (Ali et al., 2021). Another study by Kim et al. (2014), revealed that nano zerovalent iron (ZVI) contributes to the degradation of pectin found in plant cell walls via hydroxyl radical reaction. This action increases their mobility within plant tissues. The authors also highlighted that the plant is selectively permeable, meaning that polar compounds such as water and other ions fail to diffuse into the phospholipid bilayer and are therefore translocated via the apoplast. This is because this pathway is found in several key locations, viz., outside the membrane, through cell walls, intercellular spaces, and xylem vessels. The apoplast allows for lipid bilayer restrictions, which allows for bulk flow of water and solutes until they encounter the Casparian strip in the endodermis, where selective uptake into the symplast is forced (Farvardin et al., 2020; Gámez-Arjona et al., 2022). Another factor is that the issue of engineered nanoparticles (ENMs) can trigger a complex transport of nanoparticles and their transformation, regulated by three critical factors such as particle size, surface coating and environmental aging (Islam, 2025b).

Both pattern trends of nanoparticle effects, based on extremely small or larger particles, were reflected in the current study, as C1 and C7 showed ultra-small and scattered nanoparticles with sizes of 4-8 nm. These sizes ensured that both the stem diameter and the production of flowers were improved. In contrast, larger particles represented by C3 (540 nm) and C8 (289 nm) showed dominance in biomass and leaf improvement. Together, the presented data demonstrate that diverse effects associated with different nanoparticle sizes yield distinct benefits. These can range from instantaneous signaling effects to the sustained release of nutrients, thus dismantling the universal notion that performance ranking is best determined by particle size. This is supported by recent findings by Djanaguiraman et al. (2024), who indicated that “nanoparticles exhibit positive and negative impacts on biota due to their size, surface property, concentration within the system, and species or cell type under test.”

Regarding plant height, a classic pattern based on dosage was observed: 4 mL (moderate treatment) enhanced shoot elongation compared to 16 mL (higher dosage), which suppressed it. This “low-dose stimulation/high-dose inhibition” trend has also been reported from other plant extract treatments. For instance, Deepana et al. (2021) applied 12.5 kg/ha of seaweed extract (SWE) when growing rice in soil, coupled with a 0.5% foliar application, which yielded the highest plant height (46.6 cm). However, higher SWE failed to improve plant height (33.6 cm) and only became superior in enhancing plant available nutrients such as N, P, K, Ca, Mg, S and micronutrients as a result of plant growth regulators such as auxin, gibberellins and cytokinin within the SWE (Deepana et al., 2021). Other researchers examined the impact of green seaweed *Ulva intestinalis* (gutweed). on the germination and root development of *Arabidopsis thaliana* (Thale cress). In their findings, they reported that only SWE below 1% was most effective in promoting root growth, whereas higher concentrations inhibited lateral root formation (Ghaderiardakani et al., 2019). Furthermore, Ghaderiardakani et al. (2019) warned that algal extracts such as this should be used cautiously, as higher concentrations outweigh the fertilizer benefits for crops, especially for the investigated crop. Independently, Di Filippo-Herrera et al. (2021) investigated the potential of seaweed liquid extract (SLE) from microalgae species to determine their performance as a biostimulant on *Vigna radiata* L. (mung beans). The results revealed that the SLEs at low concentrations (0.12-0.5%) stimulated root length, shoot length and dry weight. On the contrary, higher doses (1.0-2.0%) inhibited growth, yielding shorter roots and reduced biomass. These studies align with the findings of the current study and also correlate with other reported findings that higher concentrations of plant extracts tend to inhibit root growth and plant height in tomato and bell pepper plants, except in retaining nutrients or biomass.

The interaction between crop type, × CPE × dose revealed that in the two experiments, tomato plants presented variation in stem diameter due to the influence of CPE × dose. The bell peppers, however, retained a stable stem diameter across the treatments. This effect suggests that the interaction with treatments is dependent on the crop type, as a result of varying physiological and genetic traits between the two crop species, as confirmed by other researchers on different crops (Cristofano & El-Nakhel, 2020; Franzoni et al., 2022; Pereira et al., 2019). In addition, fluctuations in CPE composition and complex interactions between CPE and crop type likely contributed to inconsistent results across experiments. Since there are overlapping effects and batch-to-batch differences of CPE formulations, coupled with potential interactions between CPE type and dosage application (Povero et al., 2016; Yakhin et al., 2017).It is thus impossible to identify a single CPE or specific dosage as the main driving factor to stem diameter fluctuations (Franzoni et al., 2022; Yakhin et al., 2017). Such complexity is confirmed by previous studies, which highlight challenges in specifying the impact of individual components in experiments driven by multiple factors (Yakhin et al., 2017; Franzoni et al., 2022). Based on the study findings, it is evident that CPE or its dosage(s) might not always contribute to increased stem diameter, as several other common factors present in natural products in agriculture can also affect stem diameter.

With regard to the nutrient profile of the applied green nano-fertilizers, elemental analysis demonstrated that the different plant extract composites derived from BPE, WRE, and ALvE generally displayed comparable nutrient composition, with consistent presence of essential macro-and micronutrients detected across all treatments. This implies that the observed differences in growth responses among the treatments cannot be primarily attributed to the presence or absence of specific nutrients. However, compared with the control, plant extract-based composite treatments elicited positive plant responses, highlighting improved nutrient-use efficiency associated with nanostructured delivery.

The observations from the study are in agreement with previous studies Ansari et al. (2023), Babarabie et al. (2025), Sheta et al. (2024), and Samsoon et al. (2024), showing that green synthesized nano-fertilizers exhibited superior agronomic performance compared with control treatments, primarily due to their physicochemical properties. Overall, these findings suggest that the reported agronomic benefits are mainly driven by the nutrient delivery mechanisms, rather than by differences in nutrient composition across the formulations.

4.4.3 Soil variables

The anchors of crop productivity reflect an interlink between two closely related factors, namely the soil conditions and minor fluctuations in soil chemical characteristics, which pose a significant impact on crop responses to management practices and treatments (Deng et al., 2023). Among these factors, pH and EC are especially important for understanding soil conditions and their characteristics. These can include microbial activity, nutrient cycling, inorganic carbon balance, and organic matter decomposition (Mosley et al., 2024; Ahmad et al., 2025).

The observed pH appears to have shifted post-growth, as shown in Figure 4.21, likely reflecting rhizosphere acidification influenced by the release of protons and low-molecular-weight organic acids from actively growing roots (Santoro et al., 2024). Root-mediated acidification has been well documented as a mechanism that enhances nutrient solubility and mobilization in the rhizosphere, especially for phosphorus and other nutrients. This process helps plants acquire nutrients during early stages of growth (Bilyera et al., 2022; Holz et al., 2024; Mimmo et al., 2018).

In this study, the moderate decline in soil pH coincided with treatments that promoted higher seed emergence and improved vegetative growth. As observed in the tomato plants, this effect suggests that the acidification remained within an acceptable range and improved nutrient availability rather than inducing chemical stress. Baccari and Krouma (2023) reported that *Vicia faba* L. (feba bean) genotypes associated with lower soil pH promoted better growth, photosynthesis, and phosphorous uptake. These genotypes also handled stress better, indicating that a small pH drop helped with nutrient availability without affecting the plants. Several studies have confirmed that slightly acidic soils promote enzyme activation and improve nutrient uptake during germination and seedling establishment, thereby improving early plant vigour (Ngosong et al., 2022; Yuan et al., 2025).

The differences observed in the soil pH between tomato and bell pepper plants further suggest species-species variation in the quantity and composition of root exudates, which are heavily influenced by plant genotype and developmental stage (McLaughlin et al., 2023). Root exudate profiles vary considerably among plant species, leading in unique rhizosphere chemical environments and nutrient acquisition strategies (Adeniji et al., 2025; Chen and Liu, 2024; Qu et al., 2024; Sakib et al., 2025). This aligns well with the consistent vegetative growth response observed in both experiments for tomato crops. This indicates a more efficient capacity in manipulating soil chemical conditions, which supports sustained nutrient uptake.

Figure 4.22 shows a marked drop in EC after crop growth, which likely reflects the depletion of soluble ions in the soil solution due to nutrient uptake by plant roots during active plant development (Chu et al., 2018; Yekutiel et al., 2024). As EC measures the total dissolved ionic content of soil and water, it is a sensitive indicator of changes in nutrient dynamics and crop establishment (Hmidi et al., 2025; Shin et al., 2026). Notably, the reduced EC alone is insufficient to substantiate direct nutrient uptake. This is because the EC indicates the cumulative behaviour of all dissolved ions and is heavily influenced by soil texture, moisture and the formulation and characteristics of the fertilizer (Kim and Park, 2024; Shin et al., 2026).

Although all the formulations reduced soil EC, the formulation with the highest amount of ALvE resulted in lower seed emergence percentages. This can be explained by several interrelated factors: EC is strongly modulated by soil moisture and texture, not only ion removal (Lipiec and Usowicz, 2024; Bo-Seong et al., 2022). Moreover, thick polysaccharide shells can slow nutrient release from nano-fertilizers. Similarly, high ALvE formulation, rich in polysaccharides, may form diffusion barriers or promote particle aggregation, thereby delaying nutrient availability during germination. Collectively, the findings demonstrate that optimal seed emergence and plant growth were associated with balanced soil chemical conditions that facilitated efficient nutrient availability during early development, beyond soil pH and EC. They also sustained the uptake of nutrients throughout the growth cycle.

4.5 Conclusion

The shift towards sustainable agriculture has increased dependence on organic nutrient sources that support soil health and reduce chemical fertilizer use. Findings from this study showed that formulations containing a lower concentration of ALvE (5 mL) applied at a lower dose (4 mL) resulted in higher seed emergence percentages (93.3%). Regarding crop types, tomatoes maintained a consistent rate of structural biomass accumulation, while bell peppers showed superior leaf expansion and chlorophyll content. The CPEs and nanoparticles exerted unique effects owing to differences in nanoparticle size and CPE composition. Rapid signaling and translocation were enhanced by ultra-small nanoparticles. Larger nanoparticles contributed to sustained nutrient release and biomass accumulation, contradicting the fact that small-sized nanoparticles always yield superior results. Additionally, a dose-dependent trend was observed: moderate applications stimulated growth, whereas higher concentrations inhibited it, underscoring the importance of precise dosage application of treatments. The application of nano-fertilizer composites significantly reduced soil pH and EC post-crop growth, indicating active nutrient uptake and improved soil conditions that allow easy release and assimilation into plant biosystems.

Additional investigations are required to compare the agronomic performance of the developed nano-fertilizers with conventional fertilizers across a range of crops and soil environments. Comparative evaluations under greenhouse and field conditions are vital for establishing the efficiency of nano-fertilizers in terms of nutrient release kinetics, nutrient use efficiency, crop productivity, and environmental safety.

CHAPTER 5

SYNTHESIS OF FINDINGS, SIGNIFICANCE, AND PROSPECTS

5.1 Summary

The study demonstrates the feasibility of producing efficient nano-fertilizers from fruit peels as extracts and shows how their properties can be manipulated via simple formulation modifications. Through the materials used, measurable enhancements were realized in plant performance and in soil conditions. This was to confirm their functional engagement within the soil and plant biosystem. In summary, the work presented proposes a practical foundation for developing nano-fertilizers that are not only sustainable but also derived from waste, highlighting their potential for targeted application across various crop production systems.

5.2 Implications of the findings of this study

The study demonstrates the potential of producing true nano-fertilizers using plant extracts as primary functional components under mild and low-energy processes. Being able to prove that BPs, WRs, and *Aloe vera* gel can form stable, nutrient-rich nanoparticles without the introduction of inorganic precursors opens a new frontier in advancing sustainable, circular nanomaterial development methodology. Central to this work is the deliberate modification of nanoparticle size and behavior through optimized formulation. As reported in Chapter 3 of this study, adding small amounts of *Aloe vera* gel extracts to the composite of BPE and WRE produced much smaller and more scattered particles. However, increasing the amount of *Aloe vera* gel extract in the composite of BPE and WRE led to the formation of larger, agglomerated particles. This adjustment-capable property reflects that extract ratios influence control over nanoparticle properties. Thus, this approach forms the foundation for designing formulations that align with specific, intended agronomic objectives.

At the same level of importance, the observed effects when the produced nano-fertilizer was applied provided further insight into nanomaterial property fabrication. It was found that nanoscale particles do not guarantee uniform agronomic performance. As such, seed emergence has been found to be the highest in formulations with *Aloe vera* content applied at lower dosage, only to later contrast the trend during growth. Smaller-particle formulations, such as C1 and C7 improved the stem diameter and flower production, while larger-particle formulations, such as C3 and C8, enhanced the development of leaves and the accumulation of biomass. These biological transformations were associated with soil changes in both pH and EC, which declined post-application. This indicates active ion exchange, nutrient uptake and modifications to the soil solution. Therefore, such reductions demonstrate that the composites interacted effectively with the soil-plant system rather than behaving as inert materials.

Concerning scholars and innovators within the agricultural diaspora, this work showcases proof that waste-derived nanomaterials are not only fixated on chemical performance but can also deliver measurable agronomic benefits. To policymakers, the findings present low-hazard, circular approaches that can produce functional fertilizers without having to rely on mined or artificial input materials. In a nutshell, the significance of the study draws its value in bridging the synthesis of nanomaterials with real plant performance. Placing an emphasis that efficient nano-fertilizer fabrication needs both precision in design and the application of materials used.

5.3 Recommendations and directions for future research

To further develop a better understanding, application and design of nano-fertilizers, several future research endeavors lie in wait for exploration. This entails clarifying their release mechanisms alongside a deep understanding of their physicochemical behavior. Another would be to assess nutrient release in real-world settings beyond small plots or hydroponic systems. To achieve these proposals, advanced analytical equipment such as DLS, zeta potential, FTIR, Raman, XRD, and TGA/DSC is required, as they would reveal exactly how size, composition and surface chemistry of the prepared nano-fertilizer impact nutrient stability and their availability.

On another note, research on the application of nano-fertilizers should extend to running efficient crop assessments beyond the early or mid-growth stages, and to consider full crop growth cycles and postharvest soil assessments. Future studies may also examine seed germination and emergence dynamics, including parameters such as mean emergence time, emergence rate, emergence uniformity, and seedling vigor index. This will help determine whether nano-fertilizers can enhance early seed establishment, particularly in seeds that exhibit dormancy or are typically difficult to germinate. This will provide insight into the persistence, transformational and long-term soil impact of the composites. The test for future nano-fertilizers should also be diverse, accounting for varying soil types, climates, and settings of the field. This will be vital in determining their scalability and identification of environments in which they would perform best or be better suited. Yet, running comparison tests between nano-fertilizers and conventional fertilizers will help place them within already existing managerial frameworks. Together, all these efforts will yield a broad socio-economic and environmental assessment, culminating in the circulation of nano-fertilizers, costs and sustainability implications. Ultimately supporting the development of nano-fertilizers whose materials have been sourced from waste as viable and responsible agricultural innovations.

5.4 Conclusions

From the study, a clear feasibility procedure of converting fruit-waste extracts into functional nano-fertilizers possessing nanoscale properties has been demonstrated. Further showcasing that these properties can be modified via formulation control. The findings yielded highly apparent improvements specific to each crop growth stage. Accompanying fluctuations in soil chemistry parameters, including EC and soil pH, reflect the successful impact of the composites on the soil environment via a combination of chemical and biological activities within the soil. Summarizing all the findings, a credible foundation for the design of waste-derived nano-fertilizers with modified intended agronomic functions has been established. Finally, the work proposes an advanced approach to sustainable material design and its practical integration into environmentally conscious agriculture.

REFERENCES

Abady, M.M., Mohammed, D.M., Soliman, T.N., Shalaby, R.A. and Sakr, F.A., 2025. Sustainable synthesis of nanomaterials using different renewable sources. *Bulletin of the National Research Centre*, 49(1), pp.24.

Abdel Latef, A.A.H., Srivastava, A.K., El-sadek, M.S.A., Kordrostami, M. and Tran, L.S.P., 2018. Titanium dioxide nanoparticles improve growth and enhance tolerance of broad bean plants under saline soil conditions. *Land Degradation & Development*, 29(4), pp.1065-1073.

Abdelmigid, H.M., Hussien, N.A., Alyamani, A.A., Morsi, M.M., AlSufyani, N.M. and Kadi, H.A., 2022a. Green synthesis of zinc oxide nanoparticles using pomegranate fruit peel and solid coffee grounds vs. chemical method of synthesis, with their biocompatibility and antibacterial properties investigation. *Molecules*, 27(4), pp.1236.

Abdelmigid, H.M., Morsi, M.M., Hussien, N.A., Alyamani, A.A., Alhuthal, N.A. and Albukhaty, S., 2022b. Green synthesis of phosphorous-containing hydroxyapatite nanoparticles (nHAP) as a novel nano-fertilizer: preliminary assessment on pomegranate (Punica granatum L.). *Nanomaterials*, 12(9), pp.1527.

Adetimirin, V.O., 2008. Stand establishment and early field vigour variation in a tropicalised shrunken-2 maize population. *Field Crops Research*, 108(2), pp.143-149.

Abhiram, G., 2023. Contributions of nano-nitrogen fertilizers to sustainable development goals: a comprehensive review. *Nitrogen*, 4(4), pp.397-415.

Acun, S., Gül, H. and Seyrekoğlu, F., 2025. Comprehensive analysis of physical, chemical, and phenolic acid properties of powders derived from watermelon (*Crimson Sweet*) by-products. *Journal of Food Science*, 90(3), pp.e70092.

Adeniji, A., Huang, J., Li, S., Lu, X. and Guo, R., 2025. Hot viewpoint on how soil texture, soil nutrient availability, and root exudates interact to shape microbial dynamics and plant health. *Plant and Soil*, 511(1), pp.69-90.

Adnan, A., Naumann, M., Mörlein, D. and Pawelzik, E., 2020. Reliable discrimination of green coffee beans species: A comparison of UV-Vis-based determination of caffeine and chlorogenic acid with non-targeted near-infrared spectroscopy. *Foods*, 9(6), pp.788.

Adnan, M., Siddiqui, A.J., Ashraf, S.A., Ashraf, M.S., Alomrani, S.O., Alreshidi, M., Tepe, B., Sachidanandan, M., Danciu, C. and Patel, M., 2023. Saponin-derived silver nanoparticles from *phoenix dactylifera* (Ajwa Dates) exhibit broad-spectrum bioactivities combating bacterial infections. *Antibiotics*, 12(9), pp.1415.

Afroz, M., Agrahari, S. and Tandon, P.K., 2020. Nanomaterials synthesis and their eco-friendly applications. In *Handbook of Nanomaterials and Nanocomposites for Energy and Environmental Applications* (pp. 1-32). Cham: Springer International Publishing.

Agathokleous, E., Liu, C.J. and Calabrese, E.J., 2023. Applications of the hormesis concept in soil and environmental health research. *Soil & Environmental Health*, 1(1), pp.100003.

Aguilar, M.N., Perez-Aguilar, J. l, González-Coronel, V.J., Soriano Moro, J.G., Sanchez-Gaytan, B.L., 2021. Polymers as Versatile Players in the Stabilization, Capping, and Design of Inorganic Nanostructures. *ACS Omega*, 6(51), pp.35196-35203.

Ahmad, M.N., Anuar, M.I., Abd Aziz, N. and Murdi, A.A., 2025. Function and application of Soil Electrical Conductivity (EC) sensor in agriculture: A Review. *Advances in Agricultural and Food Research Journal*, 6(1).

Ahmad, N.M., Mohamed, A.H., Hasan, N., Abidin, N.Z.-, Nawahwi, M.Z., Azzeme, A.M., 2024. Effect of optimisation variable and the role of plant extract in the synthesis of nanoparticles using plant-mediated synthesis approaches. *Inorganic Chemistry Communications* 161, pp.111839.

Ahmed, N.K., Abbady, A., Elhassan, Y.A. and Said, A.H., 2023. Green synthesized titanium dioxide nanoparticle from *Aloe vera* extract as a promising candidate for radiosensitization applications. *BioNanoScience*, 13(2), pp.730-743.

Ahuja, I., Dauksas, E., Remme, J.F., Richardsen, R. and Løes, A.K., 2020. Fish and fish waste-based fertilizers in organic farming–With status in Norway: A review. *Waste Management*, 115, pp.95-112.

Al-Hajj, N.Q., 2021. in vitro Evaluation of Antimicrobial and Antioxidant Activity of *Carica papaya* L. Seeds Grown in the Republic of Yemen. *Electronic Journal of University of Aden for Basic and Applied Sciences*, 2(3), pp.93-102.

Ali, A., Bordoh, P.K., Singh, A., Siddiqui, Y. and Droby, S., 2016. Post-harvest development of anthracnose in pepper (*Capsicum* spp): Etiology and management strategies. *Crop Protection*, 90, pp.132-141.

Ali, J., Mukarram, M., Ojo, J., Dawam, N., Riyazuddin, R., Ghramh, H.A., Khan, K.A., Chen, R., Kurjak, D. and Bayram, A., 2024. Harnessing phytohormones: advancing plant growth and defence strategies for sustainable agriculture. *Physiologia Plantarum*, 176(3), pp.e14307.

Ali, M.M., Hashim, N., Bejo, S.K. and Shamsudin, R., 2017. Rapid and nondestructive techniques for internal and external quality evaluation of watermelons: A review. *Scientia Horticulturae*, 225, pp.689-699.

Ali, O., Ramsubhag, A. and Jayaraman, J., 2021. Biostimulant properties of seaweed extracts in plants: Implications towards sustainable crop production. *Plants*, 10(3), pp.531.

Ali, Q., Perveen, R., El-Esawi, M.A., Ali, S., Hussain, S.M., Amber, M., Iqbal, N., Rizwan, M., Alyemeni, M.N., El-Serehy, H.A. and Al-Misned, F.A., 2020. Low doses of Cuscuta reflexa extract act as natural biostimulants to improve the germination vigor, growth, and grain yield of wheat grown under water stress: Photosynthetic pigments, antioxidative defense mechanisms, and nutrient acquisition. *Biomolecules*, 10(9), pp.1212.

Ali, S., Mehmood, A. and Khan, N., 2021. Uptake, translocation, and consequences of nanomaterials on plant growth and stress adaptation. *Journal of Nanomaterials*, 2021(1), pp.6677616.

Alkhader, A.M., 2023. Nanofertilizers as an alternative to inorganic fertilizers: a review. *African Journal of Food, Agriculture, Nutrition and Development*, 23(6), pp.23956-23974.

Alkhlefawi, A. M. K., 2022. Growth response of peppermint to nano copper and Algacifo fertilizer and their effect on the active substances. *Euphrates Journal of Agricultural Science*, 14(3), pp. 9–19.

Al-Ma'athedi, A.F. and Mohammad, E.H., 2019. Effect Of Gibberellic Acid On Seed Germination Percentage And Growth Performance Of Two *Cassia* Species. *Scientific Journal of Flowers and Ornamental Plants*, 6(2), pp.99-104.

Amanullah. 2025. Chapter 12 Nanofertilizers: shaping the future of field crop production. *Crop Nutrition: Enhancing Healthy Soils, Food Security, Environmental Sustainability and Advancing SDGs*. Berlin, Boston: De Gruyter, pp. 479-505

Anand, U. and Rai, N.R., 2024. Pesticide Reduction through Organic Farming for Promoting Public Health Management and Food Security. *The South Eastern European Journal of Public Health*, 23, pp.246-250.

Anaya-Esparza, L.M., Mora, Z.V.D.L., Vázquez-Paulino, O., Ascencio, F. and Villarruel-López, A., 2021. Bell peppers (*Capsicum annum* L.) losses and wastes: Source for food and pharmaceutical applications. *Molecules*, 26(17), pp.5341.

Anbarasan, S. and Ramesh, S., 2021. The Role of Plant Roots in Nutrient Uptake and Soil Health. *Plant Science Archives*, 5(08), pp.2655-1837.

Añibarro-Ortega, M., Dias, M.I., Petrović, J., Pereira, A., Soković, M., Barros, L. and Pinela, J., 2025. Nutrients, Phytochemicals, and In Vitro Antioxidant and Antimicrobial Activities of Lulo (*Solanum quitoense* Lam.) Fruit Pulp, Peel, and Seeds. *Foods, 14(12),* pp.2083.

Ansari, M., Ahmed, S., Abbasi, A., Hamad, N.A., Ali, H.M., Khan, M.T., Haq, I.U. and Zaman, Q.U., 2023. Green synthesized silver nanoparticles: a novel approach for the enhanced growth and yield of tomato against early blight disease. *Microorganisms*, 11(4), pp.886.

Aqeel, U., Aftab, T., Khan, M.M.A., Naeem, M. and Khan, M.N., 2022. A comprehensive review of impacts of diverse nanoparticles on growth, development and physiological adjustments in plants under changing environment. *Chemosphere*, 291, pp.132672.

Arora, P.K., Tripathi, S., Omar, R.A., Chauhan, P., Sinhal, V.K., Singh, A., Srivastava, A., Garg, S.K. and Singh, V.P., 2024. Next-generation fertilizers: the impact of bionanofertilizers on sustainable agriculture. *Microbial Cell Factories*, 23(1), pp.254.

Aryal, J.P., Sapkota, T.B., Krupnik, T.J., Rahut, D.B., Jat, M.L. and Stirling, C.M., 2021. Factors affecting farmers' use of organic and inorganic fertilizers in South Asia. *Environmental Science and Pollution Research*, 28(37), pp.51480-51496.

Asadu, C.O., Ezema, C.A., Ekwueme, B.N., Onu, C.E., Onoh, I.M., Adejoh, T., Ezeorba, T.P.C., Ogbonna, C.C., Otuh, P.I., Okoye, J.O. and Emmanuel, U.O., 2024. Enhanced efficiency fertilizers: Overview of production methods, materials used, nutrients release mechanisms, benefits and considerations. *Environmental Pollution and Management*, 1, pp.32-48.

Asafa, R. F., Elizabeth, O. A., Yusuf, S. Y., & Akanbi, W. B. 2024. Assessment of Vitamins, Minerals and Phytochemical Variability in Watermelon (*Citrullus lanatus*) Varieties from South-West Nigeria. *Trends in Agricultural Sciences*, 3(3), pp. 220–230.

Ashoka, S., Shamshad, B.S., Vijayalaxm, K.G., 2022. Physico-chemical properties and Nutritional Composition of Watermelon (*Citrullus lanatus*) and its Rind Flour. *Biological Forum*.

Astija, A., 2020. Soil pH influences the development of tomato root organ (*Solanum lycopersicum* L.). *Eurasian Journal of BioSciences*, 14, pp.6903-6908.

Aswathi, V.P., Meera, S., Maria, C.A. and Nidhin, M., 2023. Green synthesis of nanoparticles from biodegradable waste extracts and their applications: a critical review. *Nanotechnology for Environmental Engineering*, 8(2), pp.377-397.

Avellan, A., Yun, J., Morais, B.P., Clement, E.T., Rodrigues, S.M. and Lowry, G.V., 2021. Critical review: role of inorganic nanoparticle properties on their foliar uptake and in planta translocation. *Environmental Science & Technology*, 55(20), pp.13417-13431.

Avila-Quezada, G.D., Ingle, A.P., Golińska, P. and Rai, M., 2022. Strategic applications of nano-fertilizers for sustainable agriculture: Benefits and bottlenecks. *Nanotechnology Reviews*, 11(1), pp.2123-2140.

Ayenew, B.M., Satheesh, N., Zegeye, Z.B. and Kassie, D.A., 2025. A review on the production of nanofertilizers and its application in agriculture. *Heliyon*, 11(1).

Azad, A., Zafar, H., Raza, F. and Sulaiman, M., 2023. Factors influencing the green synthesis of metallic nanoparticles using plant extracts: a comprehensive review. *Pharmaceutical Fronts*, 5(03), pp.e117-e131.

Babarabie, M., Zolfaghary, P., Sardoei, A.S., Fotoohiyan, Z., Ghorbanzadeh, A., Danyaei, A. and Afsharipour, S., 2025. The effect of foliar application of silver nanoparticles synthesized by Moringa oleifera on improving the yield and quality of *Pelargonium hortorum* under drought stress. *Scientific Reports*, 15(1), pp.23239.

Baccari, B. and Krouma, A., 2023. Rhizosphere acidification determines phosphorus availability in calcareous soil and influences faba bean (*Vicia faba*) tolerance to p deficiency. *Sustainability*, 15(7), pp.6203.

Bahrulolum, H., Nooraei, S., Javanshir, N., Tarrahimofrad, H., Mirbagheri, V.S., Easton, A.J. and Ahmadian, G., 2021. Green synthesis of metal nanoparticles using microorganisms and their application in the agrifood sector. *Journal of Nanobiotechnology*, 19(1), pp.86.

Bailey, S.J., Blackwell, J.R., Williams, E., Vanhatalo, A., Wylie, L.J., Winyard, P.G. and Jones, A.M., 2016. Two weeks of watermelon juice supplementation improves nitric oxide bioavailability but not endurance exercise performance in humans. *Nitric Oxide*, 59, pp.10-20.

Bairwa, P., Kumar, N., Devra, V. and Abd-Elsalam, K.A., 2023. Nano-biofertilizers synthesis and applications in agroecosystems. *Agrochemicals*, 2(1), pp.118-134.

Banerjee, K., Pramanik, P., Maity, A., Joshi, D.C., Wani, S.H. and Krishnan, P., 2019. Methods of using nanomaterials to plant systems and their delivery to plants (mode of entry, uptake, translocation, accumulation, biotransformation and barriers). In *Advances in phytonanotechnology* (pp. 123-152). Academic Press.

Banjara, R.A., Kumar, A., Aneshwari, R.K., Satnami, M.L. and Sinha, S.K., 2024. A comparative analysis of chemical vs green synthesis of nanoparticles and their various applications. *Environmental Nanotechnology, Monitoring & Management*, 22, pp.100988.

Basavegowda, N. and Baek, K.H., 2021. Current and future perspectives on the use of nanofertilizers for sustainable agriculture: the case of phosphorus nanofertilizer. *3 Biotech*, 11(7), pp.357.

Bashir, M., Ali, S. and Farrukh, M.A., 2020. Green synthesis of Fe2O3 nanoparticles from orange peel extract and a study of its antibacterial activity. *Journal of the Korean Physical Society*, 76(9), pp.848-854.

Batool, M., Khurshid, S., Daoush, W.M., Siddique, S.A. and Nadeem, T., 2021. Green synthesis and biomedical applications of ZnO nanoparticles: Role of PEGylated-ZnO nanoparticles as doxorubicin drug carrier against MDA-MB-231 (TNBC) cells line. *Crystals*, 11(4), pp.344.

Begum, T., Agarwal, S., Bhuyan, P., Das, J., Verma, A.K., Guha, A. and Ganguly, M., 2025. Aloe vera gel mediated green synthesis of ruthenium nanoparticles and their potential anticancer activity. *Next Nanotechnology*, 7, pp.100095.

Ben Romdhane, M., Bouallegue, A., Bourhia, M., Bougatef, A., Salamatullah, A.M., Ellouz-Chaabouni, S. and Haddar, A., 2024. Watermelon rind dietary fibers as natural source to enhance texture of wheat bread. *Foods*, 13(18), pp.2909.

Bhattacharjee, L., Gopakumar, A.N., Beheshtimaal, A., Jazaei, F., Ccanccapa-Cartagena, A. and Salehi, M., 2025. Mechanisms of microplastic generation from polymer-coated controlled-release fertilizers (PC-CRFs). *Journal of Hazardous Materials*, 486, pp.137082.

Bilyera, N., Hummel, C., Daudin, G., Santangeli, M., Zhang, X., Santner, J., Lippold, E., Schlüter, S., Bertrand, I., Wenzel, W. and Spielvogel, S., 2022. Co-localised phosphorus mobilization processes in the rhizosphere of field-grown maize jointly contribute to plant nutrition. *Soil Biology and Biochemistry*, 165, pp.108497.

Bishnoi, S., Sharma, S. and Agrawal, H., 2023. Exploration of the potential application of banana peel for its effective valorization: A review. *Indian Journal of Microbiology*, 63(4), pp.398-409.

Borges-Argáez, R., Chan-Balan, R., Cetina-Montejo, L., Ayora-Talavera, G., Sansores-Peraza, P., Gómez-Carballo, J. and Cáceres-Farfán, M., 2019. In vitro evaluation of anthraquinones from Aloe vera (*Aloe barbadensis* Miller) roots and several derivatives against strains of influenza virus. *Industrial Crop and Products*, 132, pp.468-475.

Borowska, S., Tomczyk, M., Strawa, J.W. and Brzóska, M.M., 2020. Estimation of the chelating ability of an extract from Aronia melanocarpa L. berries and its main polyphenolic ingredients towards ions of zinc and copper. *Molecules*, 25(7), pp.1507.

Bo-Seong, S.E.O., Jeong, Y.J., Nu-Ri, B.A.E.K., Hyun-Jin, P.A.R.K., Yang, H.I., Se-In, P.A.R.K. and Woo-Jung, C.H.O.I., 2022. Soil texture affects the conversion factor of electrical conductivity from 1: 5 soil-water to saturated paste extracts. *Pedosphere*, 32(6), pp.905-915.

Božena, Š.E.R.Á., 2023. Methodological contribution on seed germination and seedling initial growth tests in wild plants. *Notulae Botanicae Horti Agrobotanici Cluj-Napoca*, 51(2), pp.13164-13164.

Brinker, C.J., Lu, Y., Sellinger, A. and Fan, H., 1999. Evaporation-induced self-assembly: nanostructures made easy. *Advanced Materials*, 11(7), pp.579-585.

Brydson, R., Brown, A., Hodges, C., Abellan, P. and Hondow, N., 2015. Microscopy of nanoparticulate dispersions. *Journal of Microscopy*, 260(3), pp.238-247.

Burdulis, D., Kašėtaitė, A., Trumbeckaitė, S., Benetis, R., Daukšienė, J., Burdulienė, K. and Raudonė, L., 2025. Cultivation of Watermelon (*Citrullus lanatus* (Tunb.)) in a Temperate Climate: Agronomic Strategies and Phytochemical Composition. *Agronomy*, 15(4), pp.933.

Burgess, S., 2022. Determining accurate detection limits for EDS analysis using simulated spectra. Oxford Instruments.

Cabrera, R.I. and Solis-Perez, A.R., 2017. Mineral nutrition and fertilization management.

Cantarella, H., Otto, R., Soares, J.R. and de Brito Silva, A.G., 2018. Agronomic efficiency of NBPT as a urease inhibitor: A review. *Journal of Advanced Research*, 13, pp.19-27.

Carmona, F.J., Dal Sasso, G., Bertolotti, F., Ramírez-Rodríguez, G.B., Delgado-López, J.M., Pedersen, J.S., Masciocchi, N. and Guagliardi, A., 2020. The role of nanoparticle structure and morphology in the dissolution kinetics and nutrient release of nitrate-doped calcium phosphate nanofertilizers. *Scientific Reports*, 10(1), pp.12396.

Castillo, M., de Guzman, M.J.K. and Aberilla, J.M., 2023. Environmental sustainability assessment of banana waste utilization into food packaging and liquid fertilizer. *Sustainable Production and Consumption*, 37, pp.356-368.

Castillo-Quevedo, C., Cabellos, J.L., Aceves, R., Núñez-González, R. and Posada-Amarillas, A., 2020. Cu-doped KCL unfolded band structure and optical properties studied by DFT calculations. *Materials*, 13(19), pp.4300.

Chakraborty, S., Mandal, M., Chakraborty, A.P. and Majumdar, S., 2022. Zinc solubilizing rhizobacteria as soil health engineer managing zinc deficiency in plants. In *Rhizosphere Engineering* (pp. 215-238). Academic Press.

Chandel, V., Biswas, D., Roy, S., Vaidya, D., Verma, A. and Gupta, A., 2022. Current advancements in pectin: Extraction, properties and multifunctional applications. *Foods*, 11(17), pp.2683.

Channab, B.E., Idrissi, A.E., Ammar, A., Dardari, O., Marrane, S.E., El Gharrak, A., Akil, A., Essemlali, Y. and Zahouily, M., 2024. Recent advances in nano-fertilizers: synthesis, crop yield impact, and economic analysis. *Nanoscale*, 16(9), pp.4484-4513.

Chen, H., Wang, L., Guo, S., Li, M., Tian, Z., Han, B., Tang, X. and Liu, B., 2023. Effects of light intensity on seedling emergence and early growth of *Liquidambar formosana* Hance. *Forests*, 14(5), pp.867.

Chen, J., Lü, S., Zhang, Z., Zhao, X., Li, X., Ning, P. and Liu, M., 2018. Environmentally friendly fertilizers: A review of materials used and their effects on the environment. *Science Of The Total Environment*, 613, pp.829-839.

Chen, L. and Liu, Y., 2024. The function of root exudates in the root colonization by beneficial soil rhizobacteria. *Biology*, 13(2), pp.95.

Cheng, J., Han, S., Verrelst, J., Zhao, C., Zhang, N., Zhao, Y., Lei, L., Wang, H., Yang, G. and Yang, H., 2023. Deciphering maize vertical leaf area profiles by fusing spectral imagery data and a bell-shaped function. *International Journal of Applied Earth Observation and Geoinformation*, 120, pp.103355.

Cheng, Y., Li, M. and Xu, P., 2024. Allelochemicals: A source for developing economically and environmentally friendly plant growth regulators. *Biochemical and Biophysical Research Communications*, 690, pp.149248.

Choi, W.J. and Yang, M., 2025. Probabilistic Deep Learning Framework for Greenhouse Microclimate Prediction with Time-Varying Uncertainty and Covariance Analysis. *Agriculture*, 15(23), pp.2461.

Chowdary, M.Y., Rana, S.S. and Ghosh, P., 2022. Banana inflorescence and their potential health benefits as future food. *Quality Assurance and Safety of Crops & Foods*, 14(2), pp.131-136.

Chu, S., Zhang, D., Zhi, Y., Wang, B., Chi, C.P., Zhang, D., Liu, Y. and Zhou, P., 2018. Enhanced removal of nitrate in the maize rhizosphere by plant growth-promoting Bacillus megaterium NCT-2, and its colonization pattern in response to nitrate. *Chemosphere*, 208, pp.316-324.

Cristofano, F., El-Nakhel, C., 2020. Understanding Genotype X Biostimulant Interaction is Essential for Developing Biostimulant Application Programs to Improve Targeted Crop Traits.

Cristofano, F., El-Nakhel, C., Pannico, A., Giordano, M., Colla, G. and Rouphael, Y., 2021. Foliar and root applications of vegetal-derived protein hydrolysates differentially enhance the yield and qualitative attributes of two lettuce cultivars grown in floating system. *Agronomy*, 11(6), pp.1194.

Cusola, O., Kivisto, S., Vierros, S., Batys, P., Ago, M., Tardy, B.L., Greca, L.G., Roncero, M.B., Sammalkorpi, M. and Rojas, O.J., 2018. Particulate coatings via evaporation-induced self-assembly of polydisperse colloidal lignin on solid interfaces. *Langmuir*, 34(20), pp.5759-5771.

Czech, A., Zarycka, E., Yanovych, D., Zasadna, Z., Grzegorczyk, I. and Kłys, S., 2020. Mineral content of the pulp and peel of various citrus fruit cultivars. *Biological Trace Element Research*, 193(2), pp.555-563.

da Silva, S.S., de Lima, G.S., de Lima, V.L.A., Gheyi, H.R., dos Anjos Soares, L.A., Oliveira, J.P.M., de Araújo, A.C., Gomes, J.P., 2020. Production and quality of watermelon fruits under salinity management strategies and nitrogen fertilization. *Semina:Ciencias Agrarias* 41, pp. 2923–2935.

de Angelis-Pereira, M.C., Barcelos, M.D.F.P., Pereira, R.C., Pereira, J.D.A.R. and de Sousa, R.V., 2016. Chemical composition of unripe banana peels and pulps flours and its effects on blood glucose of rats. *Nutrition & Food Science*, 46(4), pp.504-516.

Deepana, P., Bama, K.S., Santhy, P. and Devi, T.S., 2021. Effect of seaweed extract on rice (*Oryza sativa* var. ADT53) productivity and soil fertility in Cauvery delta zone of Tamil Nadu, India. *Journal of Applied and Natural Science*, 13(3), pp.1111.

Demeke, E.D., Benti, N.E., Terefe, M.G., Anbessa, T.T., Mengistu, W.M. and Mekonnen, Y.S., 2025. A comprehensive review on nano-fertilizers: preparation, development, utilization, and prospects for sustainable agriculture in Ethiopia. *Nanoscale Advances,* 7(8), pp.2131-2144.

Demir, I., Ermis, S.I.T.K.I., Mavi, K.A.Z.I.M. and Matthews, S., 2008. Mean germination time of pepper seed lots (*Capsicum annuum* L.) predicts size and uniformity of seedlings in germination tests and transplant modules. *Seed Science and Technology*, *36*(1), pp.21-30.

Deng, M., Ma, H., Sadeghpour, A., Yang, G., Hu, Y. and Yang, D., 2023. Responses of crop production and soil health to chemical nitrogen fertilization in a maize-wheat rotation system. *Frontiers in Environmental Science*, 11, pp.1108288.

Deng, Y., Feng, X., Yang, D., Yi, C. and Qiu, X., 2012. π-π Stacking of The Aromatic Groups In Lignosulfonates. *BioResources*, 7(1).

Denham, T., 2014. Maize: Origins and Development. In *Encyclopedia of Global Archaeology* (pp. 4612-4614). Springer, New York, NY.

Devi, O.B., Singh, A., Raising, L.P., Sherpa, T.L., Haokip, S.W., Hazarika, S. and Khan, A., 2023. Fruit peels as biofertilizers and biopesticides for sustainable agriculture and horticulture: A review. *International Journal of Environment and Climate Change*, 13(9), pp.3403-3413.

Devi, P., Perkins-Veazie, P. and Miles, C., 2020. Impact of grafting on watermelon fruit maturity and quality. *Horticulturae*, 6(4), pp.97.

Di Filippo-Herrera, D.A., Hernández-Herrera, R.M., Ocampo-Alvarez, H., Sánchez-Hernández, C.V., Muñoz-Ochoa, M. and Hernández-Carmona, G., 2021. Seaweed liquid extracts induce hormetic growth responses in mung bean plants. *Journal of Applied Phycology*, 33(2), pp.1263-1272.

Diao, T., Liu, R., Meng, Q. and Sun, Y., 2023. Microplastics derived from polymer-coated fertilizer altered soil properties and bacterial community in a Cd-contaminated soil. *Applied Soil Ecology*, 183, pp.104694.

Ding, X., Yu, L., Jiang, Y., Yang, S., He, L., Zhou, Q., Yu, J. and Huang, D., 2020. Changes in leaf length, width, area, and photosynthesis of fruit cucumber in a greenhouse production system. *HortScience*, 55(7), pp.995-999.

Djanaguiraman, M., Anbazhagan, V., Dhankher, O.P. and Prasad, P.V., 2024. Uptake, translocation, toxicity, and impact of nanoparticles on plant physiological processes. *Plants*, 13(22), pp.3137.

Djanaguiraman, M., Belliraj, N., Bossmann, S.H. and Prasad, P.V., 2018. High-temperature stress alleviation by selenium nanoparticle treatment in grain sorghum. *ACS omega*, 3(3), pp.2479-2491.

Du, J.S., Chen, P.C., Meckes, B., Kluender, E.J., Xie, Z., Dravid, V.P. and Mirkin, C.A., 2018. Windowless Observation of Evaporation-Induced Coarsening of Au–Pt Nanoparticles in Polymer Nanoreactors. *Journal of the American Chemical Society*, 140(23), pp.7213-7221.

Dubey, S., Rajput, H. and Batta, K., 2021. Utilization of watermelon rind (*Citrullus lanatus*) in various food preparations: a review. *Journal of Agricultural Science and Food Research*, 14, pp.1-3.

Dufková, H., Greplová, M., Hampejsová, R., Kuzmenko, M., Hausvater, E., Brzobohatý, B. and Černý, M., 2023. Secondary metabolites, other prospective substances, and alternative approaches that could promote resistance against *Phytophthora Infestans*. *Agronomy*, 13(7), pp.1822.

Dziza, K., Krzan, M., Jarek, E., Szyk-Warszyńska, L., Kudłacik-Kramarczyk, S., Warszyński, P., Santini, E., Liggieri, L. and Ravera, F., 2025. Adsorption of Saponin and Saponin–Chitosan Mixture at Water–Oil Interface and Stabilization of Oil-in-Water Emulsions. *Molecules,* 30(11), pp.2281.

Egbuonu, A.C.C., 2015. Comparative assessment of some mineral, amino acid and vitamin compositions of watermelon (*Citrullus lanatus*) rind and seed. *Asian Journal of Biochemistry*, 10(5), pp.230-236.

Ekinci, A., Kutluay, S., Şahin, Ö. and Baytar, O., 2023. Green synthesis of copper oxide and manganese oxide nanoparticles from watermelon seed shell extract for enhanced photocatalytic reduction of methylene blue. *International Journal of Phytoremediation*, 25(6), pp.789-798.

El-Nakhel, C., Cristofano, F., Colla, G., Pii, Y., Secomandi, E., De Gregorio, M., Buffagni, V., Garcia-Perez, P., Lucini, L. and Rouphael, Y., 2023. Vegetal-derived biostimulants distinctively command the physiological and metabolomic signatures of lettuce grown in depleted nitrogen conditions. *Science Horticultural, 317,* pp.112057.

Elsabagh, S.S., Elkhatib, E.A. and Rashad, M., 2024. Eco-friendly nano-enabled fertilizers derived from date industry waste for sustainable and controlled-release of P, K and Mg nutrients: sorption mechanisms, controlled-release performance and kinetics. *Bioresources and Bioprocessing*, 11(1), pp.3.

El-Serafy, R.S., El-Sheshtawy, A.N.A. and Dahab, A.A., 2023. Fruit peel soil supplementation induces physiological and biochemical tolerance in Schefflera arboricola L. grown under heat conditions. *Journal of Soil Science and Plant Nutrition*, 23(1), pp.1046-1059.

El Shafey, A.M., 2020. Green synthesis of metal and metal oxide nanoparticles from plant leaf extracts and their applications: A review. *Green Processing and Synthesis*, 9(1), pp.304-339.

El-Shetehy, M., Moradi, A., Maceroni, M., Reinhardt, D., Petri-Fink, A., Rothen-Rutishauser, B., Mauch, F. and Schwab, F., 2021. Silica nanoparticles enhance disease resistance in *Arabidopsis* plants. *Nature Nanotechnology, 16(3),* pp.344-353.

Erugo, A.I., Sunday, K. and Olusesi, F.Y., 2022. Optimization of Bio-fertilizer Production From Watermelon Peels Using Response Surface Methodology.

Fadzil, N.I., Masdor, A., Nor, M., Rosmi, M., Wahid, S., Karim, S.A., Firdaus, M., Anuar, M., 2024. Effects of MARDI Nano-Fertilizer Application Frequency on the Growth of Rock Melon. I*nternational Journal of Nanoelectronics and Materials (IJNeaM),* 17, pp.137-141.

Faizan, M., Singh, A., Eren, A., Sultan, H., Sharma, M., Djalovic, I. and Trivan, G., 2024. Small molecule, big impacts: Nano-nutrients for sustainable agriculture and food security. *Journal of Plant Physiology*, 301, p.154305.

Farshad, M. and Rasaiah, J., 2023. Kinetics of nanoparticle nucleation, growth, coalescence and aggregation: A theoretical study of (Ag) n nanoparticle formation based on population balance modulated by ligand binding. *Chemical Physics*, 573, pp.112002.

Farvardin, A., González-Hernández, A.I., Llorens, E., García-Agustín, P., Scalschi, L. and Vicedo, B., 2020. The apoplast: a key player in plant survival. *Antioxidants*, 9(7), pp.604.

Fathy, M.A., Abdellatif, A.A., Emara, E.I., Malik, K., Bhardwaj, A.K. and HAMED, L.M., 2023. Synthesis, characterization, and uses of nanofertilizers and nano-agrochemicals for sustainable agriculture. In *Nanofertilizers for Sustainable Agroecosystems: Recent Advances and Future Trends* (pp. 181-203). Cham: Springer Nature Switzerland.

Fernando, W.A.S.R. and Weerasinghe, T.K., 2023. Efficacy of compost made of food wastes with organic amendments for a sustainable and environment-friendly agricultural system. *Int J Life Sci Res Arch*, 4(1), pp.086-102.

Fidler, M., Perez-Lugones, D. and Gómez, C., 2025. Effect of Nitrogen Concentration on Compact Tomato and Pepper Plants during Production and Fruiting Phases. *HortTechnology*, 35(1), pp.52-61.

Finch-Savage, W.E. and Bassel, G.W., 2016. Seed vigour and crop establishment: extending performance beyond adaptation. *Journal of experimental botany*, *67*(3), pp.567-591.

Finch-Savage, W.E. and Leubner-Metzger, G., 2006. Seed dormancy and the control of germination. *New phytologist*, *171*(3), pp.501-523.

Franzoni, G., Cocetta, G., Prinsi, B., Ferrante, A. and Espen, L., 2022. Biostimulants on crops: Their impact under abiotic stress conditions. *Horticulture*, 8(3), pp.189.

Freitas, C.M.P., Coimbra, J.S.R., Souza, V.G.L. and Sousa, R.C.S., 2021. Structure and applications of pectin in food, biomedical, and pharmaceutical industry: A review. *Coatings*, 11(8), pp.922.

Gamagedara, T.P., Rathnayake, U.M. and Rajapakse, R.M.G., 2018. Facile synthesis of hydroxyapatite nanoparticles by a polymer-assisted method: morphology, mechanical properties and formation mechanism. *The Journal of Clinical Investigation*, 1(1), pp.1-5.

Gámez-Arjona, F.M., Sánchez-Rodríguez, C. and Montesinos, J.C., 2022. The root apoplastic pH as an integrator of plant signaling. *Frontiers in Plant Science*, 13, pp.931979.

Gansukh, E., Gopal, J., Paul, D., Muthu, M., Kim, D.H., Oh, J.W. and Chun, S., 2018. Ultrasound mediated accelerated Anti-influenza activity of Aloe vera. *Scientific Reports*, 8(1), pp.17782.

Garg, D., Sridhar, K., Stephen Inbaraj, B., Chawla, P., Tripathi, M. and Sharma, M., 2023. Nano-biofertilizer formulations for agriculture: A systematic review on recent advances and prospective applications. *Bioengineering*, 10(9), pp.1010.

Garibo, D., Borbón-Nuñez, H.A., de León, J.N.D., García Mendoza, E., Estrada, I., Toledano-Magaña, Y., Tiznado, H., Ovalle-Marroquin, M., Soto-Ramos, A.G., Blanco, A. and Rodríguez, J.A., 2020. Green synthesis of silver nanoparticles using *Lysiloma acapulcensis* exhibit high-antimicrobial activity. *Scientific Reports*, 10(1), p.12805.

Gaytancıoğlu, O. and Yılmaz, F., 2024. Sustainable Paddy Farming in Edirne: Evaluating the Impacts of Excessive Fertilizer and Pesticide Use. *Sustainability*, 16(17), pp.7814.

Georgakilas, V., Tiwari, J.N., Kemp, K.C., Perman, J.A., Bourlinos, A.B., Kim, K.S. and Zboril, R., 2016. Noncovalent functionalization of graphene and graphene oxide for energy materials, biosensing, catalytic, and biomedical applications. *Chemical Reviews*, 116(9), pp.5464-5519.

Ghaderiardakani, F., Collas, E., Damiano, D.K., Tagg, K., Graham, N.S. and Coates, J.C., 2019. Effects of green seaweed extract on Arabidopsis early development suggest roles for hormone signalling in plant responses to algal fertilisers. *Scientific Reports*, 9(1), pp.1983.

Gharibshahian, E., Tafreshi, M., 2021. Study on the effect of L-Alanine concentration as capping agent on size, structural quality and morphology of KTiOPO4 nanoparticles synthesized by Co-precipitation method. *Iranian Journal of Crystallography and Mineralogy* 29, 249–256.

Ghasemi, A. and Zahediasl, S., 2012. Normality tests for statistical analysis: a guide for non-statisticians. *International Journal of Endocrinology and Metabolism*, 10(2), pp.486.

Ghimirey, V., Chaurasia, J. and Marahatta, S., 2024. Plant nutrition disorders: insights from clinic analyses and their impact on plant health. *Agriculture Extension in Developing Countries*, 2(1), pp.09-17.

Giampieri, F., Mazzoni, L., Cianciosi, D., Alvarez-Suarez, J.M., Regolo, L., Sánchez-González, C., Capocasa, F., Xiao, J., Mezzetti, B. and Battino, M., 2022. Organic vs conventional plant-based foods: A review. *Food Chemistry*, 383, pp.132352.

Giordano, M., Petropoulos, S.A. and Rouphael, Y., 2021. The fate of nitrogen from soil to plants: Influence of agricultural practices in modern agriculture. *Agriculture*, 11(10), pp.944.

Girgel, U., 2025. System-specific determinants of seed yield in common bean: insights from conventional and organic path analyses. *Legume Research - An International Journal*, pp.1–10

Gladvin, G., Sudhaakr, G., Swathi, V. and Santhisri, K.V., 2017. Mineral and vitamin compositions contents in watermelon peel (Rind). *International Journal of Current Microbiology and Applied Sciences*, 5(5), pp.129-133.

Goh, H.T., Cheok, C.Y. and Yeap, S.P., 2023. Green synthesis of silver nanoparticles using banana peel extract and application on banana preservation. *Food Frontiers*, 4(1), pp.283-288.

Goldan, E., Nedeff, V., Barsan, N., Culea, M., Panainte-Lehadus, M., Mosnegutu, E., Tomozei, C., Chitimus, D. and Irimia, O., 2023. Assessment of manure compost used as soil amendment—A review. *Processes*, 11(4), pp.1167.

Gomiero, T., 2016. Soil degradation, land scarcity and food security: Reviewing a complex challenge. *Sustainability*, 8(3), pp.281.

González-Melendi, P., Fernández-Pacheco, R., Coronado, M.J., Corredor, E., Testillano, P.S., Risueño, M.C., Marquina, C., Ibarra, M.R., Rubiales, D. and Pérez-de-Luque, A., 2008. Nanoparticles as smart treatment-delivery systems in plants: assessment of different techniques of microscopy for their visualization in plant tissues. *Annals of Botany*, 101(1), pp.187-195.

Gosavi, V.C., Daspute, A.A., Patil, A., Gangurde, A., Wagh, S.G., Sherkhane, A., Deshmukh, V.A., 2020. Synthesis of green nanobiofertilizer using silver nanoparticles of Allium cepa extract Short title: Green nanofertilizer from *Allium cepa*. *International Journal of Chemical Studies* 8 (4), pp.1690–1694.

Govinda, K., Bhavya, N. and Krishna Murthy, R., 2023. Heavy metal content in chemical fertilizers and its implications on agroecosystems and human health. *Recent Advances in Agricultural Sciences and Technology*.

Goyal, A., Chavan, S.S., Mohite, R.A., Shaikh, I.A., Chendake, Y. and Mohite, D.D., 2025. Emerging trends and perspectives on nano-fertilizers for sustainable agriculture. *Discover Nano*, 20(1), pp.97.

Gu, I., Balogun, O., Brownmiller, C., Kang, H.W. and Lee, S.O., 2023. Bioavailability of citrulline in watermelon flesh, rind, and skin using a human intestinal epithelial Caco-2 cell model. *Applied Sciences*, 13(8), pp.4882.

Guo, L., Yu, H., Kharbach, M. and Wang, J., 2021. The response of nutrient uptake, photosynthesis and yield of tomato to biochar addition under reduced nitrogen application. *Agronomy*, 11(8), pp.1598.

Grevsen, K., Fretté, X.C. and Christensen, L.P., 2009. Content and composition of volatile terpenes, flavonoids and phenolic acids in Greek oregano (*Origanum vulgare* L. ssp. hirtum) at different development stages during cultivation in cool temperate climate. *European Journal of Horticultural Science*, 74(5), pp.193.

Ha, N., Seo, E., Kim, S. and Lee, S.J., 2021. Adsorption of nanoparticles suspended in a drop on a leaf surface of Perilla frutescens and their infiltration through stomatal pathway. *Scientific Reports*, 11(1), pp.11556.

Hamzah, M.A., Alias, A.B. and Ahmad, N.E., 2019. Production of biofuel (bio-ethanol) from fruitwaste: Banana peels. *International Journal of Engineering and Advanced Technology*, 9(1), pp.5897-5901.

Hariram, N.P., Mekha, K.B., Suganthan, V. and Sudhakar, K., 2023. Sustainalism: An integrated socio-economic-environmental model to address sustainable development and sustainability. *Sustainability*, 15(13), pp.10682.

Hariyono, Mulyono, Ayunin, I.Q., 2021. Effectiveness of Banana Peel-Based Liquid Organic Fertilizer Application as Potassium Source for Eggplant (*Solanum melongena* L.) Growth and Yield. In *IOP Conference Series: Earth and Environmental Science* 752, pp.012022.

Hasan, M.M., Islam, M.R., Haque, A.R., Kabir, M.R., Khushe, K.J., Hasan, S.M.K., 2024. Trends and challenges of fruit by-products utilization: insights into safety, sensory, and benefits of the use for the development of innovative healthy food: a review. *Bioresources and Bioprocessing*, 1(1), pp.10.

Hassan, D.U. and Abdulsalam, S., 2017. Assessement of bio-fertilizer quality of anaerobic digestion of watermelon peels and cow dung. *Chemical and Biomolecular Engineering*, *2*(3), pp.135-141.

Hausmann, J.N., Traynor, B., Myers, R.J., Driess, M., Menezes, P.W., 2021. The pH of Aqueous NaOH/KOH Solutions: A Critical and Non-trivial Parameter for Electrocatalysis. *ACS Energy Letters*, 6(10), pp.3567-3571.

He, M., Ye, Z., Lin, G., Yin, S., Huang, X., Zhou, X., Yin, Y., Gui, B., Wang, C., 2023. Research Progress of Porphyrin-Based Covalent Organic Frameworks in Photocatalysis . *Acta Chimica Sinica*, 81(7), pp.784.

Hema, Bhatt, T., Pant, T., Dhondiyal, C.C., Rana, M., Chowdhury, P., Joshi, G.C., Arya, P. and Tiwari, H., 2020. Computational study of the intermolecular interactions and their effect on the UV-visible spectra of the ternary liquid mixture of benzene, ethanol and propylene glycol. *Journal of Molecular Modeling*, 26(10), pp.268.

Hmidi, O., Srarfi, F., Brahim, N., Bambina, P. and Lo Papa, G., 2025. Predicting Soil Electrical Conductivity of Saturated Paste Extract Using Pedotransfer Functions in Northeastern Tunisia. *Sustainability*, 17(20), pp.9177.

Holz, M., Zarebanadkouki, M., Benard, P., Hoffmann, M. and Dubbert, M., 2024. Root and rhizosphere traits for enhanced water and nutrients uptake efficiency in dynamic environments. *Frontiers in Plant Science*, 15, pp.1383373.

Hong, K., Cheng, W., Xue, E., Wang, B. and Amin, A., 2025. Green growth in belt and road initiative countries: exploring the interplay of agriculture production, technological innovation and environmental pollution. *Clean Technologies and Environmental Policy*, 27(8), pp.3601-3621.

Huang, R., Fedeli, S., Hirschbiegel, C.M., Zhang, X. and Rotello, V.M., 2023. Modulation of Gold Nanoparticle Ligand Structure–Dynamic Relationships Probed Using Solution NMR. *ACS Nanoscience Au*, 4(1), pp.62-68.

Hussain, H., Mamadalieva, N.Z., Hussain, A., Hassan, U., Rabnawaz, A., Ahmed, I. and Green, I.R., 2022. Fruit peels: Food waste as a valuable source of bioactive natural products for drug discovery. *Current Issues in Molecular Biology*, 44(5), pp.1960-1994.

Hussain, S.F., Reddy, M.L.N. and Porika, H.K., 2016. Nutrition in banana.

Hussain, W.S., Ahmed, H.F., Al-Saffar, R.S. and Taher, N.A.H.A., 2023. Effect of bio fertilization using banana and apple peels on flax plant's vegetative characteristics. *Al-Azhar Journal of Agricultural Research*, 48(3), pp.395-400.

Hussein, H.S., Shaarawy, H.H., Hussien, N.H. and Hawash, S.I., 2019. Preparation of nano-fertilizer blend from banana peels. *Bulletin of the National Research Centre*, 43(1), pp.1-9.

Ibrahim, O.M.S., Abed, A.M., Yahea, N.Z., 2020. Evaluation of biological activity of greenly synthesized silver nanoparticles using aloe vera gel extract as antibacterial agent In-vitro and In-vivo. *The Iraqi Journal of Agricultural Science* 51(6),pp. 1706–1715.

Ikhuoria, E.U., Uwidia, I.E., Okojie, R.O., Ifijen, I.H., Chikaodili, I.D. and Fatiqin, A., 2024. Advancing green nanotechnology: harnessing the bio-reducing properties of *Musa paradisiaca* peel extract for sustainable synthesis of iron oxide nanoparticles. *Journal of Multidisciplinary Applied Natural Science*, 4(1), pp.108-119.

Iqbal, M., Umar, S. and Mahmooduzzafar, F., 2019. Nano-fertilization to enhance nutrient use efficiency and productivity of crop plants. In *Nanomaterials and plant potential* (pp. 473-505). Cham: Springer International Publishing.

Islam, M., Halder, M., Siddique, M.A., Razir, S.A.A., Sikder, S. and Joardar, J.C., 2019. Banana peel biochar as alternative source of potassium for plant productivity and sustainable agriculture. *International Journal of Recycling of Organic Waste in Agriculture*, 8(Suppl 1), pp.407-413.

Islam, S., 2025a. Agriculture, food security, and sustainability: a review. *Exploration of Foods and Foodomics*, 3, pp.101082.

Islam, S., 2025b. Toxicity and transport of nanoparticles in agriculture: effects of size, coating, and aging. *Frontiers in Nanotechnology*, 7, pp.1622228.

Jafari, B., Kordrostami, M. and Ghasemi-Soloklui, A.A., 2024. Maximizing Tomato Seed Germination: Quantifying Cardinal Temperatures and Thermal Time Requirements. *International Journal of Horticultural Science & Technology,* 11(1).

Jang, Y., Moon, J.H., Kim, S.G., Kim, T., Lee, O.J., Lee, H.J. and Wi, S.H., 2022. Effect of low-temperature tolerant rootstocks on the growth and fruit quality of watermelon in semi-forcing and retarding culture. *Agronomy*, 13(1), pp.67.

Jaroszewska, A., Jedrejek, D., Sobolewska, M., Kowalska, I. and Dzięcioł, M., 2023. Mineral, nutritional, and phytochemical composition and baking properties of teff and watermelon seed flours. *Molecules*, 28(7), pp.3255.

Javed, R., Zia, M., Naz, S., Aisida, S.O., Ain, N.U. and Ao, Q., 2020. Role of capping agents in the application of nanoparticles in biomedicine and environmental remediation: recent trends and future prospects. *Journal of Nanobiotechnology*, 18(1), pp.172.

Jeol, 2025. Electron Optic Documents. Jeol Solutions for Innovation.

Jerszurki, D., Saadon, T., Zhen, J., Agam, N., Tas, E., Rachmilevitch, S. and Lazarovitch, N., 2021. Vertical microclimate heterogeneity and dew formation in semi-closed and naturally ventilated tomato greenhouses. *Scientia Horticulturae*, 288, pp.110271.

Jia-Yi, Y., Meng-Qiang, S., Zhi-Liang, C., Yu-Tang, X., Hang, W., Jian-Qiang, Z., Ling, H., Qi, Z., 2022. Effect of foliage applied chitosan-based silicon nanoparticles on arsenic uptake and translocation in rice (*Oryza sativa* L.). *Journal of Hazardous Material* 433,pp 128781.

John Isa, J.F., 2024. Phytonutrients Composition of Nigerian Banana Fruits (*Musa* species) And Their Peel Extracts. *International Journal of Human and Health Sciences*, 8(2), 170–176.

Joshi, V., Joshi, M., Silwal, D., Noonan, K., Rodriguez, S. and Penalosa, A., 2019. Systematized biosynthesis and catabolism regulate citrulline accumulation in watermelon. *Phytochemistry*, 162, pp.129-140.

Kaeswurm, J.A., Scharinger, A., Teipel, J. and Buchweitz, M., 2021. Absorption coefficients of phenolic structures in different solvents routinely used for experiments. *Molecules*, 26(15), pp.4656.

Kak, V., Kishor, K. and Singh, K., 2024. Nanofertilizers: A New Frontier in Agriculture. In *Nanobiostimulants: Emerging Strategies for Agricultural Sustainability* (pp. 13-27). Cham: Springer Nature Switzerland.

Kalibbala, H.M., Olupot, P.W. and Ambani, O.M., 2023. Synthesis and efficacy of cactus-banana peels composite as a natural coagulant for water treatment. *Results in Engineering*, 17, pp.100945.

Kamala Nalini, S.P., 2020. Vijayaraghavan K. Green synthesis of silver and gold nanoparticles using Aloe vera gel and determining its antimicrobial properties on nanoparticle impregnated cotton fabric. *Journal of Nanotechnology Research*, 2(3), pp.42-50.

Kamble, S.D., Gatade, A.A., Sharma, A. and Sahoo, A., 2022. Physico-chemical composition and mineral content of Aloe vera (*Aloe barbadensis* miller) gel. *International Journal of Multidisciplinary Educational Research*, 11(4), pp.73-79.

Kanabar, P., Wu, Y. and Nandwani, D., 2024. Enhancing sustainable cultivation of organic bell pepper through Fulvic Acid (FA) application: impact on phytochemicals and antioxidant capacity under open-field conditions. *Sustainability*, 16(16), pp.6745.

Kataria, D., Kaur, J., 2023. From Waste to Wellness: Exploring the Nutritional Composition, Health Benefits and Utilization of Watermelon Rind. *Journal of Food Chemistry and Nanotechnology*, 14,pp.9.

Hosseingholian, A., Gohari, S.D., Feirahi, F., Moammeri, F., Mesbahian, G., Moghaddam, Z.S. and Ren, Q., 2023. Recent advances in green synthesized nanoparticles: from production to application. *Materials Today Sustainability*, 24, pp.100500.

Keita, D.S., Koffi, K.P., Chhapia, P. and Patel, H., 2025. Impact of titanium dioxide and zinc oxide nanoparticles on soil micronutrients. *Discover Soil*, 2(1), pp.1-15.

Kekeli, M.A., Wang, Q. and Rui, Y., 2025. The role of nano-fertilizers in sustainable agriculture: Boosting crop yields and enhancing quality. *Plants*, 14(4), pp.554.

Khalifa, A.M., Safhi, F.A. and Elsherif, D.E., 2024. Green synthesis of a dual-functional sulfur nanofertilizer to promote growth and enhance salt stress resilience in faba bean. *BMC Plant Biology*, 24(1), pp.607.

Khan, I., Awan, S.A., Rizwan, M., Hassan, Z.U., Akram, M.A., Tariq, R., Brestic, M. and Xie, W., 2022. Nanoparticle's uptake and translocation mechanisms in plants via seed priming, foliar treatment, and root exposure: a review. *Environmental Science and Pollution Research*, 29(60), pp.89823-89833.

Khan, M., Arif, M., Karim, T., Khan, D., Rashid, H., Ahmad, F. and Zeeshan, M., 2022. Food safety and the effect of fertilizers on human health. *International Journal of Endorsing Health Science Research*, 11(1), pp.54-57.

Khan, M.T., Aleinikovienė, J. and Butkevičienė, L.M., 2024. Innovative organic fertilizers and cover crops: Perspectives for sustainable agriculture in the era of climate change and organic agriculture. *Agronomy*, 14(12), pp.2871.

Khang, D.T., Tien, L.T.T., Men, T.T. and Thuy, N.P., 2021. Potential of fermented fruit peel liquid in cosmetics as a skin care agent. *Cosmetics*, 8(2), pp.33.

Khanna, V., Singh, S., Sudhakar, K., Baghel, D.S., Kumar, B., Wadhawa, S., Pandey, N.K., 2024. Green Synthesis of Copper Nanoparticles From Aloe Vera Leaf Gel Concentrate and its Characterisation. *Rasayan Journal of Chemistry* 17(3), pp.957–963.

Khanyile, N., Dlamini, N., Masenya, A., Madlala, N.C., Shezi, S., 2024. Preparation of Biofertilizers from Banana Peels: Their Impact on Soil and Crop Enhancement. *Agriculture*, 14(11), pp.1894.

Kharissova, O.V., Kharisov, B.I., Oliva Gonzalez, C.M., Méndez, Y.P. and López, I., 2019. Greener synthesis of chemical compounds and materials. *Royal Society open science*, 6(11), pp.191378.

Khundi, Q., Jiang, Y., Sun, Y. and Rui, Y., 2025. Nanofertilizers for Sustainable African Agriculture: A Global Review of Agronomic Efficiency and Environmental Sustainability. *Nanomaterials*, 15(5), pp.390.

Kim, H.N. and Park, J.H., 2024. Monitoring of soil EC for the prediction of soil nutrient regime under different soil water and organic matter contents. *Applied Biological Chemistry*, 67(1), p.1.

Kim, J.H., Lee, Y., Kim, E.J., Gu, S., Sohn, E.J., Seo, Y.S., An, H.J. and Chang, Y.S., 2014. Exposure of iron nanoparticles to *Arabidopsis thaliana* enhances root elongation by triggering cell wall loosening. *Environmental Science & Technology*, 48(6), pp.3477-3485.

Kitundu, M.P., Msuya, N. and Katima, Z., 2025. Production of Potassium-Rich Biofertilizer from Composted Banana Peels and Watermelon Rinds. *Tanzania Journal of Engineering and Technology*, 44(1), pp.118-136.

Knapp, S. and Peralta, I.E., 2016. The tomato (*Solanum lycopersicum* L., Solanaceae) and its botanical relatives. In *The tomato genome* (pp. 7-21). Berlin, Heidelberg: Springer Berlin Heidelberg.

Kouniba, S., Benbiyi, A., Zourif, A. and Guendouzi, M.E., 2024. Optimization use of watermelon rind in the coagulation-flocculation process by Box Behnken design for copper, zinc, and turbidity removal. *Heliyon*, 10(10).

Kumar, S., Sharma, Y., Khandelwal, V., Rawat, K. and Patil, A., 2025. Applications of nanotechnology in fertilizers: a review study. *Sustainable Chemistry for the Environment*, pp.100247.

Kumari, N., Pandey, A.K., Singh, A.K. and Singh, A., 2024. Sustainable agriculture: Balancing productivity and environmental stewardship for future generations. *Journal of Scientific Research and Reports*, 30(8), pp.629-639.

Kumari, P., Gaur, S.S. and Tiwari, R.K., 2023. Banana and its by-products: A comprehensive review on its nutritional composition and pharmacological benefits. *eFood*, 4(5), pp.e110.

Kurganskaya, I. and Luttge, A., 2023. Probability distributions of mineral dissolution rates: the role of lattice defects. *Frontiers in Water*, 5, p.1225837.

Lakey-Beitia, J., Burillo, A.M., La Penna, G., Hegde, M.L. and Rao, K.S., 2021. Polyphenols as potential metal chelation compounds against Alzheimer's disease. *Journal of Alzheimer's Disease*, 82(s1), pp.S335-S357.

Lalitha, J., Rafath, H. and Subash, M., 2016. Effect of gibberellic acid and indole 3-acetic acid on seed germination performance of horse gram (*Macrotyloma uniflorum*) Lam (Verdc). *Journal of Applied and Advanced Research*, 1(2), pp.36-40.

Latef, A.A.H.A., Srivastava, A.K., El-sadek, M.S.A., Kordrostami, M., Tran, L.S.P., 2018. Titanium Dioxide Nanoparticles Improve Growth and Enhance Tolerance of Broad Bean Plants under Saline Soil Conditions. *Land Degradation & Development* 29(4) ,p p.1065–1073.

Lazicki, P., Geisseler, D., Lloyd, M., 2020. Nitrogen mineralization from organic amendments is variable but predictable. *Journal of Environmental Quality*, 49, pp. 483–495.

Leedy, P.D. and Ormrod, J.E., 2015. *Practical research*. Pearson Education UK.

Lesaine, A., Bonamy, D., Rountree, C.L., Gauthier, G., Impéror-Clerc, M. and Lazarus, V., 2021. Role of particle aggregation in the structure of dried colloidal silica layers. *Soft Matter*, 17(6), pp.1589-1600.

Li, Y. and Mattson, N.S., 2019. Effect of organic fertilizer source and rate on growth and nutrient leachate profile of greenhouse-grown cucumber. *HortTechnology*, 29(4), pp.450-456.

Lian, J., Liu, W., Meng, L., Wu, J., Chao, L., Zeb, A. and Sun, Y., 2021. Foliar-applied polystyrene nanoplastics (PSNPs) reduce the growth and nutritional quality of lettuce (*Lactuca sativa* L.). *Environmental Pollution*, 280, pp.116978.

Liang, Y., Deng, L., Feng, Z., Ouyang, Q., Wu, X., Quan, W., Zhu, Y., Ye, H., Wu, K. and Luo, H., 2023. A chitosan-based flocculation method for efficient recovery of high-purity B-phycoerythrin from a low concentration of phycobilin in wastewater. *Molecules*, 28(8), pp.3600.

Lin, D., Xiao, M., Zhao, J., Li, Z., Xing, B., Li, X., Kong, M., Li, L., Zhang, Q., Liu, Y. and Chen, H., 2016. An overview of plant phenolic compounds and their importance in human nutrition and management of type 2 diabetes. *Molecules*, 21(10), pp.1374.

Lin, M., Liu, P., Jun, L., Zhou, W. and Yuan, J., 2021. Phosphorus bioavailability and migration of hydroxyapatite in different sizes as phosphorus fertilizer in c*amellia oleifera* seedlings. *HortScience*, 56(9), pp.1112-1118.

Lipiec, J. and Usowicz, B., 2024. Temporal variability in water content, temperature, and electrical conductivity of sandy soil: Responses to soil-improving cropping systems (SICS). *Soil and Tillage Research*, 242, pp.106166.

Lisboa, L.A.M., Galindo, F.S., Pagliari, P.H., Goncalves, J.I.U.P., Okazuka, M.H., Cunha, M.L.O. and de Figueiredo, P.A.M., 2024. Morpho-physiological assessment of tomato and bell pepper in response to nutrient restriction. *Stresses*, 4(1), pp.172-184.

Liu, G., Zotarelli, L., Li, Y., Dinkins, D., Wang, Q. and Ozores-Hampton, M., 2014. Controlled-Release and Slow-Release Fertilizers as Nutrient Management Tools: HS1255/HS1255, 10/2014. *EDIS*, 2014(8).

Liu, J., Yang, W., Zhou, H., Zia-ur-Rehman, M., Salam, M., Ouyang, L., Chen, Y., Yang, L. and Wu, P., 2024. Exploring the mechanisms of organic fertilizers on Cd bioavailability in rice fields: Environmental behavior and effect factors. *Ecotoxicology and Environmental Safety*, 285, pp.117094.

Liu, X., Liu, S., Jin, X., Liu, H., Sun, K., Wang, X., Li, M., Wang, P., Chang, Y., Wang, T. and Wang, B., 2024. An encounter between metal ions and natural products: natural products-coordinated metal ions for the diagnosis and treatment of tumors. *Journal of Nanobiotechnology*, 22(1), pp.726.

Lu, B., Huang, Y., Chen, Z., Ye, J., Xu, H., Chen, W. and Long, X., 2019. Niosomal nanocarriers for enhanced skin delivery of quercetin with functions of anti-tyrosinase and antioxidant. *Molecules*, 24(12), pp.2322.

Juncal, M.J.L., Masino, P., Bertone, E. and Stewart, R.A., 2023. Towards nutrient neutrality: A review of agricultural runoff mitigation strategies and the development of a decision-making framework. *Science of the Total Environment*, 874, pp.162408.

Luo, X., Li, J., Guo, S., Yu, H., Zeng, X., Zhou, Z., Shangguan, Y., He, M., Ouyang, Y., Chen, K. and Chen, Z., 2025. Analysis of research status and trends on nano-agricultural application: a bibliometric study. *Frontiers in Plant Science*, 16, pp.1530629

Ma, S., Du, S., Pan, G., Dai, S., Xu, B. and Tian, W., 2021. Organic molecular aggregates: From aggregation structure to emission property. *Aggregate*, 2(4), pp.e96.

Maaz, T.M., Dobermann, A., Lyons, S.E. and Thomson, A.M., 2025. Review of research and innovation on novel fertilizers for crop nutrition. *npj Sustainable Agriculture*, 3(1), pp.25.

Maćczak, P., Kaczmarek, H. and Ziegler-Borowska, M., 2020. Recent achievements in polymer bio-based flocculants for water treatment. *Materials*, 13(18), pp.3951.

Madjar, R.M., Vasile Scăețeanu, G. and Sandu, M.A., 2024. Nutrient water pollution from unsustainable patterns of agricultural systems, effects and measures of integrated farming. *Water*, 16(21), pp.3146.

Madlala, N.C., Khanyile, N. and Masenya, A., 2024. Examining the correlation between the inorganic nano-fertilizer physical properties and their impact on crop performance and nutrient uptake efficiency. *Nanomaterials*, 14(15), pp.1263.

Mahlambi, P.N. and Moloto, M.J., 2022. Starch-capped silver oxide (Ag2O) nanoparticles: synthesis, characterization and antibacterial activity. *Digest Journal Nanomaterials and. Biostructures*, 17, pp.921-930.

Mahmud, A., Yusuf, M., Ahmed, A., Ado, D. and Adamu, Y., 2019. Studies on conversion of solid waste to bioferilizer by vermicomposting. *Trends in Science & Technology Journal*, 4, pp.137-139.

Malekzadeh, E., Tatari, A., Motlagh, M.B., Nohesara, M. and Mohammadi, S., 2024. A novel approach for the green synthesis of iron nanoparticles using marigold extract, black liquor, and nanocellulose: effect on marigold growth parameters. *International Journal of Biological Macromolecules*, 267, pp.131552.

Ma'mor, A.S., Wahida, N.H. and Firdaus, A.N., 2023, June. The application of eggshell and fruit peels as soil amendment on the growth performance and yield of corn (*Zea mays* L.). In *IOP Conference Series: Earth and Environmental Science*,1182(1), pp. 012040). IOP Publishing.

Manikishore, M., Rathee, S., Chauhan, A.S. and Patil, U.K., 2025. Watermelon Rind: Nutritional Composition, Therapeutic Potential, Environmental Impact, and Commercial Applications in Sustainable Industries. *Current Pharmaceutical Design*.

Manivannan, A., Lee, E.S., Han, K., Lee, H.E. and Kim, D.S., 2020. Versatile nutraceutical potentials of watermelon—A modest fruit loaded with pharmaceutically valuable phytochemicals. *Molecules*, 25(22), pp.5258.

Marcia, M., Vinh, C., Dolle, C., Abellán, G., Schönamsgruber, J., Schunk, T., Butz, B., Spiecker, E., Hauke, F. and Hirsch, A., 2018. Highly Integrated Organic-Inorganic Hybrid Architectures by Non-Covalent Exfoliation of Graphite and Assembly with Zinc Oxide Nanoparticles. *arXiv preprint arXiv:1805.09129*.

Marcinkowska, K., Synowiec, A., Łacka, A., Wenda-Piesik, A., Gala-Czekaj, D., Haliniarz, M., Marczewska-Kolasa, K., Domaradzki, K., Podsiadło, C. and Pytlarz, E., 2025. Temperature-dependent germination dynamics of herbicide-resistant and susceptible blackgrass (*Alopecurus myosuroides*) and silky windgrass (*Apera spica-venti*) from Poland. *Scientific Reports*.

Marković, J.M.D., Marković, Z.S., Brdarić, T.P. and Filipović, N.D., 2011. Comparative spectroscopic and mechanistic study of chelation properties of fisetin with iron in aqueous buffered solutions. Implications on in vitro antioxidant activity. *Dalton Transactions*, 40(17), pp.4560-4571.

Maseko, K.H., Regnier, T., Meiring, B., Wokadala, O.C. and Anyasi, T.A., 2024. *Musa* species variation, production, and the application of its processed flour: A review. *Scientia Horticulturae*, 325, pp.112688.

Mashela, P.W., Dube, Z.P. and Pofu, K.M., 2015. Managing the phytotoxicity and inconsistent nematode suppression in soil amended with phytonematicides. In *Organic Amendments and Soil Suppressiveness in Plant Disease Management* (pp. 147-173). Cham: Springer International Publishing.

Massimi, M. and Radocz, L., 2021. The Action of nutrients deficiency on growth biometrics, physiological traits, production indicators, and disease development in pepper (*Capsicum annuum* L.) plant: A review.

McLaughlin, S., Zhalnina, K., Kosina, S., Northen, T.R. and Sasse, J., 2023. The core metabolome and root exudation dynamics of three phylogenetically distinct plant species. *Nature Communications*, 14(1), pp.1649.

Meena, R.S., Pradhan, G., Kumar, S. and Lal, R., 2023. Using industrial wastes for rice-wheat cropping and food-energy-carbon-water-economic nexus to the sustainable food system. *Renewable and Sustainable Energy Reviews*, 187, pp.113756.

Miao, L., Wang, X., Yu, C., Ye, C., Yan, Y. and Wang, H., 2024. What factors control plant height?. *Journal of Integrative Agriculture*, 23(6), pp.1803-1824.

Michen, B., Geers, C., Vanhecke, D., Endes, C., Rothen-Rutishauser, B., Balog, S. and Petri-Fink, A., 2015. Avoiding drying-artifacts in transmission electron microscopy: Characterizing the size and colloidal state of nanoparticles. *Scientific reports*, 5(1), pp.9793.

Midde, S.K., Perumal, M.S., Murugan, G., Sudhagar, R., Mattepally, V.S. and Bada, M.R., 2022. Evaluation of nano urea on growth and yield attributes of rice (*Oryza Sativa* L.). *Chemical Science Review and Letters*, 11(42), pp.211-214.

Mim, J.J., Rahman, S.M., Khan, F., Paul, D., Sikder, S., Das, H.P., Khan, S., Orny, N.T., Shuvo, M.R.H. and Hossain, N., 2025. Towards smart agriculture through nano-fertilizer-A review. *Materials Today Sustainability*, 30, pp.101100.

Mimmo, T., Pii, Y., Valentinuzzi, F., Astolfi, S., Lehto, N., Robinson, B., Brunetto, G., Terzano, R. and Cesco, S., 2017, June. Nutrient availability in the rhizosphere: a review. In *VIII International Symposium on Mineral Nutrition of Fruit Crops 1217* (pp. 13-28).

Mo, R.J., Zhao, Y., Wu, M., Xiao, H.M., Kuga, S., Huang, Y., Li, J.P. and Fu, S.Y., 2016. Activated carbon from nitrogen rich watermelon rind for high-performance supercapacitors. *RSC Advances*, 6(64), pp.59333-59342.

Mohammed, A.S.A., Naveed, M. and Jost, N., 2021. Polysaccharides; classification, chemical properties, and future perspective applications in fields of pharmacology and biological medicine (a review of current applications and upcoming potentialities). *Journal of Polymers and the Environment*, 29(8), pp.2359-2371.

Dilip, W.S., Singh, D., Moharana, D., Rout, S. and Patra, S.S., 2017. Influence of gibberellic acid (GA3) on seed germination and seedling growth of Kagzi Lime. *Journal of Scientific Agriculture*, 1, pp.62-69.

Mohd Dom, Z., Mujianto, L., Azhar, A., Masaudin, S. and Samsudin, R., 2021. Physicochemical properties of banana peel powder in functional food products. *Food Research*, 5(1), pp.209-215.

Montejo, N.C., López, J.I.G., Naveda, A.F., Melgoza, F.A.G., Chacón, X.R. and Cortez, M.D.P.M., 2024. Agronomic Evaluation of Experimental Lines of Bell Pepper under Greenhouse Conditions. *Journal of Experimental Agriculture International*, 46(8), pp.710-722.

Moodley, V., Phophi, M.M. and Mafongoya, P.L., 2024. Regenerative agriculture: A paradigm shift for food production in South Africa. *Outlook on Agriculture*, 53(4), pp.336-350.

Morales-Cámara, S., Cardona-Carrascosa, L., Salcedo-Abraira, P., Rodríguez-Diéguez, A. and Rojas, S., 2025. Controlled Magnesium Release and Nutritional Effect of a Novel Metal–Organic Framework on Plants. *Crystal Growth & Design*.

Mosley, L.M., Rengasamy, P. and Fitzpatrick, R., 2024. Soil pH: Techniques, challenges and insights from a global dataset. *European Journal of Soil Science*, 75(6), pp.e70021.

Motasim, A.M., Samsuri, A.W., Nabayi, A., Akter, A., Haque, M.A., Abdul Sukor, A.S. and Adibah, A.M., 2024. Urea application in soil: Processes, losses, and alternatives—A review. *Discover Agriculture*, 2(1), pp.42.

Muchenski, F. and Mattoso, N., 2021. Synthesis and characterization of Ni79Fe15Mo6 nanoparticles produced by Co-precipitation in the presence of organic additives. *Journal Material Science Engeneering B*, 11, pp.89-97.

Munoz, O.M., Leal, X., Quitral, V. and Cardemil, L.J.M.A.P., 2015. Extraction, characterization and properties of the gel of Aloe vera (*Aloe barbadensis* Miller) Cultivated in Chile. *Medicine and Aromatic Plants*, 4(3), pp.2-7.

Mustafa, N., Raja, N.I., Ilyas, N., Ikram, M., Mashwani, Z.U.R. and Ehsan, M., 2021. Foliar applications of plant-based titanium dioxide nanoparticles to improve agronomic and physiological attributes of wheat (*Triticum aestivum* L.) plants under salinity stress. *Green Processing and Synthesis*, 10(1), pp.246-257.

Mutayoba, V. and Ngaruko, D., 2018. Assessing tomato farming and marketing among smallholders in high potential agricultural areas of Tanzania. *International Journal of Economics, Commerce and Management*, 6(8), pp.577-590.

MyScope, 2025. Energy Dispersive Spectroscopy. Microscopy Training -Microscopy Australia.

Nadeem, M., Navida, M., Ameer, K., Iqbal, A., Malik, F., Nadeem, M.A., Fatima, H., Ahmed, A. and Din, A., 2022. A comprehensive review on the watermelon phytochemical profile and their bioactive and therapeutic effects. *Food Science and Preservation*, 29(4), pp.546-576.

Naika, S., De Jeude, J.V.L., de Goffau, M., Hilmi, M. and van Dam, B., 2005. Cultivation of tomato. *Production, processing and marketing, Agromisa/CTA. Revised edition*.

Nakayama, H., Ichihashi, Y. and Kimura, S., 2023. Diversity of tomato leaf form provides novel insights into breeding. *Breeding Science*, 73(1), pp.76-85.

Nasir, N.A.H.A., Roslly, N.A.L., Rosli, N.M. and Razali, Z., 2020, April. Phytochemical screening and potential dpph radical scavenging activity of banana peel extract. In *Charting the Sustainable Future of ASEAN in Science and Technology: Proceedings from the 3rd International Conference on the Future of ASEAN (ICoFA)* 2019-Volume *2* (pp. 249-258). Singapore: Springer Singapore.

Nistor, A.N. and Butnariu, M., 2023. Physical properties and identification of flavonoids by ultraviolet-visible spectroscopy. *International Journal of Biochemistry & Physiology*, *8*(2), pp.239.

Nazir, M.A., Hasan, M., Mustafa, G., Tariq, T., Ahmed, M.M., Golzari Dehno, R. and Ghorbanpour, M., 2024. Zinc oxide nano-fertilizer differentially effect on morphological and physiological identity of redox-enzymes and biochemical attributes in wheat (*Triticum aestivum* L.). *Scientific Reports*, 14(1), pp.13091.

Ndikau, M., Noah, N.M., Andala, D.M. and Masika, E., 2017. Green synthesis and characterization of silver nanoparticles using *Citrullus lanatus* fruit rind extract. *International Journal of Analytical Chemistry*, 2017(1), p.8108504.

Ng, M.H. and Choo, Y.M., 2016. Improved method for the qualitative analyses of palm oil carotenes using UPLC. *Journal of Chromatographic Science*, 54(4), pp.633-638.

Ngcobo, B.L. and Bertling, I., 2021. Effect of light combined with heat treatment on colour development and fruit quality of cherry tomato (*Solanum lycopersicum* L.).

Ngole-Jeme, V. and Ntumba, C.N., 2024. Fruit and vegetable peel characteristics and their conversion to biosorbents using hydrothermal carbonization and pyrolysis: A review. *BioResources*, 19(4), pp.9853.

Ngosong, C., Tatah, B.N., Olougou, M.N.E., Suh, C., Nkongho, R.N., Ngone, M.A., Achiri, D.T., Tchakounté, G.V.T. and Ruppel, S., 2022. Inoculating plant growth-promoting bacteria and arbuscular mycorrhiza fungi modulates rhizosphere acid phosphatase and nodulation activities and enhance the productivity of soybean (Glycine max). *Frontiers in Plant Science*, 13, pp.934339.

Nissar, J., Sidiqi, U.S., Dar, A.H. and Akbar, U., 2025. Nutritional composition and bioactive potential of watermelon seeds: a pathway to sustainable food and health innovation. *Sustainable Food Technology*, 3(2), pp.375-395.

Nobahar, A., Carlier, J.D., Miguel, M.G. and Costa, M.C., 2021. A review of plant metabolites with metal interaction capacity: a green approach for industrial applications. *BioMetals*, 34(4), pp.761-793.

Nongbet, A., Mishra, A.K., Mohanta, Y.K., Mahanta, S., Ray, M.K., Khan, M., Baek, K.H. and Chakrabartty, I., 2022. Nanofertilizers: a smart and sustainable attribute to modern agriculture. *Plants*, 11(19), pp.2587.

Nurseha, N., Sedijani, P. and Japa, L., 2023. The Effect of Egg Shell and Banana Peel Organic Fertilizer on The Growth Of Green Spinach (*Amaratus tricolor* L.). *Jurnal Biologi Tropis*, 23(4), pp.19-26.

Odogwu, D.A., Olubusoye, B.S., Olaleye, B.V., Adekoya, S.B. and Adegoke, A.S.O., 2022. Effects of Storage Time on the Physico-Chemical Propertiesof Watermelon (*Citrullus lanatus*) and Carrot (*Daucus carota*) Juice. *International Journal of Innovative Science and Research Technology*, 7, pp.971-985.

Ogodo, U.P. and Abosede, O.O., 2025. The role of chemistry in achieving sustainable development goals: Green chemistry perspective. *International Research Journal of Pure and Applied Chemistry*, 26(1), pp.1-8.

Olalekan., K.K., Ojeleye., A.E., Afolabi, M.S., Murtadha, M.A., Ibrahim, W.A., Chukwu, S.C., Alawode., Y.O., 2025. Watermelon (*Citrullus lanatus* Thunb. L); A Vegetable Crop for Healthy Living and Food Security: A Review. *Journal of Forest Science and Environment,* 10(1),pp. 86–97.

Oliveira, H.C., Seabra, A.B., Kondak, S., Adedokun, O.P. and Kolbert, Z., 2023. Multilevel approach to plant–nanomaterial relationships: from cells to living ecosystems. *Journal of Experimental Botany*, 74(12), pp.3406-3424.

Ortas, I., 2013. Influences of nitrogen and potassium fertilizer rates on pepper and tomato yield and nutrient uptake under field conditions. *Scientific Research and Essays*, 8(23), pp.1048-1055.

Osorio-Guarin, J.A., Higgins, J., Toloza-Moreno, D.L., Di Palma, F., Enriquez Valencia, A.L., Riveros Munévar, F., De Vega, J.J. and Yockteng, R., 2024. Genome-wide association analyses using multilocus models on bananas (*Musa* spp.) reveal candidate genes related to morphology, fruit quality, and yield. *G3: Genes, Genomes, Genetics*, 14(8), pp.108.

Oyediran, O.K., Olagoke, O.O., Abiodun, S., 2025. Nano-Biofertilizers Application as Sustainable Approach to Enhance Crop Productivity and Soil Health: A Review. *Global Journal of Agricultural Research* 13 (1), pp. 47–71.

Oyeyinka, B.O. and Afolayan, A.J., 2019. Comparative evaluation of the nutritive, mineral, and antinutritive composition of *Musa sinensis* L.(Banana) and *Musa paradisiaca* L.(Plantain) fruit compartments. *Plants*, 8(12), pp.598.

Özgören Can, T., Aydin, Y., Utkan, G. and Altınkut Uncuoğlu, A., 2024. Green synthesis and characterization of Fe2O3, ZnO and TiO2 nanoparticles and searching for their potential use as biofertilizer on sunflower. *Physiology and Molecular Biology of Plants*, 30(9), pp.1429-1447.

Öztürk, M.A., Altay, V. and Efe, R. eds., 2022. *Biodiversity, Conservation and Sustainability in Asia* (pp. 1-1089). Cham: Springer.

Pagano, M., Lunetta, E., Belli, F., Mocarli, G., Cocozza, C. and Cacciotti, I., 2025. Advancements in agricultural nanotechnology: an updated review. *Plants*, 14(18), pp.2939.

Pal, J., Sharma, M., Tiwari, A., Tiwari, V., Kumar, M., Sharma, A., Hassan Almalki, W., Alzarea, S.I., Kazmi, I., Gupta, G. and Kumarasamy, V., 2024. Oxidative Coupling and Self-Assembly of Polyphenols for the Development of Novel Biomaterials. *ACS Omega*, 9(18), pp.19741-19755.

Pal, P., Sehgal, H., Joshi, M., Arora, G., Simek, M., Lamba, R.P., Maurya, S. and Pal, U.N., 2025. Advances in using non-thermal plasmas for healthier crop production: toward pesticide and chemical fertilizer-free agriculture. *Planta*, 261(5), pp.109.

Pandian, K., Mustaffa, M.R.A.F., Mahalingam, G., Paramasivam, A., Prince, A.J., Gajendiren, M., Mohammad, A.R.R. and Varanasi, S.T., 2024. Synergistic conservation approaches for nurturing soil, food security and human health towards sustainable development goals. *Journal of Hazardous Materials Advances*, 16, pp.100479.

Pannacci, E., Baratta, S., Falcinelli, B., Farneselli, M. and Tei, F., 2022. Mugwort (*Artemisia vulgaris* L.) Aqueous extract: Hormesis and biostimulant activity for seed germination and seedling growth in vegetable crops. *Agriculture*, 12(9), pp.1329.

Paris, H.S., 2015. Origin and emergence of the sweet dessert watermelon, *Citrullus lanatus*. *Annals of botany*, 116(2), pp.133-148.

Pattnaik, C., Mishra, R., Lenka, A., Kar, B.P., Dash, S.K., Sahoo, L.N., Tripathy, S.K., Nayak, G.C. and Sahoo, S., 2025. Exploring the versatility of carbohydrate-capped green silver nanoparticles as multi-dimensional reagents for targeted applications. *Journal of Molecular Structure*, 1319, pp.139544.

Pawar, J. and Kakde, U., 2022. Biosynthesis of silver nanoparticles from banana peel extract and its antibacterial assay. *International Journal of Researches in Biosciences, Agriculture and Technology*, 1(10), pp.92-100.

Peddi, P., 2025. Biogenic Synthesis Of Potassium Nanoparticles From *Artocarpus hirsutus* Leaf Extract: A Novel Nanofertilizer For Enhanced Growth Of *Vigna radiata*. *Research Journal Of Chemistry And Environment*, 29(3), pp.95-106.

Penuelas, J., Coello, F. and Sardans, J., 2023. A better use of fertilizers is needed for global food security and environmental sustainability. *Agriculture & Food Security*, 12(1), pp.1-9.

Pereira, C., Dias, M.I., Petropoulos, S.A., Plexida, S., Chrysargyris, A., Tzortzakis, N., Calhelha, R.C., Ivanov, M., Stojković, D., Soković, M. and Barros, L., 2019. The effects of biostimulants, biofertilizers and water-stress on nutritional value and chemical composition of two spinach genotypes (*Spinacia oleracea* L.). *Molecules*, 24(24), p.4494.

Pérez-de-Luque, A., 2017. Interaction of nanomaterials with plants: what do we need for real applications in agriculture?. *Frontiers in Environmental Science*, 5, pp.12.

Pérez-Juárez, C.M., García-Ortíz, J.D., González-Martínez, D.W., Flores-Gallegos, A.C., Cruz-Requena, M., Sáenz-Galindo, A., Ascacio-Valdes, J.A. and Rodríguez-Herrera, R., 2025. Physicochemical characterization of flours and biocompounds obtained by microwave and ultrasound assisted extraction from melon and watermelon rind flours. *Food and Humanity*, 4, pp.100479.

Perumalsamy, H., Balusamy, S.R., Sukweenadhi, J., Nag, S., MubarakAli, D., El-Agamy Farh, M., Vijay, H. and Rahimi, S., 2024. A comprehensive review on Moringa *oleifera* nanoparticles: importance of polyphenols in nanoparticle synthesis, nanoparticle efficacy and their applications. *Journal of nanobiotechnology*, 22(1), pp.71.

Pochapski, D.J., Carvalho dos Santos, C., Leite, G.W., Pulcinelli, S.H. and Santilli, C.V., 2021. Zeta potential and colloidal stability predictions for inorganic nanoparticle dispersions: Effects of experimental conditions and electrokinetic models on the interpretation of results. *Langmuir*, 37(45), pp.13379-13389.

Pohshna, C. and Mailapalli, D.R., 2023. Modeling the particle size of nanomaterials synthesized in a planetary ball mill. *OpenNano*, 14, pp.100191.

Pohshna, C., Mailapalli, D.R. and Laha, T., 2020. Synthesis of nanofertilizers by planetary ball milling. In *Sustainable Agriculture Reviews,* 40 (pp. 75-112). Cham: Springer International Publishing.

Poudel, A., Singh, S.K., Jiménez-Ballesta, R., Jatav, S.S., Patra, A. and Pandey, A., 2023. Effect of nano-phosphorus formulation on growth, yield and nutritional quality of wheat under semi-arid climate. *Agronomy*, 13(3), pp.768.

Povero, G., Mejia, J.F., Di Tommaso, D., Piaggesi, A. and Warrior, P., 2016. A systematic approach to discover and characterize natural plant biostimulants. *Frontiers in Plant Science*, 7, pp.435.

Pradeep, M., Kruszka, D., Kachlicki, P., Mondal, D. and Franklin, G., 2021. Uncovering the phytochemical basis and the mechanism of plant extract-mediated eco-friendly synthesis of silver nanoparticles using ultra-performance liquid chromatography coupled with a photodiode array and high-resolution mass spectrometry. *ACS Sustainable Chemistry & Engineering*, 10(1), pp.562-571.

Preet, T., Ghai, N. and Jindal, S.K., 2020. Ameliorating thermo-tolerance in bell pepper (*Capsicum annuum* L. var. grossum) with plant growth regulators. *Vegetable Science*, 47(2), pp.213-218.

Priya, A.K., Alagumalai, A., Balaji, D. and Song, H., 2023. Bio-based agricultural products: a sustainable alternative to agrochemicals for promoting a circular economy. *RSC Sustainability*, 1(4), pp.746-762.

Pudhuvai, B., Koul, B., Das, R. and Shah, M.P., 2024. Nano-Fertilizers (NFs) for resurgence in nutrient use efficiency (NUE): A sustainable agricultural strategy. *Current Pollution Reports*, 11(1), pp.1.

Qu, P., Wang, B., Qi, M., Lin, R., Chen, H., Xie, C., Zhang, Z., Qiu, J., Du, H. and Ge, Y., 2024. Medicinal plant root exudate metabolites shape the rhizosphere microbiota. *International Journal of Molecular Sciences*, 25(14), pp.7786.

Quddus, M.A., Ahmed, R., Islam, M., Haque, M.E., Islam, M.A., Alam, A., Rahman, M.Z., Fahad, Z.H., Islam, M.K., Gaber, A. and Bárek, V., 2025. Organic and inorganic fertilizers influence the productivity, fruit quality and nutrient use efficiency of strawberry (Fragaria× ananassa Duch.). *Scientific Reports*, *15*(1), pp.26252.

Rahman, A., Baharlouei, P., Koh, E.H.Y., Pirvu, D.G., Rehmani, R., Arcos, M. and Puri, S., 2024. A comprehensive analysis of organic food: evaluating nutritional value and impact on human health. *Foods*, 13(2), pp.208.

Rai, K.K. and Kaushik, P., 2023. Free radicals mediated redox signaling in plant stress tolerance. *Life*, 13(1), pp.204.

Rai, S., Acharya-Siwakoti, E., Kafle, A., Devkota, H.P. and Bhattarai, A., 2021. Plant-derived saponins: a review of their surfactant properties and applications. *Sci*, 3(4), pp.44.

Ranjha, M.M.A.N., Irfan, S., Nadeem, M. and Mahmood, S., 2022. A comprehensive review on nutritional value, medicinal uses, and processing of banana. *Food Reviews International*, 38(2), pp.199-225.

Rather, J.A., Akhter, N., Ayaz, Q., Mir, S.A., Singh, A., Goksen, G., Majid, D., Makroo, H.A. and Dar, B.N., 2023. Fruit peel valorization, phytochemical profile, biological activity, and applications in food and packaging industries: Comprehensive review. *Current Food Science and Technology Reports*, 1(2), pp.63-79.

Rayment, G.E. and Higginson, F.R., 1992. *Australian laboratory handbook of soil and water chemical Methods.*

Rayne, N. and Aula, L., 2020. Livestock manure and the impacts on soil health: A review. *Soil Systems*, 4(4), pp.64.

Reda, M., Ashames, A., Edis, Z., Bloukh, S., Bhandare, R. and Abu Sara, H., 2019. Green synthesis of potent antimicrobial silver nanoparticles using different plant extracts and their mixtures. *Processes*, 7(8), pp.510.

Reddy, M.K., Asthana, R., Debnath, S., Ray, P., Mandal, N., Arunachalam, A. and Koduru, J.R., 2024. Nanofertilizers for sustainable crop production: A comprehensive review. *BioNanoScience*, 14(2), pp.1918-1939.

Redko, A., 2017. Meet 5 Genius Fashion Companies Turning Fruit Fiber Into Seriously Luxe Material. Peaceful Dumpling.

Reed, R.C., Bradford, K.J. and Khanday, I., 2022. Seed germination and vigor: ensuring crop sustainability in a changing climate. *Heredity*, 128(6), pp.450-459.

Riaz, M., Khalid, R., Afzal, M., Anjum, F., Fatima, H., Zia, S., Rasool, G., Egbuna, C., Mtewa, A.G., Uche, C.Z. and Aslam, M.A., 2023. Phytobioactive compounds as therapeutic agents for human diseases: A review. *Food Science & Nutrition*, 11(6), pp.2500-2529.

Rodríguez, A., van Grinsven, H.J., van Loon, M.P., Doelman, J.C., Beusen, A.H. and Lassaletta, L., 2024. Costs and benefits of synthetic nitrogen for global cereal production in 2015 and in 2050 under contrasting scenarios. *Science of the Total Environment*, 912, pp.169357.

Rodriguez-Loya, J., Lerma, M. and Gardea-Torresdey, J.L., 2023. Dynamic light scattering and its application to control nanoparticle aggregation in colloidal systems: a review. *Micromachines*, 15(1), pp.24.

Romelle, F.D., Rani, A. and Manohar, R.S., 2016. Chemical composition of some selected fruit peels. *European Journal of Food Science and Technology*, 4(4), pp.12-21.

Rostami Ajirloo, A.A. and Amiri, E., 2022. Effects of nano-potassium fertilizer on yield and water use efficiency of soybean under water deficit conditions (case study: Moghan plain, Iran). *Communications in Soil Science and Plant Analysis*, 53(12), pp.1542-1551.

Sachdev, S., Ansari, S.A. and Ansari, M.I., 2023. Oxidative stress triggered damage to cellular biomolecules. In *Reactive oxygen species in plants: The right balance* (pp. 45-59). Singapore: Springer Nature Singapore.

Sádecká, J., Hroboňová, K., Veljović, S. and Jakubíková, M., 2025. UV-Vis absorption, synchronous fluorescence spectroscopy, and HPLC-DAD in sweet wine age research. *European Food Research and Technology*, 251(11), pp.3861-3874.

Sadiq, U., Gill, H. and Chandrapala, J., 2022. Ultrasound-Assisted Encapsulation of Anthraquinones Extracted from Aloe-Vera Plant into Casein Micelles. *Gels*, 8(9), pp.597.

Said, A., Abu-Elghait, M., Atta, H.M. and Salem, S.S., 2024. Antibacterial activity of green synthesized silver nanoparticles using *Lawsonia inermis* against common pathogens from urinary tract infection. *Applied Biochemistry and Biotechnology*, 196(1), pp.85-98.

Said, M., 2023. An overview of impact of agrochemicals on human health and natural environment. *Scientific Research Communications*, 3(2).

Saifuddin, N.N., Matussin, S.N., Fariduddin, Q. and Khan, M.M., 2024. Potentials of roots, stems, leaves, flowers, fruits, and seeds extract for the synthesis of silver nanoparticles. *Bioprocess and Biosystems Engineering*, 47(8), pp.1119-1137.

Sajjad, Y., Jaskani, M.J., Mehmood, A., Qasim, M. and Akhtar, G., 2019. Alleviation of gladiolus (*Gladiolus grandiflorus*) corm dormancy through application of 6-benzylaminopurine and gibberellic acid. *Pakistan Journal of Botany*, 52, pp.831-838.

Sakib, T.U., Nelson, N.O., Hettiarachchi, G.M., Moorberg, C.J., Nippert, J.B. and Whitaker, S., 2025. Soil phosphorus availability as affected by root exudates of cover crop species. *Scientific Reports*, 15(1), pp.33443.

Šalagovič, J., Vanhees, D., Verboven, P., Holsteens, K., Verlinden, B., Huysmans, M., Van de Poel, B. and Nicolaï, B., 2024. Microclimate monitoring in commercial tomato (*Solanum Lycopersicum* L.) greenhouse production and its effect on plant growth, yield and fruit quality. *Frontiers in Horticulture*, 3, pp.1425285

Salam, I.U., Ahmed, M.O., and Hussain, F., 2018. A Study of different parameters of osmotic potential compared with weed (*Chenopodium album*) on wheat and Chickpea crop. *Pak. J. Bot*, *50*(3), pp.963-967.

Salas-Pascual, M. and Cáceres-Lorenzo, T., 2022. The dispersal of bananas (*Musa* spp.) to the Americas in the sixteenth century. *Economic Botany*, 76(4), pp.354-367.

Saleem, A., Anwar, S., Nawaz, T., Fahad, S., Saud, S., Ur Rahman, T., Khan, M.N.R. and Nawaz, T., 2025. Securing a sustainable future: the climate change threat to agriculture, food security, and sustainable development goals. *Journal of Umm Al-Qura University for Applied Sciences*, 11(3), pp.595-611.

Saleem, M.H., Usman, K., Rizwan, M., Al Jabri, H. and Alsafran, M., 2022. Functions and strategies for enhancing zinc availability in plants for sustainable agriculture. *Frontiers in Plant Science*, 13, pp.1033092.

Samsoon, S., Azam, M., Khan, A., Ashraf, M., Bhatti, H.N., Alshawwa, S.Z. and Iqbal, M., 2024. Green-synthesized MnO2 nanofertilizer impact on growth, photosynthetic pigment, and non-enzymatic antioxidant of Vigna unguiculata cultivar. *Biomass Conversion and Biorefinery*, 14(21), pp.26943-26952.

Santoro, V., Schiavon, M. and Celi, L., 2024. Role of soil abiotic processes on phosphorus availability and plant responses with a focus on strigolactones in tomato plants. *Plant and Soil*, 494(1), pp.1-49.

Santosh, D. T., Natraj, K., Kumar, K. P., Sree, P. L. S., and Panda, A. 2022. Drip fertigation for high productivity and sustainable production of banana: A review. Indian Journal of Natural Sciences, 13(72), 44607–44611.

Santosh, D.T., Tiwari, K.N., Singh, V.K. and Reddy, A.R.G., 2017. Micro climate control in greenhouse. *International Journal of Current Microbiology and Applied Sciences*, 6(3), pp.1730-1742.

Ramkumar, S., Seethalaxmi, M., Rekha, T., Abiyoga, M., Baskar, V. and Sureshkumar, S., 2024. Biofortification of crops with nutrients by the application of nanofertilizers for effective agriculture. *Plant Physiology and Biochemistry*, 212, pp.108772.

Saurabh, K., Prakash, V., Dubey, A.K., Ghosh, S., Kumari, A., Sundaram, P.K., Jeet, P., Sarkar, B., Upadhyaya, A., Das, A. and Kumar, S., 2024. Enhancing sustainability in agriculture with nanofertilizers. *Discover Applied Sciences*, 6(11), pp.559.

Schwab, F., Zhai, G., Kern, M., Turner, A., Schnoor, J.L. and Wiesner, M.R., 2016a. Barriers, pathways and processes for uptake, translocation and accumulation of nanomaterials in plants–Critical review. *Nanotoxicology*, 10(3), pp.257-278.

Schwab, F., Zhai, G., Kern, M., Turner, A., Schnoor, J.L. and Wiesner, M.R., 2016b. Barriers, pathways and processes for uptake, translocation and accumulation of nanomaterials in plants–Critical review. *Nanotoxicology*, 10(3), pp.257-278.

Selyutina, O.Y., Ul'yanova, M.A., Chinak, O.A., Timoshnikov, V.A., Fedenok, L.G., Stepanov, A.A., Yanshole, V.V., Kulik, L.V., Vasilevsky, S.F., Polyakov, N.E. and Kontoghiorghes, G.J., 2024. Novel Anthraquinone Derivatives and Their Complexes with Metal Ions with Anticancer Activity: Structure/Redox and Chelation Activity Correlations. *Pharmaceuticals*, 17(12), pp.1717.

Sembada, A.A. and Lenggoro, I.W., 2024. Transport of nanoparticles into plants and their detection methods. *Nanomaterials*, 14(2), pp.131.

Shaikh, J.R. and Patil, M., 2020. Qualitative tests for preliminary phytochemical screening: An overview. *International Journal of Chemical Studies*, 8(2), pp.603-608.

Shalaby, T.A., Bayoumi, Y., Eid, Y., Elbasiouny, H., Elbehiry, F., Prokisch, J., El-Ramady, H. and Ling, W., 2022. Can nanofertilizers mitigate multiple environmental stresses for higher crop productivity?. *Sustainability*, 14(6), pp.3480.

Shapiro, S.S. and Wilk, M.B., 1965. An analysis of variance test for normality (complete samples). *Biometrika*, 52(3-4), pp.591-611.

Sharma, S., Sharma, U., Sharma, N., Rana, V.S., Thakur, S., Kumar, A. and Kumar, R., 2025. Exploring the valorization of fruit bio-waste for sustainable utilization in agro-food industries: A Comprehensive Review. *Food Bioscience*, 63, pp.105768.

Sharma, S.K., Khan, A.U., Khan, M., Gupta, M., Gehlot, A., Park, S. and Alam, M., 2020. Biosynthesis of MgO nanoparticles using Annona squamosa seeds and its catalytic activity and antibacterial screening. *Micro & Nano Letters*, 15(1), pp.30-34.

Sheidu, A., Maiha, B., Ahmed, A., Magaji, G., 2021. Successive Solvent Extraction, Phytochemical Screening and Thin Layer Chromatography (TLC) Profiling of *Musa cavendeshii* Linn Peel. Science Forum (*Journal of Pure and Applied Sciences*) 21, 192.

Sheta, M.H., Abd El-Wahed, A.H., Elshaer, M.A., Bayomy, H.M., Ozaybi, N.A., Abd-Elraheem, M.A., El-Sheshtawy, A.N.A., El-Serafy, R.S. and Moustafa, M.M., 2024. Green synthesis of zinc and iron nanoparticles using *Psidium guajava* leaf extract stimulates cowpea growth, yield, and tolerance to saline water irrigation. *Horticulturae*, 10(9), pp.915.

Shi, Y., Zhang, Z., Yan, Z., Chu, H. and Luo, C., 2025. Tomato mitogen-activated protein kinase: mechanisms of adaptation in response to biotic and abiotic stresses. *Frontiers in Plant Science*, 16, pp.1533248.

Shin, S.K., Lee, Y.E., Lee, S.J. and Park, J.H., 2026. Evaluation of Sensor-Based Soil EC Responses to Nitrogen and Potassium Fertilization Under Laboratory and Field Conditions. *Agriculture*, 16(2), pp.137.

Shira, V.D., Somi, Y., Bauri, F.K., 2013. Effect of post shoot application of potassium through bunch feeding on fruit quality characters of banana in West Bengal, *Journal of Crop and Weed,* 9(2),pp.196-197.

Siahaan, F.R., Sembiring, M., Hasanah, Y. and Sabrina, T., 2023, June. Chemical characteristics and plant growth regulators of organic waste as liquid organic fertilizer. In *IOP Conference Series: Earth and Environmental Science*,1188 (1), pp. 012001). IOP Publishing.

Simancas, R., Takemura, M., Chen, C.T., Iyoki, K., Okubo, T. and Wakihara, T., 2023. Amorphous aluminosilicates as efficient ion exchangers for ammonium cation removal from aqueous solutions. *Journal of Non-Crystalline Solids*, 605, pp.122172.

Singh, H., Desimone, M.F., Pandya, S., Jasani, S., George, N., Adnan, M., Aldarhami, A., Bazaid, A.S. and Alderhami, S.A., 2023. Revisiting the green synthesis of nanoparticles: uncovering influences of plant extracts as reducing agents for enhanced synthesis efficiency and its biomedical applications. *International Journal of Nanomedicine*, pp.4727-4750.

Singh, J., Kumar, S., Alok, A., Upadhyay, S.K., Rawat, M., Tsang, D.C., Bolan, N. and Kim, K.H., 2019. The potential of green synthesized zinc oxide nanoparticles as nutrient source for plant growth. *Journal of Cleaner Production*, 214, pp.1061-1070.

Singh, N., Singh, M.K., Raghuvansi, J., Yadav, R.K. and Azim, Z., 2024. Green synthesis of nano iron oxide using *Emblica officinalis* L. fruit extract and its impact on growth, chlorophyll content, and metabolic activity of *Solanum lycopersicum* L. *Biol. Biotechnol*, 12(2), pp.173-181.

Singh, N.K., Sachan, K., Bp, M., Panotra, N. and Katiyar, D., 2024. Building soil health and fertility through organic amendments and practices: a review. *Asian Journal of Soil Science and Plant Nutrition*, 10(1), pp.175-197.

Sıdır, Y.G. and Sıdır, İ., 2025. The Optical Properties, UV-Vis. Absorption and Fluorescence Spectra of 4-Pentylphenyl 4-n-benzoate Derivatives in Different Solvents. *Journal of Fluorescence*, pp.1-19.

Sogani, M., Sonu, K., Syed, Z. and Rajvanshi, J., 2023, March. Preparation of biofertilizer blend from banana peels along with its application in agriculture and plant microbial fuel cell. In *IOP conference series: Earth and Environmental Science*,1151(1), pp. 012034). IOP Publishing.

Sohal, J.K., Saraf, A., Shukla, K. and Shrivastava, M., 2019. Determination of antioxidant potential of biochemically synthesized silver nanoparticles using Aloe vera gel extract. *Plant Science Today*, 6(2), pp.208-217.

Soltani, A., Benfreha, K., Hamraoui, K., 2023. Analysis of Physico-chemical Properties, and Antimicrobial Activity of Aloe vera (*Aloe barbadensis* Miller). *Phytothérapie* 21(1), pp. 49–54.

Soltani, S., Gacem, A., Choudhary, N., Yadav, V.K., Alsaeedi, H., Modi, S., Patel, A., Khan, S.H., Cabral-Pinto, M.M., Yadav, K.K. and Patel, A., 2023. Scallion peel mediated synthesis of zinc oxide nanoparticles and their applications as nano fertilizer and photocatalyst for removal of organic pollutants from wastewater. *Water*, 15(9), pp.1672.

Somefun, O.T., Masasi, B. and Adelabu, A.O., 2024. Irrigation and Water Management of Tomatoes–A Review. *Journal of Sustainable Agriculture and Environment*, 3(4), pp.e70020.

Soppe, W.J. and Bentsink, L., 2020. Seed dormancy back on track; its definition and regulation by DOG1. *The New phytologist*, *228*(3), pp.816.

Spano, F.C. and Silva, C., 2014. H-and J-aggregate behavior in polymeric semiconductors. *Annual Review of Physical Chemistry*, 65(1), pp.477-500.

Sun, L., Li, M., Li, F., Wang, F., Liang, X. and Shou, Q., 2024. Solution-Phase Synthesis of KCl Nanocrystals Templated by PEO-PPO-PEO Triblock Copolymers Micelles. *Polymers*, 16(7), pp.982.

Sun, W. and Shahrajabian, M.H., 2023. Therapeutic potential of phenolic compounds in medicinal plants—Natural health products for human health. *Molecules*, 28(4), pp.1845.

Swamy, K.R.M., 2023. Origin, distribution, taxonomy, botanical description, genetic diversity and breeding of Capsicum (*Capsicum annuum* L.). *International Journal of Development Research*, 13(03), pp.61956–61977.

Tarkas, H., Rokade, A., Upasani, D., Pardhi, N., Rokade, A., Sali, J., Patole, S.P. and Jadkar, S., 2024. Pioneering method for the synthesis of lead sulfide (PbS) nanoparticles using a surfactant-free microemulsion scheme. *RSC Advances*, 14(7), pp.4352-4361.

Teulon, J.M., Godon, C., Chantalat, L., Moriscot, C., Cambedouzou, J., Odorico, M., Ravaux, J., Podor, R., Gerdil, A., Habert, A. and Herlin-Boime, N., 2018. On the operational aspects of measuring nanoparticle sizes. *Nanomaterials*, 9(1), pp.18.

Thakur, P., Mehta, P., Lal, P., Chaudhary, R., Pani, S.K., Singh, A.G., Devi, C., Verma, K. and Sharma, P., 2024. Agricultural produce supply chain network of *Capsicum*: empirical evidence from India. *Economies*, 12(1), pp.24.

Thomas, N., Puluhulawa, L.E., Cindana Mo'o, F.R., Rusdin, A., Gazzali, A.M. and Budiman, A., 2024. Potential of pullulan-based polymeric nanoparticles for improving drug physicochemical properties and effectiveness. *Polymers*, 16(15), pp.2151.

Tian, Y., Shi, C., Malo, C.U., Kwatcho Kengdo, S., Heinzle, J., Inselsbacher, E., Ottner, F., Borken, W., Michel, K., Schindlbacher, A. and Wanek, W., 2023. Long-term soil warming decreases microbial phosphorus utilization by increasing abiotic phosphorus sorption and phosphorus losses. *Nature Communications*, 14(1), pp.864.

Tomar, M., 2018. Watermelon: A Valuable Horticultural Crop with Nutritional Benefits.

Triana, A., Llanderal, A., García-Caparrós, P., Donoso, M., Jiménez-Lao, R., Franco Rodríguez, J.E., Lao, M.T., 2024. Preliminary Mapping of the Spatial Variability in the Microclimate in Tropical Greenhouses: A Pepper Crop Perspective. *Agriculture* 14 (11), pp.1972.

Tsado, A.N., Okoli, N.R., Jiya, A.G., Gana, D., Saidu, B., Zubairu, R. and Salihu, I.Z., 2021. Proximate, minerals, and amino acid compositions of banana and plantain peels. *BIOMED Natural and Applied Science*, 1(01), pp.032-042.

Twaij, B.M. and Hasan, M.N., 2022. Bioactive secondary metabolites from plant sources: types, synthesis, and their therapeutic uses. *International Journal of Plant Biology*, 13(1), pp.4-14.

Tyagi, P.K., Gupta, S., Tyagi, S., Kumar, M., Pandiselvam, R., Daştan, S.D., Sharifi-Rad, J., Gola, D. and Arya, A., 2021. Green synthesis of iron nanoparticles from spinach leaf and banana peel aqueous extracts and evaluation of antibacterial potential. *Journal of Nanomaterials*, 2021(1), pp.4871453.

Ukidave, V.V. and Ingale, L.T., 2022. Green synthesis of zinc oxide nanoparticles from *coriandrum sativum* and their use as fertilizer on Bengal gram, Turkish gram, and green gram plant growth. *International Journal of Agronomy*, 2022(1), pp.8310038.

Ullah, H., 2023. Natural and processed organic fertilizer. *Biomedical Journal of Scientific & Technical Research*, 49(4), pp.40852-40857.

Usman, I., Sana, S., Afzaal, M., Imran, A., Jaffar, H.M., Sukhera, S., Munir, M., Asghar, A. and Urugo, M.M., 2025. Phytochemicals in plant food waste: innovative insight and implications. *Journal of Agriculture and Food Research*, pp.101779.

Uwimana, B., Zorrilla-Fontanesi, Y., van Wesemael, J., Mduma, H., Brown, A., Carpentier, S. and Swennen, R., 2020. Effect of seasonal drought on the agronomic performance of four banana genotypes (*Musa* spp.) in the East African Highlands. *Agronomy*, 11(1), pp.4.

Varzakas, T. and Smaoui, S., 2024. Global food security and sustainability issues: the road to 2030 from nutrition and sustainable healthy diets to food systems change. *Foods*, 13(2), pp.306.

Velgosova, O., Mikulková, Z. and Lisnichuk, M., 2025. The Influence of Precursor pH on the Synthesis and Morphology of AuNPs Synthesized Using Green Tea Leaf Extract. *Crystals*, 15(8), pp.682.

Velthof, G.L., Cals, T.C., van't Hull, J.P., Lesschen, J.P., Lessmann, M., Porre, R.J., Ros, M.B., Rietra, R.P., Schoumans, O.F., Veenemans, L. and Westerik, D., 2024. Managing organic resources in agriculture: future challenges from a scientific perspective. *Frontiers in Sustainable Food Systems*, 8, pp.1393190.

Villagrán, Z., Anaya-Esparza, L.M., Velázquez-Carriles, C.A., Silva-Jara, J.M., Ruvalcaba-Gómez, J.M., Aurora-Vigo, E.F., Rodríguez-Lafitte, E., Rodríguez-Barajas, N., Balderas-León, I. and Martínez-Esquivias, F., 2024. Plant-based extracts as reducing, capping, and stabilizing agents for the green synthesis of inorganic nanoparticles. *Resources*, 13(6), pp.70.

Villaseñor-Ortiz, D., Prado, R.D.M., Luna-Romero, E., Jaramillo-Aguilar, E. and Agurto-Rodriguez, L., 2022. Critical nitrogen and potassium levels and sufficiency ranges for banana cultivation in Ecuador. *Fruits*, 77(1), pp.1-8.

Vishala, J. and Singh, G., 2021. A review on product development through pulp and peel of banana. *Plant Archives*, 21(Suppliment–1), pp.693-698.

Volino-Souza, M., Oliveira, G.V.D., Conte-Junior, C.A., Figueroa, A. and Alvares, T.S., 2022. Current evidence of watermelon (*Citrullus lanatus)* ingestion on vascular health: a food science and technology perspective. *Nutrients*, 14(14), pp.2913.

Volino-Souza, M., de Oliveira, G.V., Tavares, A.C., Souza, K. and Alvares, T., 2023. The effect of microencapsulated watermelon rind (*Citrullus lanatus*) and beetroot (*Beta vulgaris* L.) ingestion on ischemia/reperfusion-induced endothelial dysfunction: a randomised clinical trial. *Food & Function*, 14(17), pp.7959-7968.

Wahab, A., Muhammad, M., Ullah, S., Abdi, G., Shah, G.M., Zaman, W. and Ayaz, A., 2024. Agriculture and environmental management through nanotechnology: Eco-friendly nanomaterial synthesis for soil-plant systems, food safety, and sustainability. *Science of the Total Environment*, 926, pp.171862.

Wanapat, M., Suriyapha, C., Dagaew, G., Prachumchai, R., Phupaboon, S., Sommai, S. and Matra, M., 2024. The recycling of tropical fruit peel waste-products applied in feed additive for ruminants: Food manufacturing industries, phytonutrient properties, mechanisms, and future applications. *Journal of Agriculture and Food Research*, 17, pp.101234.

Wang, X., Liu, M., Ciampitti, I.A., Cui, J., Fang, K., Zhao, S., He, P. and Zhou, W., 2024. Benefits and trade-offs of replacing inorganic fertilizer by organic substrate in crop production: A global meta-analysis. *Science of The Total Environment*, *925*, pp.171781.

Wang, X., Xie, H., Wang, P. and Yin, H., 2023. Nanoparticles in plants: uptake, transport and physiological activity in leaf and root. *Materials*, 16(8), pp.3097.

Widmer-Cooper, A. and Geissler, P.L., 2016. Ligand-mediated interactions between nanoscale surfaces depend sensitively and nonlinearly on temperature, facet dimensions, and ligand coverage. *ACS Nano*, 10(2), pp.1877-1887.

Wu, H. and Briscoe, W.H., 2018. Morphogenesis of polycrystalline dendritic patterns from evaporation of a reactive nanofluid sessile drop. *Physical Review Materials*, 2(4), pp.045601.

Xiong, C. and Zhao, X., 2024. Impacts of chemical fertilizer reduction on grain yield: A case study of China. *Plos One*, 19(3), pp.e0298600.

Xu, J., Zhang, N., Wang, K., Xian, Q., Dong, J. and Chen, X., 2022. Exploring new strategies in diseases resistance of horticultural crops. *Frontiers in Sustainable Food Systems, 6,* pp.1021350.

Xu, L., Liang, H.W., Yang, Y. and Yu, S.H., 2018. Stability and reactivity: positive and negative aspects for nanoparticle processing. *Chemical Reviews*, 118(7), pp.3209-3250.

Xue, H., Zhao, J., Wang, Y., Shi, Z., Xie, K., Liao, X. and Tan, J., 2024. Factors affecting the stability of anthocyanins and strategies for improving their stability: A review. *Food Chemistry: X*, 24, pp.101883.

Yadav, A., Singh, S. and Yadav, V., 2024. Screening herbal extracts as biostimulant to increase germination, plant growth and secondary metabolite production in wheatgrass. *Scientific Reports*, 14(1), pp.607.

Yadav, A. and Yadav, K., 2025. Nanofertilizers: The Future of Farming or a Fading Fad Among Farmers?. In *Nanofertilizers for Sustainable Agriculture: Assessing Impacts on Health, Environment, and Economy* (pp. 57-75). Cham: Springer Nature Switzerland.

Yadav, A., Yadav, K. and Abd-Elsalam, K.A., 2023. Nanofertilizers: types, delivery and advantages in agricultural sustainability. *Agrochemicals*, 2(2), pp.296-336.

Yadav, D., Das, S., Dhillayan, D., Yadav, S. and Bhukal, S., 2025. Environmentally benign nanotechnology: transforming elements into nano-agrochemicals for sustainable farming. *Discover Agriculture*, 3(1), pp.67.

Yadeta Gemachu, L. and Lealem Birhanu, A., 2024. Green synthesis of ZnO, CuO and NiO nanoparticles using Neem leaf extract and comparing their photocatalytic activity under solar irradiation. *Green Chemistry Letters and Reviews*, 17(1), pp.2293841.

Yahya, M., Bouziani, A., Ocak, C., Seferoğlu, Z. and Sillanpää, M., 2021. Organic/metal-organic photosensitizers for dye-sensitized solar cells (DSSC): Recent developments, new trends, and future perceptions. *Dyes and Pigments*, 192, pp.109227.

Yakhin, O.I., Lubyanov, A.A., Yakhin, I.A. and Brown, P.H., 2017. Biostimulants in plant science: a global perspective. *Frontiers in Plant Science*, *7*, pp.2049.

Yang, X., Lim, S.H.M., Lin, J., Wu, J., Tang, H., Zhao, F., Liu, F., Sun, C., Shi, X., Kuang, Y. and Toy, J.Y.H., 2022. Oxygen mediated oxidative couplings of flavones in alkaline water. *Nature Communications*, 13(1), pp.6424.

Yasin, M., Gangan, S. and Panchal, S.K., 2025. Banana Peels: A Genuine Waste or a Wonderful Opportunity?. *Applied Sciences*, 15(6), pp.3195.

Yekutiel, Y., Rotem, Y., Arnon, S. and Dahan, O., 2024. Optimized fertilization using online soil nitrate data. *Soil*, 10(1), pp.335-347.

Yoshiyama, Y., Wakabayashi, Y., Mercer, K.L., Kawabata, S., Kobayashi, T., Tabuchi, T. and Yamori, W., 2024. Natural genetic variation in dynamic photosynthesis is correlated with stomatal anatomical traits in diverse tomato species across geographical habitats. *Journal of Experimental Botany*, 75(21), pp.6762-6777.

Yuan, J., Shi, L., Sang, W. and Yan, J., 2025. Enhancing phosphorus transformation and microbial activity in acidic soils using K-feldspar: A case study. *Journal of Environmental Management*, 388, pp.126002.

Yuuki, H. and Takeshi, S., 2023. Functionalization of cellulose materials via self-assembly of cello-oligosaccharides. *Glycoforum*, 26(5), pp.A20.

Zafar, S., Bilal, M., Ali, M.F., Mahmood, A., Kijsomporn, J., Wong, L.S., Kumar, V. and Alotaibi, S.S., 2024. Nano-biofertilizer an eco-friendly and sustainable approach for the improvement of crops under abiotic stresses. *Environmental and Sustainability Indicators*, 24, pp.100470.

Zhang, Q.F., 2024. From sustainable agriculture to sustainable agrifood systems: A comparative review of alternative models. *Sustainability*, 16(22), pp.9675.

Zhang, T., Wang, Q. and Rui, Y., 2025. The impact of nanomaterials on plant health: a review of exposure, toxicity, and control. *Environmental Science: Nano*.

Zhao, J. and Stenzel, M.H., 2018. Entry of nanoparticles into cells: The importance of nanoparticle properties. *Polymer Chemistry*, 9(3), pp.259-272.

Zhao, L. and Zheng, L., 2023. A Review on Bioactive Anthraquinone and Derivatives as the Regulators for ROS. *Molecules*, *28*(24), p.8139.

Zhao, P., Cao, L., Ma, D., Zhou, Z., Huang, Q. and Pan, C., 2018. Translocation, distribution and degradation of prochloraz-loaded mesoporous silica nanoparticles in cucumber plants. *Nanoscale*, 10(4), pp.1798-1806.

Zheng, Y., Zou, J., Lin, S., Jin, C., Shi, M., Yang, B., Yang, Y., Jin, D., Li, R., Li, Y. and Wen, X., 2023. Effects of different light intensity on the growth of tomato seedlings in a plant factory. *Plos One*, 18(11), pp.e0294876.

Zhigila, D.A., AbdulRahaman, A.A., Kolawole, O.S. and Oladele, F.A., 2014. Fruit morphology as taxonomic features in five varieties of *Capsicum annuum* L. Solanaceae. *Journal of Botany*, 2014(1), pp.540868.

Zhuang, L., Wang, P., Hu, W., Yang, R., Zhang, Q., Jian, Y. and Zou, Y., 2024. A comprehensive study on the impact of chemical fertilizer reduction and organic manure application on soil fertility and apple orchard productivity. *Agronomy*, 14(7), pp.1398.

Zia, S., Khan, M.R., Aadil, R.M. and Medina-Meza, I.G., 2024. Bioactive recovery from watermelon rind waste using ultrasound-assisted extraction. *ACS Food Science & Technology*, 4(3), pp.687-699.

Zia, S., Khan, M.R., Shabbir, M.A. and Aadil, R.M., 2021. An update on functional, nutraceutical and industrial applications of watermelon by-products: A comprehensive review. *Trends in Food Science & Technology*, 114, pp.275-291.

APPENDICES

Appendix 1: Ethical approval

UNIVERSITY OF MPUMALANGA

Creating Opportunities

MEK Ngcobo

School of Agricultural Sciences

Mbombela Campus.

Dear Nothando Clementine Madlala (201943751)

Protocol Reference Number: UMP/Madlala201943751/SAS/MSC/2024/01

Project **Evaluation of banana and watermelon composite peel extracts as green nano-fertilizer.**

Approval Notification: In response to your application received on **12/12/2024**, The Research Ethics Committee: Faculty Research Ethics Committee has considered the above mentioned application and the protocol has been granted **FULL APPROVAL**.

Any alteration/s to the approved research protocol i.e. Questionnaire/Interviews Schedule, Informed Consent form, Title of the project, Location of the study, Research Approach and methods must be reviewed and approved through the amendment/ modification prior to its implementation. In case you have further queries, please quote the above reference number.

PLEASE NOTE: Research data should be stored securely in the School/ division for a period of 5 years.

The Ethical Clearance certificate is only valid for a period of 3 years from date of issue. Thereafter, Recertification must be applied for on an annual basis.

Wishing you the best with your study.

Yours faithfully,

....

Appendix 2 :Topic change approval

FACULTY OF AGRICULTURE AND NATURAL SCIENCES

Postgraduate Studies Committee.

Certificate of Approval – Research Proposal.

Date of this Approval:	**17 NOVEMBER 2025**

Student Details

1	Student Name:	NC Madlala
2	Student Number:	201943751
3	School	School of Agricultural Sciences.
4	Degree Registered for:	MSc Agric
5	Date of First Registration:	February 2023
6	Supervisor(s):	Dr N Khanyile Dr A Masenya

Title Approved: Evaluation of banana peel and watermelon rind composite extracts as a green nano-fertilizer

Chairperson: Prof. DM Parker.

Signature:

Date & Official Stamp:

UNIVERSITY OF MPUMALANGA
CREATING OPPORTUNITIES
FACULTY OF AGRICULTURE &
NATURAL SCIENCE
PRIVATE BAG X 11283, NELSPRUIT, 1200
TEL: 013 002 0208

Appendix 3:Published manuscript

nanomaterials

MDPI

Review

Examining the Correlation between the Inorganic Nano-Fertilizer Physical Properties and Their Impact on Crop Performance and Nutrient Uptake Efficiency

Nothando Clementine Madlala [1], Nokuthula Khanyile [2,*] and Absalom Masenya [1]

[1] School of Agricultural Sciences, University of Mpumalanga, Mbombela 1200, South Africa; abby.masenya@ump.ac.za (A.M.)
[2] School of Chemical and Physical Sciences, University of Mpumalanga, Mbombela 1200, South Africa
* Correspondence: khanyile.peaceful@gmail.com

Abstract: The physical properties of nano-fertilizers (NFs) are important in determining their performance, efficacy, and environmental interactions. Nano-fertilizers, due to their small size and high surface area-to-volume ratio, enhance plant metabolic reactions, resulting in higher crop yields. The properties of nano-fertilizers depend on the synthesis methods used. The nanoparticle's nutrient use efficiency (NUE) varies among plant species. This review aims to analyze the relationship between the physical properties of NF and their influence on crop performance and nutrient uptake efficiency. The review focuses on the physical properties of NFs, specifically their size, shape, crystallinity, and agglomeration. This review found that smaller particle-sized nanoparticles exhibit higher nutrient use efficiency than larger particles. Nano-fertilizer-coated additives gradually release nutrients, reducing the need for frequent application and addressing limitations associated with chemical fertilizer utilization. The shapes of nano-fertilizers have varying effects on the overall performance of plants. The crystalline structure of nanoparticles promotes a slow release of nutrients. Amorphous nano-fertilizers improve the NUE and, ultimately, crop yield. Agglomeration results in nanoparticles losing their nanoscale size, accumulating on the outer surface, and becoming unavailable to plants. Understanding the physical properties of nano-fertilizers is crucial for optimizing their performance in agricultural applications.

Keywords: nano-fertilizers; surface area; nutrient use efficiency; physical properties; agglomeration

Citation: Madlala, N.C.; Khanyile, N.; Masenya, A. Examining the Correlation between the Inorganic Nano-Fertilizer Physical Properties and Their Impact on Crop Performance and Nutrient Uptake Efficiency. *Nanomaterials* **2024**, *14*, 1263. https://doi.org/10.3390/nano14151263

Academic Editor: Guangyang Liu

Received: 13 June 2024
Revised: 19 July 2024
Accepted: 24 July 2024
Published: 28 July 2024

1. Introduction

In recent years, the utilization of nano-fertilizers (NFs) has gained significant attention in the field of agriculture. These innovative fertilizers offer a promising solution to enhance plant nutrient uptake by employing precisely formulated delivery mechanisms [1]. Nano-fertilizers possess dimensions ranging between 1 and 100 nm [2] and exhibit distinct physicochemical properties that distinguish them from traditional bulk materials [3,4]. One of the notable distinguishing characteristics of nanoparticles, in comparison to their larger counterparts composed of identical material, lies between surface effects and quantum phenomena. These two factors contribute to the unique properties exhibited by nanoparticles [3,4]. The small particle size of nanomaterials results in high surface energy, spatial confinement, and high surface area. The size and surface area of any material determine how it interacts with any biological system [5]. The adoption of this innovative approach for agricultural improvement is increasingly gaining momentum as a viable alternative to traditional fertilizers [6–8]. The classification of nano-fertilizers is primarily based on their formulation, which can be categorized into three main types, as depicted in Figure 1.

Appendix 4:Published manuscript

agriculture

MDPI

Review

Preparation of Biofertilizers from Banana Peels: Their Impact on Soil and Crop Enhancement

Nokuthula Khanyile [1,*], Ndumiso Dlamini [1], Absalom Masenya [2], Nothando Clementine Madlala [2] and Sabelo Shezi [2]

[1] School of Chemical and Physical Sciences, Faculty of Agriculture and Natural Science, University of Mpumalanga, Mbombela 1200, South Africa; jamesndumiso@yahoo.com

[2] School of Agricultural Sciences, Faculty of Agriculture and Natural Sciences, University of Mpumalanga, Mbombela 1200, South Africa; abby.masenya@ump.ac.za (A.M.); 201943751@ump.ac.za (N.C.M.); sabelo.shezi@ump.ac.za (S.S.)

* Correspondence: khanyile.peaceful@gmail.com

Abstract: Disposing of banana peels (BPs) as bio-organic waste is an environmental challenge. Rich in potassium, BPs are often discarded despite their agricultural value. Reports on the valorization of BP are increasing, but no review has focused on BP fertilizer preparation methods. This study aims to review and analyze these methods to guide researchers and agriculturists in optimizing BP utilization, promoting sustainable waste management, and effective agricultural practices. This review has uncovered significant findings. A composite of banana and orange peels emerged as the most favoured and widely used approach, closely followed by dried BPs. This study highlighted the substantial impact of fertilizer application methods such as top and basal dressing. Most of the results revealed that the peels significantly improved the growth parameters of various plants. However, for biochar, the plant height was insignificant between treatments, further emphasizing the importance of the application method used. Banana peels are a valuable resource for biofertilizer synthesis. The banana–orange peel composite exhibits outstanding fertilizer properties. More new studies should go beyond the seedling stage, especially to harvest. This would give more information on the performance and viability of BP fertilizers.

Keywords: fertilizers; banana peels; preparation methods; potassium; plant height

check for updates

Citation: Khanyile, N.; Dlamini, N.; Masenya, A.; Madlala, N.C.; Shezi, S. Preparation of Biofertilizers from Banana Peels: Their Impact on Soil and Crop Enhancement. *Agriculture* **2024**, *14*, 1894. https://doi.org/10.3390/agriculture14111894

Received: 5 September 2024
Revised: 30 September 2024
Accepted: 21 October 2024
Published: 25 October 2024

1. Introduction

Demand for food is driven by an ever-growing human population and changing eating habits [1]. Such factors contribute to food shortages and food insecurity, which threaten the livelihood of humans [2,3]. Researchers have developed alternative strategies to grow crops faster and enrich the soil with the necessary nutrients using chemical fertilizers to meet the demands for food [4–7]. Chemical fertilizers are industrially manufactured to contain a specific number of nutrients required by the soil to enhance plant growth [8]. The most common chemical fertilizer is NPK, i.e., nitrogen, phosphorus, and potassium, which contains nitrogen, phosphorus, and potassium in different ratios. Superphosphate, urea, and potash are also popular. For a substance to be classified as a fertilizer, it should contain a minimum of 5% N, P, or K, known as the primary or macro-nutrients [9,10]. They play a vital role in enhancing plant development and growth. Indeed, their functions and how they contribute to soil fertility are well documented [11–14]. However, due to their efficiency in increasing soil fertility and enhancing plant growth, chemical fertilizers are often applied in excess [15]. As a result, they cause adverse effects on the environment, such as global warming, biodiversity loss, depletion of the stratospheric ozone layer, and eutrophication [9,16,17]. Besides their excessive use, their huge procurement, shipping, and transportation costs make them unsustainable [18]. There are several strategies that researchers have developed to reduce and circumvent the effects that synthetic fertilizers have

Appendix 5: Book chapter invitation

Gmail **Nokuthula Khanyile <khanyile.peaceful@gmail.com>**

Chapter Invitation: Nanomaterial Properties Impact on Soil and Plant Biosystems

3 messages

Lina Alnaddaf <hatem005@gmail.com> Wed, Sep 4, 2024 at 5:08 PM
To: khanyile.peaceful@gmail.com

Dear Dr. Nokuthula Khanyile,

We are writing to cordially invite you to contribute a chapter on "**Impact of nanomaterial properties on nanofertilizers efficiency"** for inclusion in our forthcoming book **"Nanomaterial Properties Impact on Soil and Plant Biosystems"**, which is approved for publication under the Springer book series Nanotechnology in Plant .Sciences

Manuscripts are due by **January 31, 2025**. More information about the book is attached. Manuscript preparation .guidelines will be provided after receiving your confirmation

No publication charges are applied. The corresponding author will receive a complimentary printed book and all .authors will receive full access to the electronic version

.Looking forward to your response at your earliest convenience within the next 7 days. Thanks

,Best regards

Editors

Dr. Lina M. Alnaddaf
.Department of Field Crops, Albaath University, Homs 77, Syrian Arab Republic
Email: hatem005@gmail.com; lalnaddaf@albaath-univ.edu.sy
/Webpage: https://www.researchgate.net/profile/lina alnaddaf

Prof. Jameel M. Al-Khayri
Department of Agricultural Biotechnology, King Faisal University, Al-Ahsa 31982, Saudi Arabia
Email: jmkhayri@yahoo.com; jkhayri@kfu.edu.sa
/Webpage: http://www.researchgate.net/profile/Jameel_Al-Khayri

Nokuthula Khanyile <khanyile.peaceful@gmail.com> Thu, Sep 5, 2024 at 6:43 AM
To: Lina Alnaddaf <hatem005@gmail.com>

Dear Editors

We are humbled and honored to be presented with such a great opportunity. We accept the invite and look forward to receiving all necessary information and documents to start working on the chapter.

Best regards
Nokuthula

[Quoted text hidden]

Lina Alnaddaf <hatem005@gmail.com> Fri, Sep 6, 2024 at 9:53 AM
To: Nokuthula Khanyile <khanyile.peaceful@gmail.com>

Dear Dr. Nokuthula Khanyile,

Appendix 6: DSTI-Dr Ivy Matsepe-Casaburri Master's Fellowships

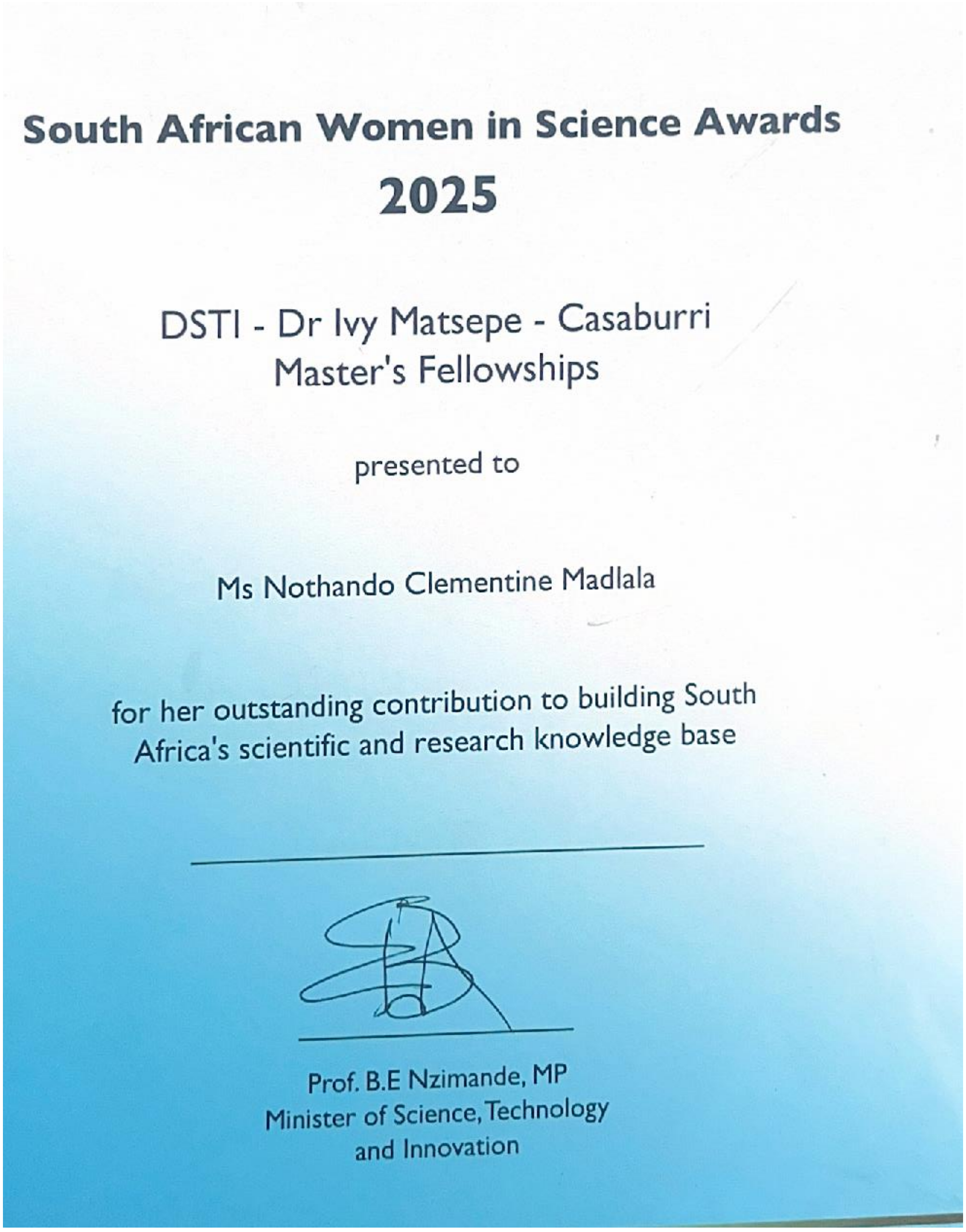

South African Women in Science Awards
2025

DSTI - Dr Ivy Matsepe - Casaburri
Master's Fellowships

presented to

Ms Nothando Clementine Madlala

for her outstanding contribution to building South Africa's scientific and research knowledge base

Prof. B.E Nzimande, MP
Minister of Science, Technology and Innovation

Appendix 7: Similarity index

NC Madlala 14 01 26_.docx

ORIGINALITY REPORT

11%	4%	8%	2%
SIMILARITY INDEX	INTERNET SOURCES	PUBLICATIONS	STUDENT PAPERS

PRIMARY SOURCES

1	Submitted to University of Mpumalanga Student Paper	2%
2	Virat Khanna, Rohit Jasrotia, Tejeet Singh, Gulab Singh. "Metal Oxides - Advances in Sustainability and Nanotechnology", Routledge, 2025 Publication	<1%
3	ulspace.ul.ac.za Internet Source	<1%
4	Shrikaant Kulkarni, Hemantkumar N. Akolkar, Vijay M. Khedkar, Rajesh Ramasamy, Kirti R. Mahanwar, Nirmala R. Darekar. "Biogenic-Based Metal Nanomaterials for Sustainable Engineering Applications", Apple Academic Press, 2025 Publication	<1%
5	dokumen.pub Internet Source	<1%
6	Olaniyi Amos Fawole, İbrahim Kahramanoğlu. "Nanotechnology in Pre- and Postharvest	<1%

Appendix 8: Analysis of variance for seed emergence percentage in Experiment 1

Source	DF	SS	MS	F	P
Replications	2	53.3	26.67		
Crop	1	735.0	735.00	3.41	0.0668
CPE	9	30435.0	3381.67	15.68	0.0000
Dose	3	7005.0	2335.00	10.83	0.0000
Crop × CPE	9	2115.0	235.00	1.09	0.3735
Crop × Dose	3	1298.3	432.78	2.01	0.1153
CPE × Dose	27	6078.3	225.12	1.04	0.4148
Crop × CPE × Dose	27	10718.3	396.98	1.84	0.0112
Error	158	34080.0	215.70		
Total	239				

Appendix 9: Analysis of variance for seed emergence percentage in Experiment 2

Source	DF	SS	MS	F	P
Replications	2	310.0	155.00		
Crop	1	281.7	281.67	2.23	0.1373
CPE	9	25935.0	2881.67	22.81	0.0000
Dose	3	4271.7	1423.89	11.27	0.0000
Crop × CPE	9	2668.3	296.48	2.35	0.0164
Crop × Dose	3	125.0	41.67	0.33	0.8038
CPE × Dose	27	6845.0	253.52	2.01	0.0044
Crop type × CPE × Dose	27	2991.7	110.80	0.88	0.6430
Error	158	19956.7	126.31		
Total	239				

Appendix 10: Analysis of variance for plant height in Experiment 1

Source	**DF**	**SS**	**MS**	**F**	**P**
Replications	2	17.90	8.951		
Crop	1	294.15	294.152	8.05	0.0051
CPE	9	590.43	65.604	1.80	0.0728
Dose	3	6.54	2.179	0.06	0.9808
Crop × CPE	9	592.08	65.787	1.80	0.0719
Crop × Dose	3	25.83	8.611	0.24	0.8714
CPE × Dose	27	847.43	31.386	0.86	0.6680
Crop × CPE × Dose	27	1484.50	54.982	1.51	0.0643
Error	158	5771.54	36.529		
Total	239				

Appendix 11: Analysis of variance for plant height in Experiment 2

Source	DF	SS	MS	F	P
Replication	2	42.3	21.14		
Crop	1	1178.4	1178.38	15.69	0.0001
CPE	9	3911.2	434.57	5.79	0.0000
Dose	3	614.4	204.79	2.73	0.0460
Crop × CPE	9	909.9	101.11	1.35	0.2173
Crop × Dose	3	131.0	43.68	0.58	0.6279
CPE × Dose	27	1721.9	63.78	0.85	0.6817
Crop × CPE × Dose	27	2038.6	75.50	1.01	0.4650
Error	158	11865.5	75.10		
Total	239				

Appendix 12: Analysis of variance for stem diameter in Experiment 1

Source	DF	SS	MS	F	P
Replications	2	3.153	1.5763		
Crop	1	11.441	11.4407	18.19	0.0000
CPE	9	17.568	1.9520	3.10	0.0018
Dose	3	2.275	0.7584	1.21	0.3094
Crop × CPE	9	7.859	0.8733	1.39	0.1973
Crop × Dose	3	0.431	0.1436	0.23	0.8766
CPE × Dose	27	19.300	0.7148	1.14	0.3051
Crop × CPE × Dose	27	31.269	1.1581	1.84	0.0112
Error	158	99.354	0.6288		
Total	239				

Appendix 13: Analysis of variance for stem diameter in Experiment 2

Source	**DF**	**SS**	**MS**	**F**	**P**
Replications	2	14.012	7.0062		
Crop	1	71.942	71.9415	32.98	0.0000
CPE	9	121.168	13.4632	6.17	0.0000
Dose	3	8.495	2.8316	1.30	0.2771
Crop × CPE	9	58.063	6.4515	2.96	0.0028
Crop × Dose	3	18.572	6.1905	2.84	0.0399
CPE × Dose	27	62.372	2.3101	1.06	0.3957
Crop × CPE × Dose	27	46.167	1.7099	0.78	0.7676
Error	158	344.701	2.1817		
Total	239				

Appendix 14 :Analysis of variance for chlorophyll content in Experiment 1

Source	**DF**	**SS**	**MS**	**F**	**P**
Replications	2	12.149	6.07433		
Crop	1	4.988	4.98817	2.81	0.0955
CPE	9	23.955	2.66165	1.50	0.1518
Dose	3	2.741	0.91377	0.52	0.6723
Crop × CPE	9	13.224	1.46930	0.83	0.5907
Crop × Dose	3	0.772	0.25746	0.15	0.9326
CPE × Dose	27	38.135	1.41240	0.80	0.7515
Crop × CPE × Dose	27	25.169	0.93218	0.53	0.9741
Error	158	280.170	1.77323		
Total	239				

Appendix 15: Analysis of variance for chlorophyll content in Experiment 2

Source	**DF**	**SS**	**MS**	**F**	**P**
Replications	2	864.5	432.27		
Crop	1	3465.6	3465.60	47.05	0.0000
CPE	9	1139.5	126.61	1.72	0.0887
Dose	3	151.9	50.65	0.69	0.5609
Crop × CPE	9	980.3	108.92	1.48	0.1600
Crop × Dose	3	55.3	18.42	0.25	0.8612
CPE × Dose	27	1979.9	73.33	1.00	0.4782
Crop × CPE × Dose	27	1974.3	73.12	0.99	0.4821
Error	158	11638.0	73.66		
Total	239				

Appendix 16 :Analysis of variance for leaf length in Experiment 1

Source	DF	SS	MS	F	P
Replications	2	3.45	1.73		
Crop	1	1450.42	1450.42	480.06	0.0000
CPE	9	64.37	7.15	2.37	0.0155
Dose	3	7.01	2.34	0.77	0.5107
Crop × CPE	9	15.01	1.67	0.55	0.8343
Crop × Dose	3	7.62	2.54	0.84	0.4734
CPE × Dose	27	58.13	2.15	0.71	0.8488
Crop × CPE × Dose	27	98.65	3.65	1.21	0.2336
Error	158	477.37	3.02		
Total	239				

Appendix 17: Analysis of variance for leaf length in Experiment 2

Source	DF	SS	MS	F	P
Replications	2	5.30	2.65		
Crop	1	1115.43	1115.43	131.56	0.0000
CPE	9	578.03	64.23	7.58	0.0000
Dose	3	3.67	1.22	0.14	0.9332
Crop × CPE	9	48.14	5.35	0.63	0.7695
Crop × Dose	3	3.02	1.01	0.12	0.9490
CPE × Dose	27	285.11	10.56	1.25	0.2028
Crop × CPE × Dose	27	310.03	11.48	1.35	0.1287
Error	158	1339.56	8.48		
Total	239				

Appendix 18: Analysis of variance for leaf width in Experiment 1

Source	DF	SS	MS	F	P
Replications	2	0.429	0.215		
Crop	1	402.227	402.227	408.95	0.0000
CPE	9	20.077	2.231	2.27	0.0204
Dose	3	0.140	0.047	0.05	0.9862
Crop × CPE	9	7.903	0.878	0.89	0.5332
Crop × Dose	3	1.274	0.425	0.43	0.7305
CPE × Dose	27	19.338	0.716	0.73	0.8324
Crop × CPE × Dose	27	31.150	1.154	1.17	0.2678
Error	158	155.404	0.984		
Total	239				

Appendix 19: Analysis of variance for leaf width in Experiment 2

Source	DF	SS	MS	F	P
Replications	2	6.20	3.098		
Crop	1	372.75	372.753	132.05	0.0000
CPE	9	134.41	14.935	5.29	0.0000
Dose	3	3.03	1.011	0.36	0.7833
Crop × CPE	9	23.89	2.654	0.94	0.4920
Crop × Dose	3	2.10	0.699	0.25	0.8628
CPE × Dose	27	95.39	3.533	1.25	0.1980
Crop × CPE × Dose	27	80.48	2.981	1.06	0.3993
Error	158	446.02	2.823		
Total	239				

Appendix 20: Analysis of variance for leaf area in Experiment 1

Source	DF	SS	MS	F	P
Replications	2	24	12.0		
Crop	1	71463	71463.3	561.64	0.0000
CPE	9	2917	324.1	2.55	0.0093
Dose	3	237	79.0	0.62	0.6022
Crop × CPE	9	479	53.2	0.42	0.9239
Crop × Dose	3	294	97.8	0.77	0.5130
CPE × Dose	27	2520	93.3	0.73	0.8265
Crop × CPE × Dose	27	4301	159.3	1.25	0.1976
Error	158	20104	127.2		
Total	239				

Appendix 21: Analysis of variance for leaf area in Experiment 2

Source	**DF**	**SS**	**MS**	**F**	**P**
Replications	2	510	254.8		
Crop	1	81756	81756.5	146.46	0.0000
CPE	9	25651	2850.1	5.11	0.0000
Dose	3	572	190.7	0.34	0.7953
Crop × CPE	9	7145	793.9	1.42	0.1827
Crop × Dose	3	604	201.3	0.36	0.7815
CPE × Dose	27	23522	871.2	1.56	0.0490
Crop × CPE × Dose	27	21947	812.9	1.46	0.0811
Error	158	88196	558.2		
Total	239				

Appendix 22: Analysis of variance for number of flowers in Experiment 1

Source	DF	SS	MS	F	P
Replications	2	0.633	0.3167		
Crop	1	23.438	23.4375	21.12	0.0000
CPE	9	19.454	2.1616	1.95	0.0490
Dose	3	2.046	0.6819	0.61	0.6066
Crop × CPE	9	8.687	0.9653	0.87	0.5537
Crop × Dose	3	1.746	0.5819	0.52	0.6662
CPE × Dose	27	40.329	1.4937	1.35	0.1336
Crop × CPE × Dose	27	52.296	1.9369	1.75	0.0189
Error	158	175.367	1.1099		
Total	239				

Appendix 23: Analysis of variance for number of flowers in Experiment 2

Source	DF	SS	MS	F	P
Replications	2	30.86	15.429		
Crop	1	198.02	198.017	55.43	0.0000
CPE	9	54.48	6.054	1.69	0.0944
Dose	3	8.88	2.961	0.83	0.4798
Crop × CPE	9	49.32	5.480	1.53	0.1403
Crop × Dose	3	1.48	0.494	0.14	0.9369
CPE × Dose	27	126.62	4.690	1.31	0.1540
Crop × CPE × Dose	27	135.85	5.031	1.41	0.1012
Error	158	564.47	3.573		
Total	239				

Appendix 24: Analysis of variance for number of fruits in Experiment 1

Source	DF	SS	MS	F	P
Replications	2	1.9750	0.98750		
Crop	1	4.0042	4.00417	27.08	0.0000
CPE	9	0.8375	0.09306	0.63	0.7707
Dose	3	0.2458	0.08194	0.55	0.6460
Crop × CPE	9	0.7042	0.07824	0.53	0.8517
Crop × Dose	3	0.1125	0.03750	0.25	0.8586
CPE × Dose	27	5.5458	0.20540	1.39	0.1102
Crop × CPE × Dose	27	5.6792	0.21034	1.42	0.0947
Error	158	23.3583	0.14784		
Total	239				

Appendix 25: Analysis of variance for number of fruits in Experiment 2

Source	DF	SS	MS	F	P
Replications	2	0.07500	0.03750		
Crop	1	0.03750	0.03750	3.08	0.0813
CPE	9	0.08750	0.00972	0.80	0.6186
Dose	3	0.01250	0.00417	0.34	0.7950
Crop × CPE	9	0.08750	0.00972	0.80	0.6186
Crop × Dose	3	0.01250	0.00417	0.34	0.7950
CPE × Dose	27	0.36250	0.01343	1.10	0.3439
Crop × CPE × Dose	27	0.36250	0.01343	1.10	0.3439
Error	158	1.92500	0.01218		
Total	239				

Appendix 26: Analysis of variance for fruit mass in Experiment 1

Source	**DF**	**SS**	**MS**	**F**	**P**
Replications	2	118.02	59.011		
Crop	1	225.39	225.389	22.81	0.0000
CPE	9	49.33	5.482	0.55	0.8322
Dose	3	31.82	10.606	1.07	0.3621
Crop × CPE	9	40.21	4.468	0.45	0.9043
Crop × Dose	3	21.79	7.264	0.74	0.5325
CPE × Dose	27	345.64	12.801	1.30	0.1654
Crop × CPE × Dose	27	330.06	12.224	1.24	0.2096
Error	158	1561.15	9.881		
Total	239				

Appendix 27: Analysis of variance for fruit mass in Experiment 2

Source	DF	SS	MS	F	P
Replications	2	4.930	2.46493		
Crop	1	2.358	2.35796	1.68	0.1968
CPE	9	11.573	1.28593	0.92	0.5125
Dose	3	3.199	1.06637	0.76	0.5182
Crop × CPE	9	11.690	1.29888	0.93	0.5046
Crop × Dose	3	3.197	1.06552	0.76	0.5185
CPE × Dose	27	39.042	1.44601	1.03	0.4319
Crop × CPE × Dose	27	39.045	1.44609	1.03	0.4318
Error	158	220.303	1.40320		
Total	239				

Appendix 28: Analysis of variance for dry shoot mass in Experiment 1

Source	**DF**	**SS**	**MS**	**F**	**P**
Replications	2	6.264	3.13205		
Crop	1	0.059	0.05891	0.10	0.7567
CPE	9	5.633	0.62586	1.02	0.4238
Dose	3	2.191	0.73024	1.19	0.3140
Crop × CPE	9	2.434	0.27049	0.44	0.9103
Crop × Dose	3	1.605	0.53494	0.87	0.4557
CPE × Dose	27	5.638	0.20882	0.34	0.9991
Crop × CPE × Dose	27	8.828	0.32695	0.53	0.9711
Error	158	96.637	0.61163		
Total	239				

Appendix 29: Analysis of variance for dry shoot mass in Experiment 2

Source	**DF**	**SS**	**MS**	**F**	**P**
Replications	2	9.89	4.947		
Crop	1	188.63	188.629	39.22	0.0000
CPE	9	147.71	16.412	3.41	0.0007
Dose	3	17.04	5.680	1.18	0.3188
Crop × CPE	9	76.26	8.474	1.76	0.0795
Crop × Dose	3	2.75	0.916	0.19	0.9028
CPE × Dose	27	168.02	6.223	1.29	0.1666
Crop × CPE × Dose	27	155.06	5.743	1.19	0.2476
Error	158	759.93	4.810		
Total	239				

Appendix 30: Analysis of variance for fresh root mass in Experiment 1

Source	DF	SS	MS	F	P
Replications	2	43.57	21.7851		
Crop	1	4.50	4.4991	0.43	0.5111
CPE	9	216.57	24.0638	2.32	0.0177
Dose	3	11.67	3.8896	0.38	0.7711
Crop× CPE	9	152.94	16.9937	1.64	0.1086
Crop × Dose	3	21.06	7.0203	0.68	0.5674
CPE × Dose	27	205.17	7.5989	0.73	0.8274
Crop × CPE × Dose	27	213.66	7.9134	0.76	0.7928
Error	158	1638.59	10.3708		
Total	239				

Appendix 31: Analysis of variance for fresh root mass in Experiment 2

Source	DF	SS	MS	F	P
Replications	2	37.27	18.633		
Crop	1	470.37	470.372	13.45	0.0003
CPE	9	826.19	91.799	2.62	0.0074
Dose	3	47.87	15.956	0.46	0.7133
Crop × CPE	9	457.22	50.803	1.45	0.1703
Crop × Dose	3	66.05	22.017	0.63	0.5970
CPE × Dose	27	702.75	26.028	0.74	0.8148
Crop × CPE × Dose	27	724.55	26.835	0.77	0.7879
Error	158	5526.77	34.980		
Total	239				

Appendix 32: Analysis of variance for dry root mass in Experiment 1

Source	DF	SS	MS	F	P
Reps	2	4.234	2.11716		
Crop type	1	0.019	0.01908	0.04	0.8361
CPE	9	4.460	0.49557	1.11	0.3553
Dose	3	0.809	0.26975	0.61	0.6115
Crop× CPE	9	4.652	0.51690	1.16	0.3225
Crop × Dose	3	1.430	0.47661	1.07	0.3626
CPE × Dose	27	9.276	0.34354	0.77	0.7810
Crop × CPE × Dose	27	8.740	0.32371	0.73	0.8323
Error	158	70.233	0.44451		
Total	239				

Appendix 33: Analysis of variance for dry root mass in Experiment 2

Source	DF	SS	MS	F	P
Replications	2	1.011	0.5055		
Crop	1	15.729	15.7286	17.11	0.0001
CPE	9	20.927	2.3253	2.53	0.0098
Dose	3	4.004	1.3347	1.45	0.2298
Crop × CPE	9	9.875	1.0973	1.19	0.3025
Crop × Dose	3	0.210	0.0700	0.08	0.9728
CPE × Dose	27	28.393	1.0516	1.14	0.2973
Crop × CPE × Dose	27	22.720	0.8415	0.92	0.5893
Error	158	145.225	0.9191		
Total	239				

Appendix 34: Analysis of variance for pH in Experiment 1

Source	**DF**	**SS**	**MS**	**F**	**P**
Crop	1	0.74401	0.74401	5.14	0.0270
CPE	9	1.67876	0.18653	1.29	0.2618
Dose	3	0.62170	0.20723	1.43	0.2423
Error	60	8.68219	0.14470		
Total	73				

Appendix 35: Analysis of variance for pH in Experiment 2

Source	**DF**	**SS**	**MS**	**F**	**P**
Crop	1	0.1176	0.11760	0.29	0.5925
CPE	9	3.3882	0.37647	0.93	0.5085
Dose	3	1.0240	0.34133	0.84	0.4770
Error	60	24.3635	0.40606		
Total	73				

Appendix 36: Analysis of variance for EC in Experiment 1

Source	DF	SS	MS	F	P
Crop	1	0.10519	0.10519	6.80	0.0115
CPE	9	0.69830	0.07759	5.02	0.0000
Dose	3	0.00147	0.00049	0.03	0.9924
Error	60	0.92794	0.01547		
Total	73				

Appendix 37: Analysis of variance for EC in Experiment 2

Source	DF	SS	MS	F	P
Crop	1	0.00351	0.00351	0.15	0.7024
CPE	9	1.17078	0.13009	5.46	0.0000
Dose	3	0.02434	0.00811	0.34	0.7963
Error	60	1.43059	0.02384		
Total	73				